



Università Politecnica delle Marche

Facoltà di ingegneria

Scuola di Dottorato di Ricerca in Scienze dell'Ingegneria

Curriculum in:

Ingegneria Civile, Ambientale, Edile e Architettura

XXX° ciclo

***A mechanically derived vulnerability index method for
seismic risk assessment of existing RC school buildings***

Candidato

Pardo Antonio Mezzapelle

Tutor

Prof. Stefano Lenci

Acknowledgments

I wish to express my deep gratitude to my supervisor Prof. Stefano Lenci for the opportunity he gave me to take part to the Ph.D. course and for the support constantly provided during the period of my research work.

Particular thanks are due to Francesco Clementi, researcher at the Università Politecnica delle Marche, for the help provided to me in many situations.

I would like to thank the provinces of Ancona and Macerata for the documentation made available relatively the high school buildings.



*A mamma,
papà,
Rosanna e
Maria Lucia*

Abstract

The seismic vulnerability of RC school buildings is a very important issue in Italy, as shown from the recent earthquakes (Molise 2002, L'Aquila 2009 and Amatrice 2016) causing the collapse and heavy damage of several school buildings. Most of Italian schools were built between the 50s and the 90s and so were usually designed considering only vertical loads, without or with low seismic resistance criteria.

In this study a methodology for rapid risk assessment of RC school buildings is shown. It is based on the vulnerability index method, considering 15 vulnerability indicators to which assign scores on the base of expert judgment. The scores were determined through pushover analyses performed on several structural models representative of the main characteristics of the Pre and Post 1974 school building stocks. To this aim a set of about 40 high schools (for a total of 105 independent buildings) were analysed to determine typical and specific vulnerabilities, and a simulated design procedure was carried according to the Codes in force in the two reference periods.

Correlations between the global vulnerability index I_v and the capacity in terms of PGA, for both slight damage and collapse, were determined to obtain trilinear damage curves such as in the 2nd level GNDT method.

Numerical validation of the rapid method was made by comparing the trilinear damage curves obtained for the two prototype buildings, representative in average of the Pre and Post 1974 school buildings, with analytical curves provided by both pushover and incremental dynamic analyses.

Also, experimental validation was carried out by comparing, for every high school building of the provinces of Ancona and Macerata, the damage occurred because of the Centre Italy 2016 seismic sequence with the damage estimated for the same intensity level through the proposed method. Both validation procedures have confirmed a good reliability of the proposed method for rapid and comparative evaluations.

Then two typologies of rapid damage scenarios were developed for both building stocks, in order to estimate physical, human and economic losses. The first typology considers uniform hazard on the whole territory and increasing intensity levels, instead the second one considers single events on the base of the fault system of the region (epicentres, magnitude and depth), thus the PGA values are calculated by means an attenuation law.

CONTENTS

Introduction	1
1. Seismic vulnerability of existing buildings	4
1.1. General aspects	4
1.2. Seismic response of RCMF structures	11
References chapter 1	26
2. Methods for seismic vulnerability assessment of buildings	30
2.1. Rapid methods	34
2.1.1. Macroseismic methods	35
2.2. Analytical methods	52
2.2.1. Simplified nonlinear procedures	53
References chapter 2	65
3. Seismic risk assessment	71
3.1. General aspects	71
3.2. Methods for risk assessment	77
3.3. Seismic hazard	84
3.3.1. Intensity measure parameters	95
3.4. Physical damage	96
3.4.1. Fragility curves	101
3.5. Human and economic losses	104
References chapter 3	110
4. The RC school building stock	119
4.1. The RC school building typology	119
4.2. Description of the building stock	127
References chapter 4	137
5. Proposal of a vulnerability index method for RC school buildings	139
5.1. General criteria and definition of the parameters	139
5.2. Simulated design for prototype buildings	144

5.3. Parametric analyses	150
5.3.1. Structural modelling and pushover analyses	150
5.3.2. Analysis results	155
5.4. Proposed method for school buildings	165
5.4.1. Iv – PGA relationship	171
References chapter 5	181
6. Rapid seismic vulnerability assessment for the school building stock	185
6.1. Assessment with macroseismic method	185
6.1.2. Macroseismic intensity – PGA relationship	189
6.2. Assessment with vulnerability index method	193
6.2.1. 2nd level GNDT method	194
6.2.2. Proposed method	197
6.2.3. Comparison between methods	204
6.2.4. Trilinear damage curves for the classes	215
References chapter 6	217
7. Numerical validation through nonlinear analyses	218
7.1. Assessment of the prototype buildings	219
7.1.1. Incremental dynamic analysis (IDA)	219
7.1.2. Pushover analysis	229
7.1.3. Comparison of the results	237
7.2. Assessment of case studies	240
References chapter 7	244
8. Experimental validation: the 2016 Centre Italy earthquake	248
8.1. The seismic sequence and the damage suffered to the building stock	248
8.2. Rapid damage estimation for the building stock	254
8.3. Analytical damage estimation for a case study	260
8.3.1. Non-linear dynamic analysis (NLDA)	263
8.3.2. Pushover analysis	267
References chapter 8	271
9. Rapid damage scenario for the building stock	274
9.1. Seismic hazard of the region	275
9.1.1. Determination of the seismic intensity level	280
9.2. Exposure data	287

9.3. Uniform hazard scenarios	289
9.4. For single event scenarios	297
References chapter 9	311
Conclusions	313
Appendix A_Data sheets of high school buildings (province of Ancona)	

Introduction

The work illustrated in this Ph.D. thesis born from the needed to rapidly assess the seismic safety level of the widespread Italian school building heritage, in order to carry out risk mitigation interventions.

In fact, recent earthquakes (Molise 2002, L'Aquila 2009 and Amatrice 2016) highlighted the quite high vulnerability of this building typology. Further, recent studies and reports about school buildings provided a general unsafe condition.

This problem, in general, involves the whole Italian built heritage because the most part was built in absence or with low seismic resistance criteria during the period 50s – 90s, when Old Seismic Code were in force and the seismic classification of the territory didn't consider the actual hazard. This mean that many reinforced concrete (RC) buildings were designed with low seismic detailing as the lack of stirrups in the column-beam joints, low quantitative of steel reinforcement in the columns leading to strong beam-weak column behaviour and many other structural irregularities (stiffness and resistance distributions).

Only after the 2003, a modern seismic Code was introduced, adopting the Capacity Design principles, and the seismic classification of the territory was improved leading to the Italy hazard map obtained by means a PSHA.

A depth description of these aspects is illustrated in chapter 1, where the seismic behaviour and main vulnerabilities of RC buildings are described.

In chapter 2 and 3 are shown the procedures to assess respectively the seismic vulnerability and risk. The latter involves also the seismic hazard and the exposure estimation.

In chapter 4 the school building topology is investigated referring to the RC high school building stock of the province of Ancona (105 RC independent structures). The main structural and morphological characteristics are detected, and the typical and specific vulnerabilities are shown distinguishing between PRE and POST 1974 classes.

The PRE 1974 class is representative of buildings designed according to the R.D. 2229 dated 1939, while the POST 1974 represents those designed according to law n. 1089 date 1971 and the relative successive Decrees.

The main differences between the two classes are in the:

- type of design adopted, considering only static load for the PRE 1974 buildings, while the seismic action is considered for most part of the POST 1974 buildings.
- Type of steel employed, smooth for the PRE 1974 and ribbed for the POST 1974 period.

Then the practical aspects of the work (elaborations and results) can be summarized in two main parts:

-
1. **The first part**, in which a vulnerability index method for RC school buildings is developed (chapter 5) and validated by means both numerical (chapters 7) and experimental procedures (chapter 8). Further the evaluation of the building stock is made through the macroseismic method, referring to the EMS-98 scale, and the 2nd level GNDT and proposed methods (chapter 6).
 2. **The second part**, in which rapid damage scenarios for the school building stock of the province of Ancona and Macerata were developed considering several intensity levels (chapter 9) and accounting for the exposure data as the scholar population and replacing cost of every school building.

The proposed vulnerability index method is mechanically-derived. In fact, many pushover analyses on 50 structural models with lumped plasticity, generated in a deterministic manner to represent the vulnerabilities detected for the PRE and POST 1974 classes and according to simulated design procedure, were carried out in order to compare the capacities of the models and so to determine the scores to assign to the vulnerability indicators. The capacity parameter assumed is the area comprised under the average equivalent bilinear curve of the 8 curves obtained for each model from the pushover analysis.

A total of 15 indicators are considered, against the 11 of the 2nd level GNDT method.

Also, relationships between the global vulnerability index (I_v) and peak ground acceleration (PGA) with respect the slight damage (PGAs) and the collapse (PGAc) are proposed in chapter 6, leading to the trilinear damage curves PGA – damage index (DI), then employed to develop rapid damage scenarios.

The numerical validation consists in the comparison of the vulnerability curves PGA – DI, obtained for the two prototype buildings representing in average the PRE and POST 1974 classes, with the trilinear damage curves provided from the rapid methods (GNDT and the proposed one) for the same prototype buildings. To this aim both pushover and incremental dynamic analyses (IDAs) were developed, obtaining first the fragility curves (the probability of exceedance a certain damage state DS_k given an intensity level) and then the vulnerability curves by introducing the seismic hazard for the region of interest.

Further ten case studies are evaluated through pushover analyses and the capacities in terms of PGA compared with those coming from the rapid methods.

The experimental validation has been possible considering the damage occurred on the school buildings under investigations after the Centre Italy 2016 seismic sequence, with strong earthquakes reaching the $M_w = 6.5$.

Thus, the estimated damage by means the rapid method is compared with those occurred for all buildings belonging to the stock and more in depth in a case study, for which the damage level has been estimated also by means pushover and NLDAs, employing the acceleration signal recorded in station close to the school.

Finally, rapid damage scenarios were developed for the entire high school building stock (province of Ancona and Macerata), assuming different hazard levels. In particular three different approach have been employed:

- *Maximum historical macroseismic intensity* recorded for every municipalities of interest.
- *Uniform hazard*, assuming the PGA values relative to the same return period for the whole area of interest. Five return periods are considered: 200, 475, 912, 1462 and 2475 years.
- *Per event scenarios*, in which three events were simulated by fixing hypocentres-magnitude pairs on the basis of the seismogenic sources present in the region. The epicentres were located in the municipalities with the highest exposure in order to estimate maximum expected losses and the attenuation law provided by (Sabetta e Pugliese 1987) was employed to calculate the PGA away from the epicentres.

For each scenario the losses in terms of physical damage, referring to the 5 levels of the EMS-98 scale, casualties and repair cost were determined and compared to each other.

In this way the owners of the building stock have an overview of the risk levels due to different scenarios and so they can to establish which is the acceptable risk level and to implement mitigation interventions based on it.

Chapter 1

1. Seismic vulnerability of existing buildings

1.1. General aspects

The seismic vulnerability of a building is the propensity to suffer a certain damage level under an earthquake of a given intensity. Thus, the vulnerability assessment is a fundamental step in seismic risk analyses and in the damage scenario for earthquakes of a certain intensity level.

When an earthquake occurs, the physical damage of structural and non-structural elements, the casualties and injuries, the loss of contents and the indirect economic losses due from the business interruption, not depend only from the vulnerability of the buildings, but also from the level of *seismic hazard* of the site (maximum expected intensity) and from the *exposure* (number of people that live or work in the building, economic values of the construction and of its content, the type of activity performed within the building).

Vulnerability, hazard and exposure are the components of the seismic risk and they have to be assessed and merged together when a scenario risk analysis have to be developed.

Several methods can be used to assess the seismic vulnerability (please see chapter 2), so empirical, analytical or hybrid procedure can be performed. The use of a specific method often depends on the scale of the loss assessment; for a single building, analytical methods are suggested, while in the case of a large-scale with a great number of buildings simultaneously assessed, also empirical or hybrid methods are useful.

The vulnerability of existing structures is a very important issue in Italy, because of the very high number of ancient historical centres, mainly made of unreinforced masonry buildings (URM), and a lot of reinforced concrete structures (RC), built up mainly in the period between the 50's and the 90's. About the 40% of the RC buildings was designed according to the law n.64/1974, that introduced basic seismic provisions, so they have low earthquake resistant criteria if the building was built within a zone declared as seismic (not likely because most of the Italian territory was declared as seismic prone area only after 1983).

Thus, the most part of RC buildings ca be considered as PRE Code buildings, that is the lack of earthquake resistance criteria, because or they were designed previously the 1974 (the 60%) or they were designed after the 1974 (the 40%) but they weren't within a seismically zone.

It worth noting that also the PRE 1974 buildings could have been built within a zone declared as seismically dangerous, thus equivalent horizontal loads were considered in design, but they only increased the stiffness and resistance of the structure, not the ductility for the lack of adequate details (quantity of longitudinal bars and stirrups in the members).

The “*Casa Italia Report*”, published from the Italian government on June 2017, has identified for each region (tab. 1.1) the number of both RC and masonry buildings with high vulnerability and localized in the cities with the highest seismic hazard ($a_{g_{max}} > 0.25$). The evaluation has been done starting from data the 2011 ISTAT census.

Table 1.1. Number of buildings with the highest seismic risk in each region
(font: “*Casa Italia Report*”, 2017)

Region	Masonry buildings	RC buildings built before the 1971
Abruzzo	34385	3380
Basilicata	21690	1630
Calabria	189608	35163
Campania	72336	4576
Emilia-Romagna	0	0
Friuli-Venezia Giulia	23902	3354
Lazio	17020	887
Liguria	0	0
Lombardia	0	0
Marche	0	0
Molise	23907	1374
Piemonte	0	0
Puglia	0	0
Sardegna	0	0
Sicilia	89687	18648
Toscana	0	0
Trentino-Alto Adige/Südtirol	0	0
Umbria	0	0
Valle d'Aosta/Vallée d'Aoste	0	0
Veneto	22370	2682
Total	494905	71694

Also, the seismic vulnerability of the Italian built heritage has been shown experimentally from several strong earthquakes occurred since the beginning of the 1900 to nowadays. They have shown the weakness of the Italian built up heritage, causing many casualties, physical damage (fig. 1.1) and economic losses (tab.1.2). The latter includes also indirect losses, tax reliefs and exemptions and in tab. II they have been actualized at the 2014 to be comparable each other (font: *Centro Studi CNI - Consiglio Nazionale Ingegneri*).



Figure 1.1. Earthquakes: 1908 Messina (upper-left), 1915 Avezzano (upper-right), 1976 Friuli (lower-left), Irpinia 1980 (lower-right).

Table 1.2. Main destructive events in Italy from 1900 to nowadays

<i>Major Earthquake in Italy</i>	<i>Date</i>	<i>Mw</i>	<i>MCS</i>	<i>Casualties</i>	<i>Economic losses [Bln €]</i>
<i>Stretto di Messina</i>	1908	7.2	XI-XII	120000	-
<i>Avezzano</i>	1915	7.0	XI	33000	-
<i>Vulture</i>	1930	6.7	X	1404	-
<i>Belice</i>	1968	6.1	X	370	9,2
<i>Friuli</i>	1976	6.4	X	989	18,5
<i>Irpinia</i>	1980	6.9	X-XI	2914	52,0
<i>Umbria-Marche</i>	1997	6.0	IX	11	13,5
<i>Molise</i>	2002	5.7	VIII-IX	30	1,4
<i>L'Aquila</i>	2009	6.3	IX-X	309	13,7
<i>Emilia Romagna</i>	2012	5.9	VIII	27	13,3
<i>Centro Italia</i>	2016	6.5	X	299	23,0

It is worth noting as the losses are directly linked with the magnitude of the events.

During these earthquakes, mainly *URM buildings* collapsed or suffered heavy damage. They were usually built with poor materials (fig.1.2), such as rounded stones and inconsistent mortar, and weak connections between walls, walls and floor/roof slabs, thus they exhibit brittle local mechanisms of collapse, such as disaggregation or rocking of the external walls, instead of a global and more ductile response of the whole structure.



Figure 1.2. Collapse of masonry walls made of poor materials (Grisciano (AP), 2016 Centre Italy earthquake)

Also, *RC buildings* collapsed or suffered heavy damage during the strongest earthquakes. The main weakness exhibit by RCMF buildings are:

- *column-beam joints*, where the lack of stirrups and the strong beam-weak column effect have made them very vulnerable to seismic excitement, causing the rupture of the top of the columns (fig.1.3).



Figure 1.3. Rupture due to weak column-beam joint effect (Amatrice, 2016 Centre Italy earthquake)

- *soft storeys* due to irregularity in the arrangement of masonry infills along the elevation of the building, causing the collapse of many columns at the same storey and the pan-cake effect (fig. 1.4).



Figure 1.4. Collapse due to soft storey: (a) Norcia, 2016 Centre Italy earthquake; (b) L'Aquila, 2009 L'Aquila earthquake.

- *short columns* due to short walls within the frames, knee-beams of the stairs or irregularity in the vertical alignment of storeys, causing the rupture of the free part of the columns (fig. 1.5).



Figure 1.5. Rupture of short columns (Visso, 2016 Centre Italy earthquake)

Further, during the 2012 Emilia Romagna (Magliulo et al, 2014; Belleri et al, 2015) and 2016 Centre Italy earthquakes many industrial pre-cast buildings collapsed (fig.1.6) because of the lack of connections between columns and beams or/and beams and rooftops.



Figure 1.6. Partial collapse of a pre-cast RC industrial building (Norcia, 2016 Centre Italy earthquake)

After the 2002 Molise earthquake, when a school building collapsed killing many children and their teacher. many things changed in Italy with regard to the seismic design of structures and the classification of the seismic prone areas.

A new hazard map for Italy was developed in 2004 and updated over time (Stucchi et al, 2011) by means a probabilistic seismic hazard analysis (PSHA), identifying a 5x5 Km grid with values of the hazard parameters PGA, F_0 and T_c for each grid-point. Thus, for each point of the map the probability to exceed a certain intensity level in a given reference period can be estimated (fig. 1.7).

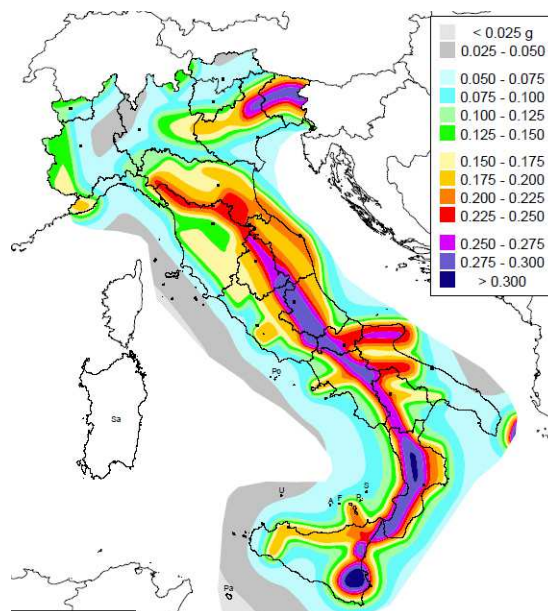


Figure 1.7. Italy seismic map for a probability of exceedance of 10% in 50 years.

Then the O.P.C.M. n. 3519 dated 2006/04/28 assigned to each city one of the four seismic zones provided:

Zone A - high seismicity: $ag_{max} > 0.25$ g.

Zone B - medium seismicity: ag_{max} ranged between 0.15g and 0.25 g.

Zone C - moderate seismicity: ag_{max} ranged between 0.05g and 0.15 g.

Zone D - low seismicity; $ag_{max} < 0.05$ g.

The performance based seismic design approach (PBSDA) (Priestely, 1997, Sullivan et al. 2003) was adopted in the last Italian seismic Code (*Norme tecniche per le costruzioni – NTC 2008*), adopting the same four performance levels (or limit states) of Eurocode 8 (fig.1.8). The Capacity Design was introduced too, providing the strong column-weak beam behaviour and that the brittle shear failure occurs later the ductile flexural failure in each structural member.

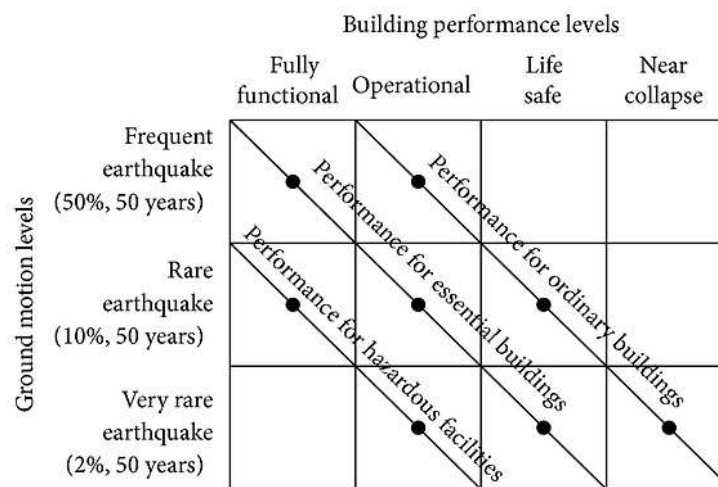


Figure 1.8. Performance levels in PBSDA

Further provisions for the seismic vulnerability assessment of existing buildings were introduced, regarding the knowledge level (KL) to reach and the confidence factor (CF) to use in order to take into account the epistemic uncertainties in constructive details and mechanical properties of materials. Nonlinear static and dynamic analysis procedures were also indicated as the main tools for the evaluation of the seismic response of structures.

1.2. Seismic response of RCMF structures

RC structures in which the load-bearing capacity is due by columns, beams and slabs, rigidly linked each other, are called moment frame structures (RCMF, fig. 1.9). They are widespread in Italy, while shear walls RC structures, also known as “dual system”, are very common in earthquake-prone areas but not in Italy.

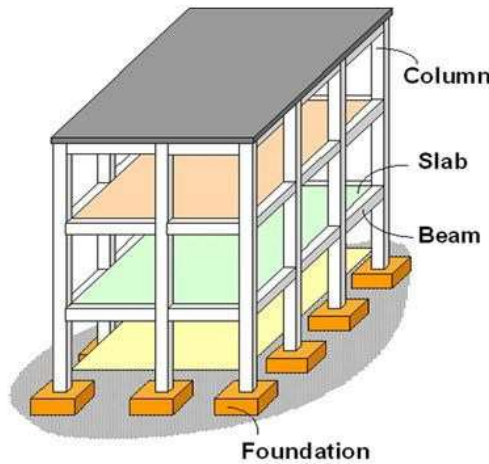


Figure 1.9. Members of a RCMF structure

The Italian RCMF buildings in the most part was designed in absence of a modern seismic Codes, that require to apply the hierarchy of resistance, until to 2003. The lack of adequate constructive details in the structural members is the main reason of the low ductility offered from these types of structures (fig. 1.10 – b).

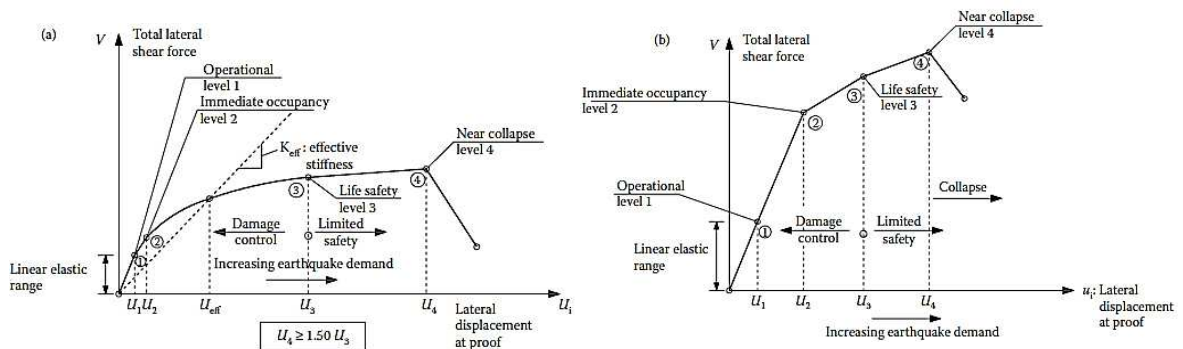


Figure 1.10. Ductile (a) and brittle (b) behaviour

Until about the ‘80s RCMF were usually conceived as composed by parallel plane frames, with high beams only in one direction, while in the other direction often only slabs made of RC joists and hollow bricks were arranged. Thus, these structures were able to bear only vertical loads and exhibited a not good response during earthquakes.

Subsequently the parallel frames were integrated with load-bearing elements also in the other direction, so a better resistant scheme against seismic action was formed.

However, in both cases the capacity design procedure wasn't provided in the Codes, thus usually in the buildings we can find weak columns - strong beams ratios and the lack of adequate constructive details to guarantee ductility in the members.

Only recently, after the 2003, the capacity design procedure was introduced and the seismic behaviour of RCMF improved very much.

Thus, there are several subtypes of existing RCMF buildings:

- Non-ductile RC frames with/without infill walls.
- Non-ductile RC frames with reinforced infill walls.
- Ductile RC frames with/without infill walls.

The masonry infills play an important role in the seismic response of RC framed buildings as described in the final part of this chapter.

The expected seismic response of RCMF structures can be well associated with the age of the buildings, according to the aspects below exposed.

1. Regulations

Generally, in all over the world Code requirements related to design and detailing of RC frame buildings in seismic zones were significantly changed in the early 1970s. Earlier codes focused on the strength requirements—that is, on providing adequate strength in structural members to resist the lateral seismic forces. However, based on research evidence and lessons learned from earthquakes in the early 1970s, code requirements have become more focused on the proportioning and detailing of beams, columns, and joints with the objective to achieve a certain amount of ductility in addition to the required strength.

Ductility is one of the key features required for desirable seismic behaviour of building structures and it needed of adequate constructive details.

The principles and rules of seismic detailing of reinforced concrete structures have been emerging over time and are mainly reflected in seismic provisions of building codes.

In Italy several Codes that regulated the design of RC structures with different levels of earthquake resistance provisions, have succeeded over time. The main Codes are:

- Royal Decree n. 193 dated 18th April 1909 “*Norme tecniche ed igieniche obbligatorie per le riparazioni ricostruzioni e nuove costruzioni degli edifici pubblici e privati nei luoghi colpiti dal terremoto del 28 dicembre 1908 e da altri precedenti elencati nel R.D. 15 aprile 1909 e ne designa i Comuni.*”

- Royal Decree n. 431 dated 13th March 1927 “*Norme tecniche e igieniche di edilizia per le località colpite da terremoti*”.
- Royal Decree n. 2105 dated 22th November 1937 “*Norme tecniche ed igieniche per le riparazioni, ricostruzioni e nuove costruzioni degli edifici pubblici e privati nei comuni o frazioni di comune dichiarati zone sismiche.*”
- Royal Decree n. 2229 dated 16th November 1939 “*Norme per la esecuzione delle opere in conglomerato cementizio semplice od armato*”,
- Law n. 1684 dated 25th November 1962 “*Provvedimenti per l'edilizia, con particolari prescrizioni per le zone sismiche*”.
- Law n. 1086 dated 5th November 1971 “*Norme per la disciplina delle opere di conglomerato cementizio armato, normale e precompresso, ed a struttura metallica*”.
- Law n. 64 dated 2th February 1974 “*Provvedimenti per le costruzioni con particolari prescrizioni per le zone sismiche*”.
- Ministerial Decree dated 3th March 1975 “*Approvazione delle Norme tecniche per le costruzioni in zone sismiche*”.
- Ministerial Decree dated 12th February 1982 “*Criteri generali per la verifica della sicurezza delle costruzioni e dei carichi e sovraccarichi*”.
- Ministerial Decree dated 19th June 1984 “*Norme tecniche relative alle costruzioni sismiche*”.
- Ministerial Decree dated 24th January 1986 “*Norme tecniche relative alle costruzioni antisismiche*”.
- Ministerial Decree n. 285 dated 20th November 1987 “*Norme tecniche per la progettazione, esecuzione e collaudo degli edifici in muratura e per il loro consolidamento*”.
- Ministerial Decree dated 14th February 1992 “*Norme tecniche per le opere in c.a. normale e precompresso e per le strutture metalliche*”.
- Ministerial Decree dated 9th January 1996 “*Norme tecniche per il calcolo, l'esecuzione ed il collaudo delle strutture in c.a. normale e precompresso e per le strutture metalliche*”.
- Ministerial Decree dated 16th January 1996 “*Norme tecniche per le costruzioni in zone sismiche*”.
- Ministerial Decree dated 16th January 1996 “*Norme tecniche relative ai criteri generali di verifica di sicurezza delle costruzioni e dei carichi e sovraccarichi*”.
- Ordinance of the Council of Ministers n. 3274 dated 20th March 2003 “*Primi elementi in materia di criteri generali per la classificazione sismica del territorio nazionale e normative tecniche per le costruzioni in zona sismica*”.
- Ordinance of the President of the Council of Ministers n.3431 dated 3th May 2005 “*Ulteriori modifiche ed integrazioni all'O.P.C.M. 20 marzo 2003 n. 3274, recante «Primi elementi in*

materia di criteri generali per la classificazione sismica del territorio nazionale e di normative tecniche per le costruzioni in zona sismica»

- Ministerial Decree dated 14th January 2008 “*Norme Tecniche per le Costruzioni*”.

Also, technical manuals were employed by engineers, such as those known as “*Santarella*” and “*Pagano*”.

These regulations essentially prescribed the minimum resistance of concrete and steel, the maximum admissible values of tension within the cross sections, sometimes the minimum geometrical dimensions of elements and the minimum quantitative of longitudinal rebars and stirrups, the minimum anchor length, the formulation to calculate the bending moment in the members and the values to adopt for dead and live loads.

The 1974 is an important year because, after many years, new provisions were provided for buildings in seismic prone areas.

In the PRE 1974 period the main used design code was the *Royal Decree n. 2239 dated 1939*. It provided extremely poor rules concerning both design and construction activities, particularly with regard to reinforcement details. No rules were given for design actions and structural details, whereas the concrete was classified by means of the average cubic resistance (R_{cm}) at 28 days of ageing. R_{cm} had to be at least three times the resistance value adopted in the calculations and contained in the range 120–180 kg/cm².

Steel, generally in smooth bars, was characterized by nominal allowable strength values variable in 1400 – 2400 kg/cm² range, according to the adopted type. Ribbed bars appeared for the first time in 1957 and the most used were the “*TOR*” and the “*Twisteeel*” types. These rebars reached the yielding strength of 6000 kg/cm² but they had to be used with concrete with cubic resistance of 225 - 250kg/cm² at least.

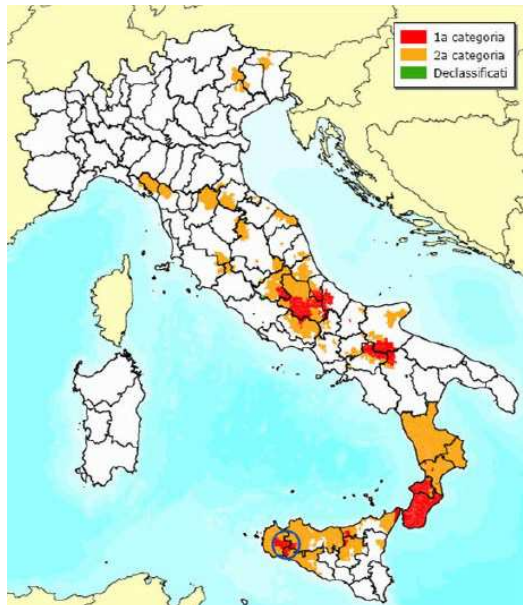
Another important aspect regulated from the Codes is the seismic classification of the Italian territory. It started after the Messina earthquake and it was updated every time a new strong earthquake occurred, by adding the cities hit to the seismic map. Fig. 1.11 show the classification at the 1909, 1935, 1975, 1984, 2003, 2015.



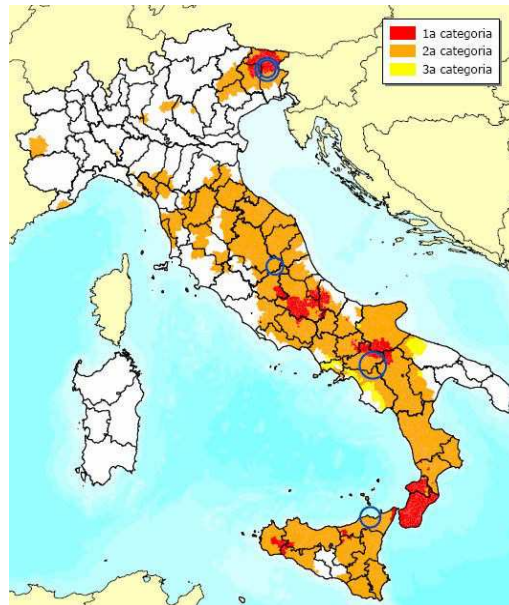
a)



b)



c)



d)

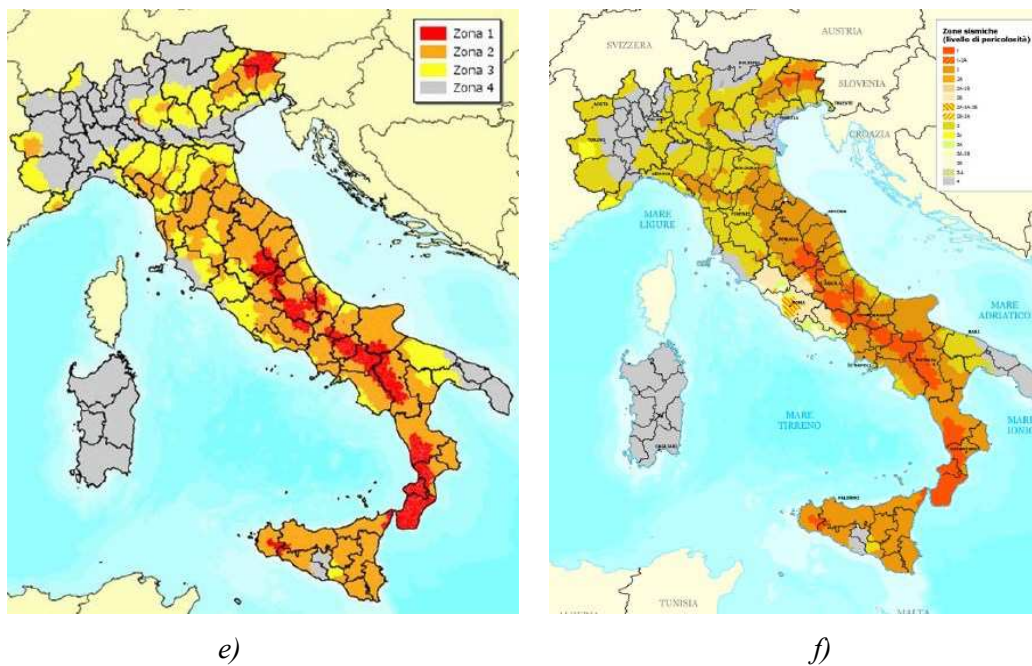


Figure 1.11. Seismic classification of Italy: 1909 (a), 1935 (b), 1975 (c), 1984 (d), 2003 (e), 2015 (f)

It is worth noting that after 1984 the classification spread very much and involved the most part of the territory.

Thus, for the seismic areas the regulations determined the level of hazard to assume (seismic categories) and the entity of the seismic forces to apply at the storey as equivalent horizontal loads (% of the storey weight depending on the seismic category of the zone).

2. Mechanical properties of the materials

Further, the type of steel used for reinforcement and the mechanical properties of concrete depending on the reference period. In fact, the industrial production improved over time and so the quality of materials and the constructive techniques.

Until to '70 usually smooth steel bars were used (tab. 1.3), anchored by bending their extremities according to a hook shape, while in the subsequent period ribbed steel bars (tab. 1.4) were largely used.

Table 1.3. Type of smooth steel bars

	Aq 42	Aq 50	Aq 60	Feb 22K	Feb 32K
<i>Yield strength [N/mm²]</i>	> 230	> 270	310	220	315
<i>Ultimate strength [N/mm²]</i>	420	500	600	335	490
<i>Minimum elongation [%]</i>	20	18	14	24	23

Table 1.4. Type of ribbed steel bars

	Feb 38K	Feb 44K
<i>Yield strength [N/mm²]</i>	375	430
<i>Ultimate strength [N/mm²]</i>	450	540
<i>Minimum elongation [%]</i>	14	12

Thus, is possible to individuate 3 main reference periods for Italian RC structures:

- PRE 1974, in which most of buildings are designed only for vertical static loads (PRE Code buildings) and smooth bars were used as reinforcement.
- POST 1974, in which most of buildings in seismic area keep in account seismic loads and they have a low level of earthquake resistant design (Low Code buildings). Ribbed rebars were used as reinforcement.
- POST 2003, in which buildings are designed according to the Capacity Design procedure and they account for the expected intensity level provided from the last hazard map (High Code buildings).

The buildings belonging to each period differ for the quality of materials employed, for the values of live loads and for constructive details such as:

- Minimum cross section of members.
- Quantity of longitudinal bars.
- Quantity of stirrups.
- Anchor length.

The PRE and POST 1974 non-ductile RCMF buildings, although sometimes designed to resist to lateral forces, did not incorporate modern ductile seismic detailing provisions. As a result, the main seismic deficiencies include:

- *Inadequate column detailing.* The two main detailing problems include inadequate column lap splices for main flexural reinforcement and a lack of adequate transverse reinforcement (ties) within the column. As an example, column lap splices were typically placed just above the floor level in the zone of high stresses. In addition, the column lap splices were generally too short, often in the order of 30-bar diameters, or less, and were typically not confined with closely spaced column ties (as required by modern codes).
- *Lack of strong column/weak beam design approach.* A capacity design approach was not followed in the design of the beam flexural reinforcement, as the beams were generally designed for the code level forces. The effects of post-yield behaviour were not considered, thus

increasing the chances for undesirable shear failure in either the beams or columns. Shear failure is rather brittle and sudden, and should be avoided in reinforced concrete structures located in seismic zones.

- *Inadequate anchorage of beam reinforcement.* The top reinforcing bars in beams were often terminated in the column or just away from the column face, whereas the bottom bars were typically discontinued at the face of the supporting column or provided with only a short lap-splice centered on the column.
- *Excessive tie-spacing.* Spacing of ties in beams and columns was excessively large by today's standards. Column ties often consisted of a single hoop with 90-degree hooks spaced at 20 to 30 cm on the whole length of the column. Today's ties generally require 135-degree hooks to ensure adequate confinement. Beam ties, often sized only for gravity shear loads, were spaced closely near the column face but were widely spaced or even discontinued in the mid-span region of the beam.
- *Inadequate beam/column joint ties.* The lack of ties in the beam/column joint created a weak zone and likely failure mechanism within the joint.

Further, the seismic performance of RC buildings could be poor because of the presence of some deficiencies that for several reasons affect the construction:

- Alteration of the member sizes during the construction phase from specifications in the design drawings
- Noncompliance of the detailing work with the design drawings.
- Inferior quality of building materials and improper concrete-mix design.
- Modifications in the structural system performed by adding/removing components without engineering input.
- Reduction in the amount of steel reinforcement as compared to the design specifications.
- Poor construction practice.

The seismic response of RCMF structures designed according to Old Codes has been investigated from several authors employing different procedures:

- Empirical analysis of damaged buildings after earthquakes (*Manfredi et al. 2010, Ricci et al. 2010, Manfredi et al. 2014*).
- Numerical investigations through nonlinear analysis (*Fardis 1997, Masi et al. 2003, Magliulo et al. 2007, Makarios et al. 2012, Mohammad et al. 2016*).
- Experimental investigations in laboratory on single RC members (columns, beams, beam-column joints) (*Hakuto et al. 2000, Braga et al. 2000, Di Ludovico et al. 2014*) and on

full/partial scale of plane or spatial frames (shake table or static tests) (*Pinto et al. 1999, Calvi et al. 2002, Albanesi et al. 2008*).

These investigations highlighted several important aspects, summarized in the following part. RCMF buildings exhibit, under strong earthquakes, plastic deformations lumped on the extremity of beams and columns, also involving the beam-column joints on the base of the quantity of longitudinal bars and stirrups within structural elements converging in the joint. In fact, a lot of longitudinal bars and the low quantity of stirrups can determine the occurrence of a brittle shear collapse before the ductile flexural collapse.

The strong beams - weak columns effect (Park and Paulay, 1975) is due to the low quantity of longitudinal rebars in the columns.

The most favourable mechanisms of collapse forbid the brittle shear rupture of beam-column joints and of the other elements, while involving the plasticization of the largest number of members, such as the beams of the all levels and the columns at the ground floor (strong column-weak beam behaviour). The occurrence of this ductile mechanism requires to design the structure according to the *Capacity Design* principles (EC 8).

Generally, the Capacity Design principles and the regularity in plan and in elevation are not considered in the design of existing RC buildings. Thus, it is more likely the occurrence of a soft storey mechanism (fig. 1.12 – a), involving mainly the columns at the same floor, instead of ductile mechanism (fig. 1.12 - b).

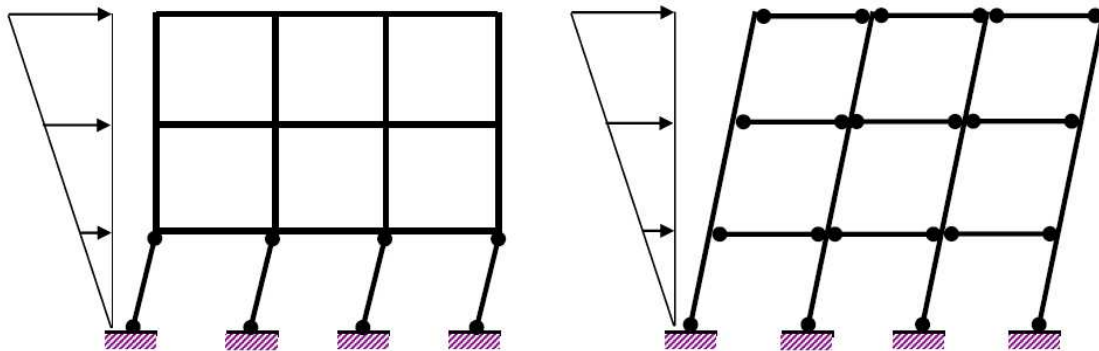


Figure 1.12. Soft-storey (a) and ductile (b) mechanisms of collapse.

In many applications, architectural considerations result in a taller first story, which causes a soft-story formation due to drastic change in the stiffness between adjacent stories. The presence of a soft story results in a localized excessive drift that causes heavy damage or collapse of the story during a severe earthquake. Another typical case of soft story arises when the first floor is left open (that is, no infills) to serve a commercial function (stores) or as a parking garage, while upper floors are infilled with unreinforced masonry walls.

A relatively rare case results when the strength of the two adjacent stories is significantly different (weak story) leading to localized deformations similar to the soft-story mechanism. Thus, the collapse mechanism could involve only a floor (the weakest) with the formation of plastic hinge to the ends of the columns. This is a brittle collapse mechanism because of both the low number of dissipative elements involved and the limited ductility capacity of the columns subjected to high axial loads (rigid-brittle behaviour).

Other typical non- ductile failure mechanisms are:

- *Shear failure and concrete crushing failure in concrete columns.* Brittle shear mechanisms are caused by the low quantity of stirrups in columns, particularly in the end zones and in the column-beam joints (fig. 1.13).

These are the most undesirable nonductile modes of failure and they can lead to the loss of gravity load-bearing capacity in the columns and potentially a total building collapse.



Figure 1.13. *Shear failure and concrete crushing failure in concrete columns*

- *Short-column effects.* The short or captive column failure (fig. 1.14) occurs due to partial restraining of the columns that are, in turn, subjected to high shear stresses and fail in shear if unable to resist these stresses.



Figure 1.14. *Short column effects*

Another important aspect of the vulnerability of RC buildings is the medium compression stress in columns. In fact, it influences the ductile capacity of columns and so the behaviour factor of the whole structure. High levels of compression lead to higher rotational stiffness and lower ductility. Further the compression level in columns is strongly correlated with other aspects, such as the structural masses and the dimensions of columns, thus with the seismic forces and the resistance of the columns that directly influence the vulnerability.

In the SAVE project (Dolce et al. 2005-a), the correlation between the compression level in columns of the ground floor and the vulnerability was investigated analysing several buildings by means the VC method (Dolce et al. 2005-b) and the results are shown in fig. 1.15 (on the X axis the medium compressive stress in columns, on the Y axis the structural capacity in terms of PGA).

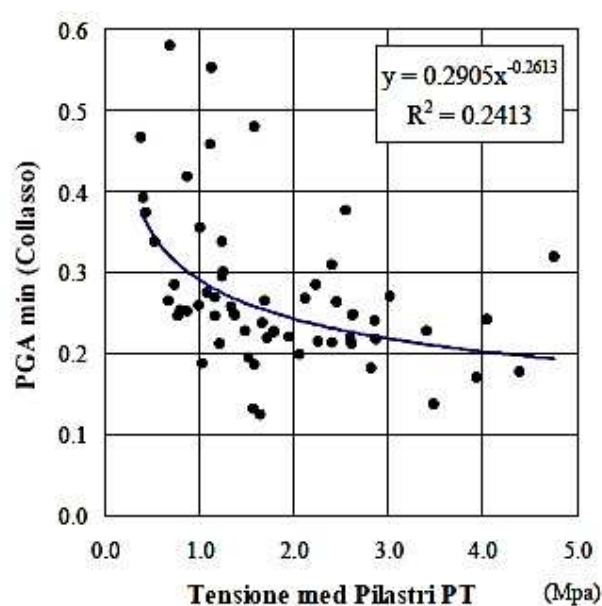


Figure 1.15. Correlation between medium compression in columns and collapse capacity

It worth noting as the maximum medium values founded in each building assume values higher than 4 MPa, meaning that the local values in columns could be very high with respect the compressive resistance of the concrete used in the '60 and '70, usually lower than 20 MPa

Further, the capacity assumes high values for medium compressive stresses lower than 1 MPa, while the capacity decreases for higher values of the stress in columns.

Structural irregularities

The simplicity, symmetry and regularity in terms of both resistance and stiffness distributions are important factors governing seismic response of RC structures.

In fact, frame structures that have performed remarkably well during earthquakes have had regularity and symmetry about two orthogonal axes in plan and regularity in elevation. If a building

is symmetric about orthogonal axes in plan, then it does not twist during the action of earthquake and the seismic demand doesn't increase on columns.

Further if the building has rigid floor diaphragms, then all columns are subjected to the same inter-storey drifts.

Whereas, those that have not performed well during earthquakes had non-symmetric and non-regular plans and/or vertical irregularities in the form of weak and/or soft stories, buildings undergone major structural alterations-addition of floors, removal of load resisting members, and structures constructed on weak, unstable, or different foundation soil systems.

Shape irregularity (fig. 1.16), which often results in structural irregularity, determines the concentration of stresses and so of the damage in specific parts or storeys of a building, and may even cause collapse.

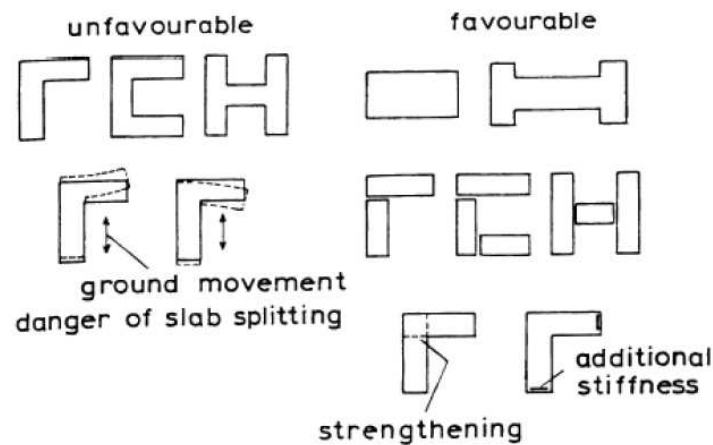


Figure 1.16. Unfavourable and favourable planar shapes (After Penelis and Kappos 1997)

Typically, stiffness and strength distributions of Old Code buildings are not symmetric in both principal directions in plan because structures were calculated without taking into account the three-dimensional effects (only plane effects). Further stiffness and strength usually are not regular even along the height of the building (fig. 1.17).

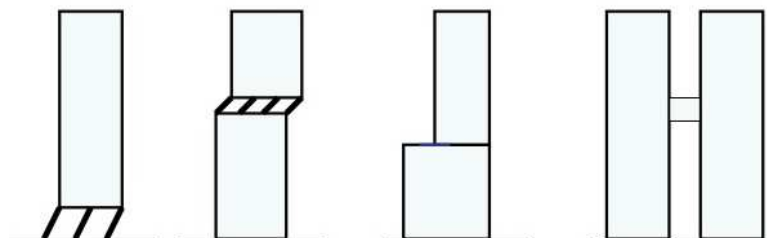


Figure 1.17. Irregularities in elevation

The presence of columns having a constant quantitative of longitudinal bars along the height, determines a structural irregularity in terms of storey resistances, being the ratio between the maximum resistant shear and the external shear forces significantly variable between storeys.

Especially for those building designed for gravity loads only, frames are usually present in one direction, generally the longer one (longitudinal), identifying a strong direction, whilst in the orthogonal direction the frames are present on the external sides only in order to withstand the weight of external walls.

Due to this characteristic, the transverse direction can be considered the weak direction.

Further the gravity load design procedure determines modest dimensions of the columns, low quantitative of steel reinforcement and an irregular stiffness distribution in elevation.

These lead to a lower lateral stiffness and in a consistent difference between the stiffness of the two main directions, being the transverse direction more deformable than the longitudinal one.

Thus, two similar buildings designed according to different Codes but with the same masses, have different fundamental vibration period and this condition should to be valid also when the buildings reach the non-linear range.

In fact, in Old Code buildings the modest dimensions of the cross sections, the low percentage of steel reinforcement, the different mechanical characteristics of the materials determine a lower resistance and a higher deformability in the post elastic range.

The stairs, usually arranged along the transverse direction, have a stiffening effect that decrease with the height of the building. For low rise buildings (2 or floors) the fundamental vibration period for the transverse direction can be lower than those for the longitudinal direction.

Further, the stairs, which are usually placed in an eccentric position, often emphasize the irregular stiffness distribution provided by position in plan of the infill panels. These features may result in global torsional effects and brittle collapse.

The longitudinal direction, having parallel plane frames, is characterized from an increasing stiffness with the surface of the plan, because of increase also the number of both spans and parallel frames. The same is for the transverse direction, even if the stiffness increase less than the other direction because only the number of the spans in the perimetrical frames contributes to the increment.

Then the seismic behaviour of RCMF structures can be strongly affected by the presence of *masonry infill walls* especially in those cases in which the external walls are made with “strong” infill panels. Their influence was assessed from several authors (*Panagiotakos et al. 1995, Dolsek et al. 2008, Asteris 2012, Sattar et al. 2016*) and they can lead to either an increase or a decrease in seismic resources.

If the infill walls are arranged uniformly both in plant and elevation, and the building is not too tall, they increase the lateral stiffness and resistance of the whole structure and can both reduce the inter-storey drift demand and rise the overall resistance to horizontal actions.

Instead, an uneven distribution may have negative effects because of they cause irregularity of stiffness and strength, fostering the occurrence of unexpected behaviours and possibly increasing the seismic demand against sensitive zones where concentrations of stress and large ductility demands might prematurely cause collapse due to soft storey mechanism (*Dolsek et al. 2001, Verderame et al. 2011*).

Further, the sudden reduction of storey stiffness due to the damage of the infills during an earthquake can lead to the formation of an unexpected soft storey mechanism, which, due to the interaction with the joint damage, can occur not necessarily at the first floor and independently by the regular or irregular distribution of the infills along the elevation.

The infills can generate also dangerous local effects on the RC frame as:

- The plasticization of the extremities of columns for the presence of a considerable tension stresses due to infill (fig. 1.18).
- The local and brittle rupture of columns for the presence of irregular openings in the walls.

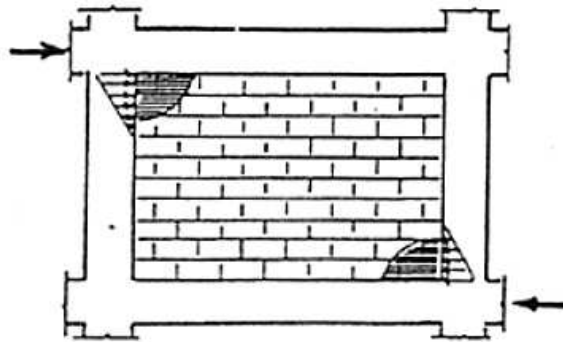


Figure 1.18. Local stresses on columns due to infill

Further, masonry infills could suffer heavy damage detaching from the frame (fig. 1.19) or rocking out of the plane (*Furtado et al. 2015 a-b*) and so becoming themselves dangerous for people.



Figure 1.19. Out of plane (left) and in-plane failure (right) of masonry infills

Given the high stiffness of the masonry infills, it is important to consider them also in structural modelling, because the elastic period of the building modelled without infills is very different to the one obtained experimentally by means in situ measurement of environmental vibrations. However, these vibrations have a very limited amplitude and so the building could be stiffer than when an earthquake occurs causing damage on the building. For these reasons the cracked stiffness of both concrete and masonry could be adopted when numerical simulations are performed.

References chapter 1

- Presidenza del Consiglio dei Ministri, Struttura di Missione Casa Italia. Rapporto sulla Promozione della sicurezza dai Rischi naturali del Patrimonio abitativo, June 2017.
- Belleri A., Brunesi E., Nascimbene R., Pagani M., and Riva P., “Seismic Performance of Precast Industrial Facilities Following Major Earthquakes in the Italian Territory,” *J. Perform. Constr. Facil.*, vol. 29, no. 5, p. 4014135, Oct. 2015.
- Magliulo G., Ercolino M., Petrone C., Coppola O., and Manfredi G., “The Emilia Earthquake: Seismic Performance of Precast Reinforced Concrete Buildings,” *Earthq. Spectra*, vol. 30, no. 2, pp. 891–912, May 2014.
- Stucchi et al., Seismic Hazard Assessment (2003–2009) for the Italian Building Code, *Bulletin of the Seismological Society of America*, Vol. 101, No. 4, pp. 1885–1911, August 2011
- Priestley, M. J. N. (1997). Displacement-Based seismic assessment of reinforced concrete buildings. *Journal of Earthquake Engineering*, 1, 157-192.
- Sullivan T.J. The limitations and performances of different displacement based design methods. *Journal of Earthquake Engineering* 7(sup001):201-241. 2003.
- Ministro dei Lavori Pubblici e dei Trasporti, “DM 14/01/2008 – NTC - Norme tecniche per le costruzioni (in Italian),” *Suppl. Ordin. Gazz. Uff. n. 29*, 2008.
- “Ordinanza del Presidente del Consiglio dei Ministri (OPCM). General criteria for the seismic classification of the national territory and technical standards for constructing in seismic zones. Ordinance no. 3274, G.U. n. 72 del 8–5-2003 (in Italian).” 2003.
- Santarella, L. (1968), "Il cemento armato – Le applicazioni alle costruzioni civili ed industriali", II volume, Edizione Hoepli.
- Pagano, M. (1968) *Teoria degli edifici – Edifici in cemento armato*, Edizione Liguori, Napoli (in Italian).

- Regio Decreto 16/11/1939 n. 2229, "Norme per la esecuzione delle opere in conglomerato cementizio semplice ed armato".
- Legge 5/11/1971 n. 1086, "Norme per la disciplina delle opere in conglomerato cementizio armato, normale e precompresso ed a struttura metallica".
- Manfredi G. et al. Preliminary analysis of a soft-storey mechanism after the 2009 L'Aquila earthquake. *Earthquake Engng Struct. Dyn.* (2010).
- Ricci P., De Luca F., Verderame G.M. 6th April 2009 L'Aquila earthquake, Italy — Reinforced concrete building performance. *Bulletin of Earthquake Engineering* 2010.
- Manfredi G. et al. 2012 Emilia earthquake, Italy: reinforced concrete buildings response. *Bulletin of Earthquake Engineering* October 2014, Volume 12, Issue 5, pp 2275–2298.
- Fardis M.N. Experimental and numerical investigations on the seismic response of RC infilled frames and recommendations for code provisions. Report ECOEST-PREC8 No 6. Prenormative research in support of Eurocode 8, 1997.
- Masi A. (2003). Seismic vulnerability assessment of gravity load designed R/C frames, *Bulletin of Earthquake Engineering*, Vol. 1, N. 3, pp. 371-395.
- Magliulo G. et al. Seismic response of three-dimensional r/c multi-storey frame building under uni- and bi-directional input ground motion. *Earthquake Engng Struct. Dyn.* 2007; 36:1641–1657.
- Makarios et al. Numerical Investigation of Seismic Behavior of Spatial Asymmetric Multi-Storey Reinforced Concrete Buildings with Masonry Infill Walls. *The Open Construction and Building Technology Journal*, 2012, 6, (Suppl 1-M8) 113-125.
- Mohammad et al. Seismic performance of older R/C frame structures accounting for infills-induced shear failure of columns. *Engineering Structures*, 122 (2016), 1-13.
- Hakuto, S, Park, R and Tanaka, H, Seismic Load Tests on Interior and Exterior Beam- Column Joints with Substandard Reinforcing Details, *ACI Structural Journal*, 97(1), 2000, 11-25

- Braga et al. R/C Existing Structures with Smooth Reinforcing Bars: Experimental Behaviour of Beam-Column Joints Subject to Cyclic Lateral Loads. *The Open Construction and Building Technology Journal* 3(1):52-67. May 2009.
- Di Ludovico M. et al. Cyclic Behavior of Nonconforming Full-Scale RC Columns. *Journal of Structural Engineering* Volume 140 Issue 5 - May 2014.
- Pinto A, Verzeletti G, Molina J, Varum H, Pinho R, Coelho E (1999) Pseudo-dynamic tests on non-seismic resisting RC frames (bare and selective retrofit frames). Joint Research Centre, Ispra.
- Calvi G.M., Magenes G., Pampanin S., Experimental Test on a Three Storey Reinforced Concrete Frame Designed for Gravity Only, 12th European Conference on Earthquake Engineering, paper n.727, London 2002.
- Albanesi T., Biondi S., Candigliota E., Le Maout, A. and Nuti, C. (2008), “Seismic full-scale test son a 3D infilled RC frame”, Proceedings of 14th WCEE, CD-ROM, Beijing, China.
- Park P., Paulay T., 1975. Reinforced Concrete Structures, Wiley. CEN (Comité Européen de Normalisation), “Eurocode 8: Design of structures for earthquake resistance – Part 1: General rules, seismic actions and rules for buildings (EN 1998-1)” 2004.
- Dolce M., Martinelli A. Inventario e vulnerabilità degli edifici pubblici e strategici dell’Italia centro-meridionale, Vol. II - Analisi di vulnerabilità e rischio sismico, INGV/GNDT, L’Aquila, 2005.
- Dolce M., Moroni C., 2005. La valutazione della vulnerabilità e del rischio sismico degli edifici pubblici mediante le procedure VC e VM. Progetto SAVE, Atti di Dipartimento N. 4/2005
- Penelis G.G., Kappos A.J., Earthquake Resistant concrete structures, E&F Spon, London, 1997.
- Panagiotakos T.B. and Fardis M.N., (1996), “Seismic response of infilled RC frames structures”, 11th World Conference on Earthquake Engineering, paper 225.

- Dolšek M. and Fajfar P., (2008), “The effect of masonry infills on the seismic response of a four storey reinforced concrete frame - A deterministic assessment”, *Engineering Structures*, 30(11), 1991-2001.
- Asteris P., & Cotsovos D. (2012). Numerical investigation of the effect of infill walls on the structural response of RC frames. *The Open Construction and Building Technology Journal*, 6 (Suppl 1-M11), 164-181.
- Sattar S., Liel A.B. (2016) Seismic Performance of Nonductile Reinforced Concrete Frames with Masonry Infill Walls—II: Collapse Assessment. *Earthquake Spectra*: May 2016, Vol. 32, No. 2, pp. 819-842.
- Dolšek M., Fajfar P., (2001). “Soft storey effects in uniformly infilled reinforced concrete frames”, *Journal of Earthquake Engineering*, 5(1), 1-12.
- Verderame G.M., De Luca F., Ricci P. and Manfredi G., (2011), “Preliminary analysis of soft-storey mechanism after the 2009 L'Aquila earthquake”, *Earthquake Engineering and Structural Dynamics*, 40, 925-944.
- Furtado et al. 2015. Influence of the in Plane and Out-of-Plane Masonry Infill Walls’ *Procedia Engineering*. Interaction in the Structural Response of RC Buildings. Volume 114, 2015, 722-729.
- Furtado et al. 2015. Experimental Characterization of the In-plane and Out-of-Plane Behaviour of Infill Masonry Walls. Volume 114, 2015, 862-869.

Chapter 2

2. Methods for seismic vulnerability assessment of buildings

The seismic vulnerability of a building is the susceptibility to suffer damage due an earthquake of a certain intensity. From this definition born the need to establish a correlation able to provide the expected damage level for each intensity level, identifying appropriate damage and intensity measure parameters.

Several possibilities exist to choose the parameters and a lot of the methods, different in purposes and procedures, are available to explicit this relationship. Further, the latter can be obtained from both a deterministic or probabilistic approach.

The criteria to classify the methods for vulnerability assessment are shown in tab. 2.1.

Table 2.1. Seismic vulnerability assessment methods

Metodology classification	Types of techniques	Description
ON THE BASE OF THE TYPE OF RESULT	<i>Direct</i>	They provide the result as a forecast of the estimated damage.
	<i>Indirect</i>	They first determine a vulnerability index (V) and then they use a relationship intensity-damage that is function also of V.
	<i>Conventional</i>	They are heuristic. According to several criteria they allow to assign an index V, they don't associate a forecast of the damage and they are useful to compare building located in area with different seismic hazard level.
ON THE VASE OF THE TYPE OF MEASURE	<i>Quantitative</i>	They provide the result (damage) in a numerical form (probabilistic or deterministic).
	<i>Qualitative</i>	They sue descriptions in terms of qualitative levels (low, medium, high).
ON THE BASE OF THE TYPE OF ELABORATION	<i>Statistical</i>	They research the result by means the statistical elaboration of the observed data, in particular those of damage and vulnerability observed after earthquakes.
	<i>Modelling</i>	They research the result by means the study of the seismic response.

	<i>Expertise</i>	They are based on the judgment of experts.
	<i>Hybrid</i>	They combine more techniques.
ON THE BASE OF THE WAY OF CONCEPTION OF THE STRUCTURAL SYSTEM	<i>Typological</i>	They differentiate the seismic behaviour of buildings by assuming typological classes in function of the quality of materials, of the constructive techniques etc. They need of a modest effort and thus they are suitable to be used for large scale assessment.
	<i>Semeiotics</i>	They consider the buildings as organisms in which the vulnerability (V) can be described through the observation of some behavioral symptoms, that are translated into parameters affecting with different weights the vulnerability. They need of a certain expertise in the data detecting, that can use also for other purposes.
	<i>Mechanistic</i>	They need to model the seismic response of the buildings as realistic as possible. They are useful to assess a single building or few buildings of the same typology. They can support the other techniques in order both to transfer on single buildings the results for typological classes and to validate the attribution of the vulnerability levels through the behaviour factors.

One of the more complete criteria considers several techniques: direct, indirect and conventional (*Corsanego and Petrini 1994*). Direct techniques are subdivided in typological and mechanical, while the indirect ones are an evolution of the conventional methods. Hybrid techniques merge elements come from two or more techniques above cited.

In direct methods, the correlation is directly found, while in the indirect ones a vulnerability index is first calculated and then the correlation is found.

Direct methods provide an absolute vulnerability, that are vulnerability functions representing the mean damage on the seismic intensity, or probability conditional distributions of the occurrence of a certain damage level given the seismic intensity. The latter represent Damage Probability Matrices – DPMs (fig. 2.1 – a) (*Whitman et al. 1974*), if a discrete intensity measure is used, or fragility curves (fig. 2.1 – b), if the seismic parameter is continuous.

Fragility curves are cumulative probability functions that can obtained through analytical or empirical procedure.

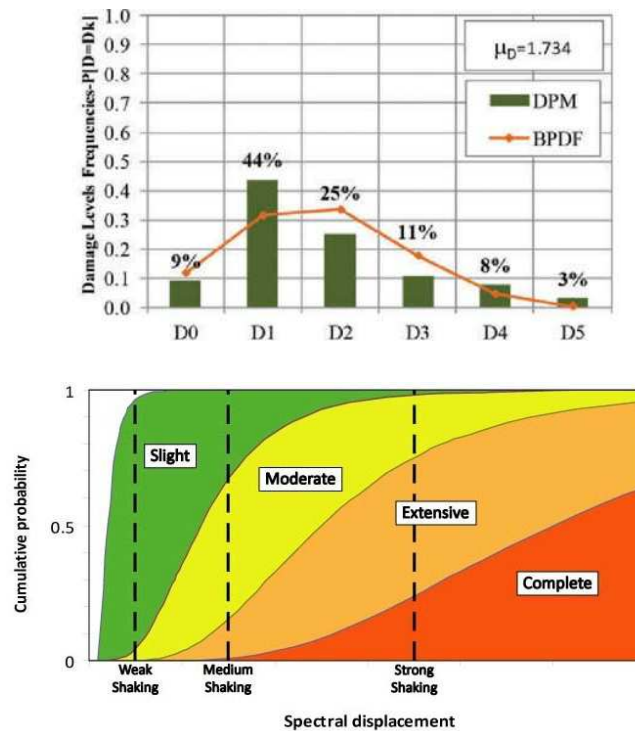


Figure 2.1. (left) DPM for damage levels of EMS-98 scale; (right) fragility curves for damage states

Indirect methods provide a relative vulnerability, that is vulnerability indices obtained empirically or experimentally. After that a relation between indices and damage expected for the intensity levels can be found.

Direct typological methods usually are based on real experiment of strong earthquakes, whose data on damage are processed through statistical regressions in order to obtain DPMs for a limited number of building categories. Therefore, they are empirical methods and their application requires a census of the main qualitative parameters that allow to classify the buildings according to defaults types, to each of them can be associated a BTM (Building Typology Matrix).

The BTMs, like the DPMs, directly provides the conditional probability (P) to reach a certain damage level (D) once individuated the typological class (T) and for a given intensity level (I):

$$P [d | T, I]$$

In Italy, the first empirical DPMs were developed in the 1980 after the Irpinia earthquake (Braga *et al.* 1982).

As the available data are often limited and do not concern all the building typologies and all the intensities that it would be necessary to represent in a model, the probabilistic processing of the observed data, at the root of observational methods, is supported or completely replaced by other approaches such as expert judgement (ATC-13 1987), neural network system (Dong *et al.* 1988) or Fuzzy Set Theory (Sanchez-Silva *et al.* 2001).

Recently, methods based on the EMS-98 macroseismic scale (*Grunthal et al. 1998*) are widely used for rapid vulnerability assessment on large scales (i.e. urban, regional or national scale).

Direct typological methods provide a good robustness in statistical terms, but on the other side they can't provide plausible results for the single building.

Direct mechanical techniques are based on numerical analyses with different complexity, performed on a single building or on a category of buildings.

The application of mechanical techniques requires a cataloguing of constructions, which includes their mechanical characteristics, and identifying the structural type of each construction. The results of the evaluations are then processed by means of statistical procedures whose result consists in the determination of the level of damage expected for a single construction or for a single category.

Between the analytical methods, those based on the Capacity Spectrum procedure (*Freeman 1998, Fajfar 1996*) are widely used in risk assessment framework such as the HAZUS (*FEMA 1999*) and Risk UE (*Milutinovic et al. 2003*) methods.

Indirect conventional techniques are based on virtual experiments of experts (expert judgment) with statistical processing of the data. The result is a conventional score (vulnerability index) attributed to a construction or a category by assessing the factors which govern the seismic response. The application of these techniques requires a field survey, sometime performed in a rapid or simplified way, of typological, structural, geometric, constructive characteristics. Some of these methods are the Rapid Visual Screen - RVS method provided by (*ATC-21 1988*) and the 2nd level GNDT method provided in the first form by (*Benedetti and Petrini 1989*).

The hybrid techniques combine the previous techniques in order to obtain the methods more complete and reliable. In fact, it can happen that there is a lack of data relative to the damage observed for certain levels of macroseismic intensity then it is possible to integrate the empirical data with those from non-linear analysis of representative structural models (*Kappos et al. 2016*). In the same way, data from expert judgment may be supported by more detailed numerical evaluations as in RE.S.I.STO method (*Savoia et al. 2013*).

Some papers (*Calvi et al. 2006, Lumantarna et al. 2014*) provide a more depth description of the several methods available for seismic vulnerability assessment of existing RC buildings.

Generally, the choice of the methods depends on the number of buildings to analyse. When a single or few buildings have to be assessed, it should be carried out *mechanical models*, that take into account the non-linear behaviour of structural elements (i.e. lumped inelastic hinges or spread plasticity models) and numerical analyses (i.e. non-linear static or dynamic analysis). While in the case the assessment of a large amount of buildings is request, numerical models could be too expansive to develop, thus it is preferable to adopt more rapid methods such as the macroseismic ones or those base on the expert judgment.

It is particularly interesting to apply the different methods of estimation of seismic vulnerability in order to grasp similarities and weaknesses of each method, taking as reference the detailed analysis performed on nonlinear models that are more reliable.

The development of methods for seismic vulnerability assessment that have a precise validity, providing a reliable estimate on single building rather than an estimate in statistical sense, requires careful verification of the reliability of the results.

This is because the application of these methods was born usually from the need to compare the conditions of risk for different buildings in different sites, thus they can be ordered in a ranking of risk to perform the mitigation policies through the intervention on individual buildings with special features, rather than sets of buildings with common characteristics.

Assessments, therefore, must be reliable not merely in conservative sense, as it is usually required for the methods of analysis for the design and verification of structural safety, but estimating the most likely value of the earthquake resistance and of the action that can determine the limit conditions for the structure

In the following part of the chapter is illustrated a brief description of the several methods available in the literature and in the practice.

2.1. Rapid methods

The use of rapid methods become important when many buildings have to be assessed and the available resources are limited. These methods usually assign a vulnerability class (macroseismic methods) to the buildings on the base of the knowledge of few structural characteristics such as the type of the vertical structure, type of floor slabs etc.

The vulnerability index method is more expansive because accounts for more details, but it is at the same time a rapid method for large scale vulnerability assessment.

Thus, rapid methods allow to compare the vulnerability levels between the buildings belonging to the stock and so to develop a ranking in order to prioritize the risk mitigation interventions.

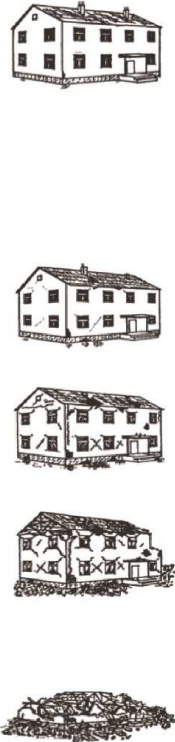
Although the results for the individual building cannot be considered reliable in the strict sense, because they are not obtained from sophisticated analyses that take adequately into account the structural characteristics and materials used (but are much more expensive in terms of time and costs because they require carrying out in situ investigations), for a comparative evaluation can be considered more than enough. In fact, the uncertainties inherent the adopted model are the same for all the buildings, then in a certain sense they cancel and what remains are the differences between buildings.

This is even more valid if a collection of buildings belonging to the same type is analyzed, as in the case of RC school buildings, whose characteristics are common and well defined.

2.1.1. *Macroseismic methods*

The basic concept of a macroseismic method is that if the aim of a macroseismic scale is the measure of an earthquake severity, from the observation of the damage suffered by the buildings, it can, in the same way, represent, for forecast purposes, a vulnerability model able to supply the probable damage distribution for a given intensity.

Therefore, typological recognition (from an appropriate inventory of buildings) leads to the assignment of a vulnerability class of and, therefore, the estimation of the expected damage with the variation of the macroseismic intensity. The latter can be represented according to different scales occurred over time such as the MSK (*Medvedev 1965, 1977*), MCS, MM, EMS-98 (*Grunthal 1999*) (fig.2.2).

EMS-98 Intensity	Felt	Impact	Magnitude (Approximat Value)	Building Damage (Masonry)
I	Not felt	Not felt	2	
II-III	Weak	Felt indoors by a few people. People at rest feel a swaying or light trembling.		
IV	Light	Felt indoors by many people, outdoors by very few. A few people are awakened. Windows, doors and dishes rattle.	4	
V	Moderate	Felt indoors by most, outdoors by few. Many sleeping people wake up. A few are frightened. Buildings tremble throughout. Hanging objects swing considerably. Small objects are shifted. Doors and windows swing open or shut.		
VI	Strong	Many people are frightened and run outdoors. Some objects fall. Many houses suffer slight non-structural damage like hair-line cracks and falling of small pieces of plaster.	5	
VII	Very strong	Most people are frightened and run outdoors. Furniture is shifted and objects fall from shelves in large numbers. Many well-built ordinary buildings suffer moderate damage: small cracks in walls, fall of plaster, parts of chimneys fall down; older buildings may show large cracks in walls and failure of in-fill walls.		
VIII	Severe	Many people find it difficult to stand. Many houses have large cracks in walls. A few well built ordinary buildings show serious failure of walls, while weak older structures may collapse.	6	
IX	Violent	General panic. Many weak constructions collapse. Even well built ordinary buildings show very heavy damage: serious failure of walls and partial structural failure.		
X+	Extreme	Most ordinary well built buildings collapse, even some with good earthquake resistant design are destroyed.	7	

© Swiss Seismological Service

Figure2.2. EMS-98 scale

Vulnerability classes are a way to group several buildings characterized by a similar behaviour with regard to the earthquake and to each one is associated a relationship between earthquake intensity and suffered damage. The definition of vulnerability classes has significantly improved in recent years, thanks to the development of the scale EMS-98 to facilitate and improve the macroseismic survey (after earthquake) for the evaluation of the local intensity. In addition to improving the attributions of the traditional buildings, highlighting however the inevitable uncertainties in the attributions, includes in the classification even buildings designed or retrofitted with seismic criteria, by extending the range of classes from the 3 (A, B, C) of the MSK scale to 6 (A, B, C, D, E, F) as shown in fig. 2.3.

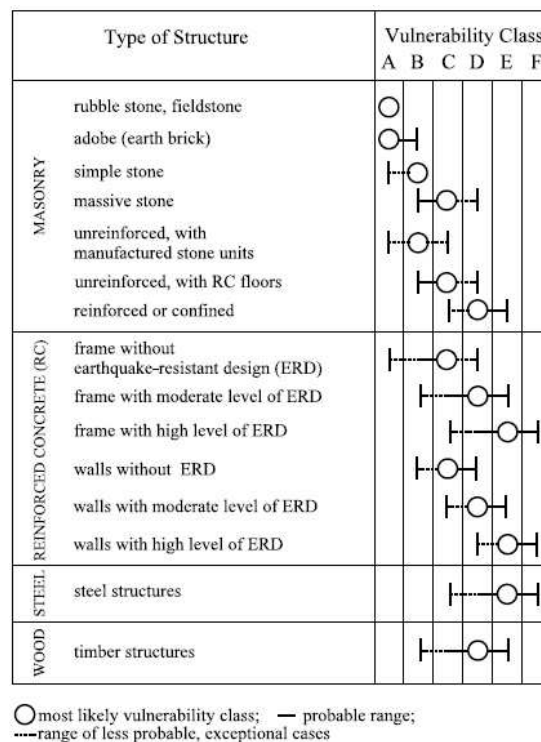


Figure 2.3. EMS-98 scale: correlation between structural typologies and vulnerability classes

The building typologies are identified on the base of the type of vertical structure by distinguishing between masonry, RC, wood and steel structure, and accounting for several earthquake design levels.

However, there are still large and unavoidable margins of judgment in the attribution of individual buildings or structural types at different vulnerability classes, as is suggested a most likely class and a range of possible classes for take into account the differences in behaviour that it may have even within the same structural typology.

It is evident that the uncertainty related to this assignment are strongly linked, on the one hand, to the general information of an international macroseismic scale, that must to be valid in areas also

profoundly different; secondly, to the purposes of the definition of classes, linked to the macroseismic assessment of the intensity of a seismic event.

In the EMS-98 scale the damage is represented in discrete form through five levels of damage (fig. 2.4), plus the situation of no damage.






DS1	DS2	DS3	DS4	DS5
				
Grade 1: Negligible to slight damage (no structural damage, slight non-structural damage)	Grade 2: Moderate damage (slight structural damage, moderate non-structural damage)	Grade 3: Substantial to heavy damage (moderate structural damage, heavy non-structural damage)	Grade 4: Very heavy damage (heavy structural damage, very heavy non-structural damage)	Grade 5: Destruction (very heavy structural damage)
Fine cracks in plaster over frame members or in walls at the base. Fine cracks in partitions and infills	Cracks in columns and beams of frames and in structural walls. Cracks in partition and infill walls; fall of brittle cladding and plaster. Falling mortar from the joints of wall panels	Cracks in columns and beam column joints of frames at the base and at joints of coupled walls. Spalling of concrete cover, buckling of reinforced rods. Large cracks in partition and infill walls, failure of individual infill panels	Large cracks in structural elements with compression failure of concrete and fracture of rebars; bond failure of beam reinforced bars; tilting of columns. Collapse of a few columns or of a single upper floor	Collapse of ground floor or parts (e. g. wings) of buildings

Figure 2.4. EMS-98 scale: correlation between structural typologies and vulnerability classes

These damage conditions relate to the physical damage, combination of structural and non-structural damage (infills, partitions, finishes, etc.). In the first two levels the structural damage is absent or very slight, while in the higher levels it predominates over judgment. Damage data collected after earthquakes in Campania/Basilicata (1980), Abruzzo (1984), Umbria-Marche (1997), Lunigiana and Garfagnana (1995) and Lazio (1999) have shown that average damage distributions following these events are well approximate from the binomial probability distribution (eq.1.1) defined by the only free parameter d (medium damage) ranged between 0 and 1:

$$p_k = \frac{5!}{k!(5-k)!} d^k (1-d)^{5-k} \quad (2.1)$$

where p_k is the probability to have a damage level D_k , with $K = 0, \dots, 5$.

The parameter d , if multiplied by five, represents the centroid abscissa μ_D of the histogram of the damage distribution, named *medium damage*, obtained also by eq. 1.2:

$$\mu_D = \sum_{K=0}^5 p_K D_K \quad (2.2)$$

with $0 \leq \mu_D \leq 5$.

Therefore, with the only medium damage it is possible to describe the whole damage distribution for each vulnerability class and each intensity level.

The information about the damage provided by the EMS-98 scale are grouped, for each vulnerability class, in the DPM that bring back the quantity of buildings damaged for a given seismic intensity and a certain damage level. Being the purpose of the EMS-98 scale the macroseismic survey in the post-earthquake, to express the quantity of damaged buildings it does not foresee an exact definition of the quantities but there are used linguistic terms (tab. 2.2): "few", "many", "most", to which percentage intervals are associated.

Table 2.2. Linguist frequencies of damage in the EMS-98 scale

<i>Dk/I</i>	0	1	2	3	4	5
<i>V</i>		Few A or B				
<i>VI</i>		Many A or B, Few C	Few A or B			
<i>VII</i>			Many B, Few C	Many A, Few B	Few A	
<i>VIII</i>			Many C, Few D	Many B, Few C	Many A, Few B	Few A
<i>IX</i>			Many D, Few E	Many C, Few D	Many B, Few C	Many A, Few B
<i>X</i>			Many E, Few F	Many D, Few E	Many C, Few D	Most A, Many B, Few C
<i>XI</i>			Many F	Many E, Few F	Most C Many D, Few E	Most B, Many C, Few D
<i>XII</i>						All A or B, Nearly All C, Most D or E or F

Then such matrixes are vague but also incomplete, because there is not information for some damage levels and for certain intensities, the scale considering only the most representative and easily observable situations.

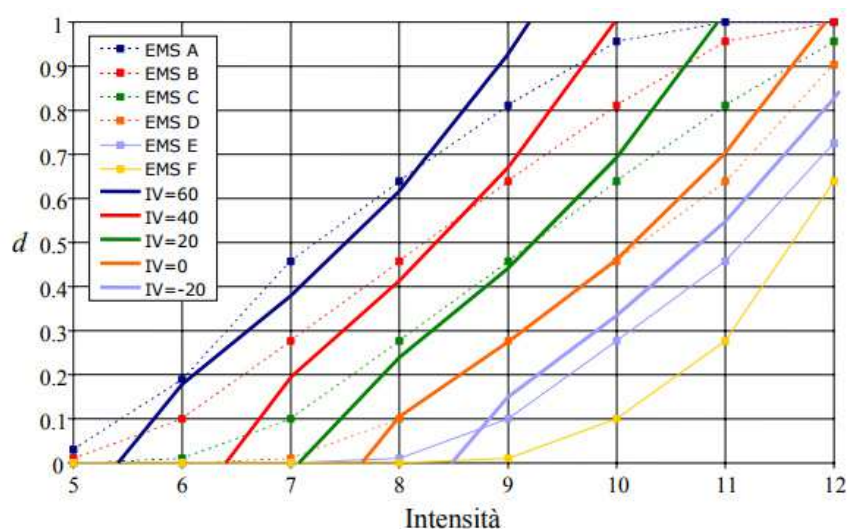
The information about the damage has been completed adopting the binomial distribution, translating the linguistic quantities in numerical values and assuming the medium percentage of the corresponding interval (few ones: 5 %, many people: 35 %, the most part: 80 %).

Then the values of the parameter d (binomial coefficients) have been estimated for each vulnerability class by varying of the macroseismic intensity (tab. 2.3).

Table 2.3. Values of the binomial coefficient for the vulnerability classes by varying the macroseismic intensity

Intensity	V	VI	VII	VIII	IX	X	XI	XII
Class A	0.03	0.190	0.457	0.639	0.811	0.957	1.000	1.000
Class B	0.0105	0.1	0.277	0.457	0.639	0.811	0.957	1.000
Class C	0	0.0105	0.1	0.277	0.457	0.639	0.811	0.957
Class D	0	0	0.0105	0.1	0.277	0.457	0.639	0.903
Class E	0	0	0	0.0105	0.1	0.277	0.457	0.725
Class F	0	0	0	0	0.0105	0.1	0.277	0.639

The vulnerability curves obtained have been then compared to those from the II level GNDT method (*GNDT 1994*). The results have shown how the trend of different families of curves is analogous and how between them a good correspondence exists (fig.2.4).

**Figure 2.4.** Comparison between damage curves from the 2nd level GNDT method and those relative to EMS-98 scale

The comparison shows that to the class A (the greater vulnerability) corresponds a $I_v = 60$, while the class C (in example representative of concrete buildings), has a $I_v = 20$. Tab. 2.4 shows the correspondence between the EMS-98 classes and vulnerability index (I_v) of the GNDT method.

Table 2.4. Relationship between vulnerability classes of the EMS-98 and vulnerability index

Classe EMS-98	A	B	C	D	E
Indice di vulnerabilità I_v	60	40	20	0	-20

In (Lagomarsino *et al*, 2004) the average damage has been obtained in a parametric way, by introducing a typological vulnerability index V_i whereby analytically estimate the expected average damage. The matrices of EMS-98 scale were completed and translated in terms of numbers by using an approach probabilistic -fuzzy and the resulting DPMs express a statistical correlation between the macroseismic intensity and apparent damage. In particular, for the completion of the matrices a discrete probability distribution of the damage, (derived from the continues β distribution) was used (eq.2.3), because there are 5 damage levels plus the no damage:

$$p_{\beta}(x) = \frac{\Gamma(t)}{\Gamma(r)\Gamma(t-r)} \frac{(x-a)^{r-1}(b-x)^{t-r-1}}{(b-a)^{t-1}} \quad (2.3)$$

with $a \leq x \leq b$.

In this case it is advisable to assign value 0 to the parameter a and value 6 to the parameter b . The parameter t affects the scatter of the distribution and if $t = 8$ is used, the beta distribution looks very similar to the binomial distribution.

Numerical translation was performed using the Fuzzy theory, under which quantitative definitions can be interpreted with the membership function X (fig. 2.5) that defines the membership of a certain parameter to a specific collection and it takes values between 0 and 1.

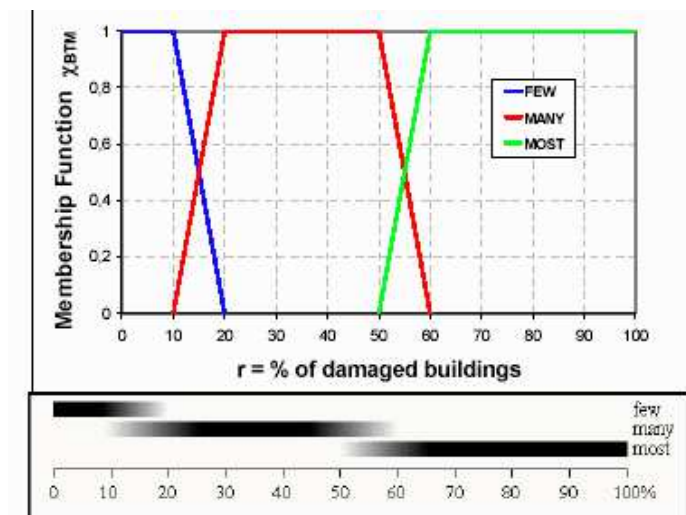


Figure 2.5. Membership function X of the damaged buildings in the linguistic terms

The percentage of damaged buildings corresponding to the term "few" is less than 10%, the one corresponding to the term "many" is between 20% and 50%, the one related to the term "most" is more than 60%. As noted in fig.2.6, there are situations in which terms overlap, for example

between 10% and 20% can be defined as both few and many, between 50% and 60% as both many and most.

To represent the membership of a building to a vulnerability class, a conventional vulnerability index (V_i) was introduced, determined according to a typological and semeiotic approach. In fact, defined the typological class of the building considered within to the Building Typology Matrix (BTM), which is representative of the European constructed, can be immediately assigned the vulnerability index that is characteristic of that particular type of building.

The values of these indices represent a measure of the fragility of the construction with respect earthquake and for simplicity it was chosen the range between 0 - 1: values close to 1 are assumed by more vulnerable constructions, those close to 0 are instead representative of an advanced seismic design.

According to fuzzy theory, these indices have a possible range ($X = 1$) and an unlikely one representative of the transition between two adjacent classes (fig.2.6).

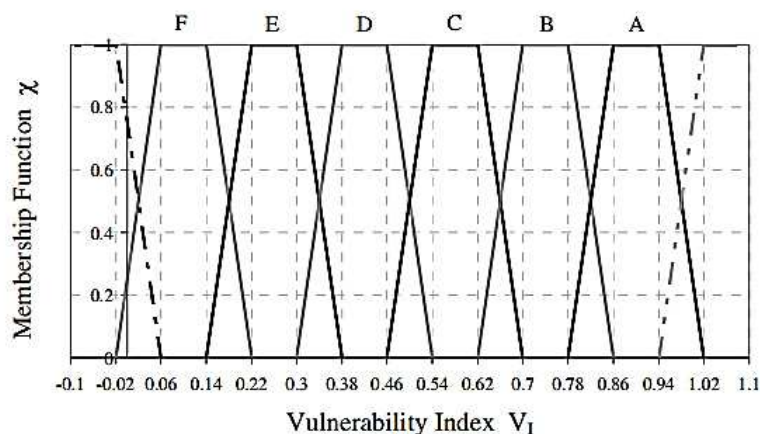


Figure 2.6. Vulnerability index membership functions for EMS-98 vulnerability classes

In tab. 2.5 the values of V_i are shown for each class.

Table 2.5. V_i values for the EMS-98 vulnerability classes

	V_{Imin}^c	V_I^{c-}	V_I^{c*}	V_I^{c+}	V_{Imax}^c
A	1.02	0.94	0.9	0.86	0.78
B	0.86	0.78	0.74	0.7	0.62
C	0.7	0.62	0.58	0.54	0.46
D	0.54	0.46	0.42	0.38	0.3
E	0.38	0.3	0.26	0.22	0.14
F	0.22	0.14	0.1	0.06	-0.02

At this point, vulnerability classes have been assigned to typological classes. The EMS-98 scale describes the different typologies belonging to vulnerability classes by means the language terms "most likely class", "probable class", "unlikely class" (tab. 2.6).

Table 2.6. Correspondence between vulnerability and typological classes according to the fuzzy definition

Typologies		Building type	Vulnerability Classes					
			A	B	C	D	E	F
Masonry	M1	Rubble stone	■					
	M2	Adobe (earth bricks)	■	■				
	M3	Simple stone	■	■	■			
	M4	Massive stone	■	■	■	■		
	M5	Unreinforced M (old bricks)	■	■	■	■	■	
	M6	Unreinforced M with r.c. floors	■	■	■	■	■	■
	M7	Reinforced or confined masonry	■	■	■	■	■	■
Reinforced Concrete	RC1	Frame in r.c. (without E.R.D)	■	■	■	■	■	■
	RC2	Frame in r.c. (moderate E.R.D.)	■	■	■	■	■	■
	RC3	Frame in r.c. (high E.R.D.)	■	■	■	■	■	■
	RC4	Shear walls (without E.R.D)	■	■	■	■	■	■
	RC5	Shear walls (moderate E.R.D.)	■	■	■	■	■	■
	RC6	Shear walls (high E.R.D.)	■	■	■	■	■	■
Stell	S	Steel structures	■	■	■	■	■	■
Tiber	W	Timber structures	■	■	■	■	■	■

Situations: ■ Most probable class; ■ Possible class; ■ Unlikely class (exceptional cases)

Again, fuzzy theory has been used to interpret language terms. Therefore, the membership of each typology to a vulnerability class is represented by determining the most probable class (Most probable class $X = 1$), the probable (Possible class $X = 0.6$) and the exceptional case (Unlikely class $X = 0.2$). The probabilities of belonging to each vulnerability class are shown in tab. 2.7.

Table 2.7. Correspondence between vulnerability and typological classes in terms of probabilities

Ti	Vulnerability classes Cj						
	Y	A	B	C	D	E	F
M1	4.5	91	4.5				
M2	4.5	73	22.5				
M3		9	86.5	4.5			
M4			22.5	68.5	9		
M5		9	82	9			
M6			22.5	68.5	9		
M7				9	68.5	22.5	
RC1		9	22.5	59.5	9		
RC2			9	22.5	46	22.5	
RC3				9	22.5	46	22.5
RC4			9	68.5	22.5		
RC5				9	68.5	22.5	
RC6					9	68.5	22.5
S				9	22.5	46	22.5
T			9	22.5	46	22.5	

It is thus possible to define the membership function to each typology (fig.2.7) as a linear combination of the membership functions to the individual vulnerability classes, each considered with their own degree of membership.

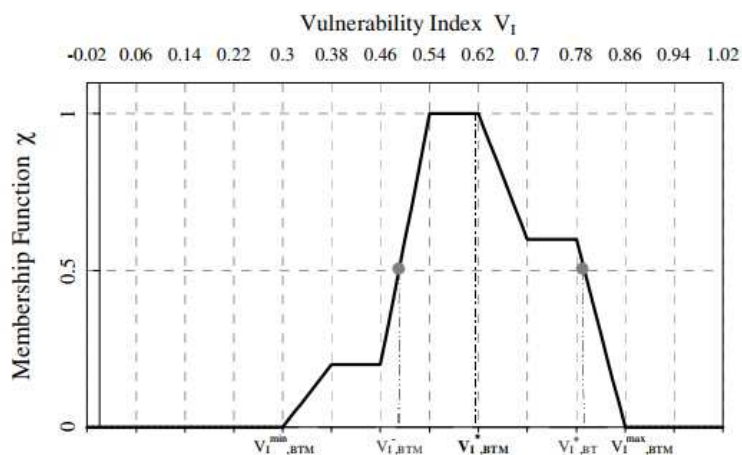


Figure 2.7. Vulnerability index membership functions for an EMS-98 vulnerability typology

From the membership function, five values of the typology vulnerability index V_I can be obtained (tab. 2.8), representing respectively:

- the most probable value V_I^* , calculated as the centroid of the membership function;
- the lower bound V_I^- and upper bound V_I^+ of the uncertainty range, corresponding to the abscissa for a value of the function equal to 0.5;
- and the values $V_{I,MIN}$ and $V_{I,MAX}$ corresponding to the boundaries of unlikely values.

Table 2.8. V_I values for the building typologies

Typologies		Building type	□ulnerabilità Classes				
			$V_{I,min}$	V_I^-	V_I^*	V_I^+	$V_{I,max}$
Masonry	M1	Rubble stone	0.62	0.81	0.873	0.98	1.02
	M2	Adobe (earth bricks)	0.62	0.687	0.84	0.98	1.02
	M3	Simple stone	0.46	0.65	0.74	0.83	1.02
	M4	Massive stone	0.3	0.49	0.616	0.793	0.86
	M5	Unreinforced M (old bricks)	0.46	0.65	0.74	0.83	1.02
	M6	Unreinforced M with r.c. floors	0.3	0.49	0.616	0.79	0.86
	M7	Reinforced or confined masonry	0.14	0.33	0.451	0.633	0.7
Reinforced Concrete	RC1	Frame in r.c. (without E.R.D)	0.3	0.49	0.644	0.8	1.02
	RC2	Frame in r.c. (moderate E.R.D.)	0.14	0.33	0.484	0.64	0.86
	RC3	Frame in r.c. (high E.R.D.)	-0.02	0.17	0.324	0.48	0.7
	RC4	Shear walls (without E.R.D)	0.3	0.367	0.544	0.67	0.86
	RC5	Shear walls (moderate E.R.D.)	0.14	0.21	0.384	0.51	0.7
	RC6	Shear walls (high E.R.D.)	-0.02	0.047	0.224	0.35	0.54
Stell	S	Steel structures	-0.02	0.17	0.324	0.48	0.7
Tiber	W	Timber structures	0.14	0.207	0.447	0.64	0.86

An analytical vulnerability curve of is then defined, which, depending on the seismic intensity, allows to estimate the degree of the average damage μ_D (eq. 2.4):

$$\mu_D = 2.5 \left[1 + \tanh\left(\frac{I+6.25 V_I-13.1}{2.3}\right) \right] \quad (2.4)$$

where the value of 2.3 to denominator represents the ductility index (Q), constant for all building types.

Eq. 2.4 was obtained by interpolation of the vulnerability curves relative to the DPMs calculated by means the beta-discrete distribution.

The value of the macroseismic vulnerability index V_1 affects the horizontal position of the curve, while the value of the ductility index is representative of the structural ductility and acts on the slope of the curve. So higher values of V_1 (greater vulnerability) shift the curve to the left, producing greater damage to the same degree of macroseismic intensity, while higher Q values make the curves less steep, thus reducing the rate of increase in damage by increasing the intensity.

The eq. is calibrated in such a way that, fixing the values of V_1 and Q , an increment of the macroseismic intensity equal to 1 corresponds to an increment of μ_d equal to 1.

The average damage curves for the 6 vulnerability classes of the EMS-98 scale, the so-called “isovulnerability curves” (because each one refers to a specific value of V_c^*), are reported in Figure 2.8.

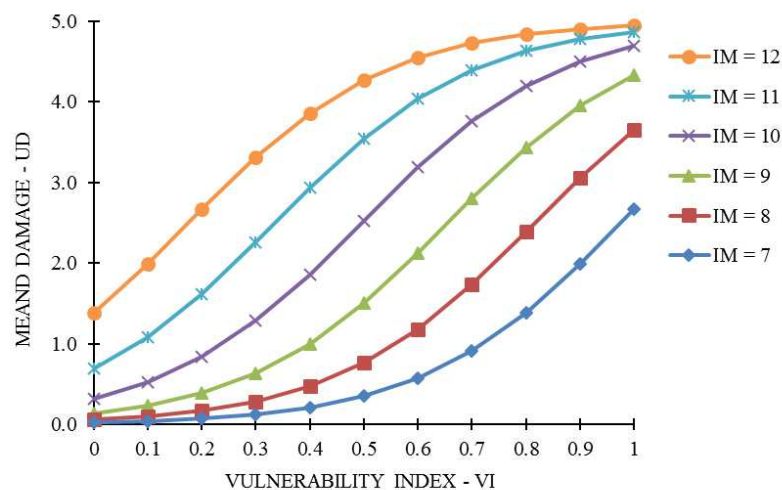


Figure 2.8. Isovulnerability curves for the 6 vulnerability classes of the EMS-98 scale

An alternative representation of the expected damage is that illustrating the variation of the average damage as a function of the macroseismic vulnerability index V_i , which range between -0.02 and 1.02. In this case, we have the macroseismic isointensity curves of fig.2.9, whose allow to determine the expected damage for any value of V_i .

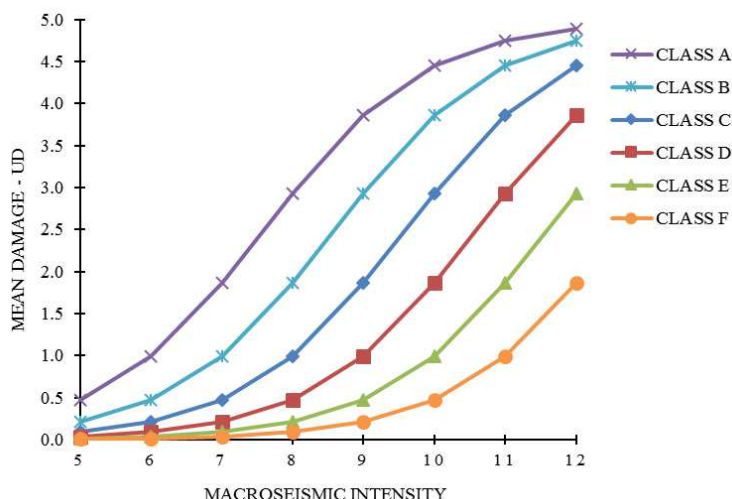


Figure 2.9. Macroseismic isointensity curves

Behavior Modifiers Factors

It is important to emphasize that the seismic behavior of a building, however, does not depend only from the structural system but involves other factors.

To obtain an assessment that takes into account not only the typology but also other influencing characteristics on the seismic response of the building, it is possible to vary the typological vulnerability index (V_I^*), considering the deviations in terms of a regional vulnerability factor ΔV_R and a contribution provided by the behavior modifiers ΔV_m (eq. 2.5):

$$V_I = V_I^* + \Delta V_R + \Delta V_m \quad (2.5)$$

In the V_I^* evaluation it is possible to exceed the values of V_{I-} and V_{I+} of the proposed range for each typology. In any case V_I must not exceed the limit values for which it has been defined (between -0.02 and 1.02).

The regional vulnerability factor ΔV_R is introduced to take into account the best or worse quality of some typology of buildings, found at regional level and attributable to traditional construction techniques or to the particular features of the materials used. The value to attribute to this factor is established on an expert basis, using the knowledge of regional construction techniques and on-site testing, if available.

The behavior modifier factor ΔV_m (tab. 2.9) calculates the contribution of all those building characteristics (height, planimetric and altimetric irregularity, maintenance status, and constructive quality) that affect the building earthquake response.

The scores relative to these modifiers were consistently attributed by means both an assessment carried out on large areas of the national territory (*Meroni et al. 2000*) and the weight attributed to the various parameters considered in the vulnerability methods provided from (*GNDT 1994*) and

the (ATC-21 1988). Where no comparison was possible, scores were assigned on an expert judgment as submultiples of 0.16, which is the deviation of V_1 corresponding to a jump of one vulnerability class. Basically, it is possible to apply the model with just essential data.

Table 2.9. Values of the behaviour modifier factors (after Lagomarsino)

Behaviour modifier	Masonry		Reinforced Concrete			
		V_{mk}	ERD Level	Pre/Low	Medium	Hight
				V_{mk}	V_{mk}	V_{mk}
State of preservation	Good	-0.04	Good	-	-	-
	Bad	+0.04	Bad	+0.04	+0.02	0
Number of floors	Low (1 or 2)	-0.08	Low (1-3)	-0.02	-0.02	-0.02
	Medium (3,4 or 5)	0	Medium (4-7)	0	0	0
	High (6 or more)	+0.08	High (8 or more)	+0.04	+0.04	+0.04
Structural system	Wall thickness					
	Wall distance	-0.04+0.04				
	Wall connections					
Plan Irregularity	Geometry	+0.04	Geometry	+0.04	+0.02	0
	Mass distribution		Mass distribution	+0.02	+0.01	0
Vertical Irregularity	Geometry	+0.04	Geometry	+0.04	+0.02	0
	Mass distribution		Mass distribution			
Superimposed flors		+0.04				
Roof	Weight, thrust and connections	+0.04				
Retrofitting Intervention		-0.08+0.08				
Aseismic Devices	Barbican, Foil arches, Butresses	-0.04				
Aggregate Building: position	Middle	-0.04	Insufficient aseismic joints	+0.04	0	0
	Corner	+0.04				
	Header	+0.06				
Aggregate Building: elevation	Staggered floors	+0.04				
	Buildings with different height	-0.04+0.04				
Foundation	Different level foundations	+0.04	Beams	-0.04	0	0
			Connected beams	0	0	0
			Isolated Footing	+0.04	0	0
			Short-column	+0.02	+0.01	0
			Bow windows	+0.04	+0.02	0

Uncertainty Range in the vulnerability assessment

The uncertainties affecting a seismic risk analysis are both epistemic and aleatory; in the proposed method only, epistemic uncertainties are considered (aleatory uncertainties will be taken into account if a PSHA analysis is performed). In particular, vulnerability evaluations are affected by an uncertainty associated with the classification of the exposed building stock into a vulnerability class or into a building typology and by the uncertainty associated with the attribution of a characteristic behaviour to the vulnerability class or building typology (Spence et al 2003).

It must be noticed how the uncertainty affecting building typologies is higher than the one computed for vulnerability classes; thus, as the building typology behaviour has been deduced from the one observed from vulnerability classes and furthermore because with few data is more difficult to classify a building into a typology rather than into a vulnerability class.

Then it is possible to consider the epistemic uncertainties in the assessment through upper and lower bounds of V_I (eq.2.6 and eq.2.7):

$$V_I^- = V_I - 3/2 \Delta V_f \quad (2.6)$$

$$V_I^+ = V_I + 3/2 \Delta V_f \quad (2.7)$$

where ΔV_f can be assumed, as suggested in (Lagomarsino et al), equal to 0.04 if data are specifically detected to carry out a seismic vulnerability assessment, otherwise it would be assumed a value equal to 0.08, significant of greater uncertainty.

2.1.2. Vulnerability index methods

These indirect methods are more accurate than the macroseismic one and they request to evaluate several typological and constructive characteristics, or vulnerability factors, that affect the seismic response of the building. The disadvantage is that it needs more time and resources.

Thus, a vulnerability index (I_v) is calculated by summing independent scores representative of the influence of single factors on the global vulnerability. It is a conventional and relative measure of the propension to damage and it allows ranking the buildings under investigation.

Vulnerability classes are not directly considered for building typologies and for this reason buildings belonging to a same class, according to the macroseismic method, can offer different level of vulnerability.

Vulnerability index methods or similar were developed from several authors to assess masonry and RC buildings (*Sucuoglu et al. 2007, Gulay et al. 2011*). They can be referred to empirical or numerical data (also together) and they often considered parameters such as the year of construction, the level of earthquake resistance design, the type and quality of the resistance system. etc.

In Italy, the 2nd level GNDT method (*Benedetti e Petrini 1984, GNDT 1994*) is largely used. It is an indirect, semeiotic, empirical method based on the survey of damage occurred in past earthquake and the relation seismic intensity – damage is deterministic and it is represented by trilinear damage curves (*Petrini et al 1989*), associated with every value of the vulnerability index, that correlate the peak ground acceleration to the damage level expressed in terms of damage index between 0 and 1 (the ratio between the repair cost and the total rebuilt cost).

However, due to the uncertainties associated with the evaluation of the structural characteristics of individual buildings, the variability of their seismic behavior, the precision of the vulnerability model, the randomness of the seismic shock, whose characteristics cannot be uniquely defined through the only intensity parameter considered and the possible local amplification effects are seldom evaluable for each individual building, thus the function that expresses the damage

according to the vulnerability index and the seismic intensity cannot be considered as deterministic (Braga et al. 1987).

For this reason, the vulnerability of the single building should be thought as an indicative parameter of belonging to a wider vulnerability range, rather than as a punctual evaluation.

The 2nd level GNDT method consists in the evaluation of 11 vulnerability factors (fig. 2.10) through expert judgment.

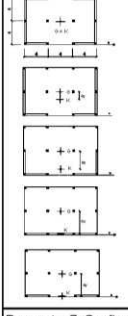
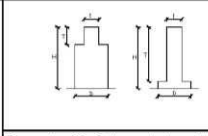
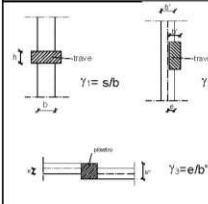
G.D.N.T. - SCHEDE DI VULNERABILITA' DI 2° LIVELLO (CEMENTO ARMATO)														
Cod. ISTAT Provincia			Cod. ISTAT Comune			N. scheda			Squadra					
PARAMETRI		Clas- si	Qual. inf.	ELEMENTI DI VALUTAZIONE				SCHEMI - RICHIAMI (CEMENTO ARMATO)						
1	TIPO DI ORGANIZZAZIONE DEL SISTEMA RESISTENTE (S.R.)	1 st	4 ^{ta}	Pareti in c.a. (cl. A)	1	Tamp. cons. e telai (cl. A)	2	Tamp. deb. e telai rig. (cl. B)	3	Tamp. deb. e telai def. (cl. C)	4	Telai non tamp. (cl. B o C)	5	Parametro 3. Resistenza convenzionale
2	QUALITA' DEL S.R.	1 st	4 ^{ta}	(vedi manuale)				$q = (A_v + A_s) \cdot h \cdot p_m / A_s + p_s$ $C = a_g \cdot \tau_i / (q \cdot N) \quad \alpha = C / (0.4 \cdot R)$ Calcolo di R Terreni tipo S ₁ : R=2.5 (T<0.35 s) R = 2.5 / (T/0.35) ^{2/3} (T>0.35 s) Terreni tipo S ₂ : R = 2.2 (T<0.8 s) R = 2.2 / (T/0.8) ^{2/3} (T>0.8 s)						
3	RESISTENZA CONVENZIONALE	1 st	4 ^{ta}	Numero di piani N	1	Area tot. cop. A _v (mq)	1	Area A _v (mq)	1	Area A _s (mq)	1	τ _i (t/mq)	1	Parametro 6. Configurazione planimetrica
4	POSIZIONE EDIFICIO E FONDAZIONI	1 st	4 ^{ta}	Pend. perc. terr.	1	Roccia	1	Terr. sc. non sp.	1	Terr. sc. sp.	1	Diff. Max. di quota Δh (m)	1	 0=e (A, I ₀) e ₁ /d ₁ =0.08 (cl. A) e ₁ /d ₁ =0.28 (cl. B) e ₁ /d ₁ =0.40 (cl. C) e ₁ /d ₁ =0.43 (cl. C)
5	ORIZZONTAMENTI	1 st	4 ^{ta}	Piani sfalsati	1	Orizz. rig. e ben coll.	1	Orizz. def. e ben coll.	2	Orizz. rig. e mal coll.	3	Orizz. def. e mal coll.	4	% or. rig. ben coll.
6	CONFIGURAZIONE PLANIMETRICA	1 st	4 ^{ta}	Rapp. perc. β ₁ = a/l	1	Rapp. perc. β ₂ = e/d	1	Rapp. perc. β ₄ = Δd/d	1	Rapp. perc. β ₅ = c/b	1		1	Parametro 7. Configurazione in elevazione
7	CONFIGURAZIONE IN ELEVAZIONE	1 st	4 ^{ta}	% aumento (+) riduz. (-) di massa	1	Rapp. perc T/H	1	Var. in elev. s.r.	1	Piano terra port.	1		1	
8	COLLEGAMENTI ED ELEMENTI CRITICI	1 st	4 ^{ta}	Rapp. perc. γ ₁ = s/b	1	Rapp. perc. γ ₂ = e/b _{min}	1	Rapp. perc. γ ₃ = e/b*	1	Rapp. max. h/b _{min}	1	% σ/Rc (approssim.)	1	Parametro C9. Colleg. ed elementi critici
9	ELEM. BASSA DUTT.	1 st	4 ^{ta}	Colleg. el. pref.	1	Largh. min. b _{min} (cm)	1	Rapp. min. h _{min} /b	1	Rapp. max. h _{max} /h _{min}	1		1	 γ ₁ = s/b γ ₂ = e/b _{min} γ ₃ = e/b*
10	EL. NON STRUTT.	1 st	4 ^{ta}	(vedi manuale)										
11	STATO DI FATTO	1 st	4 ^{ta}	(vedi manuale)										
12	Struttura a telai piani o a telai spaziali	1 st	2 ^{da}	piani	1	spaziali	2							

Figure 2.10. Vulnerability factors of the 2nd level GNDT method

In particular, some of the parameters take into account the behavior of structural and non-structural elements, others of the overall behavior of the constructive organism.

For each factor, one assigns a vulnerability class between 4 (A, B, C, D) and take the related score pi (tab. 2.10). The choice of the class to assign is based on the expert judgment about the difference surveyed with respect the optimal condition for the factor considered, represented by the class A.

Table 2.10. Vulnerability factors and relative scores for each class

<i>Vulnerability factors</i>	<i>Classes</i>			
	A	B	C	D
1 – Type of the resistant system	0	- 1	-2	-
2 – Quality of the resistant system	0	-0.25	-0.50	-
3 – Conventional resistance	0.25	0	-0.25	-
4 – Position of the building with respect the soil	0	-0.25	-0.50	-
5 – Type of slabs	0	-0.25	-0.50	-
6 - Planimetric configuration	0	-0.25	-0.50	-
7 – Elevation configuration	0	-0.50	-1.50	-
8 – Connections and critical elements	0	-0.25	-0.50	-
9 – Elements with low ductility	0	-0.25	-0.50	-
10 – Non-structural elements	0	-0.25	-0.50	-
11 – Conservation status	0	-0.50	-1	-2.45

It is worth noting as the scores relative to the same class are often equal. This mean that the method is not capable to distinguish the different influence that each factor has on the global response of the structure. This is because the method was developed with the aim to compare the buildings each other, rather than evaluate the exact vulnerability level of the single building.

Below the vulnerability factors are described in depth.

Factor n.1 considers if the structural system is composed by stiff or deformable frames, walls, strong or weak infills. Important is to detect if seismic resistant frames are arranged in both main directions of the structures.

Factor n.2 needs of the knowledge of how the structure was designed and the quality of materials used. Thus, design documents are required to detect the constructive details and the mechanical characteristics of the materials.

Factor n.3 takes into account the stories shear resistances and compares it with seismic forces for each direction, calculated for example by means a linear static analysis. The resistance of materials, dimensions of the column sections, the weight of the structure and the spectral acceleration $S_a(T)$ have to be known to. Thus, design documents and several investigations are required to assess this factor.

Factor n. 4 depends on the profile of the ground, thus if there are foundations located on different quota and parts of the soil loading the building.

Factor n. 5 considers if the slabs are stiff or deformable in their plane and if the connection between slabs and RC beams is good. The letter usually is a satisfied condition.

Factor n. 6 takes into account the geometrical shape of the horizontal section and the masses and stiffness in their plant distribution. Thus, the calculation of the stiffness distribution is required for each floor and analysis direction, in order to quantify the torsional effects.

Factor n.7 considers the elevation irregularity of the buildings, thus if there are variations in the structural system, in geometrical shape, in masses and stiffness, etc. Very important for the seismic vulnerability is the increasing of stiffness on the height of the building, particularly the presence of soft story.

Factor n. 8 take into account the quality of the connections between structural members and the presence of critical elements. The formers consider some aspects as the width ratios between columns and beams converging in the same joint and the eccentricity ratio between the axes of the members, while the latters are the extern joints, squat elements and highly loaded members.

Factor n. 9 considers elements with low ductility, like brittle and slender elements, and elements in which the ductility request is higher for structural irregularity (soft story),

Factor n. 10 regards those non-structural elements, which can affect the seismic behaviour interfering with the structural behaviour, and elements that are dangerous by itself during earthquakes such as infills, countertops, installations, furnishings etc. For the latter is important to check if the existing grade of connectivity is adequate to avoid dangerous effects.

Factor n. 11 considers the conservation status of the structural members, with respect to both the materials decay and the existing damages.

As shown, to evaluate some factors are required many operations that make the 2nd level GNDT method not very fast especially in emergency situations in which a lot of building have to be evaluated.

Finally, the single scores are summed in order to obtain the vulnerability index I_v , that can be converted by eq. 2.8 to be comprised in the range between 0 (no vulnerability) and 100 (maximum vulnerability):

$$I_v = - 10.07 \sum_i^n V_i + 2.5175 \quad (2.8)$$

So for a given seismic intensity, the damage suffered by a certain building is a growing function of the score assigned to it.

A value close to zero or very low of the index identifies a building that having almost all eleven parameters in class A, is qualitatively in a condition much closer to that of a building built according to the old seismic regulations for a seismic zone of category 1. This means that its propensity to damage should be that for which collapse is excluded and damage level guarantees a residual ability to carry vertical loads and further horizontal seismic actions. Therefore, a construction that can suffer a certain damage level, in relation to the actual level of seismic shaking.

To consider also RC structure designed with modern earthquake resistance criteria, a score equal to -25 is added to V_i in order to differentiate it with respect RC building with lower seismic design. Increasing values of the vulnerability index identify buildings that suffer higher damage until to collapse.

However, the statistical nature of this kind of assessment method implies to take precautions when a punctual use of vulnerability values for the purpose of forming vulnerability ranking is made. In fact, the criteria for attributing the vulnerability classes to the individual parameters and the subsequent additive combination of scores for the index calculation causes the loss of some significative information found detecting the evaluation elements.

The choose of an additive formulation for combining the scores assigned to the parameters may lead to buildings having equal vulnerability index value, but it results from the contribution of different parameters that also have a different weight in measuring the actual incidence on the seismic behavior. Further this incidence is often not well represented by the weights assigned to the parameters of the GDNT method.

Another weakness of the vulnerability index methods derives from how the vulnerability class of each parameter is assigned, through a threshold value: even the belonging to the higher vulnerability class (D) occurs simply by exceeding this threshold and it is not discriminated in any way the extent of its overcoming that may also be remarkable. Thus, it is possible to have cases of buildings with the same parameters into the class D but also with significantly different vulnerability conditions for the same parameters.

Essentially the index fails to grasp some extreme situations that may occur and that are still documented in the information come from the evaluation elements of the parameters.

Furthermore, the index is defined in scalar form, so it does not allow to account the differences in the response of the building along the two main directions. The directionality of the seismic action can have a relevant importance to establish the correlations between the seismic intensity level and the damage occurred.

The method was applied within the LSU-96 (*Dolce et al. 2000*) and Save (*Dolce et al. 2005*) projects in which the assessment of both masonry and RC private and public buildings (schools, hospitals) was done. The buildings first were assigned to a vulnerability classes provided by the EMS-98 scale (A,...,F), on the base of some general typological characteristics, such as the type of vertical structure, level of earthquake design etc. and then they were evaluated through the 2nd level GNDT method.

The results showed a high variability of the vulnerability indices for buildings within the same vulnerability class. Because of is the major detail request from the vulnerability index method that lead to a higher differentiation between buildings within the same class.

In addition, the buildings were ranked in descending order in terms of vulnerability, according to the belonging to one of the five classes obtained by dividing the vulnerability index range 0 - 100 in intervals of 20.

This classification does not adequately correspond to the distribution of the frequencies of values that the index calculation model provides in real cases, in which the thousands of buildings analyzed do not have cases with $I_v \geq 80$ and are extremely limited those with $70 < I_v < 80$. This is due to the rare possibility of observing buildings with all high vulnerability parameters (A), except for really extreme situations.

This observation results in the fact that the actual range of variability of the index is realistically between 0 and 80, thus the qualifiable medium value in the scale is rather one comprised between 30 and 40 than that between 40 and 60 (as it is likely if the range 0-100 is considered).

Therefore, vulnerabilities expressed by index values greater than 30 are indicative of situations to be carefully evaluated.

2.2. Analytical methods

Analytical methods assess more in depth the seismic response of buildings, but more information is requested and so they are more expensive in terms of time and resources with respect the rapid methods.

Non-linear procedures are mostly employed, such as *static analyses (pushover)*, described and compared in (Pinho et al. 2013), and *dynamic analysis -NLDA* (Otani 1980, Moehle 2005).

The latter are the best tools to assess the seismic response, but also nonlinear static procedures were proposed, with the respect of particular conditions, are able to simulate the nonlinear behaviour of a structure with good approximation and lower effort.

The dynamic behaviour of structure in the nonlinear range can be investigated in a better way by using NLDA, also performing *incremental dynamic analysis – IDA* (Vamvatsikos et al. 2002, 2004), by scaling the seismic intensity to include the response for increasing levels of intensity, or *cloud analysis* (Tsfamariam et al. 2014).

Some authors (Masi et al. 2004, Kappos et al. 2010) carried out numerous nonlinear analyses on representative buildings of some European and Italian typologies, thus developing analytical fragility curves. However, this approach is very costly and often impracticable, mainly on a large scale.

Thus, the most recent trends in the field of analytical vulnerability methods for scenario risk analysis, lead to operating with *simplified mechanical models*. Such methods are often *Capacity Spectrum based procedures* (Chopra et al. 1999, Freeman 2004), where the problem of determining the maximum response expected from an MDOF system against a certain seismic event is attributed

to that of a SDOF system rendered equivalent to the MDOF system representative of the real structure. Other simplified mechanical methods are SP-BELA (*Borzi et al. 2008*), D-BELA (*Crowley et al. 2004*), VC method (*Dolce et al. 2005-b*), storey collapse method (*Cosenza 2000*). Linear analyses, in particular dynamic one, provide useful information on the elastic behaviour of a structure and on which components are first introduced into the plastic range. However, they do not allow to detect subsequent collapse mechanisms and the redistribution of forces in the elements, so their use to establish the seismic performance is subject to restrictions. In the following part of the paragraph the simplified procedures are shown, while more complex procedures are illustrated in chapter 3.

2.2.1. Simplified nonlinear procedures

The common base of these procedures is in the use of pushover analysis, to characterize the structural system and then to consider the response directly in terms of displacement through the substitutive structure approach (*Shibata and Sozen, 1976*), in which the structure period is no longer based on the initial elastic stiffness K_e , as in force-based procedures, but on the effective stiffness K_{eff} , which corresponds to the maximum displacement.

The base concept of the pushover analysis is that the global capacity of the structure to support seismic actions can be described from equivalent static forces increased until the collapse, that is the inability to continue to carry vertical loads.

Thus, the characteristic deformations (usually roof level displacement) are plotted against the lateral load.

The system of forces must simulate as realistic as possible the inertia effects produced by the earthquake in the horizontal plane. The latter depend on the structural response, so the system of forces should be updated during the analysis (adaptive pushover) on the base of the damage suffered from the building and the consequent stiffness decay.

However, the force distribution is assumed to be fixed during the analysis. Generally, it represents the distribution of inertia forces deriving from the fundamental vibration mode (first mode), assuming it is predominant. This assumption is generally approximate for buildings with fundamental periods of up to one second, while for more flexible structures, the higher vibration modes should also be considered (multimodal analysis). In addition, if localized damage mechanisms can be detected during the analysis, it may be desirable to adopt congruent force distributions with them. For example, the triggering of a weak or soft storey at the lowest level of a building may lead to a uniform force distribution in elevation.

The pushover procedure would require the use of a nonlinear computational code, but it may also be approximated by a series of sequential elastic analyses, as suggested with different variants in the ATC-40 and FEMA-273, to allow for greater rapidity and also to reduce possible refuse in the results. In this case, the mathematical model of the structure (more precisely the stiffness matrix) is

continually updated to take into account the stiffness reduction of the elements entering the plastic range.

The main aspects of these nonlinear procedure are:

- **Seismic demand:** is a representation of the displacements and deformations required to the structure by the seismic motion of the soil.
- **Structural capacity:** is the ability of the structure to withstand seismic demand. It depends on the strength and inelastic deformation capacity of the individual components of the structure.
- **Performance:** represents the extent to which capacity absorbs demand. The structure must have the ability to withstand seismic demand in such a way the performance is compatible with the design purpose.

Therefore, the risk assessment for a building or group of buildings is the estimation of the expected losses based on the exhibited performance, that is the damage suffered depending on the vulnerability and on the seismic intensity level.

Capacity Spectrum Methods

Capacity Spectrum based procedures are approximate heuristic methods which essentially assumes that a complex non-linear multi-degree-of-freedom system such as a multi-storey building undergoing severe plastic deformations during an earthquake can be modelled as an equivalent single degree of freedom system with an appropriate level of inelasticity.

The capacity of a structure is represented by a curve which has as reference values the base shear (V), normalized with respect to the mass of the building (M), and the displacement at the roof of the building (ΔR). The capacity curve represents the lateral response of the structure under a certain horizontal load distribution.

To compare the demand spectrum with the structural capacity, it is necessary to convert the base shear in spectral acceleration (S_a) and the roof displacement in the in spectral displacement (S_d). For the conversion of the capacity curve it is necessary to know the dynamic characteristics such as the vibration period (T), modal shape (F_i), mass (m_i). For this purpose, a horizontal displacement distribution is used along the building height: usually the fundamental vibration mode is used, but other modes can also be used. In most structures dynamic behaviour is well described considering only the first vibration mode.

CSMs permit to evaluate the expected seismic performance of structures (represented by equivalent single-degree-of-freedom, SDOF, models) by the comparison, in spectral coordinates (S_d , S_a), between the seismic capacity and the seismic demand represented by the 5% damped elastic response spectra of the ground motion in the ADRS plane, adequately reduced in order to take into account the inelastic behaviour.

The capacity spectrum has an initial linear section where the slope depends on the typical natural frequency of vibration of the building class, and rises to a plateau level of spectral acceleration at which the maximum attainable resistance to static lateral force has been reached. As an example, a capacity spectrum is shown in fig. 2.11.

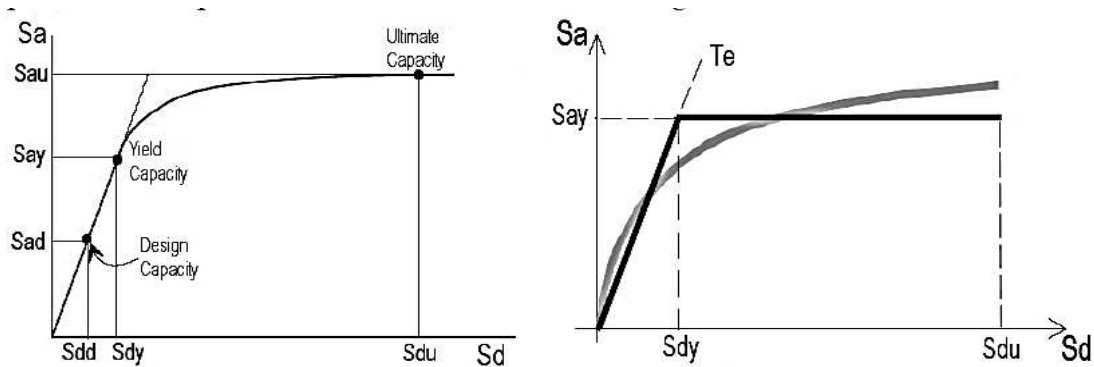


Figure 2.11. Typical capacity spectrum (left) and its bilinear form (right).

For territorial vulnerability assessment scopes, Capacity Spectrum procedures do not necessarily refer to capacity curves obtained by pushover analyses, but they ascribe to each building typology, bilinear capacity curves in terms of yielding (D_y , A_y) and ultimate (D_u , A_u) capacity points. These curves vary depending on several geometrical and technological parameters of the building (number of floors, code level, material strength, drift capacity) such provided for example in Risk-UE and HAZUS methods.

Such approach provides reliable results if applied to a built-up area characterized by a typological building homogeneity and by consolidated seismic design codes. This is not the case of European Union regions where seismic codes are very different and where various typologies of masonry buildings can be distinguished in the territory.

Then the performance of the building is then identified by the so-called “performance point” located at the intersection of the capacity and demand spectra (fig. 2.12).

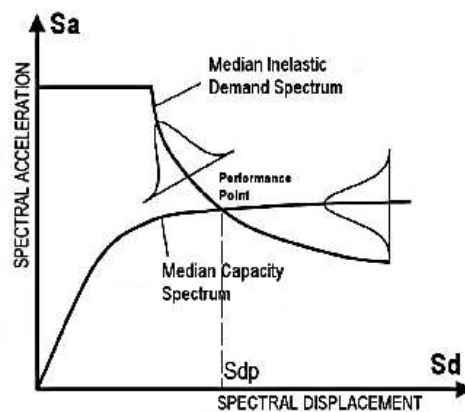


Figure 2.12. Performance point estimation

If the earthquake has a modest intensity, the response of the structure is elastic, so the determination of the performance point is immediate because it will be in the elastic part of the capacity spectrum and there is no need to reduce the elastic demand spectrum. As the seismic intensity increases, the structure response is no longer linear and the determination of the performance point is no longer immediate since the inelastic demand spectrum is function of the ductility that needs to be determined, then the performance point is searched for attempts thorough an iterative procedure.

Hence the probability that the building reaches a certain state of damage (fragility curve) can be determined as follows:

1. To define the capacity model and converting it into capacity spectrum.
2. To determine the demand spectrum.
3. To calculate the expected response from the intersection of the capacity spectrum and the demand spectrum (performance point).
4. From the fragility model, the conditional probability that for a given performance point the building will present a certain damage state is estimated.

Having the fragility curves (or damage functions) of the building, it is possible to determine the probability that the damage states d_s ("slight", "moderate", "extensively", "complete") will occur due to the realization of the spectral displacement S_d provided by the performance point.

Demand spectra

The elastic demand spectrum is used to characterize seismic demand. It allows to summarize the response of all possible linear SDOF systems for a specific seismic intensity. Generally, this spectrum is obtained for a dimming factor of 5%, representative of most structures. This curve has as reference quantities the period (T) and the elastic spectral pseudo-acceleration (S_{ae}). The values of $S_{ae}(T)$ can be directly linked to the corresponding values of the elastic displacement spectra $S_{de}(T)$ by means the factor $(T^2 / 4\pi^2)$.

To define the elastic demand, spectra with different shapes can be used.

The *Newmark-Hall spectrum* (Newmark et al. 1982) is the most convenient. It detects three regions, one with constant acceleration ($T_B \leq T \leq T_C$), one with constant speed ($T_C \leq T \leq T_D$) and one with constant displacement ($T \geq T_D$).

EC8 suggests two types of elastic acceleration response spectra for horizontal components of the ground motion: Type 1 and Type 2. The shape of the elastic response spectrum is taken the same for the two levels of seismic action.

If the earthquakes that contribute most to the seismic hazard defined for the site for the purpose of probabilistic hazard assessment has a surface-wave magnitude, M_s , not greater than 5.5, it is

recommended that the Type 2 spectrum is adopted. Type 1 spectrum is used for the earthquakes with magnitude greater than 5.5.

The horizontal elastic response spectrum is defined by:

- a_g : Design ground acceleration on type A ground
- T_B, T_C : The periods that limit the constant spectral acceleration region
- T_D : The period that define the beginning of the constant displacement range of the spectrum
- S : Soil factor
- η : Damping correction factor

The values of T_B, T_C, T_D and S for each ground type and shape of spectrum to be used as well as the damping corrections for different levels of damping are given in EC 8 part 1.

For the construction of the inelastic demand spectrum, the following steps are performed:

- the elastic demand spectrum is determined for a specific site and for a damping factor of 5% (for buildings with dumping higher than 5% a new elastic spectrum could be generated by considering an appropriate damping ratio or the demand spectrum with 5% damping could be modified).
- the elastic demand spectrum is converted into ADRS format, which have the spectral displacement (S_d) on the X axis and the elastic spectral pseudo-acceleration (S_{ae}) on the Y axis. The relationship between spectral acceleration and displacement is used.
- Starting from the demand spectrum in ADRS format, the inelastic demand spectrum is obtained to take into account the non-linearity of the structural response. The over-strength factor R_μ (Miranda et al. 1994, Cosenza et al. 1997, Fajfar 1999) is used, which is a strength reducing factor due to ductility (fig.2.13).

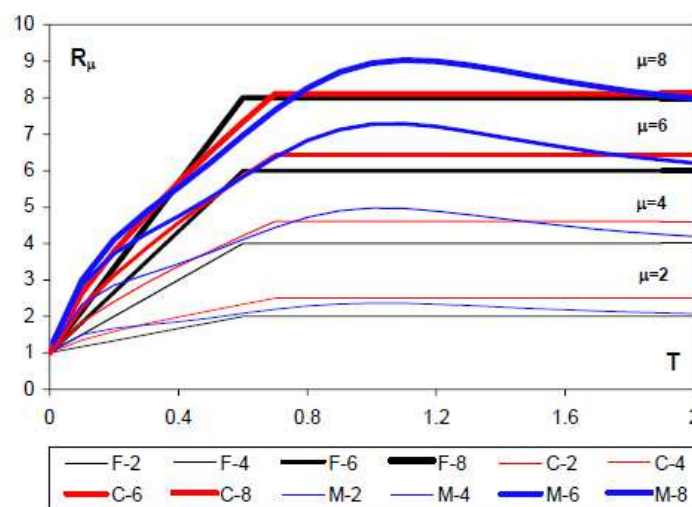


Figure 2.13. Strength reduction factors: Fajfar (black), Cosenza-Manfredi (red), Miranda (blue)

The formulation to calculate the over strength factor according to (Vidic et al. 1994; Fajfar 1999) are shown in eq. 2.9 and 2.10:

$$R_{\mu} = (\mu - 1) \frac{T}{T_c} + 1 \quad \text{if } T < T_c \quad (2.9)$$

$$R_{\mu} = \mu \quad \text{if } T \geq T_c \quad (2.10)$$

where:

- μ is the ductility factor, defined as the ratio between the maximum displacement (du) and the yield displacement (dy).
- T_c is transition period from the constant acceleration segment to the constant velocity segment; some typical values of T_c are 0.6 s (Fajfar 1999) and 0.7 s (Cosenza et al. 1997).

Thus, the relation defined as (Vidic et al. 1994) can be used to calculate the inelastic spectral parameter (eq. 2.11 and 2.12).

$$S_d(T) = \frac{S_{ae}(T)}{R_{\mu}} \quad (2.11)$$

$$S_d(T) = \frac{\mu}{R_{\mu}} S_{de}(T) = \mu \frac{T^2}{4\pi^2} S_a(T) \quad (2.12)$$

Since $S_a(T)$ or $S_d(T)$ are defined for predefined value of μ , they are often referred as “*constant ductility spectra*”.

Determination of the Performance point

The ADRS format allows the demand spectrum to be overlaid on the capacity spectrum. The intersection of the demand and capacity spectra is seismic demand (from the structure). It represents a point where demand and capacity are equal, and often is termed building ‘*Performance Point*’.

The location of the performance point must satisfy two conditions:

1. The point must lie on the capacity spectrum curve in order to represent the structure at the given displacement; and,
2. The point must lie on a spectral demand curve, reduced from the elastic 5 percent damped response spectrum, that represents the nonlinear demand at the same structural displacement.

If the performance point is located in the linear range of the capacity, it defines the actual displacement of the structure. This is not normally the case as most structures experience inelastic (nonlinear) behaviour when exposed to strong seismic action. For seismic inputs being of interest for damage/loss assessment, the performance points will regularly be out of linear, i.e., in inelastic (nonlinear) capacity range.

When the performance point is located in the nonlinear range of the capacity, in the general case, determination of the performance point requires a trial and error search for satisfying the two criteria specified above. In the following, presented are three alternate procedures. All are based on the same concepts and mathematical relations, but vary in assumptions made in solution process and the dependence on graphical versus analytical techniques.

There are several criteria for determining the performance point. The *ATC-40 (1996)* provides several methods for determining the performance point. They are all based on the calculation of the demand spectra corresponding to different equivalent damping values and on the iterative determination of the expected displacement.

Elastic-perfectly plastic representation of capacity spectrum, or **N2 method** (*Fajfar 2000*) in which the inelastic demand spectra is obtained from standardized (code-based) elastic design spectra using ductility factor based reduction factors (R_u). The N2 method (also called the Reduction Factor Method) has been implemented in the so-called “Mechanical-Based Method” of vulnerability analysis (*Lagomarsino et al. 2006*) in the RISK-UE project (*Mouroux et al. 2004*).

1. General form of the capacity spectra (*ATC-40, 1996*)

The ‘General Form of Capacity Spectra’ assumes a capacity spectrum of linear form until the yield point and nonlinear post-yield segment. The procedure presented below is designed as hand or spreadsheet iteration method of converging on the performance point.

To define performance point, a trial point (S_{dTR} , S_{aTR}) on the capacity spectrum should be selected as an initial estimate. A first choice of trial point could be the displacement obtained using the equal displacement approximation (fig.2.14), or, it may be the end point of capacity spectrum, or, any other point chosen based on the expert judgement.

Based on the spectral acceleration and the spectral displacement defining the trial point (S_{dTR} , S_{aTR}), the strength reduction factor accounting for nonlinear effects associated with it shall be calculated, and then, the the 5% damped demand spectra is reduced for calculated strength reduction factor.

The reduced demand spectrum intersects the capacity spectrum at (S_{dNEW} , S_{aNEW}) point. If the displacement at the intersection is equal to initially assumed (S_{dTR}), or is within 5 percent ($0.95 S_{dTR} \leq S_{dNEW} \leq 1.05 S_{dTR}$) of the displacement of the trial performance point, the point (S_{dNEW} , S_{aNEW}) is the performance point, i.e., the unique point where the capacity equals demand. Thus, the displacement found is the maximum expected displacement for the considered seismic event.

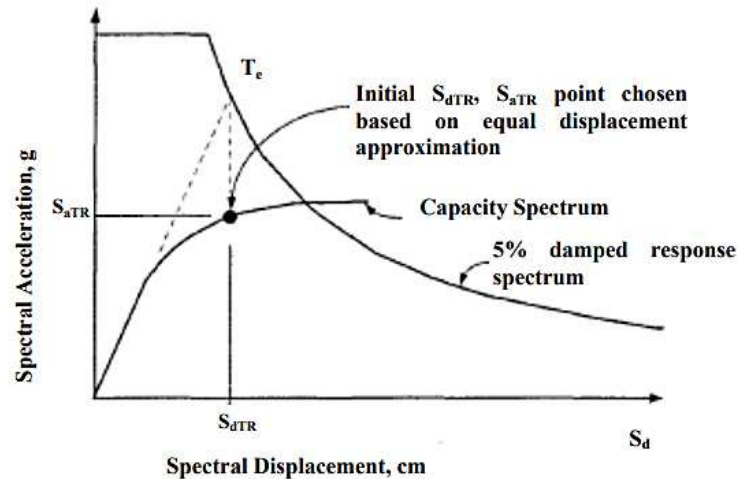


Figure 2.14. ATC-40 method: General form of the capacity spectra

If the demand spectrum does not intersect the capacity spectrum within the acceptable tolerance, a new trial point shall be selected and the procedure repeated until the accepted tolerance is reached. The choice of a new trial point might be the intersection point determined in the previous step ($S_{dTR} = S_{dNEW}$, $S_{aTR} = S_{aNEW}$), or any other point chosen based on expert judgement.

2. Bi-linear representation of capacity spectrum

In the case the capacity spectrum is represented by bilinear shape, a simplified and more direct approach can be used for defining the performance point. It is based on the assumption that not only the initial slope of the bilinear representation of the capacity model remains constant, but also the yield point and the post-yield slope. This simplifying assumption allows a direct solution without drawing multiple demand spectra (fig. 2.15).

It uses empirically derived relationships for the effective period and damping to estimate the response of an equivalent linear SDOF model. The bilinear representation is needed to quickly estimate the effective damping (equivalent) and the consequent reduction in spectral demand.

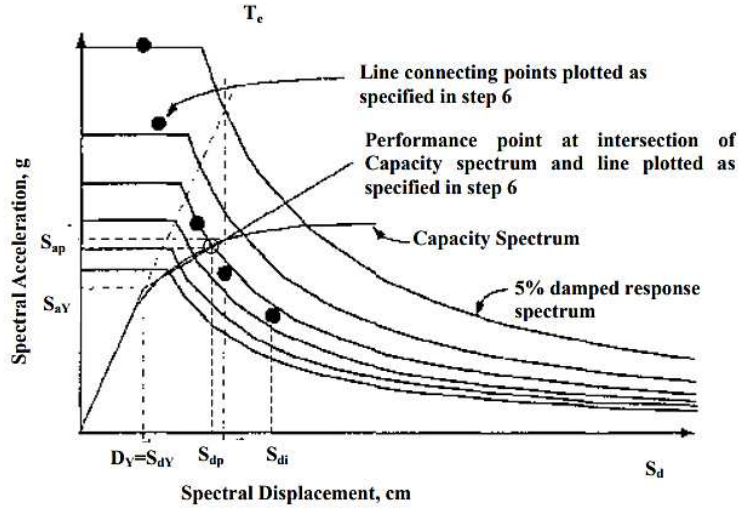


Figure 2.15. ATC-40 method: Bi-linear representation of capacity spectrum

STEP 1: Plot the 5 % damped elastic spectrum and the capacity spectrum on the same chart.

STEP 2: Chose several values of $S_{d,i}$.

$i = 1, 2, 3, \dots, N$, such as $S_{d,i} > S_{d,y}$, $S_{d,i+1} > S_{d,i}$

STEP 3: For each chosen $S_{d,i}$ define:

ductility (eq. 2.13):

$$\mu_i = \frac{S_{d,i}}{S_{d,y}} \quad (2.13)$$

spectral periods (eq. 2.14):

$$T_i = 2\pi \sqrt{\frac{S_{d,i}}{S_{a,i}}} \quad (2.14)$$

and define the spectral range (acceleration $T_i < T_C$, or velocity $T_i \geq T_C$) where it falls.

STEP 4: Calculate strength reduction factors $R_{\mu,i}$.

STEP 5: Calculate reduced spectral accelerations ($S_{a,i}$) by reducing the corresponding 5% damped elastic spectral accelerations ($S_{ae,i}$) for adequate strength reduction factor $R_{\mu,i}$ (eq. 2.15):

$$S_{a,i} = \frac{S_{ae,i}}{R_{\mu,i}} \quad (2.15)$$

STEP 6: Plot the calculated discrete acceleration/displacement spectral values ($S_{d,i}$, $S_{a,i}$) and draw a line connecting plotted points. The intersection of this piecewise linear line with the capacity spectrum is the demand spectral displacement, i.e., the performance point.

Although procedure requires plotting of multiple ($S_{d,i}$, $S_{a,i}$) points, the only ($S_{d,i}$, $S_{a,i}$) point that has any real significance is the one that lies on the capacity spectrum curve. This point defines the

intersection point of the capacity spectrum with the adequate constant damping demand spectrum, and thus defines the demand displacement.

It is evident (fig.2.15) that the $(S_{d,i}, S_{a,i})$ piecewise line steadily slopes down until intersect with the capacity spectrum. This provides opportunity for the procedure to be fully coded and completely automated.

3. The Modified Acceleration-Displacement Response Spectrum Method (FEMA 440, 2005)

Basically, differs from the Capacity Spectrum Method in the reduction of the elastic demand curve. The elastic SDOF system that is used to estimate the maximum inelastic displacement of the nonlinear system is usually referred to as the equivalent or substitute system. Similarly, the period of vibration and damping ratio of the elastic system are commonly referred to as equivalent period and equivalent damping ratio, respectively. The equivalent period is computed from the initial period of vibration of the nonlinear system and from the maximum displacement ductility ratio, μ . On the other hand, the equivalent damping ratio is computed as a function of damping ratio in the nonlinear system and the displacement ductility ratio.

4. The Coefficient Method (FEMA 356, 2000).

It is essentially a spectral displacement modification procedure in which several empirically derived factors are used to modify the response of a linearly-elastic equivalent SDOF model of the building structure.

5. Elastic-perfectly plastic representation of capacity spectrum (N2 method, Fajfar 2000)

For this particular case (fig. 2.16) there is closed mathematical solution, thus no plotting is required at all. An estimate on the displacement due to a given seismic demand is made using a simple technique called 'the equal displacement approximation'. This approximation is based on the assumption that the inelastic spectral displacement (S_d) is the same as that which would occur if the structure remained perfectly elastic (S_{de}).

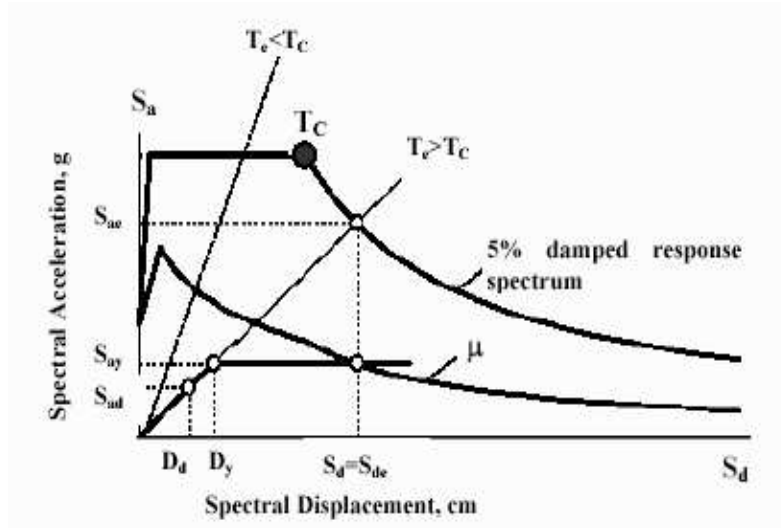


Figure 2.16. N2 method

The intersection of the radial line corresponding to the elastic period T_{el} (eq. 2.6) of idealized elastic-perfectly plastic system with the elastic 5% damped response spectra (S_{ae}) defines the acceleration (i.e. the strength) and the corresponding displacement (S_{de}) demands required for elastic (linear) behaviour of the system.

The yield acceleration (S_{ay}) represents both the acceleration demand and the capacity of the inelastic system. The ratio between the accelerations corresponding to the elastic and inelastic systems represents the strength reduction factor due to ductility (eq. 2.16):

$$R_{\mu} = \frac{S_a(T_{el})}{S_{a,y}} \quad (2.16)$$

Based on the equal displacement approximation, the inelastic displacement demand S_d is equal to the elastic displacement demand $S_{d,e}$ (eq. 2.17):

$$S_d = S_{de} = \mu * S_{dy} = \mu * d_y \quad (2.17)$$

For constant acceleration ($T_e < T_c$) and the constant velocity ($T_e \geq T_c$) spectral ranges, the ductility demands μ_p are (eq.2.18 and 2.19):

$$\mu_p = \frac{(R_{\mu} - 1) T_c}{T_e} + 1 \quad \text{if } T_e < T_c \quad (2.18)$$

$$\mu_p = \frac{S_d}{d_y} = \frac{S_{ae}(T_e)}{S_{ay}} = R_{\mu} \quad \text{if } T_e \geq T_c \quad (2.19)$$

and the coordinates of performance point are calculated as in eq. 2.20 and 2.21:

$$S_{d,p} = d_y * \mu = \frac{S_{d,e}}{R_\mu} \mu_p \quad (2.20)$$

$$S_{a,p} = S_{a,y} \quad (2.21)$$

Summary of the procedure:

STEP 1: Define the yield point coordinates for capacity spectrum (S_{dy} , S_{ay}).

STEP 2: Define the elastic period of the structure (T_e).

STEP 3: For $T = T_e$, define corresponding ordinates of 5% damped elastic acceleration response spectrum $S_{ae}(T_e)$ and $S_{de}(T_e)$.

STEP 4: Calculate the strength reduction factor R_μ .

STEP 5: Depending of the relation between T_e and T_C , calculate the demand ductility μ_d by using eq. 2.18 or 2.19.

STEP 6: Use eq. 2.20 and 2.21 to calculate the coordinates of the performance point.

The procedure is mathematically closed and easy for coding. No iteration or plotting is needed.

References chapter 2

- Corsanego A., Petrini V. Evaluation criteria of seismic vulnerability of the existing building patrimony on the national territory. *Seismic Engineering*, Patron ed. 1994; Vol. 1 pp: 16-24.
- Whitman R.V., Reed J.W., Hong S.T. Earthquake Damage Probability Matrices. Proc. 5th ECEE, Rome 1974, pp: 2531.
- Braga F., Dolce M. & Liberatore D. 1982. A statistical study on damaged buildings and an ensuing review of the M.S.K.-76 scale, Proc. of the 7th European Conference on Earthquake Engineering, Athens
- ATC-13 “Earthquake damage evaluation data for California”. Applied Technology Council, Redwood City, California, 1987.
- Dong W., Shah H., Wong F. *Expert System in Construction and Structural Engineering*. and New York: Chapman and Hall, London, 1988.
- Sanchez-Silva M., Garcia L. “Earthquake Damage Assessment Based on Fuzzy Logic and Neural Network”. *Earthquake Spectra*, 2001; Vol. 17(1), pp: 89-112.
- Grunthal G. “European Macroseismic Scale”. Centre Européen de Géodynamique et de Séismologie, Luxembourg 1998; Vol. 15.
- Freeman S.A. “The Capacity Spectrum Method”. Proc. 11th ECEE, Paris 1998
- Fajfar P. and Gašperšič P. “The N2 method for the seismic damage analysis of rc buildings,” *Earthq. Eng. Struct. Dyn.*, vol. 25, no. 1, pp. 31–46, Jan. 1996.
- HAZUS 99 “Earthquake Loss Estimation Methodology - Technical and User Manuals” Federal Emergency Management Agency, Washington, D.C. 1999.
- Milutinovic Z.V. and Trendafiloski G.S., WP4: Vulnerability of current buildings, in RISK-UE project. 2003.

- ATC-21 “Rapid Visual Screening of Buildings for Potential Seismic Hazard - A Handbook”. Applied Technology Council, Redwood City, California, 1988.
- Benedetti D. & Petrini V. 1984. On seismic vulnerability of masonry buildings: proposal of an evaluation procedure. *L’Industria delle Costruzioni*, vol. 18, pp. 66-78.
- Kappos A. J., “An overview of the development of the hybrid method for seismic vulnerability assessment of buildings,” *Struct. Infrastruct. Eng.*, vol. 12, no. 12, pp. 1573–1584, Dec. 2016.
- Savoia M. et al. “Una metodologia speditiva per la valutazione di vulnerabilità sismica di edifici in muratura e calcestruzzo armato”. *Proc. 15th ANIDIS*, Padova 2013.
- Calvi G. M., Pinho R., G. Magenes, J. J. Bommer, and H. Crowley, “Development of seismic vulnerability assessment methodologies over the past 30 years,” *Earthquake*, vol. 43, no. 472, pp. 75–104, 2006.
- Lumantarna E. et al. Review of Methodologies for Seismic Vulnerability Assessment of Buildings. Australian Earthquake Engineering Society 2014 Conference, Nov. 21–23, Lorne, Victoria.
- Medvedev S.V. “Seismic Intensity Scale M.S.K.-76”. *Publ. Inst. Geophys. Pol. Acad. Sc.*, Warsaw, 1977; A-6 (117).
- Gruppo Nazionale per la Difesa dai Terremoti - GNDT, 1994. Schede di 1° e 2° livello di vulnerabilità e di rilevamento del danno (edifici in c.a. e muratura).
- Giovinazzi S. and Lagomarsino S., “A Macroseismic Method for the Vulnerability Assessment of Buildings,” *13th World Conf. Earthq. Eng.*, no. 896, pp. 1–6, 2004.
- Meroni F., Petrini V. & Zonno G. 2000. Distribuzione nazionale della vulnerabilità media comunale. In A. Bernardini (ed), *La vulnerabilità degli edifici*, CNR-GNDT, Roma, pp.105-131.
- Spence R., Bommer J., Del Re D., Bird J., Aydinoglu N., Tabuchi S. “Comparison Loss Estimation with Observed Damage: A study of the 1999 Kocaceli Earthquake in Turkey”. *Bulletin of Earthquake Engineering*, 2003; Vol. 1, pp: 83-113.

- Sucuoglu H., et al. A Screening Procedure for Seismic Risk Assessment in Urban Building Stocks, *Earthquake Spectra* 23(2), May 2007
- Gulay F.C., P25 - Scoring Method for The Collapse Vulnerability Assessment of R/C Buildings. The Twelfth East Asia-Pacific Conference on Structural Engineering and Construction. *Procedia Engineering* 14 (2011) 1219–1228.
- Guagenti E., Petrini V., 1989. Il caso delle vecchie costruzioni: verso una nuova legge danni-intensità, *Proceedings of the 4th Italian National Conference on Earthquake Engineering*, - Milan - (Italy), 1, 145-153, Milano.
- Braga F., Dolce M., Liberatore D., (1987). Rassegna critica dei metodi per la stima della vulnerabilità. In *Atti 3° Conv. Naz. L'ingegneria Sismica in Italia*, Roma, 1987.
- Braga F., Dolce M., Liberatore D. (1987), “Statistical Calibration of Second Level Seismic Vulnerability of Buildings”, *Atti della 5th international conference on applications of statistics and probability in soil and structural engineering*, Vancouver.
- Di Pasquale G., Dolce M. & Martinelli A. 2000. Analisi della vulnerabilità, Censimento di vulnerabilità a campione dell'edilizia corrente dei centri abitati, nelle regioni Abruzzo, Basilicata, Calabria, Campania, Molise, Puglia e Sicilia (Progetto Lavori Socialmente Utili), Dipartimento della Protezione Civile, Roma, pp. 76-106.
- Dolce M., Martinelli A. *Inventario e vulnerabilità degli edifici pubblici e strategici dell'Italia centro-meridionale*, Vol. II - *Analisi di vulnerabilità e rischio sismico*, INGV/GNDT Istituto Nazionale di geofisica e Vulcanologia / Gruppo Nazionale per la Difesa dai Terremoti, L'Aquila, 2005.
- Pinho R., Marques M., Monteiro R., Casarotti C., and Delgado R. (2013) Evaluation of Nonlinear Static Procedures in the Assessment of Building Frames. *Earthquake Spectra*: November 2013, Vol. 29, No. 4, pp. 1459-1476.
- Otani S. Nonlinear Dynamic Analysis of Reinforced Concrete Building Structures. *Canadian Journal of Civil Engineering* 7(2):333-344. June 1980.

- Moehle J.P. Nonlinear analysis for performance-based earthquake engineering. December 2005. *The Structural Design of Tall and Special Buildings* 14(5):385 - 400
- Vamvatsikos D. and Cornell C. A. Incremental dynamic analysis, *Earthquake Engineering and Structural Dynamics*, 31(3): 491–514. 2002
- Vamvatsikos D. and Cornell C. A. Applied incremental dynamic analysis, *Earthquake Spectra*, 20(2): 523–553. 2004
- Tesfamariam et al. Probabilistic seismic demand model for RC frame buildings using cloud analysis and incremental dynamic analysis, Tenth U.S. National Conference on Earthquake Engineering Frontiers of Earthquake Engineering, At Anchorage, Alaska 2014.
- Masi A., Vona M. Vulnerabilità sismica di edifici in c.a. realizzati negli anni '70. XI Congresso Nazionale “L’ingegneria Sismica in Italia”, Genova 25-29 gennaio 2004.
- Kappos A.J. et al. Fragility curves for reinforced concrete buildings in Greece. *Structure and Infrastructure Engineering* 6(1-2):39-53. February 2010
- Chopra A.K., Goel R.K. (1999). “Capacity-demand-diagram methods for estimating seismic deformation of inelastic structures: SDF systems”, Report PEER-1999/02. Pacific Earthquake Engineering Research Center, University of California, Berkeley.
- Freeman S.A. Review of the development of the capacity spectrum method. *ISET Journal of Earthquake Technology*, Paper No. 438, Vol. 41, No. 1, pp. 1-13, March 2004.
- Borzi et al., Simplified pushover-based vulnerability analysis for large-scale assessment of RC buildings. *Engineering Structures* Volume 30, Issue 3, Pages 804-820, March 2008.
- Crowley et al. A Probabilistic Displacement-based Vulnerability Assessment Procedure for Earthquake Loss Estimation. *Bulletin of Earthquake Engineering* 2: 173–219, 2004.
- Dolce M., Moroni C., 2005. La valutazione della vulnerabilità e del rischio sismico degli edifici pubblici mediante le procedure VC e VM. Progetto SAVE, Atti di Dipartimento N. 4/ 2005.

- Cosenza E., 2000. Il comportamento sismico di edifici in c.a. progettati per carichi verticali, CNR—Gruppo Nazionale per la Difesa dai Terremoti, Roma, Italy (in Italian).
- Shibata A., and Sozen M. (1976). “Substitute structure method for seismic design in reinforced concrete.” J. Struct. Div., ASCE, 102(1), 1-18.
- FEMA (1997). NEHRP guidelines for the seismic rehabilitation of buildings, Report No. FEMA-273, Federal Emergency Management Agency, Washington DC.
- ATC (1996). Seismic evaluation and retrofit of concrete buildings, Report No. ATC-40, Applied Technology Council, Redwood City, CA.
- Newmark N. M. and Hall W. J., 1982. Earthquake Spectra and Design. Earthquake Engineering Research Institute (EERI) Monograph. (Oakland, CA: EERI).
- CEN (2003) Eurocode 8: design of structures for earthquake resistance—part 1: general rules, seismic actions and rules for buildings. European Committee For Standardization (CEN), Brussels.
- Miranda E., Bertero V.V. Evaluation of strength reduction factors for earthquake-resistant design. Earthquake spectra 10 (2), 357-379.
- Cosenza E., Manfredi G. (1997), The improvement of the seismic-resistant design for existing and new structures using damage concept, in “Seismic Design Methodologies for the Next Generation of Codes”, (P. Fajfar and H. Krawlinker Eds.), Balkema (ISBN: 9054109289).
- Fajfar P. Capacity spectrum method based on inelastic demand spectra. Earthquake Engng. Struct. Dyn. 28, 979 - 993 (1999).
- Vidic T., Fajfar P., and Fischinger M. (1994). Consistent inelastic design spectra: Strength and displacement, Earthquake Engineering and Structural Dynamics, 23(5): 507–521.
- Fajfar P. A nonlinear analysis method for performance-based seismic design. Earthq Spectra, 16(3):573–591 (2000).

- Lagomarsino S., Giovinazzi S. Macroseismic and mechanical models for the vulnerability and damage assessment of current buildings. *S. Bull Earthquake Eng* (2006) 4: 415.
- Mouroux et al. The European RISK-UE project: an advanced approach to earthquake risk scenarios. 13th World Conference on Earthquake Engineering Vancouver, B.C., Canada August 1-6, 2004 Paper No. 3329.
- FEMA-440 (2005), Improvement of Nonlinear Static Seismic Procedures, ATC-55 Draft, Washington.
- American Society of Civil Engineers (ASCE), “FEMA 356 - Prestandard and Commentary for the Seismic Rehabilitation of Building,” no. November, 2000.

Chapter 3

3. Seismic risk assessment

3.1. General aspects

Seismic risk assessment, as well as risk due to other natural phenomena such as floods, hurricanes, etc., essentially focuses on determining the expected losses in terms of physical damage to constructions (buildings or infrastructure), human and economic losses, direct and indirect type (business interruption), as a result of the damage suffered by the constructions.

Risk analysis can be carried out at different scales, from single building to territorial scale, for the purpose of implementing prevention and risk mitigation policies. A brief history of the development of the risk assessment over time is shown in (Scawthorn 2008).

It may concern the existing constructions but also be carried out to assess the costs of the entire lifecycle of constructions to build. In fact, the level of seismic protection that one wants to give to a building can arise from an overall cost analysis, which takes into account the initial costs plus the ones to be sustained to repair the building during its useful life, estimated on the basis of the outcome of seismic risk analysis.

In this way the so-called "*Risk-based optimum design*" (Vitiello et al. 2017) can be performed, representing the right compromise between the seismic protection level and the total costs to sustain during the life of the building.

In fig. 3.1 CI is the built cost, CFL is the expected present value of all future losses and CT is the total cost.

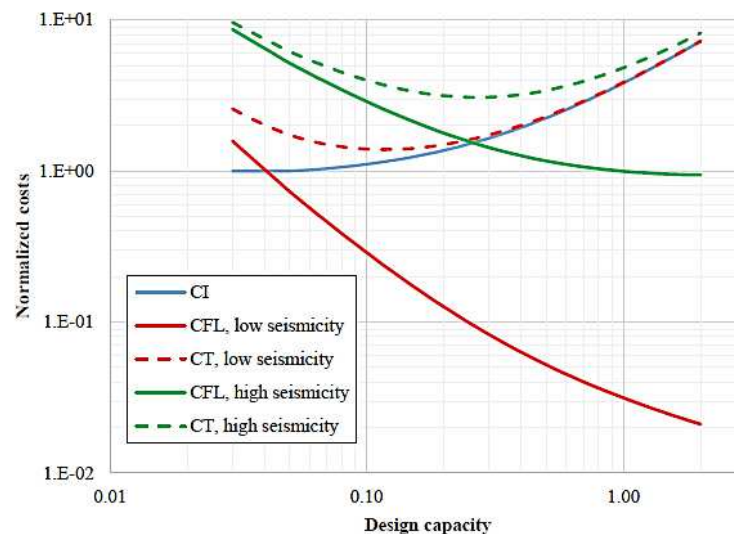


Fig. 3.1. Comparison of several relations between the level of design and the relative costs

In this evaluation a key role is played from the probability of exceedance P of a certain performance level in the exposure period T , takes as reference for the building, provided from eq. 3.1

$$P = 1 - e^{-\left(\frac{T}{TR}\right)} \quad (3.1)$$

where TR is the average return period of the ground motion for which the building should not exceed the performance level in the reference period T . In fact, if this probability is high because the reference period is large, it could be smart to increase the level of earthquake design to ensure less losses in the whole reference period.

With regard to existing buildings, the RCMF are the majority of the European built up heritage, so the assessment of seismic risk associated with them is particularly important. However, in Italy, it is very important to evaluate also the masonry heritage of which historical centres are rich.

The risk assessment procedure is the evaluation of three different components:

- *Vulnerability*
- *Seismic hazard*
- *Exposure in terms of people and economical value*

The vulnerability aspect has been widely discussed in chapters 1 and 2, so in the following discussion are treated mainly of the other aspects.

When assessing the risk, it is necessary to determine if the study is performed for preventive purposes (risk analysis) or for emergency management (scenario analysis).

In the case of a territorial study for preventive purposes, *risk analysis* is preferable as it cumulates the effects of all potential seismic sources in the area and provides a comparable assessment among the different municipalities interested by the evaluation. Instead, to analyse the aspects of civil emergency management, it is more significant a *scenario analysis*, as it reproduces a realistic distribution of the effects on the territory, which makes it possible to develop strategies for the post-earthquake intervention.

Once established the purpose, also changes the approach to use, probabilistic for risk analysis, deterministic for scenario analysis.

If the seismicity is studied in a *deterministic* fashion, by extracting one or more significant earthquakes from a historical seismicity catalogue or by simulating with numerical models the source mechanism and the propagation of seismic waves, a scenario analysis is performed and so the effects on the territory following a specific seismic event are evaluated.

In the *probabilistic* procedure (*Ellingwood 2001, Weatherill et al. 2013, Vargas et al. 2013*), however, the seismic risk represents the probability that a structure (or a portfolio of buildings)

exceeds a predetermined limit state (damage level) due to a given earthquake (event) over a fixed period. A comparison between the two approaches can be found in (*Kirchsteiger 1999, McGuire 2001*).

Once know the vulnerability level and the seismic hazard of the area under consideration, i.e. the characteristics of the expected seismic event in the region and possibly differentiated to consider local amplification effects (microzonation), the distribution of damage can be estimated.

If the hazard study is conducted in probabilistic terms, also the losses have to be expressed probabilistically.

The framework of modern risk assessment is provided by the theorem of total probability (eq. 3.2):

$$P [\text{loss} > c] = \int_s \int_{LS} \int_d P [\text{Loss} > c \mid DS = d] P[DS = d \mid LS] P[LS \mid SI = s] P[SI = s] \quad (3.2)$$

where P is the loss exceedance rate given chaining some conditional probability distributions.

In the absence of significant data on exposure, reference may be made to typological risk, which can be defined as the unconditional probability of exceeding a given limit state, for a selected typology of buildings. Typological risk can hence be obtained from the convolution of fragility with hazard curves (leaving aside exposure), according to eq. 3.3:

$$P = \int_0^{\infty} \left| \frac{dH}{dPGA} \right| p(PGA) dPGA \quad (3.3)$$

where P_f is the typological risk, H is the hazard, expressed as the annual probability of exceeding a given level of PGA and $P_f(PGA)$ is the fragility, representing the probability of damage given a certain PGA.

In fig. 3.2 the probabilistic seismic risk assessment framework is summarized.

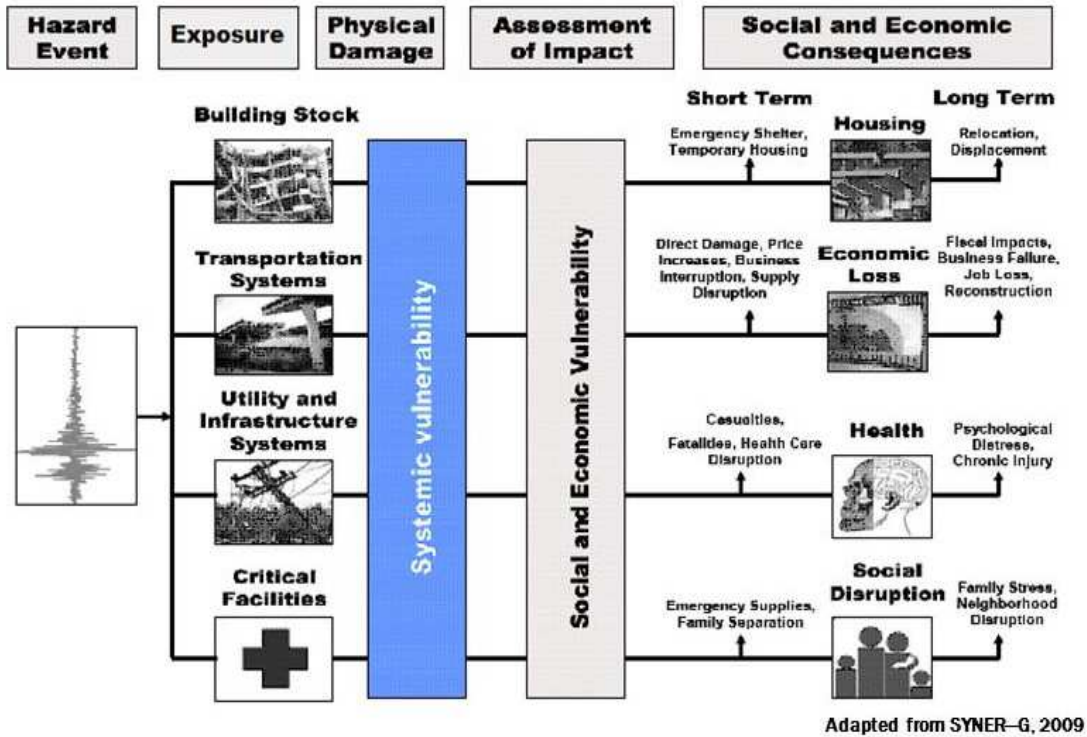


Fig. 3.2. Procedure for seismic risk assessment

From the vulnerability analysis, that assesses the level of seismic intensity for which the various damage states are attained, the fragility curves (intensity - likelihood of occurrence of damage levels) are obtained, in number equal to the damage states considered (usually: slight, moderate, extensive and complete damages).

The fragility curves (fig.3.3) Can be empirical or analytic derivation, and usually lognormal distribution is used.

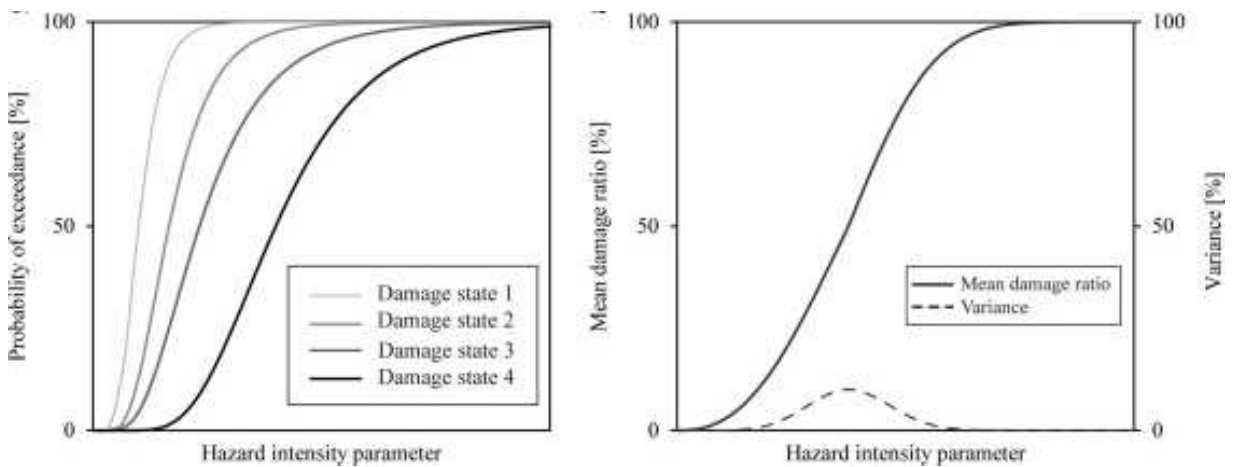


Figure 3.3. Typical fragility (a) and vulnerability curves (b)

By combining the fragility curves with the hazard level of the area, represented by the hazard curves (fig. 3.4) (Intensity - annual frequency of occurrence), the vulnerability curve (intensity measure-damage ratio) is obtained. For analytical representation of vulnerability curves, it is common to use the probabilistic beta distribution.

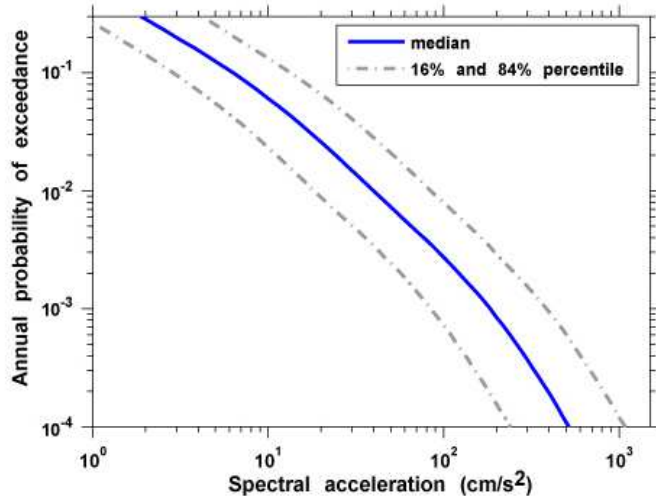


Figure 3.4. Typical hazard curves

The mean damage index, ranged between 0 and 1, represents the percentage of the replacing cost associated with a certain damage state. The mean DI can be calculated from the fragility curves (fig. 3.5) as the weighted average of the probabilities of occurrence of each damage state for a fixed seismic intensity value (eq. 3.4):

$$DI = \frac{1}{n} \sum_i K_i p_i \tag{3.4}$$

where n is the number of damage states D_k considered, p_i is the probability of occurrence of the damage state D_{ki} and K_i is its number.

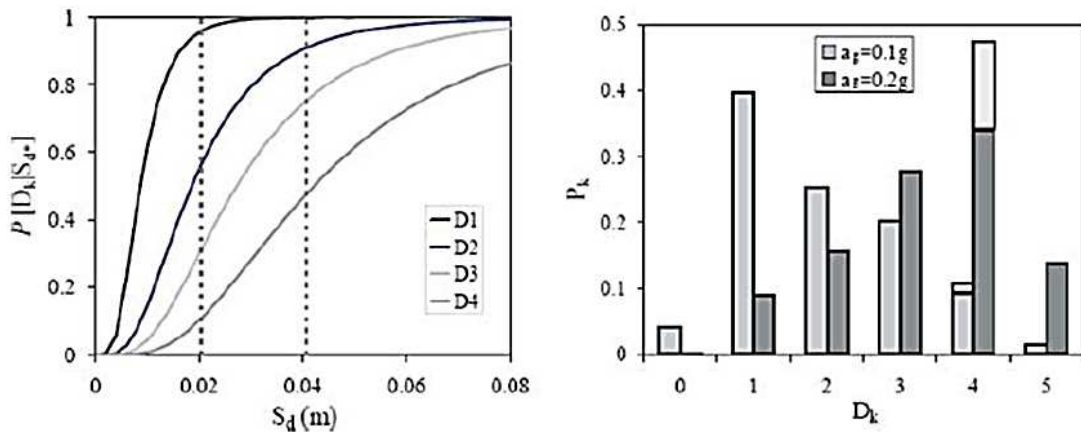


Figure 3.5. Probabilities from fragility curves

Therefore, considering the vulnerability curves and the exposure data (replacing costs, the number of people living /working in buildings), the expected economic and human losses can be determined.

Losses can be represented by means the loss curve (in fig. 3.6) with on the X axis the magnitude with which the loss has to be estimated (in example the economic loss, casualties etc.) and on the Y axis the annual frequency of occurrence λ (or the probability of exceedance PoE).

The curve can be represented also in terms of mean return period TR (the inverse of the annual frequency of occurrence), on the X axis, and losses, on the Y axes.



Figure 3.6. Typical loss curve

The annual frequency of exceedance of the performance level is obtained considering both structural fragility and seismic hazard through the *Total Probability Theorem* (eq. 3.5):

$$\lambda_{SL} = \int_0^{\infty} p_{SL}(s) \left| \frac{d\lambda(s)}{ds} \right| ds \quad (3.5)$$

where:

- S is an intensity level of the Intensity measure parameter (i.e. a value of PGA).
- p_{SL} is the probability of exceedance the LS for the intensity level equal to S, computed from the fragility curve.
- $\lambda(s)$ is the annual frequency for the intensity value S, obtained from the mean hazard curve.

The area underlying the loss curve is the average annual losses – AAL, that is the expected loss per year, averaged over many years. It is the mean of this probabilistic loss distribution is the average annual loss (AAL).

The AAL can be calculated in a discrete way by summing the product of each discrete loss state (L_i) for its annual frequency of occurrence (f_i), over all loss states (eq. 3.6):

$$AAL = \sum L_i \times \lambda_i \quad (3.6)$$

The occurrence AAL considers only losses due from the strongest event occurred in each year, while the aggregate AAL considers the losses due from all events occurred in each year.

Loss curves (EP curves) with very different shapes could provide about the same AAL.

The AAL an excellent and very popular measure of risk because it gives a rational size of the risk. Further in a simple insurance system, it is equal to the annual fair premium.

Also, the AAL ratio (AALR) can be calculated, that is a relative measure of the losses and it allows to compare losses coming from different portfolio.

More information about insurance models against earthquakes can be found in (*Porter et al. 2004, Asprone et al. 2013*).

3.2. Methods for risk assessment

In the practice, various framework and tools to assess the risk of built up area were developed. Some of them are described in (*Erdik et al. 2010*) and listed below:

- RISK-UE (*Mouroux et al. 2004*)
- HAZUS (*FEMA 1999*)
- SIGE (*Di Pasquale et al. 2004*)
- KOERILOSS (*Erdik et al. 2008*)
- ELER (*Erdik et al. 2008*)
- CAPRA (*Anderson et al. 2008*)
- SELENA (*Molina et al. 2005*)
- QUAKELOSS (*Larinov et al. 200*)

A comparative study between some tools can be find in (*Strasser et al. 2008, Spence et al. 2008*).

In the following part the RISK-UE, HAZUS and PEER (*Moehle et al. 2004*) frameworks are described in depth.

RISK-UE method

Risk-UE method provides three levels of analysis for assessing the seismic vulnerability of the European built up heritage (fig. 3.7).

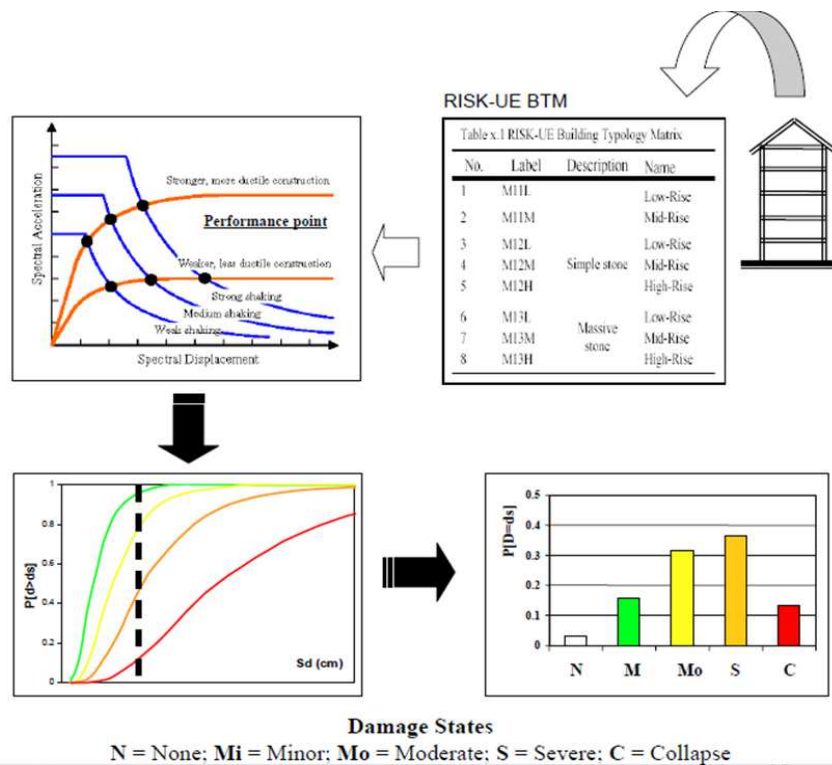


Figure 3.7. Risk-UE procedure for risk assessment

The first level is based solely on typological studies and on observed vulnerabilities, so it is therefore of macroseismic type. Once it is defined the belonging of the building to a class within the Building Typology Matrix (BTM) representative of the European built up heritage, the assessment is expressed in terms of a typological vulnerability index with which it is possible to obtain the representation of the damage, known the seismic input.

The 23 building classes of the BTM are defined on the base of the structural type (materials, resistant system, etc.). Further they are subdivided according to both the height and the seismic codes with which they were presumably designed. In the European area there are 4 classes (High-Code, Moderate-Code, Low-Code, Pre-Code) that express the quality of the structure in relation to the necessary seismic performance.

- Pre-Code are RC buildings designed in the absence of seismic regulations.
- Low-Code are instead RC buildings designed with a unique and arbitrary base shear and seismic coefficient, thus without proper seismic rules and structural details.
- Moderate-Code refers to RC buildings that do not fall into the category of Low-Code or.
- High-Code RC buildings have a seismic design level comparable to that defined in Eurocode 8. (WP1-Risk-EU project).

With regard the building height, RC buildings are divided into subgroups by three typical height classes:

- Low-rise (1-3 floors).
- Mid-rise (3-5 floors).
- High-rise (+ 6 floors).

Tab. 3.1. shows the subdivision adopted in Risk-UE for RC buildings.

Table 3.1. RC building classes in Risk-UE project

No.	Label	Description	Name	Height classes	
				No. of Stories	Height Range (m)
28	RC1L	RC moment frames	Low-Rise	1 – 2	≤ 6
29	RC1M		Mid-Rise	3 – 5	6 – 15
30	RC1H		High-Rise	6+	> 15
31	RC2L	RC shear walls	Low-Rise	1 – 2	≤ 6
32	RC2M		Mid-Rise	3 – 5	6 – 15
32	RC2H		High-Rise	6+	> 15
34	RC31L	Regularly infilled RC frames	Low-Rise	1 – 2	≤ 6
35	RC31M		Mid-Rise	3 – 5	6 – 15
36	RC31H		High-Rise	6+	> 15
37	RC32L	Irregular RC frames	Low-Rise	1 – 2	≤ 6
38	RC32M		Mid-Rise	3 – 5	6 – 15
39	RC32H		High-Rise	6+	> 15

The second level of the methodology is more detailed, in fact it provides the definition of geometry, dynamic and structural parameters of the building and it is based on the definition of capacity, demand and performance of the building. It makes use of both typological studies and simplified mechanical models.

Seismic vulnerability is assessed through the spectrum capacity model (*Freeman 1998*), so the damage scenario is defined by the intersection between the capacity spectrum and the demand spectrum that is representative of the selected earthquake. The demand spectrum is based on the 5% damped building-site specific response spectrum modified to account for structural behaviour out of the elastic domain.

This form of presentation is referred as ADRS - Acceleration-Displacement Response Spectra (*Mahaney et al. 1993*) and some methods to calculate the performance point are shown in chapter 2.

The third level requires the modelling of the building and detailed numerical analysis in order to obtain a capacity curve. The required computational effort is not suitable for a territorial study, but in a geographical area with homogeneous characteristics of the built environment it is possible to

analyse in depth a single building as prototype of a typology and then to extend the obtained results to the whole area under investigation.

Using finite element models, it is possible to define in a non-arbitrary way the limit states on the capacity curve (for example, as a fraction of the ultimate displacement), but associating them with particular condition in structural behaviour (activation of plastic hinges in some points of the structure).

HAZUS Method

Hazus method, like the Risk-UE, provides three assessment levels of increasing reliability.

Regardless of the level of analysis chosen, a building classification system based on the characteristics of the structure is provided (36 building typologies).

Four damage states are considered: Slight, Moderate, Extensive and Complete.

HAZUS damage functions for ground shaking have two basic components: capacity curves and fragility curves as shown in fig.3.8.

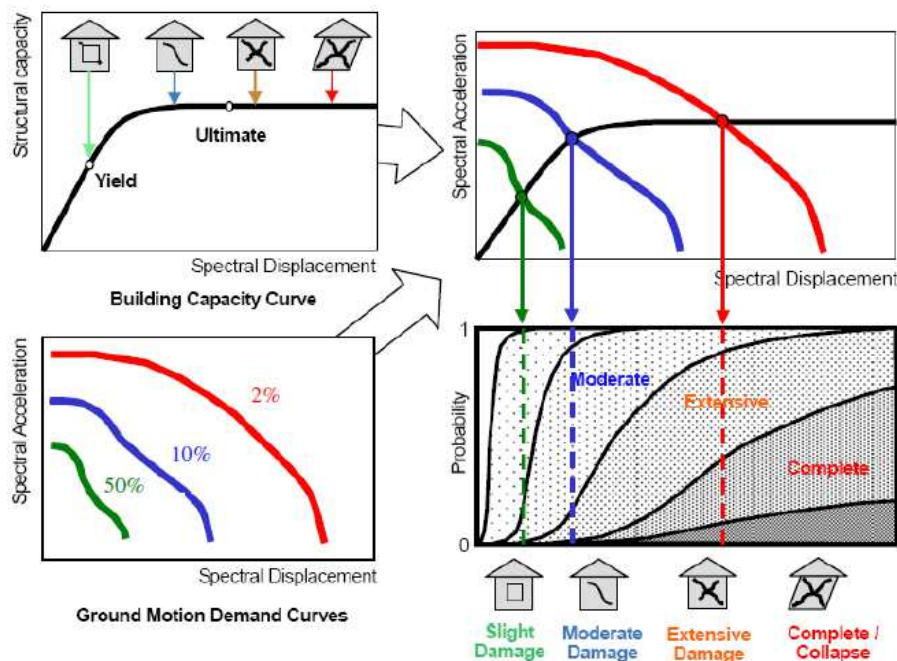


Figure 3.8. Hazus loss estimation framework

The HAZUS default building capacity curves depend on the level of seismic design: pre-code, low-code, moderate-code and high-code.

Capacity curves are defined by estimating parameters that influence design as the fundamental vibration period, over strength and ductility. Some of these parameters are obtained from the codes, once the reference level for the design is defined, others are considered as independent and assigned a priori according to the structural typology.

At the capacity curve, developed with tabulated values for each building class, it is associated lognormal uncertainty. The dispersion on the capacity curve is also provided through tabulated values and depend on the level of seismic design with which the building class is assumed to have been designed.

Capacity Spectrum Method is adopted to evaluate the demand corresponding to a given seismic intensity. To this end, the inelastic demand spectrum is obtained reducing the 5%-damped elastic response spectrum, obtained from the hazard analysis, by means of an effective damping value which is defined as the total energy dissipated by the building during peak earthquake response and is the sum of an elastic damping term, β_E , and a hysteretic damping term, β_H , associated with post-yield, inelastic response and influenced by ground motion duration. Then, peak response displacement and acceleration are determined from the intersection between the demand spectrum and the building's capacity curve.

HAZUS provides fragility curves for damage to structural system, non-structural components sensitive to drift and non-structural components (and contents) sensitive to acceleration. Fragility curves are lognormal functions defined by a median value of the demand parameter, which corresponds to the threshold of that damage state, and by the variability associated with that damage state.

A lognormal standard deviation is used to describe the total variability for structural damage state. In HAZUS it is often taken to include the variability of the ground motion as well as that of the building stock and also allows for variability of the capacity curve. A value of 0.5 for the natural log is a reasonable value if the seismic hazard is represented by uniform hazard response spectra that already contain specific allowance for variability of the input ground motion.

PEER framework

The PEER probabilistic framework (Moehle et al. 2004) identifies some basic blocks in the analytical assessment of the risk (fig. 3.9):

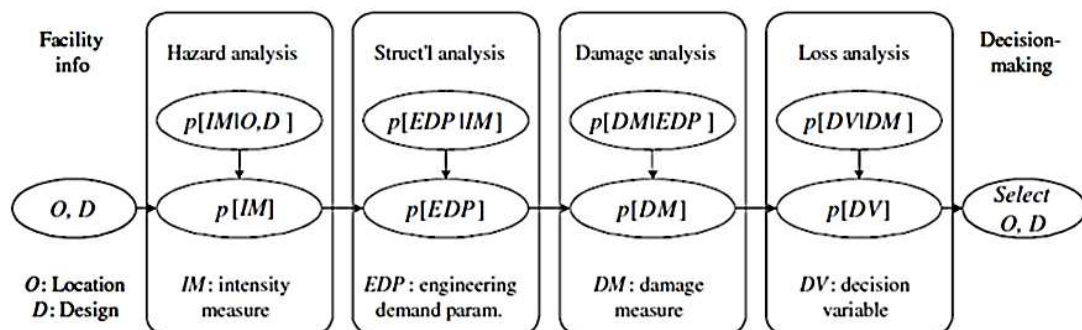


Figure 3.9. PEER probabilistic framework (after Cornell, Porter)

- Ground motion *Intensity Measure (IM)*

It defines in a probabilistic sense the salient features of the ground motion hazard that affect structural response. For standard earthquake intensity measures (such as peak ground acceleration or spectral acceleration) *IM* is obtained through conventional probabilistic seismic hazard analyses. Typically, *IM* is described as a mean annual probability of exceedance, $p[IM]$, which is specific to the location (*O*) and design characteristics (*D*) of the facility (fundamental period etc.).

- *Engineering Demand Parameters (EDP)*

They describe structural response in terms of deformations, accelerations, induced forces or other response quantities calculated by simulation of the building to the input ground motions. For buildings, the most common *EDPs* for the structural components and system are interstorey drift ratios, inelastic component deformations and associated forces. For non-structural components and contents, the most common are interstorey drift ratios, floor accelerations, and floor velocities. Relationships between *EDP* and *IM* are typically obtained through inelastic analyses, in order to obtain the conditional probability, $p(EDP|IM)$, which can then be integrated with the $p[IM]$ to calculate mean annual probabilities of exceeding the *EDPs*.

- *Damage Measures*

They describe the condition of the structure and its components (loss of capacity) in order to quantify the necessary repairs along with functional or life safety implications of the damage. The conditional probability relationships, $p(DM|EDP)$, can then be integrated with the *EDP* probability, $p(EDP)$, to give the mean annual probability of exceedance for the *DM*.

Collapse of older existing reinforced concrete buildings commonly results from the loss of vertical load-carrying capacity of columns. Research on shear critical columns has established relations between drift ratio at axial load failure and relevant parameters including column details and axial load.

The *DM* with respect the damage states can be determined in a deterministic way, through *EDP* threshold values, or in a probabilistic fashion by means fragility curves.

There exists a tremendous gap in knowledge to characterize all the necessary *DMs* and *EDP-DM* relations for buildings, for several reasons:

- Much prior testing emphasized strength and ductility capacity, with insufficient attention to damage measures such as residual crack width, spalling, permanent displacement, etc.
- Non-structural components and contents damage are the primary source of loss in most buildings during earthquakes, yet there is a paucity of experimental data on these.

- *Decision Variables*

Finally, given a detailed probabilistic description of damage, the process culminates with calculations of *Decision Variables* (fig. 3.10), which translate the damage into quantities that enter into risk management decisions, such as repair costs, downtime, and casualty rates. The evaluation of alternative performance metrics (DVs) dictates the choice of DMs and EDPs.

In a similar manner as done for the other variables, the *DVs* are determined by integrating the conditional probabilities of *DV* given *DM*, $p(DV|DM)$, with the mean annual *DM* probability of exceedance, $p(DM)$. The relationship $p(DV|DM)$ is described by *loss functions*.

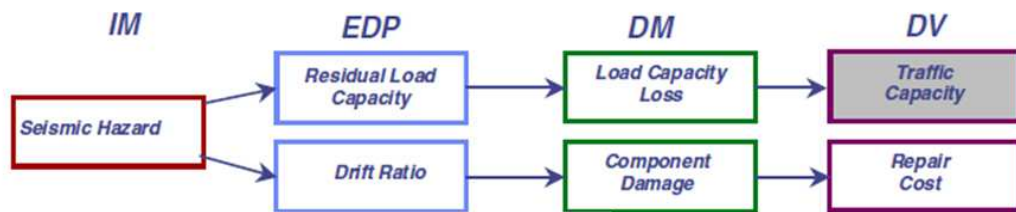


Figure 3.10. Flow chart for the calculation of the Decision variable

The relation between *EDPs* and *IMs* can be found by means the incremental dynamic analysis procedure (IDA) (Vamvatsikos *et al.* 2002 and 2004, Dolsek 2009), in which a building structure is subjected to an input ground motion having specified amplitude of the *IM* for which the response *EDP* is calculated. The process is repeated for increasing values of the *IM* by scaling the ground motion record, resulting in a continuous relation between the input *IM* and the resulting *EDP*.

This process is repeated for a series of input ground motion records that have characteristics consistent with the site conditions, resulting in a series of relations between *IM* and *EDP* (fig. 3.11). One can calculate relevant statistical relations (i.e. median and standard deviation) between *IM* and *EDP*, and establish the probability that the *EDP* will exceed a set value given *IM* (fragility curves).

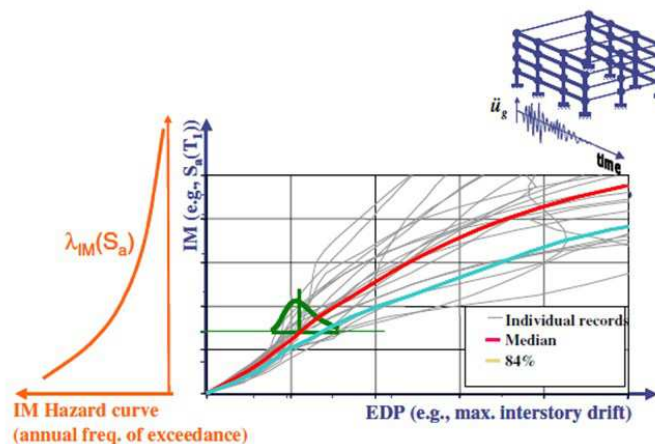


Figure 3.11. Plot of the results from an IDA analysis (after Krawinkler)

Typically, lognormal distributions are used to model the distribution of EDP at each hazard level. The statistical parameters of these lognormal distributions vary over hazard levels. Researchers used trendlines to express these parameters as functions of the hazard level. These trendlines were obtained by minimizing the error in estimating the sample mean and the sample standard deviation values at each hazard level (nonlinear regression technique on the IDA data).

Also, multi-IDA can be performed, involving multiple IM vs. EDP curves for a suit of acceleration records, which is used commonly in probabilistic seismic demand analysis (PSDA).

Another procedure alternative to the IDAs is the so-called “Cloud analysis” (*Tesfamariam et al. 2014*), in which different sets of ground motion records are selected to be compatible to several hazard levels. The cloud of points that establish the relation between the intensity measure and the demand parameter is shown in fig. 3.12.

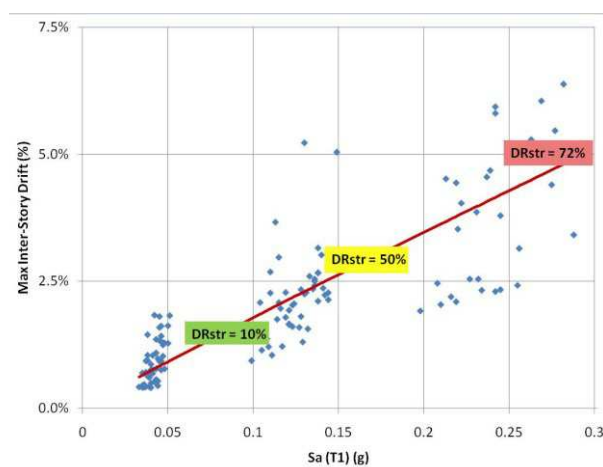


Figure 3.12. Plot of the results from a cloud analysis

For each ground motion the maximum EDP value is plotted in function of the relative IM value and then data are treated through simple or multiple linear or nonlinear regression.

3.3. Seismic hazard

The seismic hazard of a territory depends on the presence of seismogenic sources that can cause earthquakes with a certain intensity and frequency over time. Faults are characterized by a predominant focal mechanism that indicates the type and orientation of the fault, so if the tectonic regime responsible for its formation is compressive, extensible or translucent (fig. 3.13).

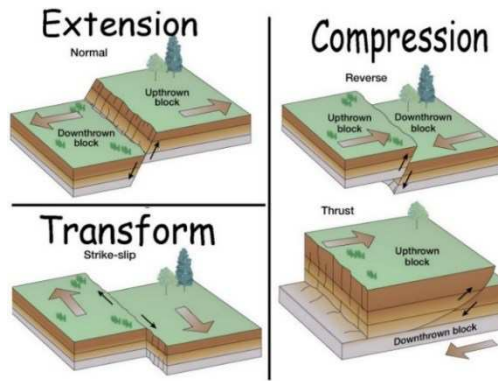


Figure 3.13. Fault mechanisms

All the methods used for hazard analysis are characterized by three basic elements:

- the catalogue of seismic events;
- seismogenic zoning;
- attenuation laws.

Initially, the method used for the estimation of hazard was the observational one, classifying as seismic areas those where earthquakes occurred. Further, depending on the magnitude of the earthquake, a category of seismicity was assigned to which corresponded a certain level of expected acceleration.

Other methods that have been developed as a result of advances in the research on the active faults systems are the probabilistic method (PSHA) (Cornell 1968, Kramer 1996) and the deterministic one (DSHA) (Bommer 2002, McGuire 2001).

In fig. 3.14 is summarized by the probabilistic method proposed by Cornell.

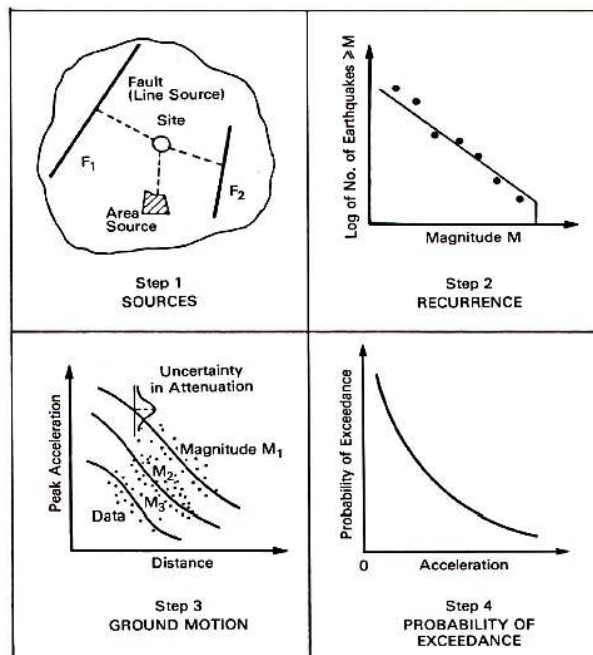


Figure 3.14. Probabilistic seismic hazard analysis (after Cornell 1968)

The probabilistic approach allows you to get the "forecasts" of future events in a given site, in particular, to determine the probability of having an event that exceeds a certain severity over a given time period, through probabilistic analysis of past events.

To this purpose, the effects of all potential seismogenic sources of the area are aggregated, producing, by means attenuation laws (*Douglas 2017*), representative maps of the expected seismic level at each point of the territory for predefined return times.

The result of these approaches is essentially the function of probabilistic distribution at the sites of the seismic parameters for earthquakes that may occur at the site itself.

The source zone method is one of the most used probabilistic methods for hazard analysis, also used for the hazard map of Italy (*Stucchi et al. 2011*). It is based on two hypotheses:

- Uniform space distribution of events in the seismogenic zones. This hypothesis is equivalent to assume that in a given source zone, the probability of an event occurs in a subzone (such as an area of 20 x 20 km) is the same for all the sub-zones in which the source zone can be subdivided. This is a very strong hypothesis, rarely verified, which can lead to significant errors in estimating the site hazard, especially when the size of the areas is significant.
- Poissonian distribution of the occurrences of events. This hypothesis is equivalent to assume that given a time interval Δt (e.g. 50 years), the average number of events in that range does not change over the centuries. This hypothesis is often not verified and may have significant consequences on the results.

Despite the limitations due to these two hypotheses, this approach is very often used for its simplicity and because it is applicable even when the amount of data base is not very large.

If we consider as base data the magnitude (M) of seismic events, remembering that every seismogenic zone is characterized by a single distribution of M and, for stationary hypotheses, by an average number of annual events (λ), the steps that characterize this procedure are the following:

- determination of sources on a tectonic basis;
- determination of the number of events grouped for magnitude classes N (M) for each zone;
- subdivision of each area into "small enough" areas to make irrelevant the location of the epicentre within it for the purposes of the site effects. Each small area is thus characterized by a distribution of the number of events N'(M) defined by eq. 3.7:

$$N'(M) = \frac{N(M) \cdot A_i}{A_{tot}} \quad (3.7)$$

- application of the attenuation law to the events in each small are, determining the significant events over a minimum threshold, for example in terms of A_{max} (maximum acceleration), and thus

determining the average number of events that annually affect the site (rate of occurrence for shaking classes);

- determination of the number of events that affect the site, grouped in acceleration classes $N(y)$ (y is the A_{max}/g ratio), by adding the contributions of all zones;

- the hazard curves are defined, thus the probability of annual occurrence is estimated for each value of seismic intensity.

Attenuation laws allow to determine the propagation of the phenomenon with the distance from the epicentre and, consequently, the variation of the parameters that define its severity. There are several types of attenuation models depending on some factors, in particular depending on the severity parameter that is considered: magnitude or intensity.

Considering the magnitude as a parameter, the attenuation laws existing in literature are very numerous, especially at international level, and they are much dispersed. The most reliable are those at the regional scale.

This model allows you to directly extract the values of many seismic parameters to the site (acceleration peak, peak velocity, shift peak, Arias intensity, spectral order, etc.). The main disadvantage of such attenuation models is that they need of accelerometric records.

In Italy, records are available only for the most recent events (since 1971) that are a little bit. Thus, it is only possible to determine a single medium law for the whole national territory.

The attenuation laws commonly used in Italy are those provided by *Ambraseys* (1995), *Ambraseys et al.* (1996, 2005), and *Sabetta and Pugliese* (1987, 1996).

are also valid for the horizontal spectral acceleration with generic vibration period, so they can be used, within the Cornell method, to obtain spectrum response with constant hazard.

The Ambraseys relationships (1995 and 1996) are calibrated over a larger database and can be applied in a greater range of data with respect the attenuation laws developed for Italy by Sabetta and Pugliese (1987) (fig.3.15).

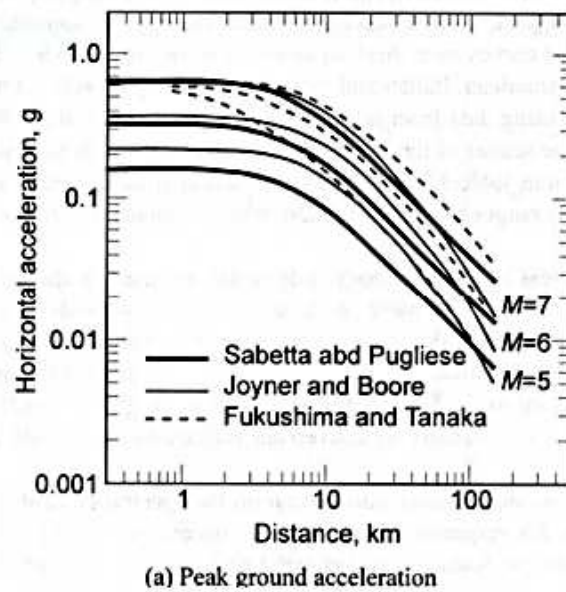


Figure 3.15. Attenuation laws

The *Sabetta e Pugliese* (1987) relationship is (eq. 3.8):

$$\log_{10}(Y) = a + bM + c * \log_{10} \sqrt{R^2 + h^2} + e1 * S1 + e2 * S2 \pm \sigma \quad (3.8)$$

where Y is the seismic parameter to be evaluated, M is magnitude, R is the distance from the epicenter, S1 and S2 are two parameters referring to the site from a geological point of view, while a, b, e1, e2, σ (standard deviation) are the parameters that vary according to the parameter to be determined.

Relations of Ambraseys et al. (1996) and Sabetta and Pugliese (1996) were used in the seismic hazard study conducted by the National Institute of Geophysics and Volcanology to carry out the national hazard map

Tab. 3.2 shows the relationships used for the different hazard maps made for Italy.

Table 3.2. Comparison of different hazard maps made for Italy

	GNDT - 1998	SSN – 1998	New hazard maps
<i>Background zones</i>	9 zones	None	None
<i>Soft edges</i>	Depth variable from 1 to 15 km	No	No
<i>Maximum magnitude</i>	Historical maximum + 0.3 for 28 ZS	Historical maximum	Historical maximum
<i>Completeness of the historical catalogue</i>	Statistical tests for 4 macroareas/30/	Statistical tests on only one macroarea /31/	Influence area for each ZS
<i>Recurrence laws</i>	individual seismicity rates + precautionary conditions	Gutenberg - Richter	Entire catalogue weighted with the reliability of the several periods /10/
<i>Attenuation laws (PGA and response spectra)</i>	Ambraseyes /9/ with st. dev.	Sabetta & Pugliese /8/ with st.dev.	Average between Ambraseyes /12/ and Sabetta & Pugliese /8/ with st. dev.
<i>Attenuation for volcanic zones (PGA)</i>	Ambraseyes /9/ without st. dev.	Sabetta and Pugliese /8/ without st.dev.	Specific attenuation for the Etna region
<i>Attenuation laws (MCS)</i>	Grandinori law differentiate for every ZS /14/	Blake /15/ modified	Grandinori law differentiate for every ZS /16/

In probabilistic methods, the typical hazard indicator is the probability of exceedance a given value of the parameter assumed to evaluate ground shaking (peak acceleration, spectral ordinate, etc.) over a given windows time T.

In the hypotheses of a stationary process, this quantity can also be expressed by the value of the seismic parameter having a given return period (the average time between an occurrence and the next). In this hypothesis the two dimensions are related by means eq. 3.1. and the probability of exceedance is constant whatever the instant from which the T is calculated.

Other indicators can be used, such as the expected average annual damage, referred to a standard building that gives an "integral" measure of the hazard, because it depends on the entire probabilistic distribution that describes the site hazard and thus it avoids the inconvenience of the dependency of the result from the reference return period chosen.

The expected average annual value of the cost due to damage to buildings resulting from future earthquakes can be assessed by considering earthquakes of all severities to the site, or only those

that can cause collapse or, in a complementary way, the only earthquakes that can cause damage but are not cause collapse.

This subdivision is particularly useful in order to distinguish situations characterized by relatively frequent but moderate energy events from those characterized by fairly rare but highly destructive. The starting point for calculating this indicator is, however, the distribution function of the A_{\max} ($F_y(y)$), which, as mentioned above, is considered in its entirety and not limited to a value depending on the return period.

The expected annual average damage, when calculated for real buildings, is commonly used as an indicator of the risk levels. However, it can also be a synthetic hazard measure if it is assessed with reference to the same standard building in all sites.

In the deterministic method, no reference is made to the probability of occurrence of any intensity value, but a reference earthquake (from historical catalogues, study of surrounding faults, PSHA disaggregation) can be assumed and indications are given about pairs Magnitude - Epicentre distance that allow to get it.

Thus, it is considered a single event on a certain site and its propagation in the surrounding areas, allowing to study its effects (scenario of damage). The shaking parameter typically used is the peak of acceleration due to the event considered.

Some Authors believe that the two methods are mutually exclusive, while others consider that a hazard assessment have to take into account both methods in an integrated manner.

In general, for the purpose of assessing seismic risk, all possible earthquakes can be taken into account in the different zones and seismogenic structures capable of generating significant events for that territory (probabilistic approach), and finally selecting critical ones for the management of the emergency (deterministic approach). Seismogenic areas are those that can be considered homogeneous from a geological and above all kinematic point of view.

The seismogenic model used in Italy, introduced specifically for the development of the hazard map dated 2004, is the so-called ZS9 zoning (*Meletti et al. 2004*) for which the Italian territory has been subdivided into 36 different zones, numbered from 901 to 936, plus 6 more zones, identified by "A" to "F" letters outside the national territory (A, B, C) or considered to have scarce influence (D, E, F) (fig. 3.16).

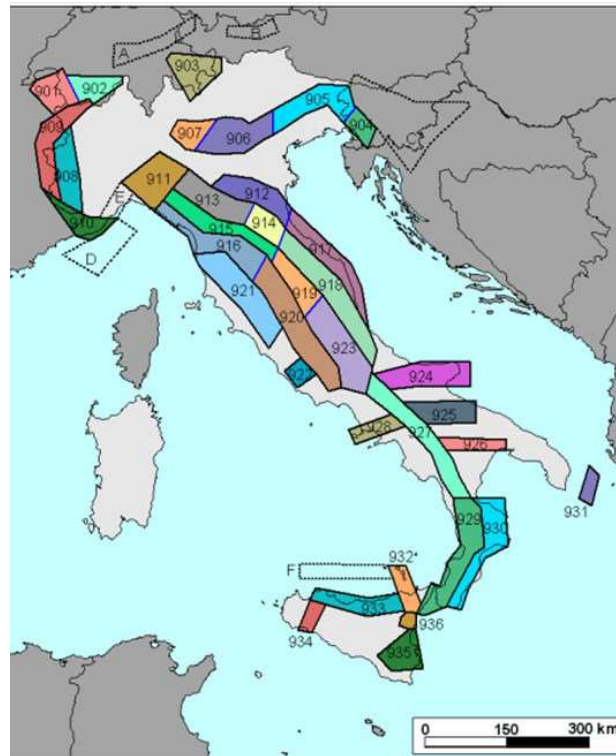


Figure 3.16. Seismogenic zones for Italy

For each seismogenic zone an estimation of the average depth of the hypocentre and of the prevalent fracture mechanism was performed. Further the degree of uncertainty in the definition of the boundaries of the zones was assessed.

Each seismogenic zone is characterized by its own seismicity defined through the distribution of events according to their severity.

Practically to develop a distribution function of the severity of events, first the events to consider among those catalogued as belonging to the area concerned have to be selected.

Taking as reference data the whole list of the events in the area could lead to significant errors in the evaluation due to the incompleteness of the catalogue itself. In fact, as the severity decreases, it is more likely that some events were not recorded in the chronicles of the time, while greater was the severity and higher is the likelihood that events were recorded, even if it occurred in a remote past. It is therefore necessary to fix limits, intervals of completeness depending on the severity (for intensity or magnitude classes). In practice, for each zone and for each severity class, the year from which the catalogue can reasonably be considered complete is fixed.

Two different representations were used in developing the Italian hazard map date 2004: an exponential event distribution and a discrete distribution by assigning the average annual number of events subdivided for magnitude classes.

Then two sets of intervals of completeness obtained with different methodologies were determined. These are "predominantly historical" and "predominantly statistical" intervals. As can be seen from

the names, the first ones are essentially based on an assessment of the completeness of historical event information, while for the second one, purely statistical procedures have been followed, starting from a hypothesis about the type of occurrence process (stationary process) and verifying in which time intervals this hypothesis is respected.

Fig. 3.17 shows the national hazard maps in terms of PGA and $S_a(T)$ (for $T = 0.4$ s), relative to the 50th percentile and for a probability of exceeding of 10% in 50 years.

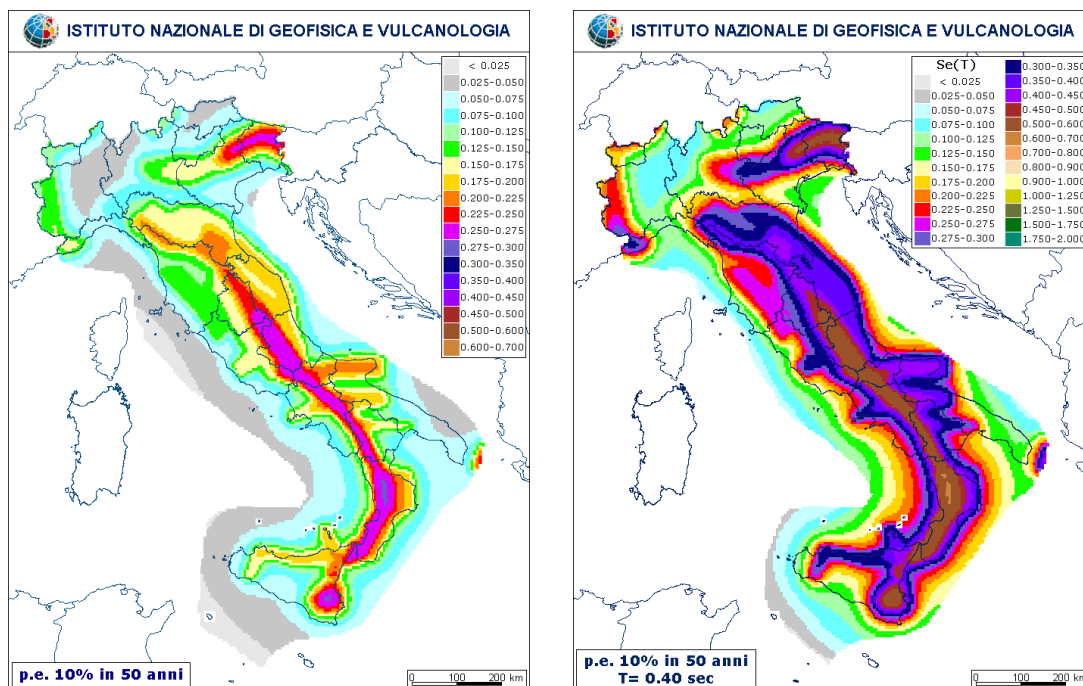


Figure 3.17. Italy hazard map in terms of PGA (left) and $S_a(T)$ (right) for a probability of exceedance of 10% in 50 years.

The maps provide, on a regular grid of 0.05° and in terms of % g, PGA and $S_a(T)$ values on horizontal rigid soil, relative to different probability of exceedance (9 values from 2% to 81 %) in 50 years and for each one is given the 50th percentile (median map), 16th and 84th percentile values (indicating the variability of estimations) of the probabilistic distribution of the maximum values obtained from hazard analysis.

Fig. 3.18 shows a zoom of the hazard map on the Marche Region.

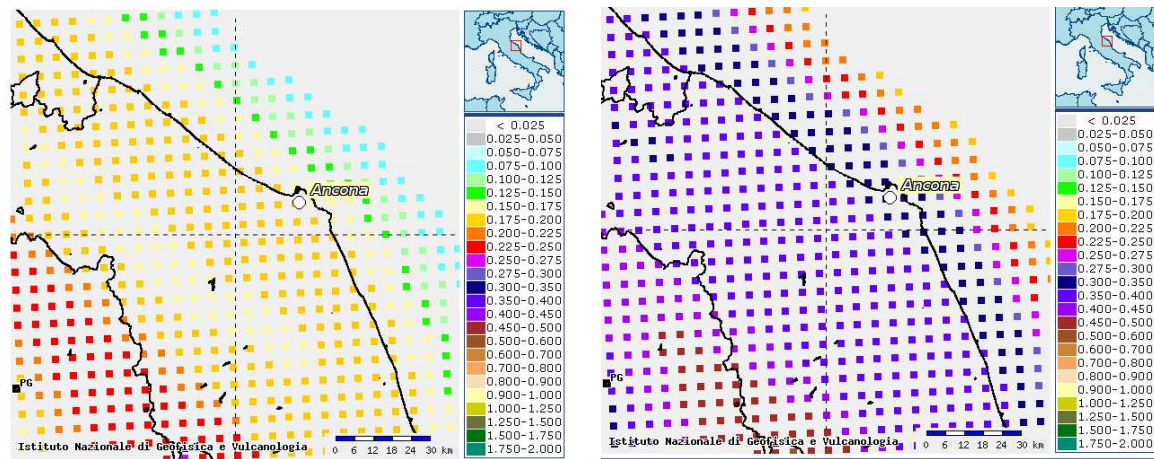


Figure 3.18. Hazard maps for the Marche region

It is worth noting that at a 0.40 sec vibration period, the spectral acceleration in a point increases of about the 50% compared to the ground values.

From hazard maps it is possible to obtain the hazard curve for a given point, which provides the PGA trend for several annual probabilities of exceedance and the relative values of magnitude and epicentral distance derived from the disaggregation analysis. This type of analysis allows the detection of the seismogenic source that mostly contributes to produce the estimated shaking value, in probabilistic terms, and it is also useful in microzonation analysis.

Fig. 3.19 shows, on the left side, the hazard curves in terms of PGA on horizontal rigid soil, while, on the right side, the disaggregation (Bazzurro et al. 1999) for a node of the grid located in the municipality of Ancona, assuming $P_{vr} = 10\%$ in 50 years. The source that mostly contributes to the hazard of the node is characterized by the following parameter values:

Magnitude = 5.11

Distance = 8.99 Km

Epsilon = 0.718

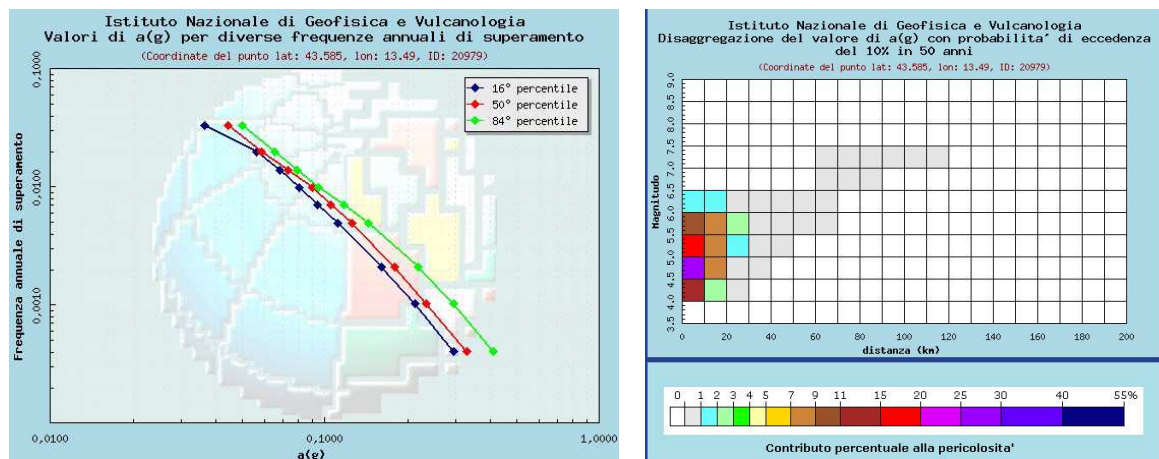


Figure 3.19. Hazard curves (left) and disaggregation data (right) for a grid node of the hazard map located in municipality of Ancona

From the maps in terms of $S_a(T)$, the UHS - Uniform Hazard Spectra (for the 16th, 50th and 84th percentile) can be derived for every node of the grid and for the several probabilities of exceedance in a reference period of 50 years (ie for several seismic return periods), evaluated for 10 vibration periods of engineering interest (from 0.1 to 2 sec). UHSs respect the actual level of the site hazards for all frequencies, separately calculating the hazard for frequency ranges but at the same time using the same source model, that is a regionally applicable spectral attenuation model.

Fig. 3.20 shows UHSs for the same grid node of fig. 3.19.

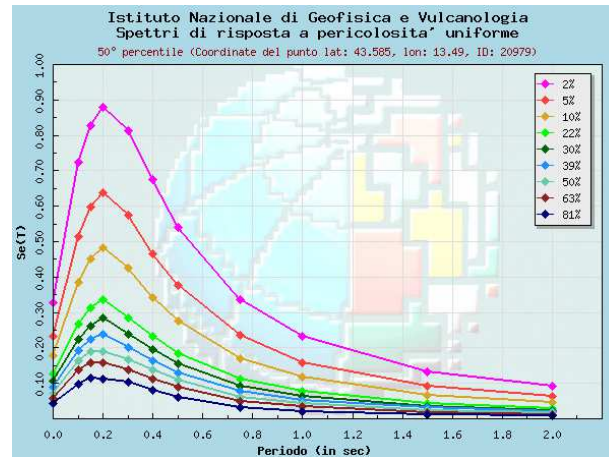


Figure 3.20. Uniform hazard spectra for the several probabilities of exceedance

It is to be noted that the hazard map relates to the horizontal bad rock, so it does not take into account the local amplification effects, due to subsoil type and topographic condition (fig. 3.21), that are of fundamental importance in determining the value of the seismic action on buildings.

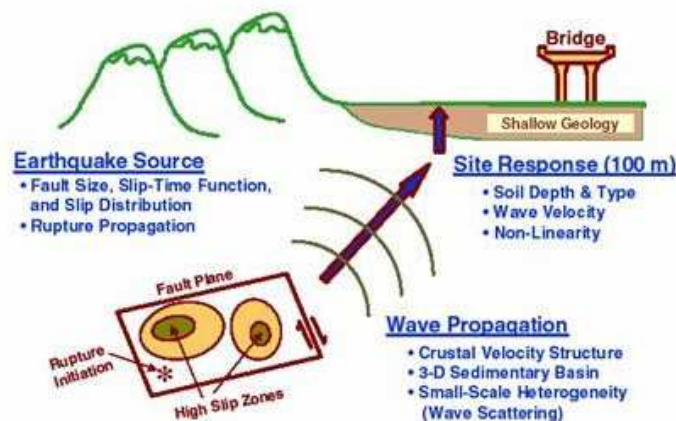


Figure 3.21. Site effect amplification of the ground motion

Local amplification effects can be considered in a simplified fashion, by using the stratigraphic and topographic coefficients provided by the regulations, or by conducting in situ investigations in order to determine the local seismic response.

In fig. 3.22 the response spectra relative to the several subsoil conditions provided by EC8 are shown.

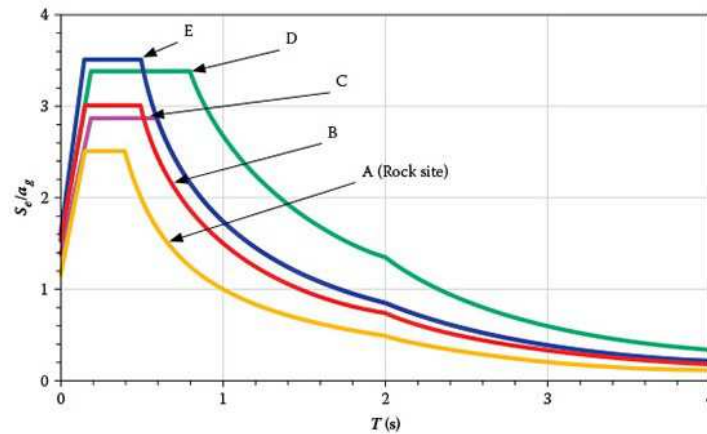


Figure 3.22. EC8 design spectra for different subsoil conditions

3.3.1. Intensity measure parameters

Several intensity parameters can be used in earthquake risk assessment. Their influence on the seismic response of buildings and on the consequent loss estimation can be found in (*Weatherill et al. 2015, Kohrangi et al. 2016*).

Some of them provide an objective measure of the energy released to the source, such as the global and local magnitude (Richter), but they do not give information about damage suffered to buildings. Other parameters such as PGA, PGV, Sa, Sd, HI (*Housner 1952*), AI (*Arias 1970*), however, have greater engineering value because they give an idea of the seismic action suffered by the building and so of the expected damage. Further several authors have pointed out as the HI and Sa provides a better correlation with the damage than the PGA.

Also, it is important the effect of the duration of the ground motion on the building response and damage, as described in (*Iervolino et al. 2006, Hancock et al. 2006, Chandramohan 2013, Raghunandan 2013*).

Finally, the macroseismic intensity (MI) provides a measure of the damage suffered by the buildings regardless of the energy released, so implicitly considers their vulnerability. Indeed, in a highly vulnerable context, even a weak earthquake can cause high damage and so the macroseismic intensity will have a high value.

There are several macroseismic scales developed over time: MM (Modified Mercalli), MCS (Mercalli, Cancani, Sieberg), MSK (Medvedev, Sponheuer, Karnik), EMS-98, correlated each other as shown in tab. 3.3 (*Musson et al. 2009*):

Table 3.3. Correlation between macroseismic scales

RF	EMS-98	MCS	EMS-98	MMI 56	EMS-98	MSK	EMS-98	JMA-96	EMS-98
1	1	1	1	1	1	1	1	0	1
2	2	2	2	2	2	2	2	1	2 or 3
3	3	3	3	3	3	3	3	2	4
4	4	4	4	4	4	4	4	3	4 or 5
5	5	5	5	5	5	5	5	4	5
6	5	6	6	6	6	6	6	5L	6
7	6	7	7	7	7	7	7	5U	7
8	7 or 8	8	8	8	8	8	8	6L	8
9	9	9	9	9	9	9	9	6U	9 or 10
10	— ^a	10	10	10	10	10	10	7	11
		11	11	11	— ^a	11	11		
		12	— ^a	12	— ^a	12	— ^a		

^aThis intensity is defined in such a way that it relates to phenomena that do not represent strength of shaking, e.g. those due to surface faulting, or reaches a saturation point in the scale where total damage refers to total damage to buildings without antiseismic design

As a consequence of seismic events, macroseismic intensity is obtained from the detection of the damage suffered from the buildings, that are catalogued in vulnerability classes of the EMS-98 scale in example. Thus, the intensity is obtained crossing data (e.g. C class with damage level 4, then $I = IX$).

3.4. Physical damage

Physical damage relates to both structural and non-structural elements. For RC buildings it was investigated by several authors (*Park et al. 1985, Ghobarah et al. 1999, Cosenza et al. 2000*).

Physical damage should be correctly represented through a damage model able to take in to account the occurrence of the different damage states, determined through a clear description of structural and non-structural damage. Further to each limit state must be associated a threshold between the different damage conditions, that can be expressed according to several damage measure parameters.

Generally, threshold values of the 4 limit states (or performance levels) provided by the seismic Code such as EC8 and FEMA 273, can be associated with the 5 damage levels provided by the EMS-98 scale (*Grunthal 1998*), as shown in tab. 3.4, in order to classify the building into a vulnerability class of the macroseismic method and to develop vulnerability curves.

Table 3.4. Correlation between damage scales

DL_k EMS-98	DS_k	Damage description	<i>Eurocode</i>	<i>FEMA</i>
DL0	DS0	No damage	Fully operational	Operational
DL1	DS1	Slight		
DL2	DS2	Moderate	Operational	Immediate occupancy
DL3	DS3	Extensive	Operational	Damage control
DL4	DS4	Complete	Life safety	Life safety
DL5			Near collapse	Collapse prevention

DL1 of the EMS-98 scale can be equalled to DL0 and it is assumed that the system remains essentially elastic for this damage levels, thus it is usable without reparation.

DL3 and DL2 indicate respectively unusable buildings on long periods and those usable after simpler retrofitting or reparation.

DL4 indicates that the structure has suffered at least heavy damage, with low residual lateral strength and stiffness. Thus, DL4 is obviously considered hardly, or more often, not repairable.

A damage model should be adopted to differ damage states through quantitative thresholds.

In the EMS-98 scale the thresholds between the damage levels are not clearly defined because damage levels are determined by means the observed damage on structural and non-structural elements.

In literature (*Bramerini et al. 1995, Dolce et al. 2000*) several damage scales based on the damage index DI are provided. It can be assumed as the ratio between the repair cost and the total replacing cost for a construction.

Correlations between each damage level of the EMS-98 scale and the threshold values of the damage index are shown in tab.3.5.

Table 3.5. Correlation between EMS-98 damage scale and several damage index scales

<i>Damage levels EMS-98</i>	DI [%]				
	Bramerini et al (1995)	Dolce et al (2000)	HAZUS (1999)	ATC-13 (1985)	Park et al (1985)
D0	0.00	0.00	0.00	0.00	0.00
D1	0.01	0.035	0.02	0.05	0.10
D2	0.10	0.145	0.10	0.20	0.25
D3	0.35	0.305	0.50	0.55	0.40
D4	0.75	0.80	1.00	0.90	1.00
D5	1.00	1.00	1.00	1.00	1.00

The values in tab. 3.5 indicate the variability of the damage index due to the sensibility to local economic factor.

In (*Hill et al. 2008-a*) a comparison between damage scales is provided, while in (*Hill et al. 2008-b*) a critical review on the capacity of several damage scales to meet the needs of seismic loss estimation is done.

A correlation between the mean damage grade μ_D , employed in macroseismic method, and the damage index DI is provided in (*Giovinazzi et al. 2004*) as in eq. 3.9:

$$\mu_d = 5 * DI^{0.57} \quad (3.9)$$

While in analytical method for each limit state is associated an analytical characterization using a Damage Measure parameter (DM).

The main distinction in terms of DM is between local and global. The first is a structural response parameter due to single structural members, while the second is referred to whole structure.

The choice of local or global DM is strongly linked with the modelling and analysis methods used. For example, if the equivalent SDOF is considered as in CSM based methods, the limit states cannot be defined in a detailed way (e.g. based on members behaviour, local strains or hinge mechanisms, etc.) and so in these cases, the global DM will be defined in terms of simplified global parameters. Generally, the interstorey drift (ID) is considered as global DM because it is a good damage index for RCMF structures. Under earthquake shaking, building damage is primarily a function of the interstorey drift. In the inelastic range of the response, more severe damage would result from increased interstorey drift although lateral force would remain almost constant or even decrease. Hence, successful prediction of earthquake damage to buildings requires accurate estimation of the ID in the inelastic range.

To this aim capacity curves obtained from pushover provide a simple and reasonably accurate means of predicting inelastic building displacement response for damage estimation purposes.

Several authors (*Vona 2014, Ghobarah 2004*) provided thresholds values in terms of interstorey drift ratio (IDR) for the damage states (tab. 3.6).

Table 3.6. IDR thresholds for damage states of Nonductile RCMF structures

	DL0	DL1	DL2	DL3	DL4	DL5
<i>Ghobarah 2004</i>	0.1 %	0.2 %	0.5 %	0.8 %	1.0 %	> 1.0%
<i>Vona 2014</i>	0.1 %	0.25 %	0.5 %	1.0 %	1.5 %	> 1.5 %

It is worth noting as the values provided by (*Vona 2014*) are about the half of those provided by (*Ghobarah 2004*). Generally different thresholds of IDR are associated to different structural typologies, considering their different ductility member levels after their different structural responses.

With regard the *local DM parameters*, they could be the strain level in materials and the chord rotation in structural elements.

A good index for RC structures is the ductility ratio DR, that is the ratio between the ductility demand and capacity in columns and beams. In this case, some references for limit states thresholds could be the instructions contained in Codes, such as in EC8.

The IDR is a good structural and non-structural damage estimator, but in some cases, more reliable results could be reached considering the damage as a function of both IDR and the mean ductility ratio (i.e., in terms of chord rotation) in the structural elements for each floor. In (*Tesfamariam et al. 2015*) a framework to assess the seismic performance for non-Code conforming buildings is provided.

For columns and beams considered as primary components, the deformation for the DS3 performance level (Life safety) shall not exceed 75% of the ultimate value. Instead, if the DS1 must be considered to minimize cost and repair time for immediate occupancy, for columns and beams considered as primary components, the deformation shall not exceed 10% of the ultimate value. In tab. 3.7 DR thresholds obtained through NLDA in (*Vona 2014*) are shown.

Table 3.7. DR thresholds for damage states of Non-ductile RCMF structures

	DS0	DS1	DS2	DS3	DS4
<i>Vona 2014</i>	0 - 0.1 %	0.1 - 0.25 %	0.25 - 0.75 %	0.75 - 1.0 %	> 1.0 %

Fig. 3.23 (Masi et al) shows the response of several structural schemes of two storeys buildings (bare infilled and pilotis frames) in terms of IDR, effective acceleration (A_{eff}) and ductility ratio on columns for both external and internal frames.

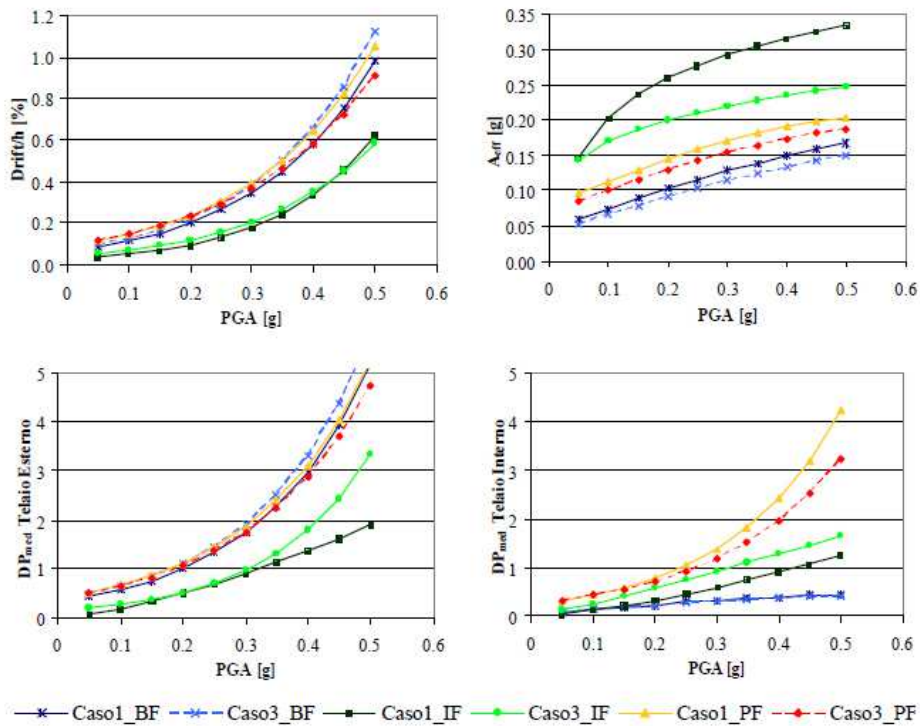


Figure 3.23. Response of several structural schemes of two storeys RC buildings, according to different EDP

In tab. 3.8 (Masi et al. 2012) the correlation coefficients between the IDR and the DR for both columns and beams (DR_C and DR_B respectively) are reported, by distinguishing between PRE and POST 1971 buildings and for 2, 4 and 8 storeys.

Table 3.8. Correlation coefficients values for PRE and POST 1971 RC buildings:

IDR- DR_C and IDR- DR_B

Ante71 and Post71 types: correlation coefficient values Drift- DRC_{max} , Drift- DRB_{max} .

	2 storey		4 storey		8 storey	
	DRC_{max}	DRB_{max}	DRC_{max}	DRB_{max}	DRC_{max}	DRB_{max}
<i>Ante71</i>						
BF	0.84	0.76	0.95	0.83	0.84	0.71
IF	0.80	0.77	0.94	0.84	0.90	0.83
PF	0.77	0.73	0.84	0.73	0.82	0.75
<i>Post71</i>						
BF	0.91	0.86	0.95	0.83	0.84	0.72
IF	0.85	0.77	0.94	0.84	0.89	0.80
PF	0.82	0.78	0.84	0.73	0.81	0.77

It is worth noting as the coefficients in most cases are quite close to 1, above all those relative to ID-DRC. Further the higher correlation is provided from the 4 storeys buildings in the cases of bare and infilled frames.

3.4.1. Fragility curves

Once hazard and damage model have been defined, the fragility curves can be developed for the damage states.

Fragility curves for existing RC frame were developed by several authors through analytical procedures, empirical and semi-empirical methods.

The curves are mainly based on analytical methods, while empirical studies are conditioned to the information available for this type of structures. The method that should be adopted to derive fragility curves essentially depends on the scale of the assessment (i.e. large scale or single building assessment) and from the quality and quantity of available data. When the assessment is performed for a class of buildings on a large scale, a statistical treatment of the damage data surveyed after earthquakes can be used (*Rossetto et al. 2003, Rota et al. 2008, Crowley et al. 2008, D'Ayala et al. 2011, Verderame et al. 2017*) providing an empirical relationship (*Rossetto et al. 2013*). Otherwise numerical analyses can be performed, providing analytical relationship (*Vona 2014, Rossetto et al 2005, Silva et al. 2014*). Furthermore, hybrid methods (*Yakut et al. 2005, Kappos 2016*) are employed when surveyed damage data are poor (i.e. statistical data are available only for some level of ground motion intensity) and they must be completed through numerical investigations and homogenised each other.

Although, when the vulnerability assessment of a single building is carried out, only the analytical procedure should be performed and the nonlinear response can be obtained through nonlinear static or dynamic analysis.

Analytical fragility of a building or of a single structural or non-structural component is the conditional probabilities of exceeding a specific damage states (d_s) at specified levels of ground motion (y_k):

$$P_{sk} [D_s > d_s | Y = y_k]$$

The conditional probability of being in a specific damage state can then defined as the difference between adjacent fragility curves.

Equation commonly used in literature to develop the fragility curves is:

$$p(\text{LS} | \text{IM} = x) = \Phi \left[\frac{\ln(x - \mu)}{\beta_R} \right] \quad (3.10)$$

where:

- $p(\text{LS} | \text{IM} = x)$ is the probability that a ground motion with $\text{IM} = x$ (or a Damage Parameter $(\text{DM}) = x$) will cause the reaching of the LS.
- $\Phi()$ is the standard normal Cumulative Distribution Function (CDF).
- μ is the median of the fragility function, the IM level (or DM value) with 50% probability of reaching the LS.
- β_R is the standard deviation of the $\ln(\text{IM})$ (or the $\ln(\text{DM})$), given by the sum of aleatoric and epistemic uncertainties (eq. 3.11):

$$\beta_R = \sqrt{\beta_{RR}^2 + \beta_{RU}^2} \quad (3.11)$$

where:

β_{RU} epistemic uncertainty in modelling.

β_{RR} is the aleatoric uncertainty calculated as in eq. 3.12:

$$\beta_{RR} = \sqrt{\beta_{DISa}^2 + \beta_C^2} \quad (3.12)$$

where:

β_{DISa} is the aleatoric uncertainty in seismic demand.

β_C is the aleatoric uncertainty in capacity, that should capture the uncertainty with respect to the assumption in the threshold values for the performance levels.

Eq. 3.10 implies that the IM values of ground motions which causes the achievement of the LS are lognormally distributed.

Analytical fragility curves can be obtained from both static and dynamic nonlinear analyses.

NLDAs are considered the best tool to obtain analytical fragility curves because they allow to consider the cyclic response of the structural members, even for increasing levels of the ground motions. Differently the monotonic analysis, namely nonlinear static or pushover, does not capture the cyclic decay of the mechanical parameters and usually lead to non-conservative results.

The aleatory uncertainty in the seismic demand is considered through the selection of several GMs, while the uncertainty in the structural capacity should be considered in the same way by generating several models with specific techniques (e.g. Monte Carlo or Latin Hypercube simulations).

In example in (Masi *et al.* 2012) many NLTHs on several configurations of RC frame (bare, infill and pilotis frames) were performed, highlighting the influence of the infill distributions on the fragility of this type of buildings.

In general, the analytical procedure request to develop the following step:

- Generation of adequate sample of structural models able to represent the real geometrical, structural and mechanical variability. Monte Carlo or other similar techniques should be used.
- Selection of ground motion and intensity measure. The seismic input plays a key role in fragility curves definition, thus if NLDAs are performed, accelerograms recorded during real earthquakes should be considered. Further the seismic intensity should be able to represent the potential damage due to ground motion. The seismic hazard is most commonly described by the pseudo-spectral acceleration corresponding to the fundamental mode ($S_a(T)$), or by the peak ground acceleration (PGA).
- Structural modelling and evaluation of the seismic response through nonlinear numerical analyses.

Parameters representative of the structural damage are evaluated such as the request in terms of interstorey drift (IDR), ductility demand in the structural members (chord rotation), maximum effective acceleration $A_{eff} = T_b/W$, if nonlinear dynamic analyses are performed, or the capacity curves, if pushover analyses are carried out.

- Definition of damage model.
- Construction of fragility curves. The way depends on the type of analysis performed.

In each step, a probabilistic approach should be used, because a high degree of uncertainty involved each of them. If structural capacity and seismic demand are random variables that roughly conform to either a normal or log-normal distribution then, following the central limit theorem, it can be shown that the composite performance outcome will be log-normally distributed.

In several cases, it is excessive consider probabilistic some topics, especially when their variation is negligible and not affect substantially the structural behaviour. Further, a probabilistic approach requires an accurate and extensive investigation in order to obtain reliable probability distributions.

In the fragility assessment, a critical choice consists on the Intensity Measure (IM) parameter, representative of the seismic action, and on the Damage Measure (DM), representative of the structural and non-structural damaging, which must be adequately correlated (*Elenas 2000, Kostinakis 2015, Massumi et al. 2016*).

As previously mentioned the IDR and the DR are good parameters to understand the damage suffered from the buildings. In (*Morfidis et al. 2013*) a comparative valuation of different damage measures for reinforced concrete buildings is illustrated.

With regard to IM, the Peak Ground Acceleration (PGA) is commonly used since it is the simplest parameter extracted by the GM records, even if sometimes it leads to large scattering when structures with a long fundamental period are considered (*Asprone et al. 2016*).

The choice on the adopting IM also depends on the type of analysis performed: if fragility curves are derived from pushover analyses, the spectral acceleration $S_a(T)$ (or displacement $S_d(T)$) at the

fundamental period is used. Typically, the elastic period is adopted, but it is not very representative of the dynamic behaviour when slightly damage occurred. Instead, if IDAs are performed, the choice may fall on the PGA, Sa(T), PGV or on integral parameters as the Arias Intensity (IA) and the Housner Intensity (IH) (Masi *et al.* 2012).

Further, IM must be well correlated with the damage parameters adopted. For example, for the inter-story drift the IH, IA and the Peak Ground Velocity (PGV) seem to provide better correlations than the PGA.

In (Masi *et al.* 2012) many NLDAs were performed in order to establish which is the IM parameter that provided the best correlation with the IDR for RCMF buildings. As shown in tab. 3.9 for the POST 1971 RCMF buildings, integral seismic parameters, such as Arias Intensity IA and Housner Intensity IH seem more effective with regard to peak or spectral parameters.

Table 3.9. Correlation coefficients between IDR and several IMs (after Masi *et al.* 2012).

	Pearson correlation coefficient		
	2 storey	4 storey	8 storey
Drift- I_H	0.92	0.90	0.83
Drift-PGA	0.36	0.23	0.19
Drift-PGV	0.90	0.89	0.83
Drift- I_A	0.75	0.67	0.64
Drift- t_d	0.22	0.42	0.45

However, the PGA is usually adopted as intensity measure. This choice came from the large use of this seismic parameter in the fragility assessment and then the obtained curves could be simply compared with those available in the literature.

Last generation of fragility curves use EDP parameters (i.e. the IDR) instead IM parameters.

3.4. Human and economic losses

Loss in terms of casualties/injuries and economic value are a consequence of the physical damage suffered from buildings and other constructions during earthquakes. In the following part is shown a brief description of some methods available to estimate human and economic losses.

- **Human losses**

Human losses estimation procedure evaluates the number of injuries, casualties etc. To this aim different methods can be used according to the scale of the assessment (territorial scale or urban scale).

Analytical human loss models use building damage and consequential physical damage (e.g. post-earthquake fire, explosion, hazmat release) as the starting point for the evaluation of casualties. This casualty assessment approach requires the knowledge of building occupancy data and the

probability of several levels of injury and death for different building types with given states of building damage.

Fig. 3.24 shows the correlations between the magnitude and the casualties occurred in some earthquakes (Vacareanu et al, 2004):

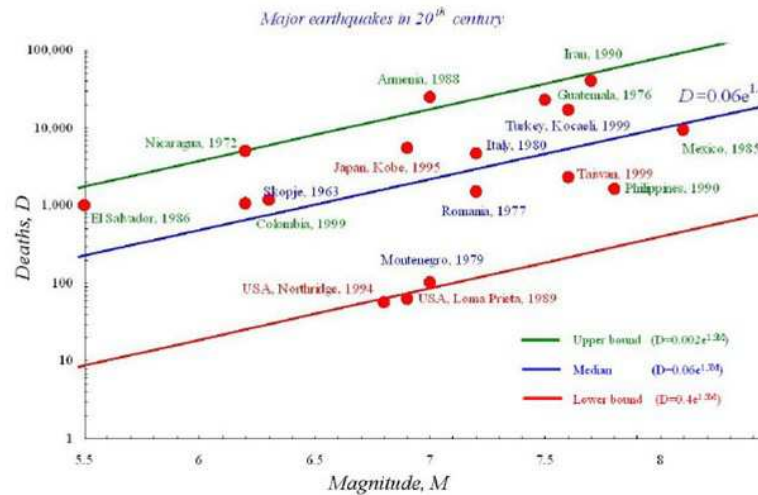


Figure 3.24. Correlation of deaths with earthquake magnitude (after Vacareanu et al., 2004)

A correlation between deaths and magnitude has been derived (eq. 3.13):

$$D = c e^{1.5M} \quad (3.13)$$

where D is the number of deaths, M is the magnitude of the earthquake and c is a coefficient assuming different values for lower, median and upper bounds (respectively $c = 0.002$, $c = 0.06$, $c = 0.4$). As it can be seen uncertainties in such correlations can reach two orders of magnitude.

Coburn and Spence Method (1992)

For the estimation of the fatalities due to structural damage (K_s parameter), which is the controlling factor for most destructive earthquakes, the equation 3.14 is proposed in (Coburn et al. 2002):

$$K_s = T_C [M1 * M2 * M3 * (M4 + M5 * (1 - M4))] \quad (3.14)$$

where:

- T_C is the total number of collapsed buildings.
- $M1$ is the factor taking into account regional variation of population per building.
- $M2$ is the factor taking into account variation of occupancy depending on the time.
- $M3$ is the factor taking into account percentage of trapped occupants under collapsed buildings.
- $M4$ is the factor taking into account different injury levels of trapped people.
- $M5$ is the factor taking into account change of injury levels of trapped people with time.

Using eq. 3.14 the casualty rates applicable immediately after the earthquake for masonry and reinforced concrete buildings are calculated.

Risk-UE Casualty - Vulnerability relationships

The casualty vulnerability relationships used in the Risk-UE project are based on the findings of (Bramerini *et al.* 1995) that studied the statistics on casualties, severely injured and homeless people in Italy. The study of Bramerini resulted in the correlations of tab. 3.10 between damage grades and effects of these on population:

Table 3.10. Correlation between damage level and their effects on the built environment and population

Effects to people and impact on the built environment		
BUILDINGS	Unusable	40% of buildings with damage grade 3 and 100% of buildings with damage grades 4 and 5
	Collapsed	Buildings with damage grade 5
PEOPLE	Homeless	100% of the population living in unusable buildings – casualties and severely injured
	Casualties and severely injured	30% of the population living in collapsed buildings

HAZUS method

The casualty estimation in Level 2 analysis is based on HAZUS-99 and HAZUS-MH methodology. The output from the module consists of a casualty breakdown by injury severity level, defined by a four-level injury severity scale (tab. 3.11).

Table 3.11. Description of injury severity levels

INJURY SEVERITY	INJURY DESCRIPTION
Level 1	Injuries requiring basic medical aid without requiring hospitalization
Level 2	Injuries requiring medical care and hospitalization, but not expected to progress into a life threatening status
Level 3	Injuries that pose an immediate life threatening condition if not treated adequately and expeditiously. The majority of these injuries result because of structural collapse and subsequent collapse or impairment of the occupants.
Level 4	Instantaneously killed or mortally injured

The HAZUS casualty rates were obtained by revising those suggested in ATC-13 (1985) using limited post-earthquake fatality data. The casualty model itself in fact is based on the models suggested by (Coburn *et al.* 1992, Murakami 1992, Shiono *et al.* 1991). However, unlike other approaches, the methodology is in event-tree format (fig. 3.25) and thus is capable of taking into account non-collapse related casualties.

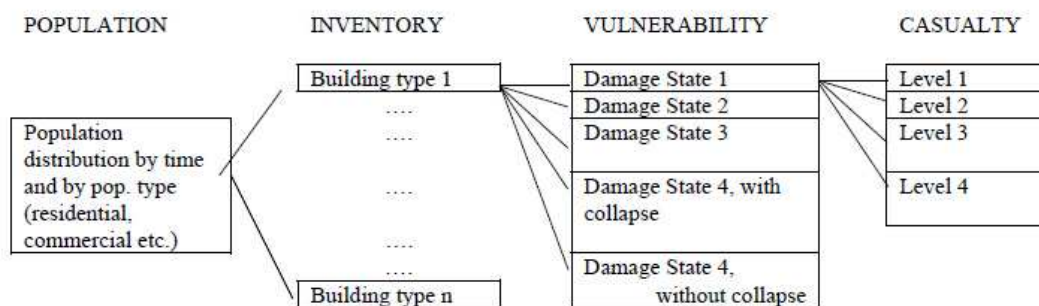


Figure 3.25. Event tree used for estimation of casualties in HAZUS-MH

To estimate the casualties from structural damage, it is needed to consider occupancy data for the time event, the probability p_k of being in the damage states (D1-slight, D2 moderate, D3 Extensive, D4 Complete, D5 complete with collapse structural damage) for the building typology and the probability for people involved in an earthquake to suffer a certain injury severity level. The latter depends on the casualty rate associated to p_k (tabs. 3.12 and 3.13).

Table 3.12. Casualty rates for RCMF structures (HAZUS 99)

Table 34. Casualty rates for Reinforced Concrete Moment Frame Structures (HAZUS99)

Injury Severity	Casualty Rates for R/C structures (%)			
	Slight Damage	Moderate Damage	Extensive Damage	Complete Damage
Severity 1	0.05	0.2	1	5* - 50**
Severity 2	0.005	0.02	0.1	1* - 10**
Severity 3	0	0	0.001	0.01* - 2**
Severity 4	0	0	0.001	0.01* - 2**

*the smaller values are related with partial collapse of the buildings

**the larger values are given for total collapse (the pancake type of collapse)

Table 3.13. Casualty rates for RCMF structures (HAZUS MH)

Table 36. Casualty rates for Reinforced Concrete Moment Frame Structures (HAZUS-MH)

Injury Severity	Casualty Rates for R/C structures (%)			
	Slight Damage	Moderate Damage	Extensive Damage	Complete Damage
Severity 1	0.05	0.25	1	5* - 40**
Severity 2	-	0.03	0.1	1* - 20**
Severity 3	-	-	0.001	0.01* - 5**
Severity 4	-	-	0.001	0.01* - 10**

*the smaller values are related with partial collapse of the buildings

**the larger values are given for total collapse (the pancake type of collapse)

Then, casualties for any given building type, building damage level and injury severity level can be calculated by eq. 3.15:

$$K_{ij} = PB * ND_j * CR_{ij} \quad (3.15)$$

where:

PB is the population per building

ND_j is the number of buildings with damages state j

CR_{ij} is the casualty rate for severity level i and damage state j

- **Economic losses**

Economic losses due to catastrophic events are of two types: direct, due to the repair cost to sustain in order to repair or rebuilt damaged constructions; indirect, due to business interruptions. The latter essentially depend on the type of the activity performed within the construction, while the repair cost is based on the local market for construction. Further the costs of both materials and manpower change over time.

Thus, it is not possible to develop a unique relation that is valid everywhere and that is constant over time.

In the practice, usually direct economic losses from building damages are estimated with the use of loss ratios (also known as damage indices DI) defined for each damage state. The loss ratio is defined as the ratio between repair and replacing costs of a structure (eq. 3.16).

$$DI = \frac{C}{C_{TOT}} \quad (3.16)$$

Thus, for the calculation of economic loss, replacing cost of each building is multiplied with the loss ratio which is determined from the building damage state.

Generally, a low damage level implies intervention only on non-structural components, while higher damage level implies more expansive intervention both on structural and non-structural components. When the damage level is upper than D4, from an economical point of view is better to demolish and rebuilt the building.

Thus, the economic model should consider the repair cost for each damage level (from DL 1 to DL 5) and the replacing cost for a typical building.

In (*KOERI 2003*) default values of direct economic loss for structural and non-structural systems are based on the following assumptions of the loss ratio corresponding to each state of damage:

- D1 damage state would correspond to a loss of 5% of replacement cost

- D2 damage state would correspond to a loss of 20% of replacement cost
- D3 damage state would correspond to a loss of 50% of replacement cost
- D4 damage state would correspond to a loss of 80% of replacement cost
- D5 damage state would correspond to a loss of 100% of replacement cost

In *HAZUS-MH (FEMA, 2003)* the correspondence is:

- Slight damage would be a loss of 2% of building's replacement cost
- Moderate damage would be a loss 10% of the building's replacement cost
- Extensive damage would be a loss of 50% of the building's replacement cost
- Complete damage would be a loss of 100% of the building's replacement cost.

For Italy, a good reference for the repair cost after earthquakes is given by (*Di Ludovico et al. 2016 a-b, De Martino et al. 2017*), where the analysis of the reconstruction process due to the quite recent L'Aquila 2009 earthquake is done.

References chapter 3

- Scawthorn, C. (2008) A Brief History of Seismic Risk Assessment (Chapter 1 in: Risk Assessment, Modeling, and Decision Support: Strategic Directions, edited by Ann Bostrom, Steven French and Sara Gottlieb), Springer
- Vitiello, U., Asprone, D., Di Ludovico, M. et al. Life-cycle cost optimization of the seismic retrofit of existing RC structures. *Bulletin of Earthquake Engineering* May 2017, Volume 15, Issue 5, pp 2245–2271.
- Ellingwood B.R. Earthquake risk assessment of building structures. *Reliability Engineering & System Safety* Volume 74, Issue 3, December 2001, Pages 251-262.
- Weatherill G. et al. Exploring Strategies for Portfolio Analysis in Probabilistic Seismic Loss Estimation. Congress on Recent Advances in Earthquake Engineering and Structural Dynamics. 28-30 August 2013, Vienna, Austria Paper No. 303
- Vargas Y. F. et al. Capacity, fragility and damage in reinforced concrete buildings: a probabilistic approach. *Bull Earthquake Eng* (2013) 11:2007–2032.
- Kirchsteiger C. On the use of probabilistic and deterministic methods in risk analysis. *Journal of Loss Prevention in the Process Industries* 12 (1999) 399–419.
- McGuire R.K. Deterministic vs. probabilistic earthquake hazards and risks. *Soil Dynamics and Earthquake Engineering* 21 (2001) 377–384.
- Porter, K.A., J.L. Beck, R.V. and Shaikhutdinov R. (2004). “Simplified performance based earthquake engineering estimation of economic risk for buildings”, *Earthquake Spectra*, 20 (4), 1239-1263.
- Asprone D. et al. Seismic insurance model for the Italian residential building stock. *Structural Safety*, 44 (2013), 70-79.
- Erdik M., Sesetyan K., Demircioglu M.B., Hancilar U., Zulfikar C. (2010) Rapid Earthquake Loss Assessment After Damaging Earthquakes. In: Garevski M., Ansal A. (eds) *Earthquake*

Engineering in Europe. Geotechnical, Geological, and Earthquake Engineering, vol 17. Springer, Dordrecht.

- Mouroux et al. The European RISK-UE project: an advanced approach to earthquake risk scenarios. 13th World Conference on Earthquake Engineering Vancouver, B.C., Canada August 1-6, 2004 Paper No. 3329
- HAZUS 99 “Earthquake Loss Estimation Methodology - Technical and User Manuals” Federal Emergency Management Agency, Washington, D.C. 1999.
- Di Pasquale G., Ferlito R., Orsini G., Papa F., Pizza A.G., Van Dyck J., Veneziano D. (2004) Seismic scenarios tools for emergency planning and management. In: Proceedings of the XXIX general assembly of the European seismological commission, Potsdam, Germany.
- Erdik M., Fahjan Y. (2006) Damage scenarios and damage evaluation. In: Oliveira CS, Roca A, Goula X (eds) Assessing and managing earthquake risk. Springer, Dordrecht, pp 213–237.
- Erdik M., Cagnan Z., Zulfikar C., Sesetyan K., Demircioglu M.B., Durukal E., Kariptas C. (2008) Development of rapid earthquake loss assessment methodologies for Euro-MED region. In: Proceedings of the, 14 world conference on earthquake engineering, Paper ID: S04-004
- Anderson E. (2008) Central American Probabilistic Risk Assessment (CAPRA): objectives, applications and potential benefits of an open access architecture, global risk forum, GRF Davos, August 2008.
- Molina S., Lindholm C. (2005) A logic tree extension of the capacity spectrum method developed to estimate seismic risk in Oslo, Norway. *J Earthq Eng* 9(6):877–897
- Larionov V., Frolova N., Ugarov A. (2000) Approaches to fragility evaluation and their application for operative forecast of earthquake consequences. In: Ragozin A (ed) All-Russian conference “Risk- 2000”. ANKIL, Moscow, pp 132–135
- Freeman S.A. “The Capacity Spectrum Method”. Proc. 11th ECEE, Paris 1998

- Mahaney J. A., Paret T.F., Kehoe B. E., and Freeman S. A., (1993), “The Capacity Spectrum Method for Evaluating Structural Response During the Loma Prieta Earthquake”, National Earthquake Conference, Memphis.
- Strasser F.O. A Comparative Study of European Earthquake Loss Estimation Tools for a Scenario in Istanbul. *Journal of Earthquake Engineering*, 12(S2):246–256, 200.
- Spence R. et al. Earthquake loss estimation and mitigation in Europe: a review and comparison of alternative approaches. The 14th World Conference on Earthquake Engineering October 12-17, 2008, Beijing, China
- Moehle et al. A framework methodology for performance-based earthquake engineering. 13th World Conference on Earthquake Engineering Vancouver, B.C., Canada August 1-6, 2004 Paper No. 679
- Vamvatsikos D. and Cornell C. A. Incremental dynamic analysis, *Earthquake Engineering and Structural Dynamics*, 31(3): 491–514. 2002
- Vamvatsikos D. and Cornell C. A. Applied incremental dynamic analysis, *Earthquake Spectra*, 20(2): 523–553. 2004
- Dolsek M (2009) Incremental dynamic analysis with consideration of modeling uncertainties. *Earth Eng Struct Dyn* 38(6):805–825.
- Tesfamariam S. et al. Probabilistic seismic demand model for RC frame buildings using cloud analysis and incremental dynamic analysis, Tenth U.S. National Conference on Earthquake Engineering Frontiers of Earthquake Engineering, At Anchorage, Alaska 2014.
- Cornell C.A. Engineering seismic risk analysis. *Bulletin of the Seismological Society of America*. Vol. 58, No. 5, pp. 1583-1606. October, 1968
- Kramer S.L. (1996). *Geotechnical earthquake engineering*. Upper Saddle River, N.J., Prentice Hall.
- Bommer J.J. Deterministic vs. probabilistic seismic hazard assessment: an exaggerated and obstructive dichotomy. *J. Earth. Eng.*, 06, 43 (2002).

- McGuire R.K. Deterministic vs. probabilistic earthquake hazards and risks. *Soil Dynamics and Earthquake Engineering* Volume 21, Issue 5, July 2001, Pages 377-384.
- Douglas J. Ground motion prediction equations 1964 – 2017. Report of September, 2017.
- Stucchi et al., Seismic Hazard Assessment (2003–2009) for the Italian Building Code, *Bulletin of the Seismological Society of America*, Vol. 101, No. 4, pp. 1885–1911, August 2011
- Ambraseys N. N., 1995, The Prediction of Earthquake Peak Ground Acceleration in Europe, *Earthquake Engineering and Structural Dynamics*, Vol. 24, 467-490.
- Ambraseys N. N., Simpson K. A. and Bommer J. J. (1996). “Prediction of horizontal response spectra in Europe”, *Earth. Eng. Struct. Dyn.*, n.25, 371-400.
- Ambraseys N.N., Douglas J., Sarma S.K. and Smit P.M. (2005). “Equations for the Estimation of Strong Ground Motions from Shallow Crustal Earthquakes Using Data from Europe and the Middle East: Horizontal Peak Ground Acceleration and Spectral Acceleration”, *Bulletin of Earthquake Engineering*, vol. 3, pp. 1-73.
- Sabetta, F., Pugliese A. Attenuation of Peak Horizontal Acceleration and Velocity from Italian Strong-motion Records. *Bull. Seism. Soc. Am.* Vol. 77, 1987.
- Sabetta F. and Pugliese A. (1996). “Estimation of response spectra and simulation of nonstationary earthquake ground motions”, *Bulletin of Seismological Society of America*, 86-2, 337-352.
- Meletti C., Valensise G. (a cura di); 2004: Zonazione sismogenetica ZS9-App.2 al Rapporto Conclusivo. Gruppo di lavoro per la redazione della mappa di pericolosità sismica. INGV.
- Bazzurro P., Cornell C. A. (1999). Disaggregation of Seismic Hazard. *Bulletin of the Seismological Society of America*, 89(2), 501-520.
- Weatherill, G.A., Silva, V., Crowley, H. et al. Exploring the impact of spatial correlations and uncertainties for portfolio analysis in probabilistic seismic loss estimation. *Bull Earthquake Eng* (2015) 13: 957.

- Kohrangi M., Vamvatsikos D., Bazzurro P. (2016) Implications of Intensity Measure Selection for Seismic Loss Assessment of 3-D Buildings. *Earthquake Spectra*: November 2016, Vol. 32, No. 4, pp. 2167-2189.
- Housner G.W. (1952). "Spectrum intensities of strong-motion earthquakes", *Proc. Symp. On Earthquake and Blast Effects Structures*, Los Angeles, 1952.
- Arias A. (1970) A measure of earthquake intensity, in *Seismic design for nuclear power plants* (ed. R. J. Hansen), MIT Press, Cambridge, Massachusetts, 438–483.
- Iervolino, I., Manfredi, G., and Cosenza, E. (2006). "Ground motion duration effects on nonlinear seismic response." *Earthquake Engineering & Structural Dynamics*, 35(1), 21–38.
- Hancock, J., and Bommer, J. J. (2006). "A state-of-knowledge review of the influence of strong-motion duration on structural damage." *Earthquake Spectra*, 22, 827.
- Chandramohan R., Lin T., Baker J. W., and Deierlein G. G. (2013). "Influence of ground motion spectral shape and duration on seismic collapse risk." 10th International Conference on Urban Earthquake Engineering, Tokyo, Japan, 9p.
- Raghunandan M., and Liel A. B. (2013). "Effect of ground motion duration on earthquake-induced structural collapse." *Structural Safety*, 41, 119–133.
- Musson R.M.W., Grunthal G., Stucchi M. The comparison of macroseismic intensity scales. *J Seismol* (2010) 14:413–428.
- Park Y, Ang A, Wen Y. Seismic damage analysis of reinforced concrete buildings. *Journal of Structural Engineering*, ASCE, 1985; 3(4): 740-757.
- Ghobarah et al. Response-based damage assessment of structures. *Earthquake Engng. Struct. Dyn.* 28, 79–104 (1999).
- Cosenza E. et al. Damage indices and damage measures. *Progress in Structural Engineering and Materials* 2(1):50-59. 2000.

- Grunthal G. “European Macroseismic Scale”. Centre Européen de Géodynamique et de Séismologie, Luxembourg 1998; Vol. 15.
- Bramerini F., Di Pasquale G., Orsini G., Pugliese A., Romeo R., Sabetta F., “Rischio sismico del territorio italiano. Proposta per una metodologia e risultati preliminari”. SSN/RT/95/01, Rome, 1995 (In Italian).
- Dolce M. et al. Seismic vulnerability analysis and damage scenarios of Potenza. Conference: International Workshop on Seismic Risk and Earthquake Scenarios of Potenza, At Potenza, Italy. November 2000.
- HAZUS 99 “Earthquake Loss Estimation Methodology - Technical and User Manuals” Federal Emergency Management Agency, Washington, D.C. 1999.
- Hill M., Rossetto T., Comparison of building damage scales and damage descriptions for use in earthquake loss modelling in Europe, *Bull. Earthq. Eng.*, vol. 6, no. 2, pp. 335–365, May 2008.
- Hill M., Rossetto T., Do existing damage scales meet the needs of seismic loss estimation? The 14th World Conference on Earthquake Engineering October 12-17, 2008, Beijing, China.
- Giovinazzi S. and Lagomarsino S., “A Macroseismic Method for the Vulnerability Assessment of Buildings,” 13th World Conf. Earthq. Eng., no. 896, pp. 1–6, 2004.
- Vona M. “Fragility Curves of Existing RC Buildings Based on Specific Structural Performance Levels,” *Open J. Civ. Eng.*, vol. 4, no. 2, pp. 120–134, 2014.
- Ghobarah A. “On Drift Limits Associated with Different Damage Levels,” Proceedings of International Workshop on Performance-Based Seismic Design, Department of Civil Engineering, McMaster University, Bled, 28 June-1 July 2004.
- Tesfamariam S., Goda K. (2015) Seismic performance evaluation framework considering maximum and residual inter-story drift ratios: application to non-code conforming reinforced concrete buildings in Victoria, BC, Canada. *Front. Built Environ.* 1:18.

- Masi A. and Vona M., “Vulnerability assessment of gravity-load designed RC buildings: Evaluation of seismic capacity through non-linear dynamic analyses,” *Eng. Struct.*, vol. 45, pp. 257–269, Dec. 2012.
- Rossetto T., Elnashai A., Derivation of vulnerability functions for European-type RC structures based on observational data, *Engineering Structures*, 25, 1241–1263, 2003.
- Rota M., Penna A., and Strobbia C. L., “Processing Italian damage data to derive typological fragility curves,” *Soil Dyn. Earthq. Eng.*, vol. 28, no. 10–11, pp. 933–947, Oct. 2008.
- Colombi M., Borzi B., Crowley H., Onida M., Meroni F., Pinho R. (2008). Deriving vulnerability curves using Italian earthquake damage data, *Bulletin of Earthquake Engineering*, Volume 6, Number 3, pp. 485- 504.
- D’Ayala D. et al. Developing Empirical Collapse Fragility Functions for Global Building Types. *Earthquake Spectra*, Volume 27, No. 3, pages 775–795, August 2011.
- Verderame G.M. et al. Empirical fragility curves from damage data on RC buildings after the 2009 L’Aquila earthquake. *Bulletin of Earthquake Engineering*. April 2017, Volume 15, Issue 4, pp 1425–1450.
- Rossetto T., Ioannou I., Grant D.N., 2013. Existing empirical vulnerability and fragility functions: compendium and guide for selection. GEM Technical Report 2013-X, GEM Foundation, Pavia, Italy. Available from: www.nexus.globalquakemodel.org/gem-vulnerability/posts/
- Rossetto T. et al. New analytical procedure for the derivation of displacement-based vulnerability curves for populations of RC structures. *Engineering Structures* Volume 27, Issue 3, February 2005, Pages 397-409.
- Silva V. et al. Evaluation of analytical methodologies used to derive vulnerability functions. *Earthquake Engng Struct. Dyn.* 2014; 43:181–204
- Yakut et al. Displacement-Based Fragility Functions for Low- and Mid-rise Ordinary Concrete Buildings. *Earthquake Spectra*, Volume 21, No. 4, pages 901–927, November 2005.

- Kappos A. J., “An overview of the development of the hybrid method for seismic vulnerability assessment of buildings,” *Struct. Infrastruct. Eng.*, vol. 12, no. 12, pp. 1573–1584, Dec. 2016.
- Elenas A. Correlation between seismic acceleration parameters and overall structural damage indices of buildings. *Soil Dynamics and Earthquake Engineering* 20 (2000) 93 – 100.
- Kostinakis K. et al. Correlation between ground motion intensity measures and seismic damage of 3D R/C buildings. *Engineering Structures*, 82 (2015), 151 – 167.
- Massumi A. et al. The influence of seismic intensity parameters on structural damage of RC buildings using principal components analysis. *Applied Mathematical Modelling* 40 (2016) 2161–2176.
- Morfidis K.E. et al. Comparative evaluation of different damage measures for reinforced concrete buildings considering variable incident angles. 4 th ECCOMAS Thematic Conference on Computational Methods in Structural Dynamics and Earthquake Engineering COMPDYN 2013.
- Asprone D., De Risi R., and Manfredi G., “Defining structural robustness under seismic and simultaneous actions: an application to precast RC buildings,” *Bull. Earthq. Eng.*, vol. 14, no. 2, pp. 485–499, Feb. 2016.
- Vacareanu R., Lungu D., Aldea A., and Arion C.: WP07 Report. Seismic Risk Scenarios Handbook, Risk-UE Project, Bucharest, 50 pp., 2004.
- Coburn A., Spence R. (2002) *Earthquake protection*, 2nd edn. Wiley, Chichester.
- ATC-13 “Earthquake damage evaluation data for California”. Applied Technology Council, Redwood City, California, 1987.
- Murakami H. O., 1992. A simulation model to estimate human loss for occupants of collapsed buildings in an earthquake, in *Proc. Tenth World Conference on Earthquake Engineering*, Madrid, Spain, 5969–5974.

- Shiono K., Krimgold F., Ohta Y., 1991. A method for the estimation of earthquake fatalities and its applicability to the global macro-zonation of human casualty risk, in Proc. Fourth International Conference on Seismic Zonation, Stanford, CA, III, 277–284.
 - FEMA (2003) HAZUS-MH technical manual. Federal Emergency Management Agency, Washington, DC.
1. KOERI (2003), Earthquake risk assessment for the Istanbul metropolitan area, Report prepared by Dept. Earthq. Eng., Kandilli Observatory and Earth quake Research Institute, Bogazici University Press, Istanbul.
 2. Di Ludovico M, Prota A, Moroni C, Manfredi G, Dolce M (2016-a). Reconstruction process of damaged residential buildings outside the historical centres after L’Aquila earthquake—part I: “light damage” reconstruction. Bull Earthq Eng.
 3. Di Ludovico M, Prota A, Moroni C, Manfredi G, Dolce M (2016-b). Reconstruction process of damaged residential buildings outside historical centres after the L’quila earthquake—part II: “heavy damage” reconstruction. Bull Earthq Eng.
 4. De Martino G., Di Ludovico M., Prota A. et al. Estimation of repair costs for RC and masonry residential buildings based on damage data collected by post-earthquake visual inspection. Bull Earthquake Eng (2017) 15: 1681.

Chapter 4

4. The RC school building stock

4.1. The RC school building typology

School buildings safety represent a very important issue in Italy because most of them are old buildings usually not adequate to absolve their educational function and, more important, they can't be considered as safe places for students and teachers, as shown from the evidence. In fact, in the last years some schools collapsed under the excitation of earthquakes, the first one in the 2002 with the Molise EQ (Mw=5.8) (*Augenti et al. 2004*) that killed 27 children and their teacher, the second one just the last year with the Amatrice EQ (Mw=6.0) fortunately without casualties because the school was empty.

Fig. 4.1 shows the collapse of these school buildings, total in the first case and partial in the second one.



Figure 4.1. Collapses of school buildings: San Giuliano di Puglia, 2002 (left) and Amatrice, 2016 (right).

In both cases the schools were subjected to restoration interventions that introduced heavy elements in the masonry structures and so they increased the seismic action on the buildings.

It is worth noting that the enforce Italian seismic Code considers the school buildings as construction with relevant importance when earthquakes occur, thus they should be very safe place. The recent data provided on 2017 in *XVIII Lagambiente Report* indicate a general unsafe situation for the about 42.000 school buildings and 7.800.000 students.

In fact, most of schools were built before the 1974 (about the 65%), thus without seismic provisions. Further, schools built after 1974 can't be automatically considered seismic-resistant.

Up to the first part of '80s the Regulations considered only a little part of the Country as seismically dangerous and so many schools were built considering only vertical loads and without seismic resistance criteria, thus they have strong beams-weak columns, frames arranged only in one direction, joints without stirrups, etc. In the late '80s, with the spread of the seismic hazard classification to other zones, more schools with earthquake resistance criteria were built. In particular, the arrangement of seismic resistant elements in the plant was improved and the quantity of stirrups were increased in the columns and extended to the joints.

Unfortunately, are not available data that distinguish between RC and masonry school buildings, but it's realistic to assume that after the 1960 the most of built schools have a RC structure.

The 54% of schools is in seismically zones, most of them in those with the highest hazard.

Only the 8% is designed according to the modern seismic provisions.

Buildings subjected to retrofit intervention are about the 12% with a full retrofit and the 7% for the partial retrofit.

The 27% has been subjected to a vulnerability assessment.

In tab. 4.1 data are provided and subdivided for the Italian Region.

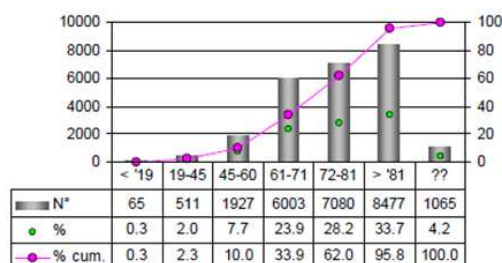
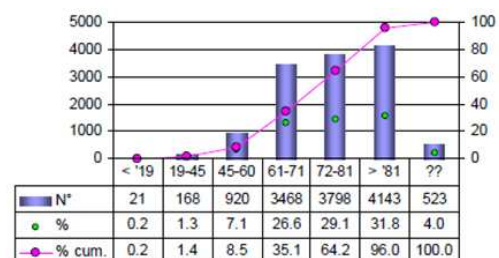
Table 4.1. Type of interventions carried out for Italian school buildings
(font: *XV Report on the safety of school buildings, 2017*)

Region	Seismic vulnerability assessment	Seismic microzonation	Improvement interventions	Retrofitting interventions
Abruzzo	51%	44%	9%	26%
Basilicata	29%	14%	15%	19%
Calabria	8%	47%	10%	5%
Campania	4%	7%	6%	4%
Emilia Romagna	8%	15%	5%	nr
Friuli Venezia Giulia	28%	76%	19%	10%
Lazio	22%	14%	3%	3%
Liguria	49%	12%	8%	3%
Lombardia	22%	32%	3,5%	nr
Marche	30%	48%	23%	12%
Molise	50%	39%	43%	29%
Piemonte	29%	8%	12%	8%
Puglia	11%	1%	5%	1%
Sicilia	nr	10%	4%	5%
Toscana	32%	55%	9%	6%
Umbria	59%	65%	25%	11%
Veneto	21%	31%	5%	nr
Media nazionale	27%	33%	12%	7%

It can be noted from data as the situation for Italian school buildings is quite critical, mostly regarding the percentages of retrofitting intervention realized. Further also the percentages of vulnerability evaluation performed is very low in some regions.

In the last 90's, the *LSU-96* project (*Cherubini et al. 1999*), and in the first 2000, the *SAVE* project (*Dolce et al. 2005*), performed evaluations on the conditions of the school heritage and on other relevant building typologies (hospitals etc.) located in the Southern Italy. Some relevant results of these projects are also showed below to better understand the characteristics of the Italian RC school building typology.

The RC school buildings were built in the most part after the 1960 (87.5%). In particular the 27% were built in the 60s, the 29% in the 70s and the 32% in the 80s (fig. 4.2).

Public RC buildings – All*Public RC buildings - Schools*

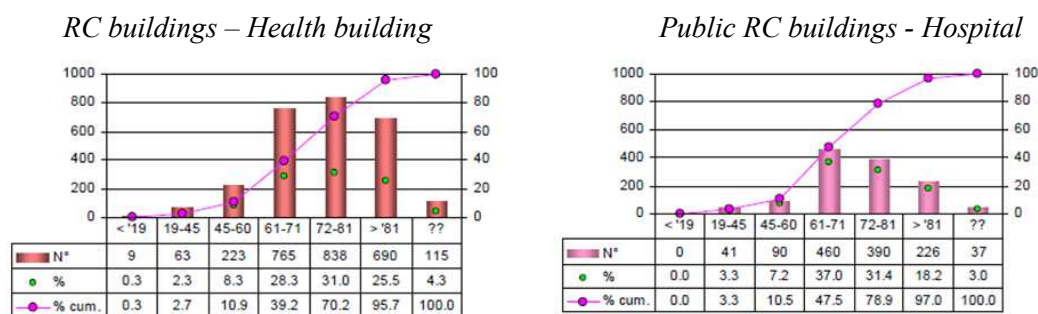


Figure 4.2. Age of school buildings (SAVE project – Task 2)

However, the buildings in which are located academies or conservators have a high frequency (about 30%) of buildings built between '46 and '60. Universities also show a tendency to be realized in more recently, as well as nursery and nursery schools, as opposed to elementary schools with about 40% of buildings built before the 1970s.

Most of RC school buildings have less than 3 floors (over 80%). Generally, increasing the education level (from maternity to university) also increases the number of storeys. This is a fairly obvious datum considering that increasing the education level also increases the user basin, while the number of buildings reduces. Similar argument is applied to volumetry.

RC schools mainly have interstorey heights ranging from 3.0 to 4.0 m (60.7% of buildings) with a good percentage of buildings (22%) with a maximum interstorey height between 4.0 and 5.0 m. With reference to the groupings made with respect to the education level of the school buildings, it is generally noted that nursery and nursery schools are characterized by lower interstorey height (more than 70% of the buildings have height less than 4 m), while higher interstorey are found for the upper education levels (approximately 50% of universities and over 60% of academies or conservatives have heights of over 4m).

They are made mainly of RC frames with consistent masonry infills (58.2%) and weak masonry infills (37.4%). About the groupings with respect to the education level, there are no significant differences in the use of the different types of vertical structures between the different types of schools under investigation.

The only relevant datum relates to the academies or conservators that for 23.5% are made with RC walls structures. Finally, universities made of RC frames have more frequently consistent infills (about 70%) with respect to other types of schools (fig. 4.3).

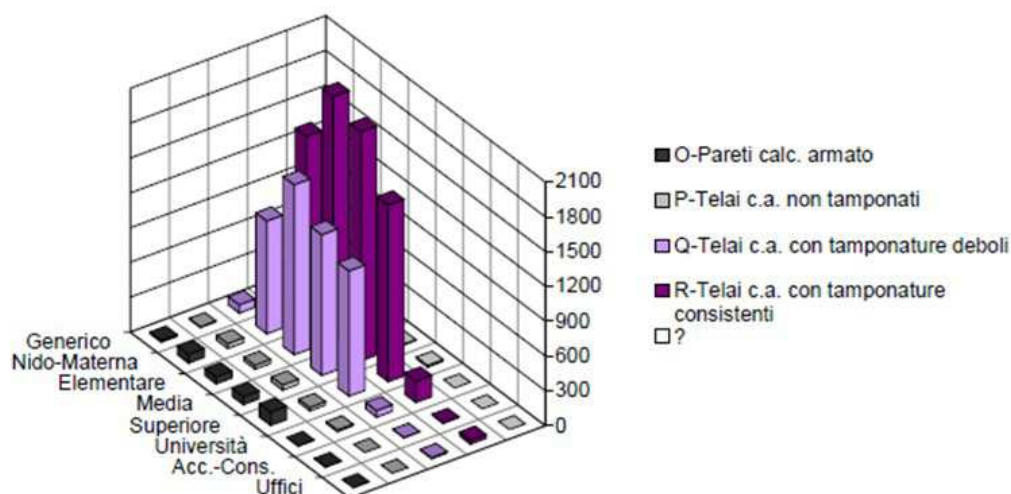


Figure 4.3. Structural typologies for different degree of education (SAVE project – Task 2)

From the examination of the data results a prevalence of buildings built before the 1980s and hence before the introduction and of the effective enforcement of the most recent national seismic codes. With respect the retrofitting interventions, in most cases (61.5%) RC school buildings have not been subject to any type of intervention or the period of the last significant intervention is not known (22.3%). Only 14.7% was subjected to maintenance intervention after 1981.

This situation agrees with the fact that RC school buildings. have been built mostly in recent times. Groupings the schools with respect to the education level, generally there are no distinctions between the situations found in the different types of schools.

However, there is a distinction between university buildings, which are characterized by more frequent buildings (74.8%) that weren't subjected to interventions, while primary schools are the more frequent buildings subjected to maintenance interventions (41.3%).

Further, data regarding interventions can be correlated with the one related to the construction period: buildings built in the past, on average, were subjected to major interventions and vice versa. Vulnerability of RC buildings was articulated into five qualitative levels, from low (B) to high (A), determined according to the construction type, construction period, and the seismic classification of the territory.

Assessing school buildings by means the 1st level GNDT method (fig. 4.4), it was determined that they belong to medium-high vulnerability class (43.2%) and to the high one (27.4%), while the percentage of buildings with a low vulnerability is insignificant (1%) (fig. 4.5).

CODICI IDENTIFICATIVI DELLE STRUTTURE VERTICALI DEGLI EDIFICI IN C.A. NELLA SCHEDA DI 1° LIV.	Età e classificazione sismica		Edifici costruiti prima del 1981, o in comuni non classificati	Edifici costruiti in comuni classificati con S=6	Edifici costruiti in comuni classificati con S=9 dopo il 1981	Edifici costruiti in comuni classificati con S=12 dopo il 1981
	Tipologia costruttiva					
O: strutture verticali in pareti in calcestruzzo armato	Telai in c.a. non tamponati o con tamponature deboli (P,Q)		*A	*MA	*M	*MB
P: telai in calcestruzzo armato non tamponati	Telai in c.a. con tamponature consistenti (R)		*MA (*M)	*M (*MB)	*MB	*MB
Q: telai in calcestruzzo armato con tamponature deboli	Pareti in c.a. (O)		*MB	*B	*B	*B
R: telai in cemento armato con tamponature consistenti						

Figure 4.4. Criteria to assign the vulnerability class based on few information (SAVE project – Task 2)

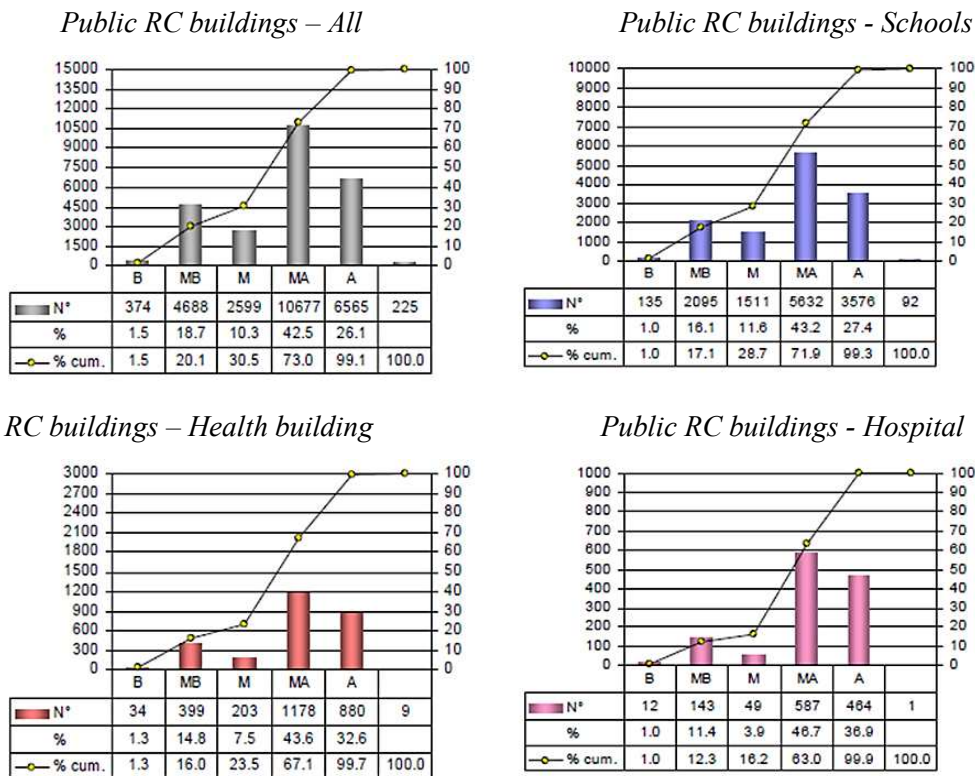


Figure 4.5. RC Building distributions in the vulnerability classes (SAVE project – Task 2)

Regarding the distinction made with respect to the education level, situations of particular importance are not highlighted (fig. 4.6). Academic or Conservatory buildings often belong to the medium-low and medium classes (almost half of the buildings), while the most vulnerable categories are represented by offices and elementary schools, where about 75% of the buildings belongs to the high and medium-high classes with the highest percentage of buildings in class A (about 30% of elementary schools).

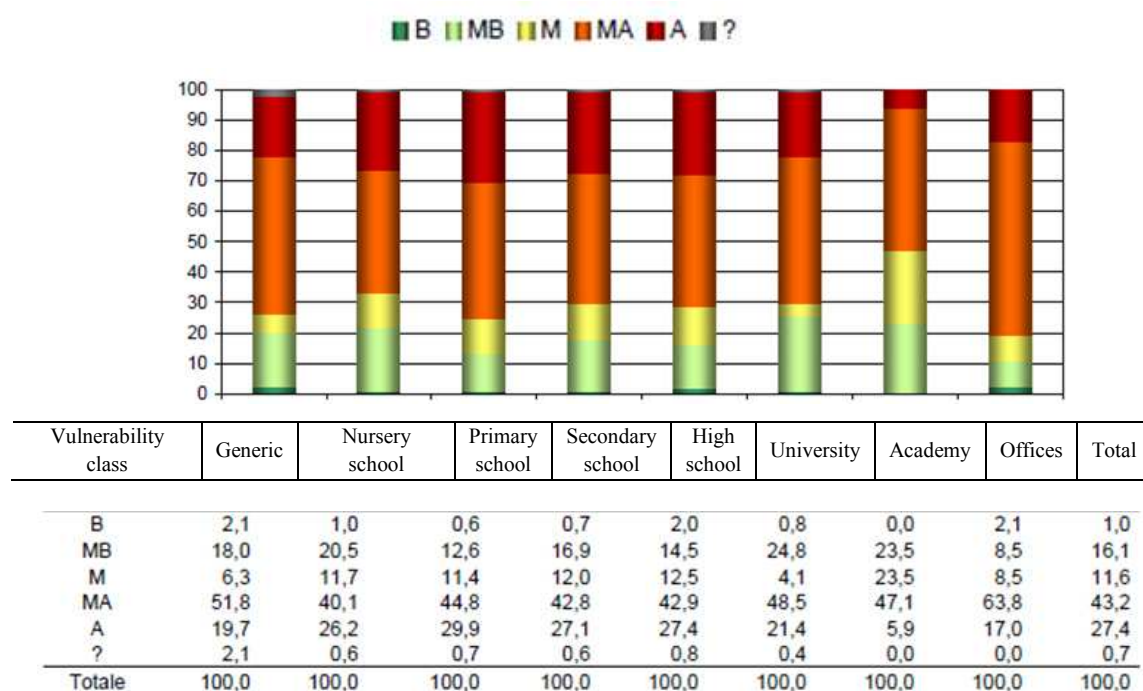


Figure 4.6. RC school building distributions in the vulnerability classes subdivided for education levels (SAVE project – Task 2)

Seismic vulnerability with respect to the collapse condition, evaluated according to the VC method (Dolce *et al.* 2005-*b*), and expressed in terms of ground acceleration that induces the ultimate state, is very variable. Very low values of about 0.1 g, indicating situations of severe structural deficiencies, were obtained from the evaluation.

This assessment, though not very robust due to the limited available data, still makes it quite clear the problem of the seismic safety of public RC buildings. It is significant if we also consider that about 30% of buildings have exceeded the age of 50 years and this certainly involves for many of them problems about quality and degradation of materials. Further about a 70% was surely built either in absence or with totally inadequate seismic criteria, especially with respect the latest conceptions introduced by the most recent seismic regulations (starting from the OPCM 3274 dated 2003).

Other authors investigated the vulnerability of Italian RC school buildings (Dolce *et al.* 2004, Grant *et al.* 2007, Borzi *et al.* 2013) highlighting the medium-high risk level and the needed of rehabilitation interventions.

Starting from this critical situation, the aim of the research performed by the author was to develop a rapid method (please see chapter 5 for a depth description) for large scale vulnerability assessment of school buildings. The rapid method allows to compare the vulnerabilities of many schools in few time and it can help the authorities to allocate correctly the few available economical resources.

In this case a vulnerability index method derived from numerical analyses was developed, taking as reference the 2nd level GNDT method.

To this purpose the building stock of high schools belonging to the Province of Ancona (Centre-East Italy) was analyzed, considering only the RC school buildings because they can be assumed as a typology with specific characteristics.

The homogeneity of typological characters is the basis of the application of empirical and semi-quantitative methods, aimed to identifying the representative building of a typological class (in example school buildings typology).

It is worth noting that secondary school complexes (fig. 4.7) often are composed from several buildings having different functions, in particular:

- The main building with the classrooms and the offices.
- The laboratories.
- The lecture halls.
- The gyms.

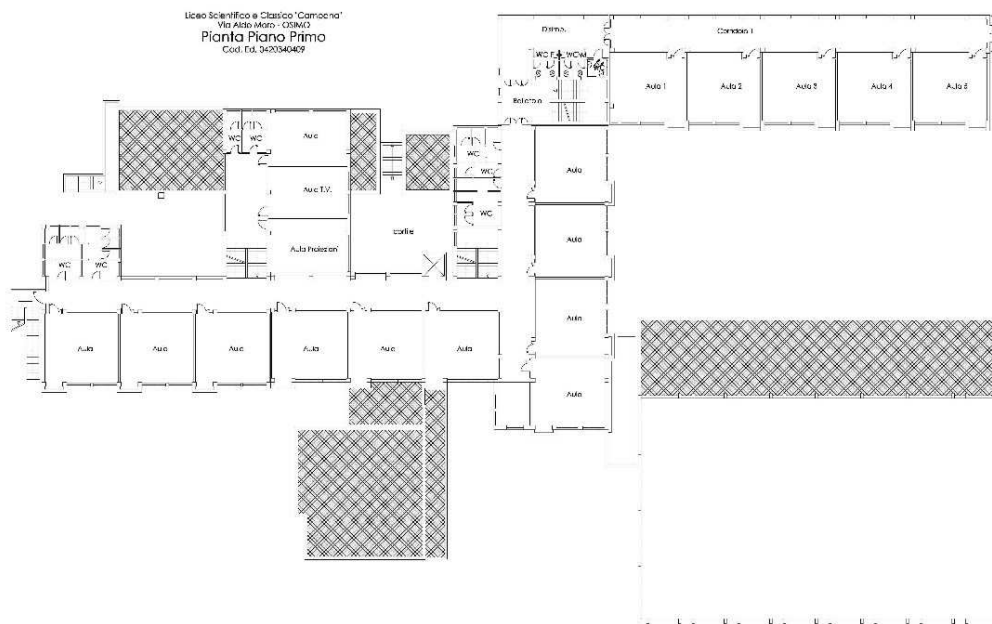


Figure 4.7. Typical high school complex: planar distribution of the several spaces (classrooms, laboratories, gym and lecture hall)

Each of these often is an independent building with own typological characteristics, structural and morphological, that identify a well-defined building typology. Sometimes classroom, laboratories and lecture halls can be within a unique building, but it is a very rare case.

In example gyms and lecture halls have a large and high space, so spans are wide and beams very high.

In this research we focus only on the main buildings (in the next called “school buildings”) because they are the most important for the seismic risk assessment, being the space where students and workers spend the most of time. Further they represent the most part (64%) of the 163 structural independent buildings that compose the whole stock of the Province of Ancona. The gyms are the 17%, the laboratories the 12%, the lecture halls the 6% and the boarding schools the 1%.

RC school buildings built up since the 50’s to the 90’s, have some common morphological characteristics, such as:

- The plant has an elongated shape, rectangular or similar (i.e. L and C shaped plant).
- Low rise (usually 3 or 4 storeys). This data is aligned with the data reported in the SAVE project in which is shown as the height of the schools increases with the order of the school (primary and secondary of first and second grade).
- Regular geometry along the height.
- Storeys with equal height (the inter storey is comprised between 3,00 and 3,50 meters).
- Infills with large windows in correspondence of classroom, while on the other sides there are small openings. Thus, the infills are irregular in their plant arrangement.
- Regular infill on the vertical direction.
- The roof is flat.

From the analysis of these characteristics can be approximately individuate the expected dynamic behaviour of this typology, overall regarding the elastic range of the structure, and some possible seismic vulnerabilities.

In fact, the regularity in the height suggest that the vibration mode could be linear with the height, while the irregularity in plant suggest the possible presence of torsional effects.

Further the large windows on the façade could weaken the relative frames and, further, short columns could be delimited.

4.2. Description of the building stock

The total number of RC school complexes investigated is 43, subdivided in 121 independent buildings from a structural point of view, given that in many cases there are separation joints within the same school building. Tab. 4.2 shows the number of schools belonging to each city of interest.

Tab. 4.2. Number of schools and f independent buildings for each city

<i>City</i>	<i>N° of school</i>	<i>N° of independent buildings</i>
Ancona	10	29
Arcevia	1	3
Fabriano	7	9
Falconara M.	2	5
Castelfidardo	1	3
Chiaravalle	1	2
Jesi	8	13
Loreto	2	6
Osimo	3	11
Sassoferrato	1	1
Senigallia	6	23
Total	43	105

In fig. 4.8 are highlighted the cities of the province of Ancona where the school buildings are located. In dark grey the cities with the higher number of school buildings (Ancona, Senigallia, Fabriano and Jesi).

**Figure 4.8.** Spatial distribution of school buildings in the province of Ancona

A description of each school building is reported in the **Appendix A**.

The RC structures are the most frequent (83%) typology within the stock, as shown in fig. 4.9, thus this endorse the choice to consider only this structural type leaving out masonry, steel and mixed structures.

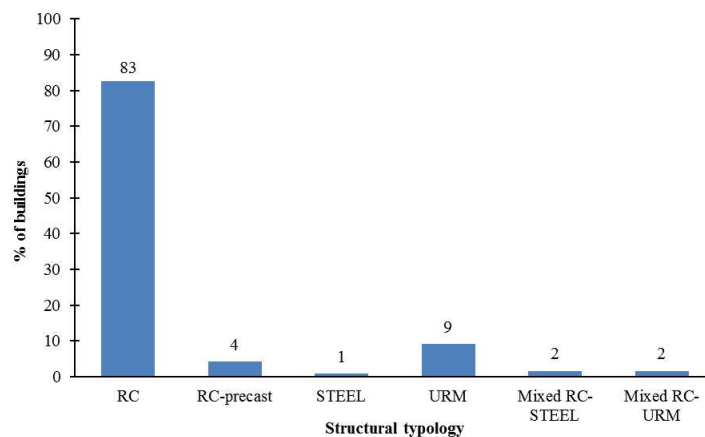


Figure 4.9. Structural typology for the building stock under investigation

Above all for masonry school buildings is very difficult to determine a typology, because usually they are historical buildings with unique architectural characteristics.

For most of the RC buildings (80%) the original design documents have been available.

The 92% of schools were built with the specific destination of school, that is a very good datum.

First the age of the buildings was found because is an essential parameter influencing the seismic vulnerability. In fact, the mechanical characteristics of concrete and steel, the structural details, such as: the type of steel, the quantity of longitudinal rebars and stirrups in beams, columns and joints, anchor length and live and seismic loads applied to the structures depend from the regulations and constructive customs of the period.

The set of schools analysed was built essentially in the period between the 50s and the 90s, as shown in fig. 4.10.

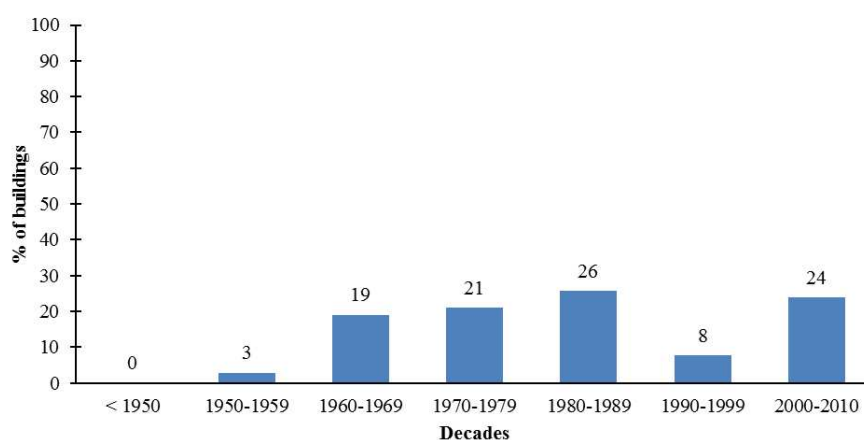


Figure 4.10. Age of RC school buildings

However, 24% of them were designed after the 2000, that is a of course a good information at least in terms of modernity of the stock under investigation. But, as shown in fig. 4.11, only the 7% were designed according to the capacity design and the seismic map introduced in the 2003. These schools have not taken in account in this study, because the aim was to evaluate buildings without or with low seismic resistant criteria.

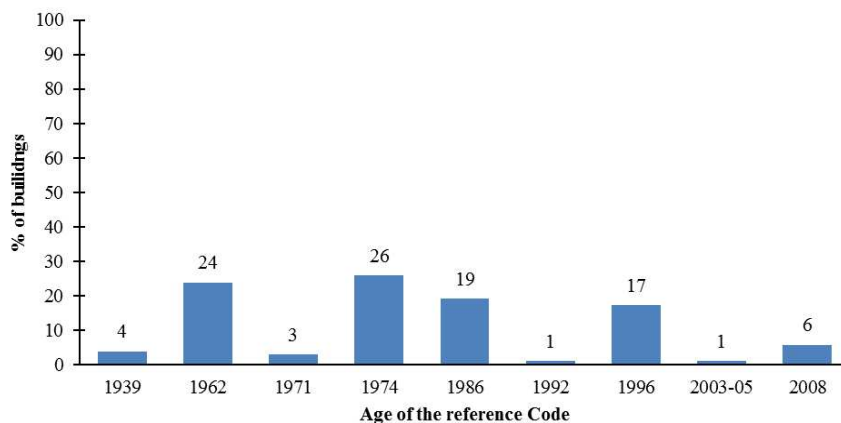


Figure 4.11. Reference Codes for RC school buildings

As described in chapter 1 for general RC buildings, from a regulatory point of view is possible to consider two main periods in which the schools were built, from the 1939 to 1974 (PRE 1974, 31% of buildings) and from 1974 to 2003 (POST 1974, 62%). The main differences between the two periods are in the type of steel used, from smooth to ribbed rebars during the '70, thus the mechanical characteristics and the grip with concrete surface were improved, and in the constructive details of the structural members, such as the minimum dimensions of the cross sections of structural members and the minimum quantity of longitudinal bars and stirrups.

Fig. 4.12 shows the frequencies of the several types of concrete and steel found in the design documents relative to the school buildings under investigation.

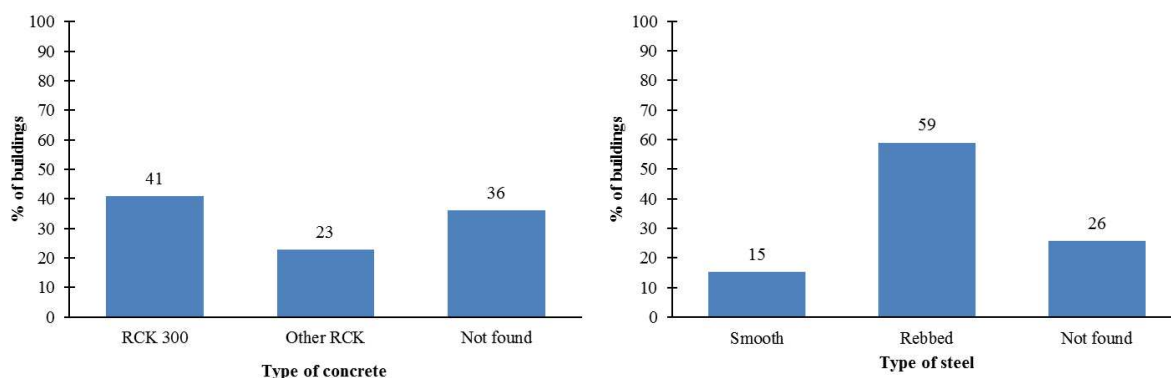


Figure 4.12. Frequencies of the types of concrete (left) and steel (right) found in the design documentation

However, ribbed steel bars (Lu 3 Rumi 4400) sometimes was used in these schools even before the 1974, overall in the beam elements that were considered more important of the columns in which always smooth rebars were used (Aq 42, Aq 50). While after the 1974 only ribbed rebars were used in both beams and columns, in particular the FeB 44K was the most used. In tab. 4.3 the mechanical characteristics of the steel mostly used over time are illustrated.

Table 4.3. Mechanical characteristics of several type of steel

	<i>Type</i>	<i>Yield strength [MPa]</i>	<i>Tensile strength [MPa]</i>	<i>Max working stress [MPa]</i>	<i>Minimum elongation [%]</i>
PRE 1974	Aq 42	230	420 - 500	115 - 140	20
	Aq 50	270	500 - 600	135 - 180	18
	Lu 3 Rumi 4400	440 - 475	600 - 680	200 - 220	12
POST 1974	FeB 38K	375	450	190 - 220	14
	FeB 44K	430	540	220 260	12

The quality of concrete and steel improved over time, so that the maximum working stresses in structural members were gradually increased.

Regarding the methods adopted to calculate stresses and strains are similar in the two reference periods. The admissible stresses method was used, in which the stresses were calculated with the traditional method of the

construction science and the maximum stress in each section must to be lower than the maximum working stresses. Thus, the materials were used only in the elastic range.

Even if both PRE and POST 1974 schools were designed without adequate seismic resistant detailing, most of them (83%) are located in areas already considered as seismic prone area when the building was designed (tab.). This means that the seismic actions were accounted in the design procedure and assumed equal to the 7 % or 10 % of the weight of each floor depending on to the hazard level. Thus, more resistant and stiffened structures were designed, but low ductility was attained for the absence of adequate structural detailing.

However, it is worth noting that all the building schools designed before the 2003 have increased their seismic hazard because, before the last seismic map, the PGA reached a maximum value of 0.1 g (the 10% of the building weight), that is lower than the current values of the PGA, comprised between 0.15 g – 0.25 g for the seismic zone II I which all schools are located.

Fig. 4.13 shows the seismic hazard map of the area of interest overlapped to the historical seismicity of the area, while tab. 4.4 shows, for each city of interest, the year of first seismic classification and the current value of the maximum PGA provided by the hazard map.

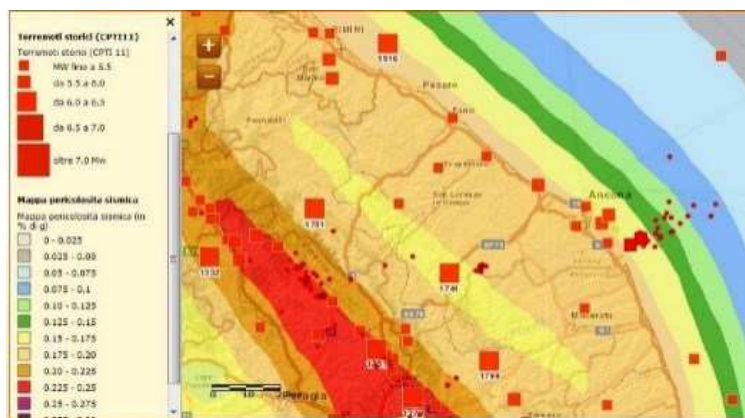


Figure 4.13. Seismic hazard map for the Marche Region

Table 4.4. Seismic classification of cities under investigation

City	Year of first classification	Current PGA
Ancona	1935	0.183
Arcevia	1983	0.177
Castelfidardo	1935	0.182
Chiaravalle	1935	0.183
Fabriano	1983	0.211
Falconara	1958	0.182
Jesi	1983	0.185
Loreto	1983	0.181
Osimo	1983	0.184
Sassoferrato	1983	0.186
Senigallia	1935	0.185

Only the 5% of the buildings designed before the 2003 was retrofitted.

This means that the 88% of the independent structures within the high school buildings belonging to the Province of Ancona doesn't satisfy the performances request from the current Italian seismic Code.

In fig. 4.14 statistical of relevant characteristics for the seismic response are illustrated. It is worth noting that there aren't relevant differences between the PRE and POST 1974 school buildings, because the way to conceive school buildings didn't changed over time.

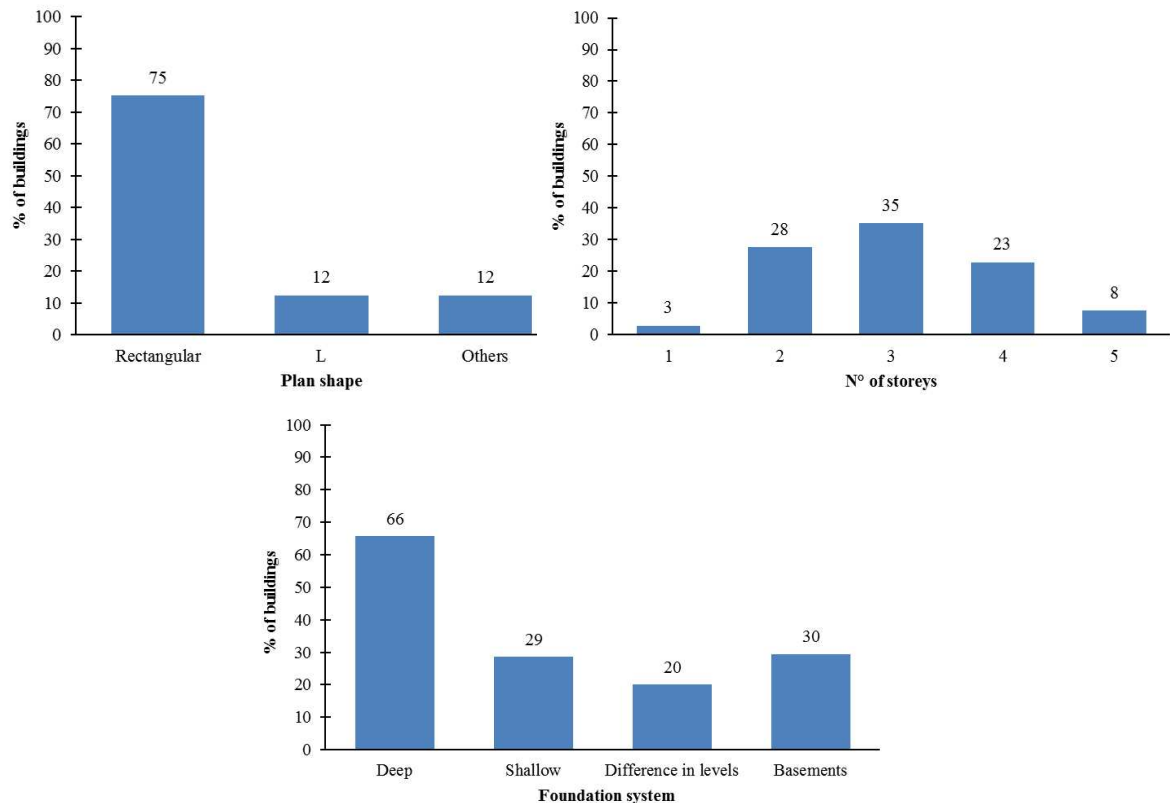


Figure 4.14. Frequencies of plan shapes (upper-left), n° of storeys (upper-right) and type of foundation (lower-centre)

The building stock analyzed have in most cases all the characteristics typical of the school buildings.

In fact:

- In the 75% of cases the plant is rectangular or similar.
- The number of storeys go from 2 to 4 (86%).
- The medium interstorey height is equal to 3.30 m.
- The slabs have a medium thickness of about 30 cm (16/20 cm + 4/5 cm for the structural part).
- Deep foundations are the most diffuse (66%).
- Masonry infills and flat roofs are present in almost all the buildings.
- The medium span length is of 5 m.
- In most cases the live loads assumed are 350 kg/m² on the intermediate levels and 150 Kg/m² on the roof.

Irregularities

The most relevant irregularities affecting the seismic response (shape in plan and elevation, irregularity in stiffness distribution, structural scheme etc.) were detected for each building of the school sample and the frequencies are shown in figs. 4.15 and 4.16.

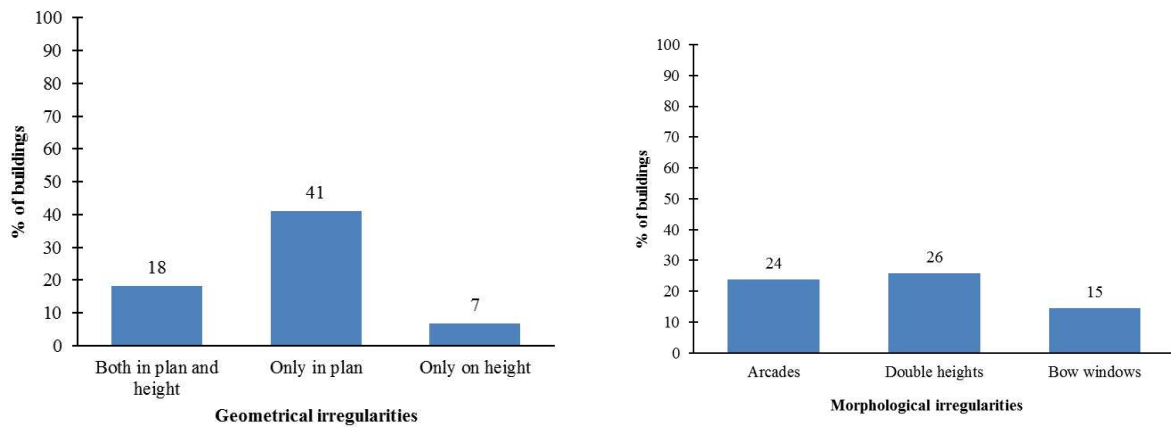


Figure 4.15. Frequencies of the geometrical irregularities

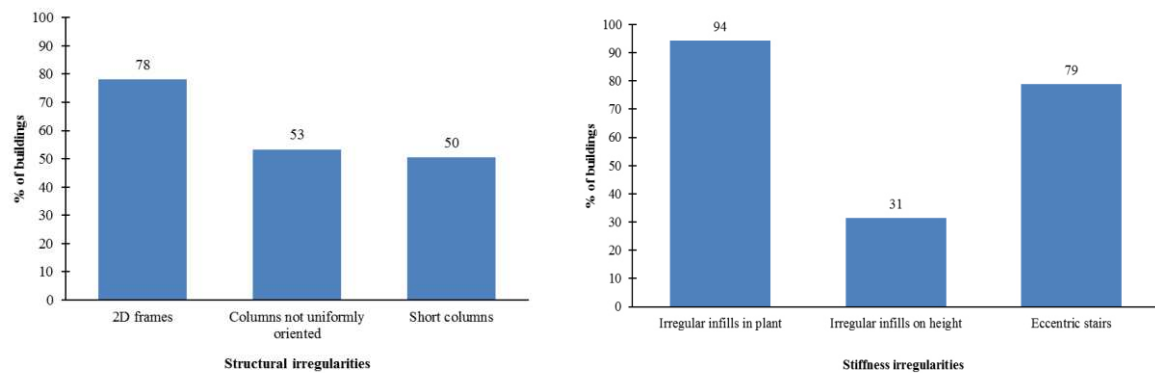


Figure 4.16. Frequencies of the structural irregularities

The 78% has mono-directionally frames (considering the direction of the high beams).

The 53% of buildings have an irregular distribution of stiffness in plant, because of the not uniform orientation of the rectangular columns or the concentration of stiff elements in a zone of the plant. In the other cases or the columns are squared or they are oriented according both main directions of the buildings.

Only few buildings, designed considering the seismic action, have two-directionally frames, columns uniformly oriented in plant and that taper in the upper storeys.

In some cases, high beams are arranged in both directions only at the first level.

In the 50% of cases there are short columns because of the presence of low infills on the façade (fig. 4.17-a) or stairs with knee-beams.

The geometrical irregularity is the most diffuse (more than 50% of cases), while those along the height of the buildings is more limited. Further almost all buildings have irregular infill distribution of in plant and stairs in eccentric position, thus torsional effects can be expected in many school buildings.

The 24% has arcades at the ground floor (fig. 4.17-b) and the 31% has irregular infill distribution on the height. This aspect is very relevant because arcades could determine a soft storey mechanism.



Figure 4.17. Arcades at the ground floor (a), short columns on the façade (b)

The 26% present a double height on the common spaces, determining an irregularity in the storey masses.

The bow-windows are present only in the 15% of cases.

Starting from these statistical data, the typical and specific vulnerabilities for the building stock have been determined (Clementi et al. 2015). The formers are present in more than the 50% of cases, while the second only in some cases.

Typical vulnerabilities

- Geometrical irregularity in plant
- Not uniformly masonry infill distribution in plant
- Not uniformly columns distribution in plant
- Eccentric stairs
- Mono-directional frames
- Short columns

Specific vulnerabilities

- C and L shaped plants
- Geometrical irregularity in elevation
- Double height
- Bow windows
- Arcades
- Foundation on different levels

Summarizing as described above, we have two structural classes within the school building stock, the PRE and POST 1974 classes. These differ essentially for the constructive details (different reference Code) and for the quality of materials, in particular for the type of steel used.

In the PRE 1974 period smooth rebars were used, after ribbed rebars became common. The POST 1974 buildings have a high probability that were designed considering also seismic action in addition to vertical loads, thus the structural scheme differs from the PRE 1974 one.

The geometrical and morphological characteristics and so the typical and specific vulnerabilities are the same for the two classes, being the school building typology invariant over time.

References chapter 4

- Augenti N., Cosenza E., Dolce M., Manfredi G., Masi A., Samela L., 2004. Performance of school buildings during the Molise earthquake sequence of October 31, November 1 2002, *Earthquake Spectra*, Special Issue on the Molise 2002 earthquake, 20 (S1), S257-S270.
- Lagambiente. XVIII Report on the quality of school construction, structures and facilities (in Italian). Rome, October 2017.
- Cittadinanzattiva. XV Report on the safety of school buildings (in Italian). 28 settembre 2017.
- Dolce M., Martinelli A. Inventario e vulnerabilità degli edifici pubblici e strategici dell'Italia centro-meridionale, Vol. I – Caratteristiche tipologiche degli edifici per L'Istruzione e la Sanità, INGV/GNDT, L'Aquila, 2005-a.
- Cherubini A, Corazza L., Di Pasquale G., Dolce M., Martinelli A., Petrini V., (1999). Vulnerabilità degli edifici in calcestruzzo armato, in *Censimento di vulnerabilità degli edifici pubblici, strategici e speciali nelle Regioni Abruzzo, Basilicata, Calabria, Campania, Molise, Puglia e Sicilia – Relazione Generale (Progetto Lavori Socialmente Utili)*, Dipartimento della Protezione Civile, L'Aquila, Vol.1, pp. 135-154.
- Dolce M., Moroni C., 2005. La valutazione della vulnerabilità e del rischio sismico degli edifici pubblici mediante le procedure VC e VM. Progetto SAVE, Atti di Dipartimento N. 4/ 2005.
- Dolce M. et al. 2004. Valutazione della vulnerabilità sismica di edifici scolastici della Provincia di Potenza, Atti del XI Convegno Nazionale L'Ingegneria Sismica in Italia, Genova, gennaio 2004.
- Grant D.N., Bommer J.J., Pinho R., Calvi G.M., Goretti A., Meroni F. 2007. A Prioritization Scheme for Seismic Intervention in School Buildings in Italy. *Earthquake Spectra* 23(2):291-314.
- Borzi B., Ceresa P., Faravelli M., Fiorini E., Onida M. (2013) Seismic Risk Assessment of Italian School Buildings. In: Papadrakakis M., Fragiadakis M., Plevris V. (eds) *Computational Methods in Earthquake Engineering. Computational Methods in Applied Sciences*, vol 30. Springer, Dordrecht.

- Clementi F., Quagliarini E., Maracchini G., and Lenci S., “Post-World War II Italian school buildings: typical and specific seismic vulnerabilities,” *J. Build. Eng.*, vol. 4, pp. 152–166, Dec. 2015.

Chapter 5

5. Proposal of a vulnerability index method for RC school buildings

5.1. General criteria and definition of the parameters

In this chapter, a vulnerability index method specific for school buildings is developed by means a numerical procedure. The aim is to obtain a more detailed *evaluation form* with respect those of the GNDT-II level that is based on empirical data from earthquake and developed for general RC buildings.

This rapid method to assess the seismic vulnerability inevitably implies some simplifications with respect more accurate methods such as the mechanical/analytical ones, but performing the same procedure on different buildings allow to directly compare their vulnerability (or capacity) levels in a quantitative fashion and so to determine the priority on which to intervene.

Further in a large-scale vulnerability assessment which involves a lot of buildings, the comparative evaluation is more important than the specific results in absolute terms, so it is necessary to capture each minimum difference between buildings, to establish a ranking as accurate as possible.

The seismic behaviour of the school buildings population was investigated through numerical analyses considering the variability in the structural, geometric and mechanical properties. Thus, a parametric study was performed on two prototype buildings representing in average the PRE and POST 1974 building stocks (shape and dimension in plant, number of storeys), designed according to a specific Code (mechanical property of materials, live and seismic loads, constructive details for beams and columns, check criteria for structural elements).

Then the main structural characteristics of the population that affect the seismic response should be identified, such as interstorey height, span width, type of slabs, number of frame for each direction, direction of columns, beam-column ratio, and type of masonry walls in the frame (resistance and stiffness), and they should be modelled as deterministic or random variables.

Once the several structural models have been determined considering some configuration of the parameters, the seismic behaviour can be developed through nonlinear static or dynamic analyses. In this work, the parametric study has been performed on the 15 vulnerability factors, defeminated on the base of the typical and specific vulnerability described in Chapter 3, in order to understand the real weight of them on the global vulnerability of both structural classes (PRE and POST 1974) representative of the RCMF building schools analyzed:

1. Age of construction
2. Reference design Code
3. Built in seismic area
4. Typology of resistance system
5. Quality of resistance system
6. Critical elements
7. Geometrical irregularity in plant
8. Geometrical irregularity in elevation
9. Stiffness irregularity in plant
10. Stiffness irregularity in elevation
11. Stairs
12. In plane slab stiffness
13. Ground level position
14. Mass distribution
15. Damage pattern and materials deterioration

The distinction between the two classes is for differences in construction period and in the design code of reference, thus a simulated design procedure was performed on two prototype buildings representing the PRE and POST 1974 classes, as described in par. 4.2.

They summarize the more frequent characteristics (detected in more than the 50 % of buildings), common for the two classes of schools, considered as fixed parameter because of a very slight variation or no variation has been found in the survey phase.

These are:

- Rectangular plant of dimensions 23m x 15 m.
- Number of storey equal to 3.
- Interstorey height equal to 3.20 m.
- Four frames on the longitudinal direction.
- Span length, assumed to be 5.00 m and 3.00 m where there are the stairs.
- Cross sections of high beams, equal to 30x60 cm.
- Masonry infills having two parallel panels made of hollow bricks and mortar with a total width of 20 cm (8 cm + 12 cm).
- Short infills on the longitudinal sides (large windows), full height infills on the transverse sides.
- Floors are made of RC joists and hollow bricks with a height of 20 cm plus 4 cm of RC slab.
- Flat roof.
- Stairs made of knee-beams.

Several authors have investigated the seismic response of RC frame considering the influence of some relevant parameters, performing nonlinear static or dynamic analyses (*Dolsek 2011, Manfredi et al. 2010*). In (*Masi et al. 2012*) was investigated the influence on interstorey drifts and ductility requests due to the age of construction (PRE 1971 and POST 1971), the number of storeys (2,4, and 8), the concrete strength (10, 18, 28 MPa) and the presence and distribution of infill walls (infill, bare and pilotis frame). To this aim nonlinear dynamic analyses were performed and the PGA and Housner Intensity were considered as intensity measures. The results show the higher influence on the vulnerability of the pilotis configuration, which increases a lot the interstorey drift and ductility ratio on the columns at the pilotis level.

Description of the vulnerability indicators

The main issue is how to model each parameter in a form as general as possible. For some of them is quite simple, for instance the geometrical irregularity in plant and elevation, while for other ones is more complicated, such as the age of construction and the damage and materials deterioration.

For every parameter, the more frequent and the extreme configurations detected have been assumed, so intermediate configurations are included implicitly in this range.

A better description of each parameter and of the configurations they assumed is reported below.

1. Building age

It considers the construction year of the building in terms of the quality of materials and construction technologies used for realization (in theory improved over time).

To this end, in parametric analysis the mechanical properties of the concrete have been changed, while the mechanical properties of steel have not changed (tab. 5.1) because they are less susceptible to uncertainty as the steel production is more controlled.

Table 5.1. Values of the concrete resistance

	$f_{cm,1}$ [N/mm ²]	$f_{cm,2}$ [N/mm ²]	$f_{cm,3}$ [N/mm ²]	$f_{cm,4}$ [N/mm ²]
PRE 1974	10	18	25	30
POST 1974	15	21	25	30

2. Reference Code

It considers the periods when a given regulation was in force and, therefore, the relative provisions were applied. Three periods are considered:

- Pre 1974, whose buildings are designed according to the Royal decree dated 1939.

- Post 1974, whose buildings are designed according to law n.1086 dated 1971 and the relative decrees.
- Post 2003, whose buildings are designed according to OPCM 3274/2003 and then to NTC 2008. The first two periods differ essentially for the type of steel adopted in reinforcement, smooth bars in the PRE 1974 period and ribbed bars in the POST 1974, while the constructive details are about the same. In both periods the admissible stress method was adopted. Instead, post 2003 buildings are designed according to the limit state method and in accordance with the principle of resistance hierarchy.

3. Seismic zone

It considers if the building was built in area already classified as seismic at the construction time. It is worth noting that in both classes there are buildings constructed considering a certain level of seismic action, even if they are much more after the 1974, and the level of the seismic intensity was different for the two periods and it depended on the seismic category in which the area was classified.

The seismic action, calculated as a percentage of the storey weight, was lower than those obtained according to the current national seismic hazard map enforced in 2003.

Furthermore, the seismic action only meant an increase in the cross sections of resistant elements. Thus, the two prototype building models, representing the PRE and POST 1974 classes, were first designed accounting only for vertical loads and then accounting also for seismic actions according to the regulations enforced on the own reference period.

4. Typology of structural system

It considers if the resistant system is made of only frames or even with masonry infills collaborating to the seismic response. Therefore, some alternative arrangements of the full height masonry infill have been considered, placing them in a more widespread manner than the prototype models, thus evaluating the increase in the global capacity.

5. Quality of the structural system

It considers if the resistant system has frames according to one or both main directions of the buildings. Therefore, for both classes, a model with high beams arranged also in the transverse direction has been evaluated.

6. Critical elements

It considers the presence of critical elements such as short columns delimited by ribbon windows and / or knee- beams of the stairs. So, the influence on the global response due to only ribbon windows, only knee-beams and of both at the same time was evaluated.

7. Irregularity in the plan shape

It indicates how much the building plan differs from a regular and compact shape in order to account for the torsional effects due to shape irregularity. The elongated rectangular shape, L-shape and C-shaped were accounted.

8. Irregularity in the elevation shape

It considers the shape irregularity in elevation, thus if there is constriction or enlargements between a storey and the next. The consequence is the abrupt variation of the storey masses, resistances and stiffness between storeys, with negative effects on global seismic behaviour.

Thus, several configurations of bow-windows and constrictions between storeys have been evaluated, varying their planar extension.

9. Irregularity in the planar stiffness distribution

It considers the arrangement in the building plan of masonry infills, so if they are arranged uniformly or not on the sides of the building (e.g. the classrooms have windows larger than the other spaces).

So, several configurations of the infills distribution were analyzed to account for the negative effects (torsion) due to the irregular stiffness distribution in the building plan.

10. Irregularity in the elevation stiffness distribution

It considers the arrangement of masonry infills along the elevation of the building, so if they are arranged uniformly or not between the various levels. This to take into account the negative effects due to the irregular stiffness distributions in elevation that could favour the concentration of stresses at some levels.

Thus, the pilotis building and other plausible variations in the infill distribution along the height of the building were analyzed.

11. Stairs types and planar position

It considers the position of the stair within the building plan, as if they are in eccentric position could be another factor for torsional amplification.

Two types of stairs were considered, with knee-beams and rampant slabs respectively, and their influence on the seismic response was considered by varying their position in the plan.

12. Stiffness of floor slabs

It considers the influence of the in-plane stiffness of the floor slabs on the overall capacity of the building, whereby the two extreme situations of rigid and deformable floor slabs have been simulated.

13. Position of the foundations on the ground

It considers whether the foundations are arranged, on a single level or on multiple levels, so as to configure an irregularity in the ground-building relationship with consequent negative effects on the structural response.

Thus, some configurations of the position of foundations on the ground were analyzed, by varying the position and extension in plan.

14. Irregularity in the mass distribution

It indicates if the mass is uniformly distributed along the building plan and elevation, or if there are zones where the mass is particularly concentrated. Irregularity in the mass distribution may lead to torsional effects because of the eccentricity with the centre of stiffness.

The continuity of the construction technique (the same type of structures, of slabs, of infills etc.), the uniform distribution of indoor spaces and of their use suggest a regular distribution of the masses.

In this case, irregularity in mass distribution has been simulated either by the presence of voids in the floor slabs (e.g. double heights are recurrent in school buildings), by varying the extension and position in the plan, and also by varying the type of live loads in some part of buildings in order to simulate the presence of archives or libraries.

15. Material degradation

It considers the presence of material degradation, such as corrosion of the reinforcement, resulting in a reduction in the diameter of the steel bars and in the removal of the concrete coverage.

The degradation was simulated by reducing the cross sections and the diameters of the reinforcement in beams and columns located in perimeteric position of the two prototypes representative of the PRE and POST 1974 classes.

A simulation of possible damage pattern was not carried out in this study because this evaluation requires a more specific and depth evaluation.

5.2. Simulated design for prototype buildings

Prototype buildings respectively for PRE 1974 and POST 1974 have been designed through a simulated design procedure (*Verderame et al. 2010*) according to the enforced Codes in the reference period. In particular, for PRE 1974 stock the reference Code is the R.D. 2229/ 1939, while for the POST 1974 is the 1974 Code.

Further a large use of technical manuals was done in those periods, in order to integrate the few provisions gave by the regulations.

The calculation method is the “*admissible tensions method*”, in Italy used up to the first years of 2000.

The two prototype buildings have the same geometrical and typological characteristics as described in the previous paragraph, so they differ for the resistance scheme, mechanical properties of the materials and for details such as the quantity of rebars and stirrups in columns and beams.

The PRE 1974 prototype considers only vertical static loads, because of the most part of PRE 1974 school buildings was built on area at the time without a seismic classification.

Thus, a scheme with parallel plane frame in the longitudinal direction (X) was considered, while in transverse direction (Y) the floor slabs are arranged, and no beams are provided, except on the perimeter (fig. 5.1 and fig. 5.2).

Column elements were assumed with a squared cross section and they were designed considering only vertical loads. However, for external columns, a small bending moment was assumed.

Beam elements were assumed with a rectangular section of dimension 30x70 cm and they were designed assuming the following bending moments:

- at the extrados of the ends: $ql^2/12$
- at the intrados of the middle: $2/3 \times ql^2/8$

Smooth rebars were used for longitudinal bars and stirrups.

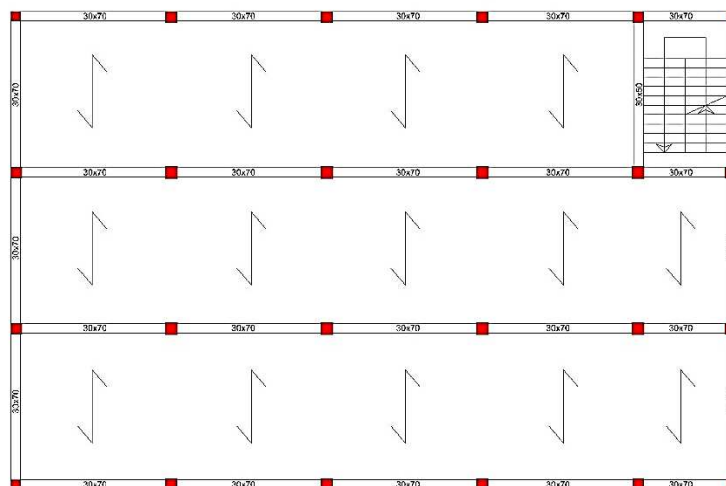


Figure 5.1. Planar scheme of the PRE 1974 prototype building

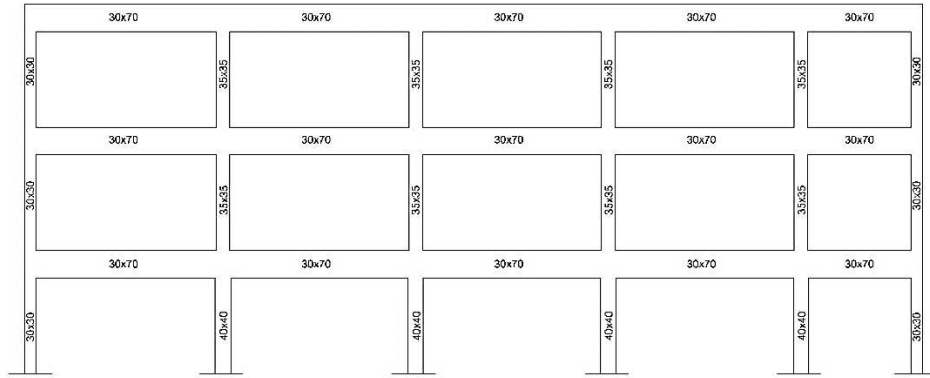


Figure 5.2. Longitudinal frame of the PRE 1974 prototype building

The POST 1974 prototype considers also the horizontal seismic loads for the level of hazard assumed on average in the reference period (1974 – 2003).

A scheme with parallel frame in the longitudinal direction (X) was considered, while in the transverse direction wide beams were provided together the floor slabs. (figs. 5.3 and 5.4)

Due to the presence of seismic forces on the longitudinal direction for the POST 1974 prototype, higher dimensions of the cross sections for columns were assumed and so rectangular sections were provided in X direction.

The stresses on the structural elements of the longitudinal frames were obtained solving the hyperstatic scheme.

Ribbed bars were used for longitudinal bars and stirrups.

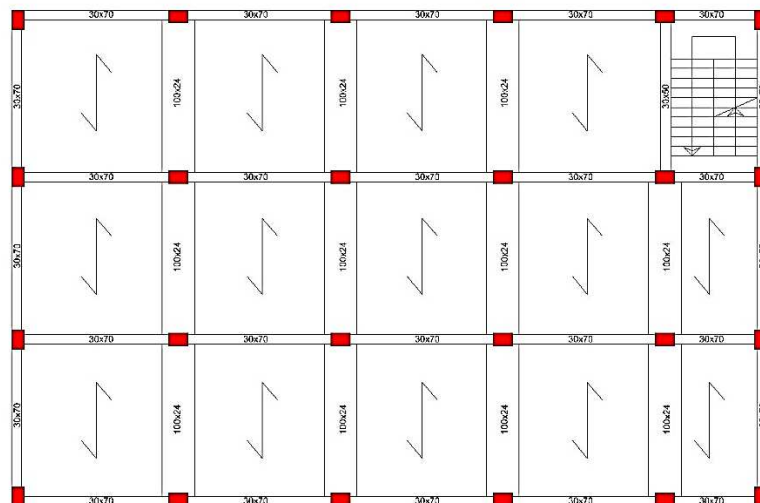


Figure 5.3. Planar scheme of the POST 1974 prototype building

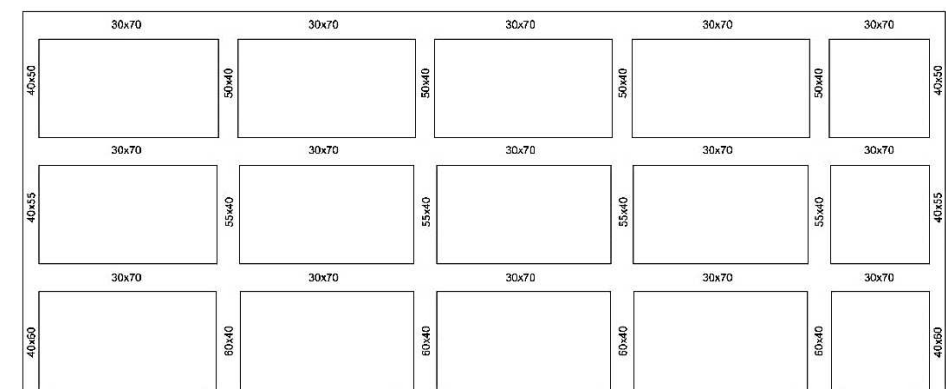


Figure 5.4. Longitudinal frame of the POST 1974 prototype building

For both PRE and POST 1974 prototype, against shear stresses a constant spacing of stirrups was adopted on the height of the columns, while for beams were used stirrups and the addition of folded bars for the final parts of the elements.

The type of floor slabs and the relative loads (dead and live) are the same for the two building stocks.

Dead loads of slabs (RC joists and hollow bricks with a height of 20 cm plus 4 cm of RC slab) are equal to 5.5 KN/m² at the 1st and 2nd floors, while 5.0 KN/m² at the roof.

Live loads, such as crowding and snow loads, are equal to 3.50 KN/m² and 1.50 KN/m² respectively.

The slabs have the RC joists along the transverse direction of the buildings (Y), so that the longitudinal frames are loaded.

Linear constant loads due the infill masonry are assumed equal to 5.5 KN/m for full height walls and 2.5 KN/m for low walls.

The resistances of concrete come from the average values of some compressive tests done on concrete carrots got from the structural elements of the buildings stock. In (*Verderame et al. 2001-a*) a description of concrete characteristics employed in the '60 is provided.

While for steel the types, most used in each period were considered, the *Aq60* type (smooth rebars) for the PRE 1974 stock and the *FeB38k* type (rough rebars) for the POST 1974 stock. In (*Verderame et al. 2001-b*) a description of steel types employed in the '60 is provided.

Average strength of concrete and steel are shown in tab. 5.2.

Table 5.2. Mechanical properties of prototype buildings

	Concrete – <i>f_{cm}</i> [N/mm ²]	Steel – <i>f_{ym}</i> [N/mm ²]
PRE 1974	18.0	310.0
POST 1974	21.0	375.0

Finally, tabs. 5.3, 5.4, 5.5 and 5.6 summarize the main differences in detailing between the two structural schemes.

The quantity of longitudinal bars and stirrups in the elements is the maximum between the minimum value by the reference Code provisions and the value that allow to satisfy the check in terms of allowable stresses.

Table 5.3. Structural details for columns in central position (left), corner (right) and side (lower).

<i>Central columns</i>	PRE 74	POST 74	<i>Corner columns</i>	PRE 74	POST 74
1st level			1st level		
Section [cm]	40x40	40x60	Section [cm]	30x30	40x60
Long. bars	6 fi 16	8 fi 14	Long. bars	4 fi 16	8 fi 12
Stirrups	2 fi 8/ 250	2 fi 8/ 150	Stirrups	2 fi 8/ 250	2 fi 8/ 150
2nd level			2nd level		
Section [cm]	35x35	40x55	Section [cm]	30x30	40x55
Long. bars	6 fi 16	8 fi 12	Long. bars	4 fi 16	8 fi 12
Stirrups	2 fi 8/ 250	2 fi 8/ 150	Stirrups	2 fi 8/ 250	2 fi 8/ 150
3rd level			3rd level		
Section [cm]	30x30	40x50	Section [cm]	30x30	40x50
Long. bars	4 fi 16	8 fi 12	Long. bars	4 fi 16	8 fi 12
Stirrups	2 fi 8/ 250	2 fi 8/ 150	Stirrups	2 fi 8/ 250	2 fi 8/ 150

<i>Side columns</i>	PRE '74	POST 74
1st level		
Section [cm]	35x35	40x60
Long. bars	6 fi 16	8 fi 12
Stirrups	2 fi 8/ 250	2 fi 8/ 150
2nd level		
Section [cm]	30x30	40x55
Long. bars	4 fi 16	8 fi 12
Stirrups	2 fi 8/ 250	2 fi 8/ 150
3rd level		
Section [cm]	30x30	40x50
Long. bars	4 fi 16	8 fi 12
Stirrups	2 fi 8/ 250	2 fi 8/ 150

Table 5.4. Perimeter longitudinal beams

Section [cm]	PRE 74	POST 74	
		<i>External span</i>	<i>Internal span</i>
	30x70	30x70	30x70
1st level			
Extremity bars	4 fi 16	5 fi 12 - 6 fi 14	6 fi 14 - 3 fi 18
Middle bars	3 fi 16	5 fi 12	5 fi 12
Stirrups	2 fi 6/ 80	2 fi 8/ 100	2 fi 8/ 100
2nd level			
Extremity bars	4 fi 16	5 fi 12 - 3 fi 18	3 fi 18
Middle bars	3 fi 16	5 fi 12	5 fi 12
Stirrups	2 fi 6/ 80	2 fi 8/ 100	2 fi 8/ 100
3rd level			
Extremity bars	3 fi 16	3 fi 12 - 4 fi 12	4 fi 12
Middle bars	2 fi 16	3 fi 12	3 fi 12
Stirrups	2 fi 6/ 120	2 fi 8/ 100	2 fi 8/ 100

Table 5.5. Internal longitudinal beams

Section [cm]	PRE 74	POST 74	
		<i>External span</i>	<i>Internal span</i>
	30x70	30x70	30x70
1st level			
Extremity bars	6 fi 16	6 fi 14	8 fi 14
Middle bars	5 fi 16	6 fi 14	6 fi 14
Stirrups	2 fi 6/ 50	2 fi 8/ 100	2 fi 8/ 100
2nd level			
Extremity bars	6 fi 16	6 fi 14	4 fi 18
Middle bars	5 fi 16	6 fi 14	6 fi 14
Stirrups	2 fi 6/ 50	2 fi 8/ 100	2 fi 8/ 100
3rd level			
Extremity bars	3 fi 16	6 fi 12	6 fi 12
Middle bars	3 fi 16	6 fi 12	6 fi 12
Stirrups	2 fi 6/ 80	2 fi 8/ 100	2 fi 8/ 100

Table 5.6. Perimeter transverse beams

Section [cm]	PRE 74	POST 74	
		<i>External span</i>	<i>Internal span</i>
	30x70	30x70	30x70
1st level			
Extremity bars	3 fi 12	3 fi 12	3 fi 12
Middle bars	3 fi 12	3 fi 12	3 fi 12
Stirrups	2 fi 6/ 250	2 fi 8/ 150	2 fi 8/ 150
2nd level			
Extremity bars	3 fi 12	3 fi 12	3 fi 12
Middle bars	3 fi 12	3 fi 12	3 fi 12
Stirrups	2 fi 6/ 250	2 fi 8/ 150	2 fi 8/ 150
3rd level			
Extremity bars	3 fi 12	3 fi 12	3 fi 12
Middle bars	3 fi 12	3 fi 12	3 fi 12
Stirrups	2 fi 6/ 250	2 fi 8/ 150	2 fi 8/ 150

5.3. Parametric analyses

5.3.1. Structural modelling and pushover analyses

Pushover analyses (*Krawinkler et al. 1998, Chopra et al. 2002*) were performed on prototype structural models of both PRE and POST 1974 classes, every time modified to obtain structural models representing the variation of a single vulnerability factor. In fig. 5.5 are shown some configurations of in plan and in elevation shapes employed in the parametric analysis.

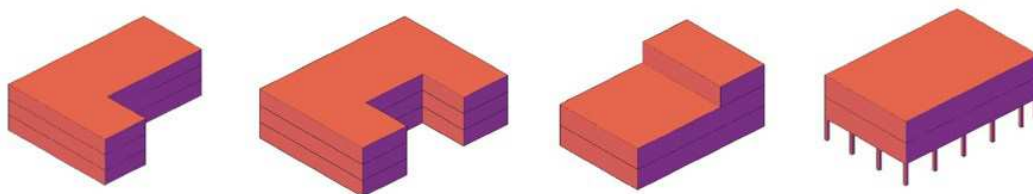


Figure 5.5. Some building configurations employed in the parametric analysis

Given that the prototype models are specific for school buildings, the results should be considered valid only for this typology, even if some of the characteristics are similar to other RC typologies such as residential buildings.

Further, the structural models were generated considering the vulnerability factors as independent deterministic variables that assume discrete values (only the more frequent values found in the survey phase). It is worth noting that the combined effect due to the presence of more parameters at the same time is not considered in this work, because of only a parameter for time is evaluated to better understand its real weight on the vulnerability.

In this way, not a very large amount of analyses needed, against a probabilistic approach in which parameters are modelled as random variables having a probabilistic distribution and so much more models are generated through, for example, a Monte Carlo simulation or the Latin Hypercube techniques (these techniques allow to consider the high number of request permutations).

Thus, 3D models were generated by using one-dimensional elements for beams and columns (*Asteris et al. 2013*). The base model is shown in fig. 5.6.

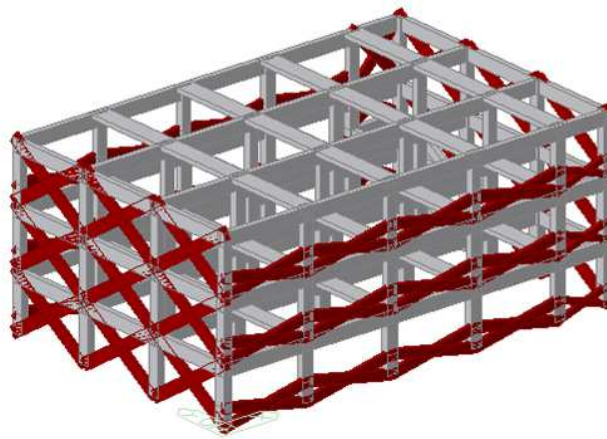


Figure 5.6. Base model for parametric analysis

The nodes at the ground level are fixed and the slabs are considered deformable in their plane because of the limited quantity of steel. Thus in-plane stiffness is that provided by the beam elements.

The applied floor loads are the same used in the simulated design procedure, except the live loads level that are assumed equal to 3.0 KN/m² at the 1st and 2nd floor and 1.20 KN/m² at the roof. The RC joist of all slabs are direct along the transverse direction (Y), so that only the longitudinal frames are loaded.

While constant linear loads are applied on the perimetrical frames for the presence of the infill walls.

The weight and the masses at each floor are shown in tab. 5.7 for the PRE 1974 prototype model and in tab. 5.8 for the POST 1974 prototype model.

Table 5.7. PRE 1974 model_Storey weights and masses

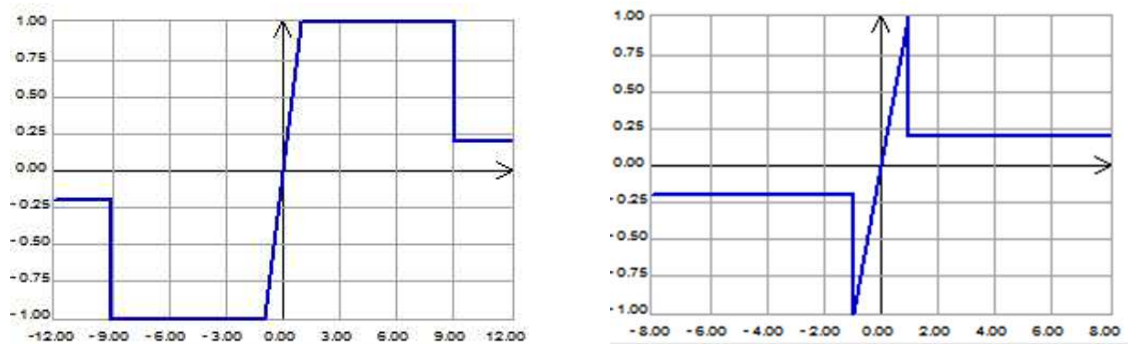
<i>Story</i>	<i>Level [m]</i>	<i>Weight [kN]</i>	<i>Translational Mass (kN/g)</i>	
Roof	9.6	2915.7	255.1	255.1
2F	6.4	4211.2	388.0	388.0
1F	3.2	4309.3	396.9	396.9

Table 5.8. POST 1974 model_Storey weights and masses

<i>Story</i>	<i>Level [m]</i>	<i>Weight [kN]</i>	<i>Translational Mass (kN/g)</i>	
Roof	9.6	3283.7	292.6	292.6
2F	6.4	4694.2	437.3	437.3
1F	3.2	4823.3	449.4	449.4

The lumped plasticity method was used to take into account nonlinearities (*Spacone et al. 2001*), so the plastic hinges were assigned to the extreme positions of both columns and beams. The plastic hinge for columns is PMM type (axial load - bending moments interaction), while no interaction is considered for beams.

Fig. 5.7 shows the constitutive laws for plastic hinges, defined by the moment-rotation curve of each element accounting for both flexure and shear.

**Figure 5.7.** Constitutive laws for plastic hinges of RC elements: ductile (left) and brittle (right)

The capacities of plastic hinges in terms of chord rotation and shear strength (*Panagiotakos et al. 2001, Biskinis et al. 2004, Fabbrocino et al. 2005, Verderame et al. 2010*) are calculated according to the Italian seismic Code and EC8 formulations.

For ultimate chord rotation, the scale factors to consider the presence of smooth longitudinal bars, equal to 0.575, and a design without detailing for earthquake resistance criteria, equal to 0.85, were considered.

The shear-bending interaction has not been considered. A study on the influence of this interaction on the global capacity of RC buildings is described in (Clementi et al. 2017).

Masonry infills were considered in the global model as equivalent struts (macro modelling approach) (fig. 5.8) with a given equivalent area/stiffness, resistance and nonlinear behaviour. Thus, a compression struts in each diagonal of the panel was employed. A study on the role of diagonal struts in RC frame can be found (Uva et al. 2012).

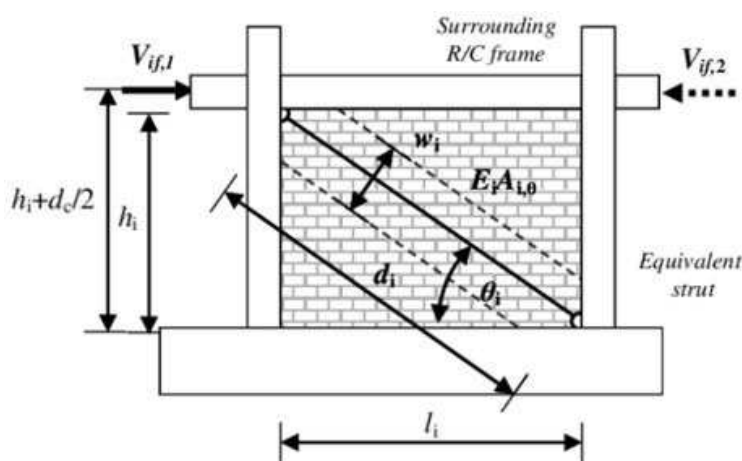


Figure 5.8. Equivalent strut model for masonry infill panels

The local effect of the infill panels on the frame was not considered in this study, because only the global response was of interest. A review of the effects of the interaction between infills and frame, and of numerical modelling of masonry infills is reported in (Crisafulli et al. 2000, Asteris et al. 2011, Spacone et al. 2015, Di Trapani et al. 2015).

Formulation for geometric dimensions and the values of peak resistances, stiffness and constitutive laws of the equivalent struts are provided from many authors (Stafford Smith 1966, Mainstone 1971 and 1974, Bertoldi et al. 1993, Panagiotakos et al. 1996, Al-Chaar 2008).

The material adopted for the masonry infills aim to reflect the characteristics of clay blocks typically used in Italy, in particular of the hollow bricks with a percentage of vacuum < 45 %. The mean values suggested by the Italian seismic Code for the resistances, elastic modulus and weight were employed:

$$f_m = 5.0 \text{ N/mm}^2$$

$$\tau_m = 0.35 \text{ N/mm}^2$$

$$E_m = 4500 \text{ N/mm}^2$$

$$G_m = 1350 \text{ N/mm}^2$$

In this study the formulation provided by (Panagiotakos et al. 1996) (fig. 5.9).

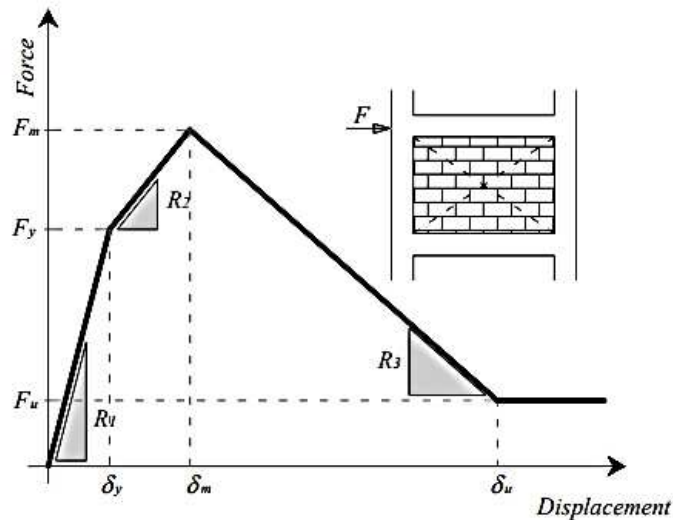


Figure 5.9. Constitutive law for the equivalent strut according to (Panagiotakos et al. 1996)

The values of the mechanical parameters calculated for the equivalent struts employed in the models (full height walls and short walls of ribbon windows) are shown in tab. 5.9.

Table 5.9. Values of the mechanical parameters of the equivalent struts

<i>Equivalent strut section [cm]</i>	<i>F_y [KN]</i>	<i>F_m [KN]</i>	<i>F_r [KN]</i>	<i>K_y [KN/m]</i>	<i>K_m [KN/m]</i>	<i>K_r [KN/m]</i>	<i>S_y [cm]</i>	<i>S_m [cm]</i>	<i>S_r [cm]</i>
20x60	350	455	35	421x 10 ³	70x10 ³	42x10 ³	0.08	0.23	1.23
20x30	350	455	35	135x 10 ³	54x10 ³	13x10 ³	0.25	0.44	3.67

Structural analyses

Modal analysis and nonlinear static analysis were performed. The former in order to study the dynamic response and obtain for each main direction the fundamental periods and the participant masses.

To this aim the modal masses are lumped in the nodes at each storey.

Non-adaptive and uni-modal pushover analyses were performed to understand the global capacity for each structural model. It consists to apply horizontal load patterns, increased step by step up to the structure collapse, separately for each direction.

Generally, this type of analysis is applied to regular structures, having few vibration modes with a high participant mass.

The following assumptions were done:

- Control in terms of displacement.

- Control point corresponds to the node on the top of a column at the last floor, located about in a central position with respect the plant shape.
- 2 load patterns for each main direction (longitudinal X and transversal Y) were considered, so 8 analyses were performed for each structural model. The first one is the pattern proportional to the fundamental mode respectively for X and Y directions, while the second one is proportional to masses (uniform distribution).

The initial load combination considers the whole dead loads and a percentage of the live loads according to the EC.

- The N2 method (please chapter 2) has been used for the bilinearization of the SDOF capacity curves.

5.3.2. Analysis results

Modal analysis

The elastic modal analysis was performed and the results in terms of vibration periods, participant masses and mode shapes for the X and Y directions were analyzed to evaluate the reliability of the models developed.

For both prototype buildings the results in tab. indicate that the fundamental period (in terms of participant mass) in X direction is lower and the participant mass is higher than the respective values in Y direction. Because of is the absence, along the Y direction, of the resistant frames, mainly for the PRE 1974 structure which provides a greater difference between the two fundamental periods. The main results of the modal analysis are shown in tab. 5.10.

Table 5.10. Fundamental period and relative participant mass for the two prototype building models

	<i>T_x</i> [s]	<i>T_y</i> [s]	<i>m_x</i> [%]	<i>m_y</i> [%]
PRE 1974	0.373	0.927	63.88	46.66
POST 1974	0.271	0.458	82.26	58.41

Further, for the POST 1974 prototype it can be noted lower values of the fundamental periods both in X and Y, meaning a higher stiffness with respect the the PRE 1974 prototype. The variation on the Y direction is about 100% because of the major stiffness of the rectangular columns with respect the squared columns of the PRE 1974 prototype.

The participant masses increase in both directions of the POST 1974 building, meaning a more regular dynamic behaviour.

The mode shapes of the fundamental period in the X direction are shown in figs. 5.10 and 5.11 respectively for the PRE 1974 and POST 1974 buildings.

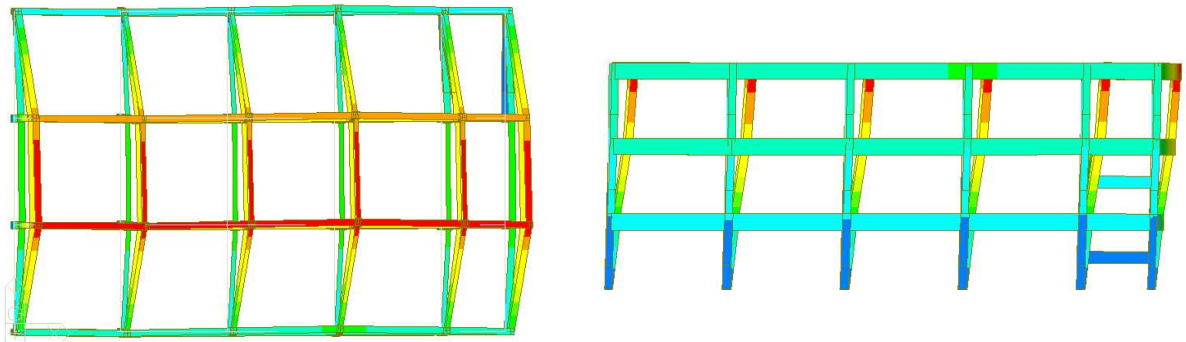


Figure 5.10. PRE 1974 model_Fundamental mode in X direction

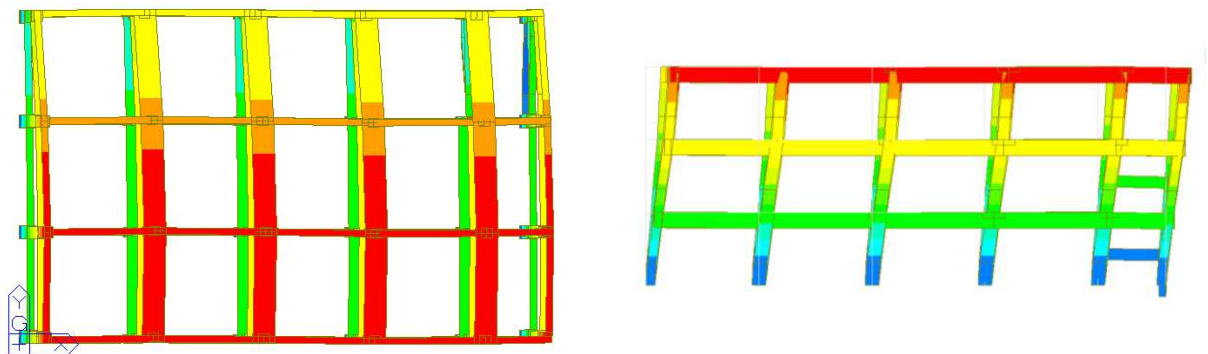


Figure 5.11. POST 1974 model_Fundamental mode in X direction

In longitudinal direction (X) the PRE 1974 prototype provides a greater translation of the two central frames, while for the POST 1974 the translation is higher for the external frame on the side opposite to the stair.

Figs. 5.12 and 5.13 shows the modal shapes for the fundamental period in the Y direction.

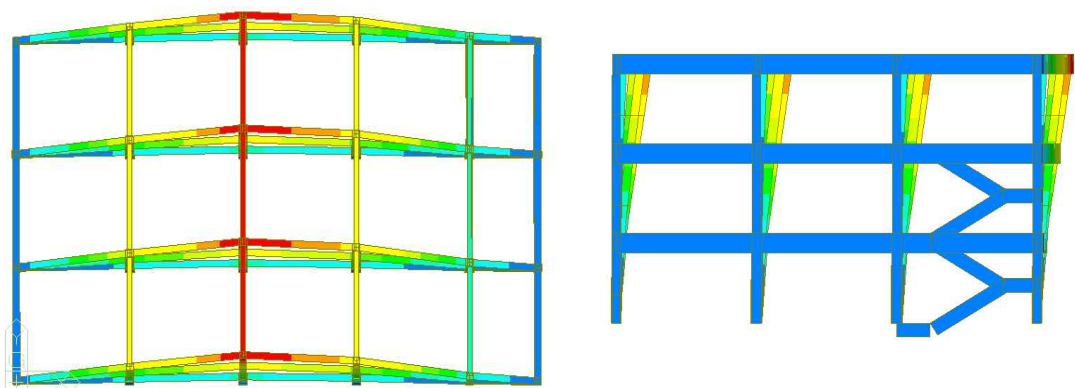


Figure 5.12. PRE 1974 model_Fundamental mode in Y direction

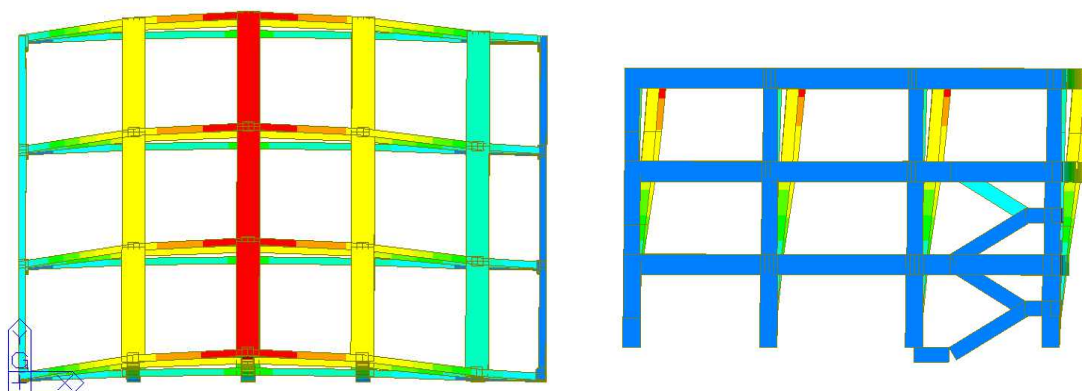


Figure 5.13. POST 1974 model_Fundamental mode in Y direction

In transverse direction (Y) the two prototypes provide the same shape, with a higher translation in the central zone of the plant and linearly increasing on the height of the buildings.

Pushover analysis

The results of the pushover analyses performed on the several buildings models representative of the typological characteristics and vulnerability factors of the PRE and POST 1974 classes were analyzed in order to capture the differences in seismic response and to obtain the scores for the vulnerability indicators in the method proposed by the author, as explained in depth in the following. Fig. 5.14 shows the bilinear curves for the two classes, both for the two prototype models and for the average of the results of all the models analyzed. It is noted in general as that of the POST 1974 class has greater resistance, stiffness and ductility than the one of the POST 1974 class.

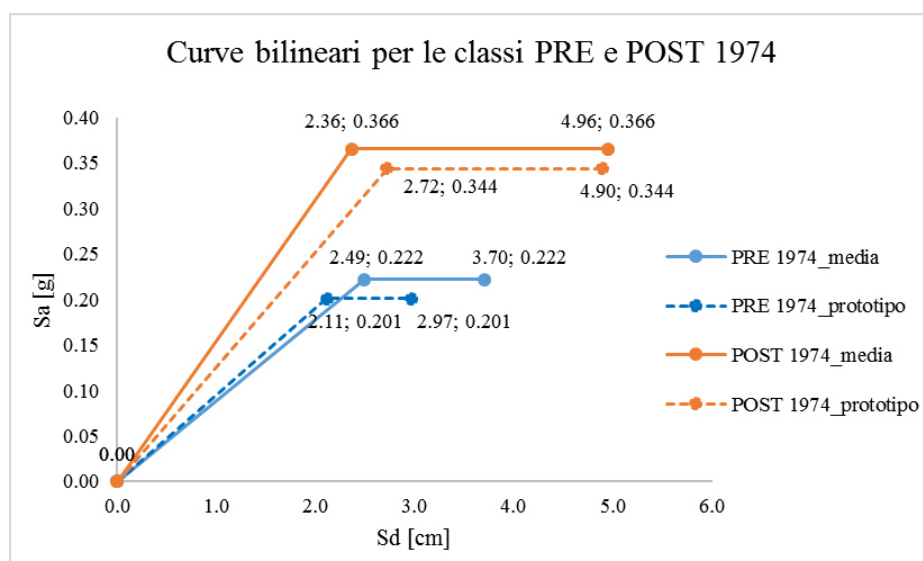


Figure 5.14. Average bilinear capacity curves for prototype buildings and for the classes

In tab. 5.11 the values of the parameters that characterize the bilinear curves are shown for the two classes, both for the prototype buildings and the for the average behaviour of all models investigated.

Table 5.11. Parameters of the equivalent bilinear curves

	a_y [m/s ²]	d_y [cm]	d_u [cm]	u	T_y [s]	T_u [s]	A [cm ²]
<i>PRE 1974_media</i>	0.222	2.49	3.70	1.48	0.662	0.820	59.54
<i>PRE 1974_prototipo</i>	0.201	2.11	2.97	1.41	0.693	0.826	32.91
<i>POST 1974_media</i>	0.366	2.36	4.96	2.10	0.459	0.648	167.54
<i>POST 1974_prototipo</i>	0.344	2.72	4.90	1.80	0.572	0.752	152.88

- a_y is the spectral acceleration for which the structure yield.
- d_y is the spectral displacement for which the structure yield.
- d_u is the ultimate spectral displacement.
- u is the ductility factor calculated as d_u/d_y .
- T_y is the elastic period.
- T_u is the effective period at the collapse.
- A is the area of the equivalent bilinear curve.

For both classes, the bilinear curves have a greater capacity if you consider the average response of all models employed in the parametric analysis rather than the response of the prototype buildings. This is especially true for the PRE 1974 class, where the areas under the bilinear curves differ nearly 100%, indicating a higher incidence of vulnerability indicators on the variability in the structural response.

In order to evaluate the reliability of the numerical analyses, the global average values were compared with some provided in the literature. In the Risk-EU project (*Mouroux et al. 2004*), for certain types of RC buildings in with different levels of seismic design (without ductile provisions and with low ductile provisions), the values of mechanical parameters such as a_y , T_y , d_y , d_u , u and of the parameters V_i and Q of the macroseismic method, were provided as shown in tab. 5.12.

Table 5.12. Parameters for vulnerability and capacity curves for RC buildings without ductile provisions (from Risk-UE project)

	BTM	V	Q	T	a_y	μ	d_y	d_u
RC1	RC1_L	0.62	2.3	0.539	0.207	3	0.0150	0.0451
	RC1_M	0.64	2.3	0.854	0.124	3	0.0224	0.0674
	RC1_H	0.68	2.3	1.304	0.072	3	0.0304	0.0915
RC2	RC2_L	0.52	2.3	0.539	0.278	3	0.0201	0.0606
	RC2_M	0.54	2.3	0.854	0.166	3	0.0300	0.0904
	RC2_H	0.58	2.3	1.304	0.097	3	0.0407	0.1227
RC3	RC3_L	0.57	2.3	0.539	0.240	3	0.0174	0.0523
	RC3_M	0.59	2.3	0.854	0.143	3	0.0259	0.0781
	RC3_H	0.63	2.3	1.304	0.083	3	0.0352	0.1060

Table 5.13. Parameters for vulnerability and capacity curves for RC buildings with low ductile provisions (from Risk-UE project)

	BTM	V	Q	T	a_y	μ	d_y	d_u
RC1 DCL	RC1-III_L	0.66	2.3	0.437	0.227	3	0.0108	0.0324
	RC1-III_M	0.64	2.3	0.642	0.164	3	0.0168	0.0504
	RC1-III_H	0.64	2.3	0.913	0.115	3	0.0239	0.0717
	RC1-II_L	0.50	2.3	0.437	0.363	3	0.0173	0.0518
	RC1-II_M	0.48	2.3	0.642	0.263	3	0.0269	0.0806
	RC1-II_H	0.48	2.3	0.913	0.185	3	0.0382	0.1147
	RC1-I_L	0.39	2.3	0.437	0.502	3	0.0239	0.0716
	RC1-I_M	0.37	2.3	0.642	0.363	3	0.0371	0.1114
	RC1-I_H	0.37	2.3	0.913	0.255	3	0.0528	0.1584
RC2 DCL	RC2-III_L	0.56	2.3	0.437	0.305	3	0.0145	0.0434
	RC2-III_M	0.54	2.3	0.642	0.220	3	0.0225	0.0676
	RC2-III_H	0.54	2.3	0.913	0.155	3	0.0321	0.0962
	RC2-II_L	0.40	2.3	0.437	0.487	3	0.0232	0.0695
	RC2-II_M	0.38	2.3	0.642	0.352	3	0.0361	0.1081
	RC2-II_H	0.38	2.3	0.913	0.248	3	0.0513	0.1538
	RC2-I_L	0.29	2.3	0.437	0.673	3	0.0320	0.0960
	RC2-I_M	0.27	2.3	0.642	0.487	3	0.0498	0.1494
	RC2-I_H	0.27	2.3	0.913	0.342	3	0.0709	0.2125
RC3 DCL	RC3-III_L	0.61	2.3	0.437	0.263	3	0.0125	0.0375
	RC3-III_M	0.59	2.3	0.642	0.190	3	0.0195	0.0584
	RC3-III_H	0.59	2.3	0.913	0.134	3	0.0277	0.0830
	RC3-II_L	0.45	2.3	0.437	0.421	3	0.0200	0.0600
	RC3-II_M	0.43	2.3	0.642	0.304	3	0.0311	0.0934
	RC3-II_H	0.43	2.3	0.913	0.214	3	0.0443	0.1328
	RC3-I_L	0.34	2.3	0.437	0.581	3	0.0276	0.0829
	RC3-I_M	0.32	2.3	0.642	0.420	3	0.0430	0.1290
	RC3-I_H	0.32	2.3	0.913	0.295	3	0.0612	0.1835

The typologies that are more similar to the two classes evaluated in this work are the RC1_L (without seismic provisions) for the PRE 1974 and the RC1-II_L (with low seismic provisions) for the POST 1974. Thus, a comparison between the results has been done, as shown in fig. 5.14 and in tabs. 5.12 and 5.13. For the PRE and POST 1974 classes the average values between all models are considered.

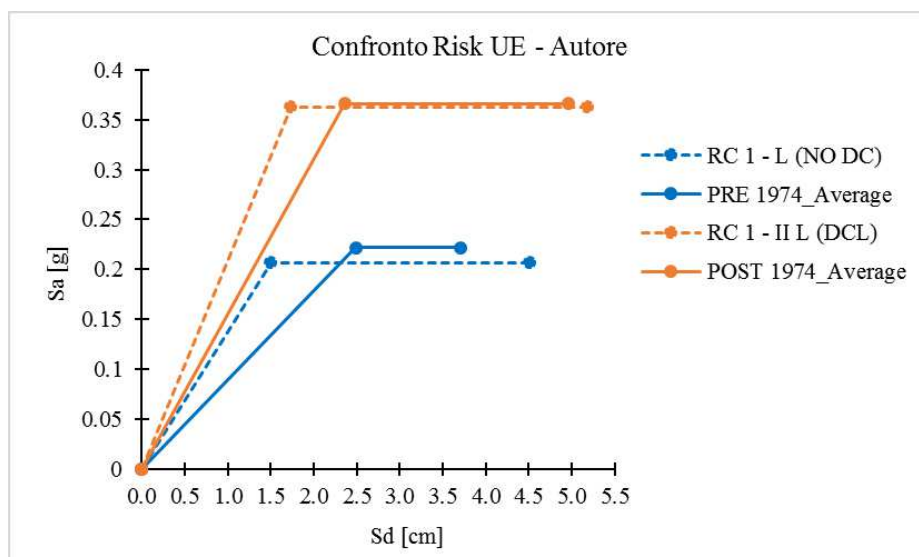


Figure 5.14. Comparison between average bilinear curves for the classes and bilinear curves provided from Risk UE project

Table 5.12. Mechanical values from parametric analyses (PRE 1974) and from Risk UE project (RC 1 - L)

	a_y [g]	d_y [cm]	d_u [cm]	u	T [s]
RC 1 - L (NO DC)	0.207	1.50	4.51	3.0	0.539
PRE 1974	0.222	2.49	3.70	1.48	0.662

Table 5.13. Mechanical values from parametric analyses (POST 1974) and from Risk UE project (RC 1 - II L)

	a_y [g]	d_y [cm]	d_u [cm]	u	T [s]
RC 1 - II L (DCL)	0.363	1.73	5.18	3.0	0.437
POST 1974	0.366	2.36	4.96	2.10	0.459

Comparing the respective values for the parameters obtained from each method, a good correspondence is found for the a_y , thus in terms of resistance, while the values of d_y and d_u appear rather discordant especially in the case of buildings designed accounting only for vertical loads. Indeed, the bilinear curves provided by the Risk-UE method have greater ductility, since the yield point is anticipated while the ultimate point is postponed if compared to the bilinear curves obtained as the average of the results of the parametric analyses. However, the fact that in the Risk-UE

method has been assigned the same value of ductility to structures with different levels of seismic design leaves a bit perplexed, so it can reasonably be said that for buildings designed accounting only for vertical loads (PRE 1974 buildings), the values provided by the author are more meaningful.

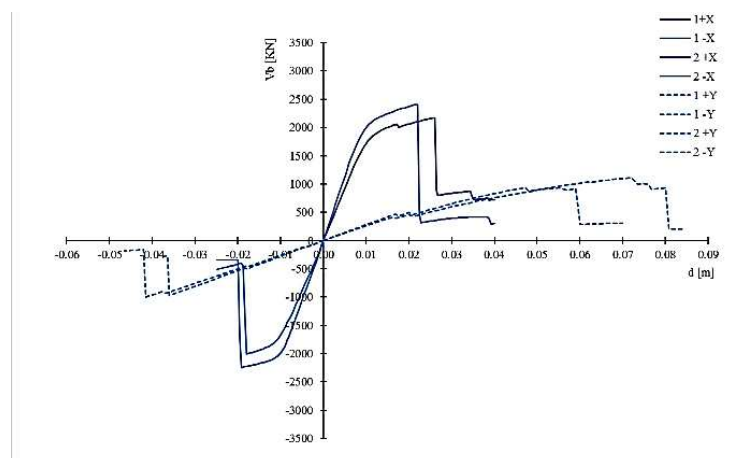
To summarize the results in terms of capacity expressed as the average area of the 8 areas under the equivalent bilinear curves, calculated for each model employed in the parametric analysis, the following statements are reported:

- For both classes and in almost all models, we have a higher capacity, especially in terms of stiffness and strength, in the X direction (the longitudinal one with parallel frames). The weak direction Y offers greater displacements but with very low values of both strength and stiffness. This can be explained by the high deformability available in the transverse direction due to the lack of frames with high beam, whereby the columns work in parallel and exhibit a cantilever behaviour. The low displacement values offered from the X direction for both classes are due to the presence of numerous short columns along the facades due to the ribbon windows. In the POST 1974 case, even if there are greater cross sections of the columns along the X direction, this is not supported by adequate constructive details to increase ductility, thus the ultimate displacement offered is again very low.

However, there is an improvement both in terms of strength and ductility compared to the PRE 1974 building.

- For a given model, the capacity in both directions of the POST 1974 class is always higher than the corresponding relative to the PRE 1974 class.

Finally, the nonlinear response of the two prototype buildings was evaluated more in depth. The capacity curves obtained through pushover analyses are shown in fig. 5.15, on the left for the PRE 1974 prototype building and on the right for the POST 1974.



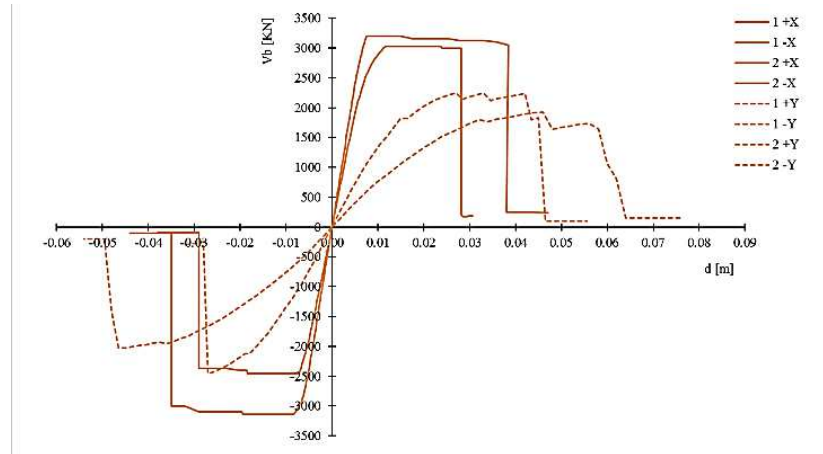


Figure 5.15. Capacity curves for the PRE 1974 (upper) and POST 1974 (lower) prototype buildings

In fig. 5.16 the response of two prototype buildings is compared with respect the two directions.

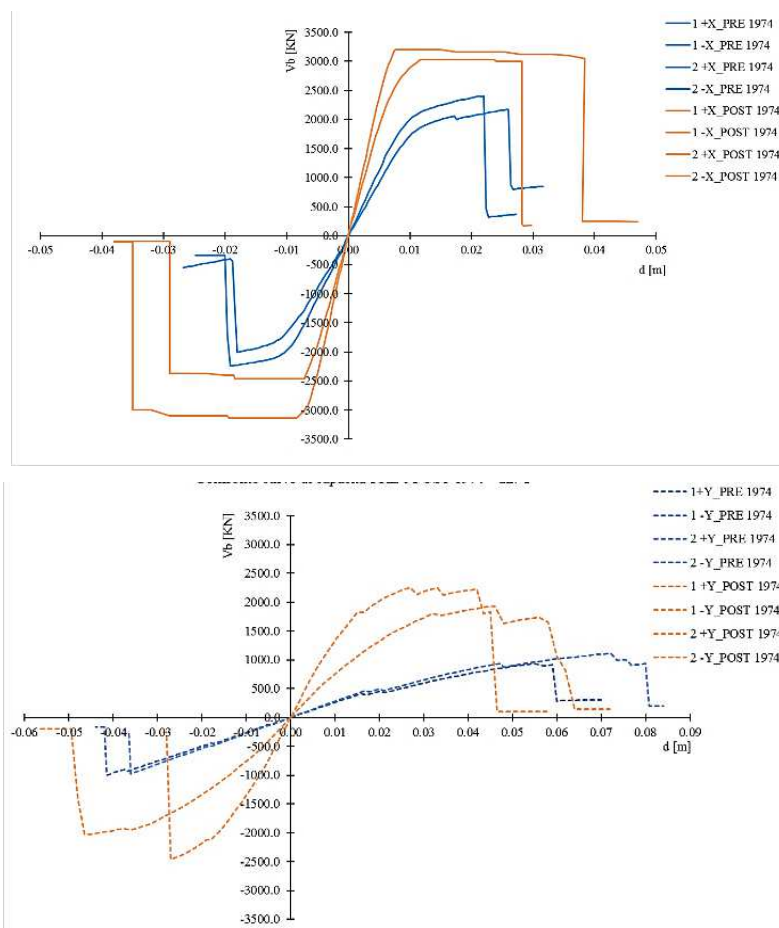


Figure 5.16. Comparison of the capacity curves for the two prototype buildings: X direction (upper) and Y direction (lower)

By evaluating the ways in which collapse occurs, we can say that, with regard to the PRE 1974 building, when the forces distribution acts in the X direction there is a progressive shear collapse of short columns on the longitudinal facades and of some perimeter beams on both sides as shown in fig. 5.17 on the left side.

While referring to the flexural collapse, it is also progressive and is achieved in many elements more widespread in the structure (fig. 5.16 right side).

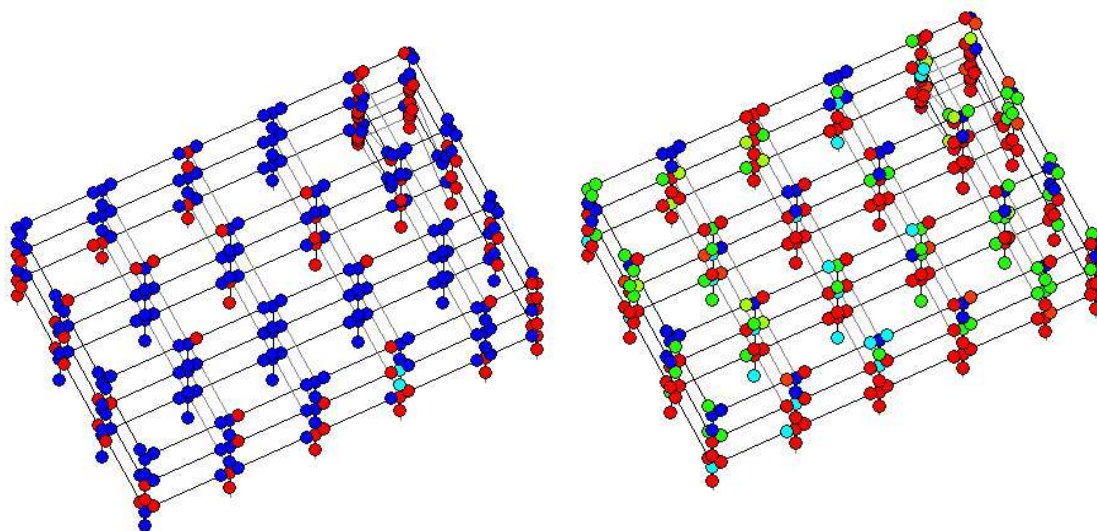


Figure 5.17. PRE 1974 building_Collapse for shear (left) and for flexural (right) due to the force distribution PUSH MASSA – X

When the forces distribution acts in the Y direction the collapse begins in correspondence of the short columns of the stairs and then it spreads to the other parts of the structure, with many elements that collapse for shear and flexure, usually at the same time, as shown in fig. 5.18.

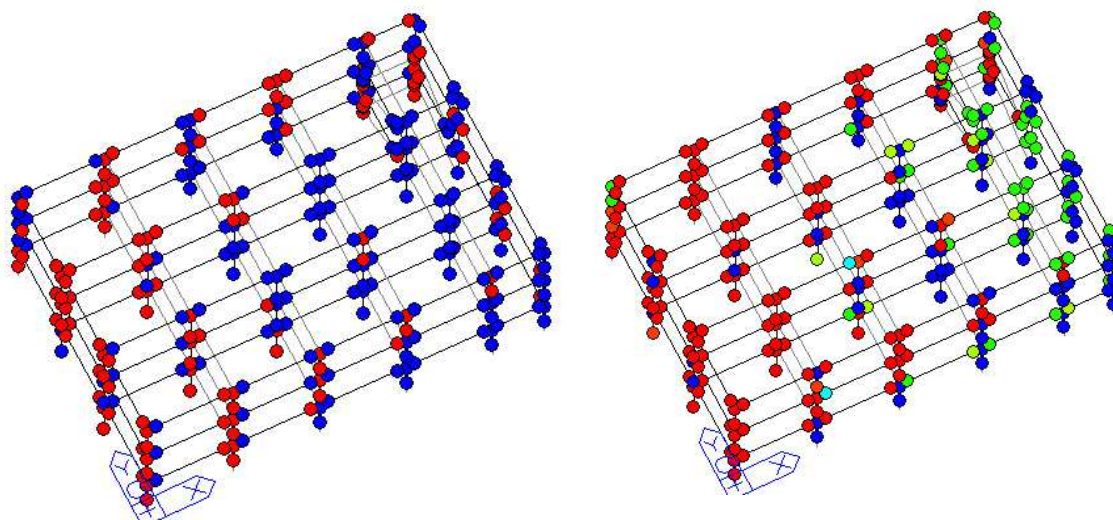


Figure 5.18. PRE 1974 building_Collapse for shear (left) and for flexural (right) due to the force distribution PUSH MODE -Y

With regard to the prototype building of the class POST 1974, the force distributions acting in the X direction causes a simultaneous collapse of almost all elements, both for shear and flexure (fig. 5.19).

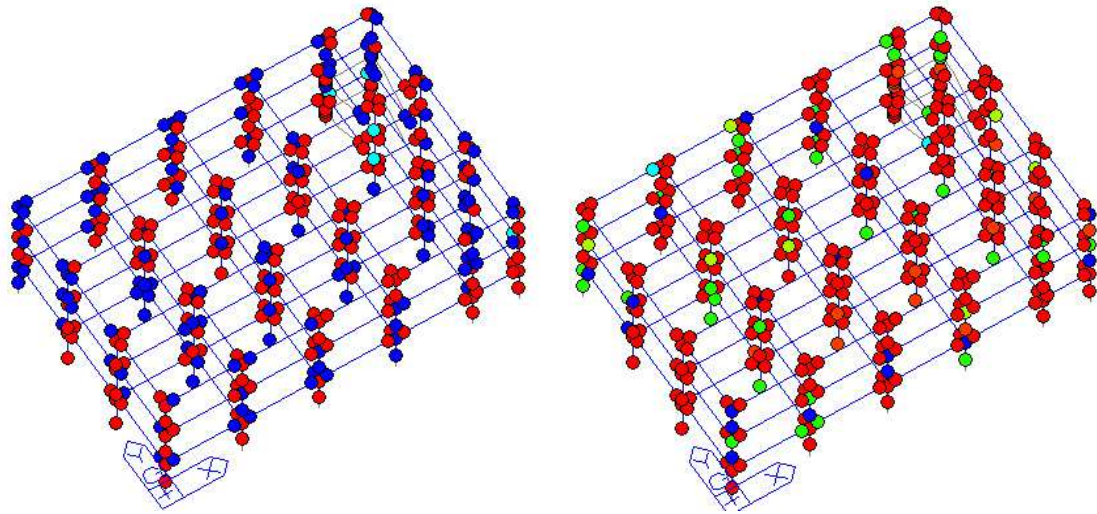


Figure 5.19. POST 1974 building_Collapse for shear (left) and for flexural (right) due to force distribution PUSH MODE +X

The force distributions acting in Y direction causes a progressive collapse of the building due to the collapse of both columns and beams (fig. 5.20).

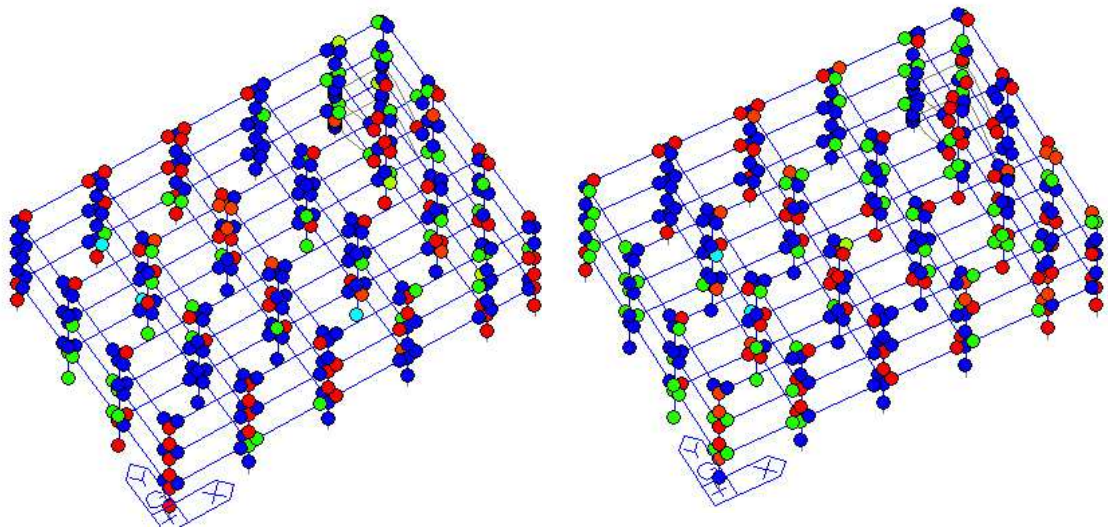


Figure 5.20. POST 1974 building_Collapse for shear (left) and for flexural (right) due to force distribution PUSH MODE -Y

5.4. Proposed method for school buildings

As showed in chapter 2, the GNDT methods does not take into account all the meaningful vulnerabilities detected in chapter 3 for the school buildings typology, since some factors are too general and do not allow evaluating the influence of the single vulnerabilities on the seismic behaviour. Thus, the aim of this work is to upgrade the GNDT schedule to school buildings typology.

The aim is to have a single vulnerability sheet that is valid for all those school buildings designed without or with low seismic details, so before the enforcing of the OPCM 3274 dated 2003.

A total of 15 parameters and 3 vulnerability classes (A, B, and C) to which correspond the scores W_i , increasing from class A to C.

At the class A, corresponding to the absence of vulnerability for the parameter investigated, a score equal to 0 is assigned.

The vulnerability index I_v is given by the sum of the scores and assumes values on a scale from 0 to 10.

So, a building that does not have any kind of vulnerability and also has a high level of seismic design (all parameters in class A) has a value of I_v equal to 0, while I_v is equal to 10 the building has the maximum vulnerability (all parameters in class C).

Generally, a building can get any value of I_v even if it has a high level of seismic design (e.g. it is in class A with respect to the parameter number 2 because it is designed after 2003, but it has other vulnerabilities).

Score assignment for vulnerability factors

For every parameter, the comparison between the structural capacity of the prototype building and of the modified buildings in order to represent the variation of the parameter has been done. To this aim several configurations of the same parameter were developed and compared each other (e.g. to assess parameter 1, using $f_{cm} = 15, 20, 25, 20$).

The area under the equivalent bilinear curve of the SDOF system has been assumed as measure of the structural capacity to perform the comparison (instead of, in example, the yielding spectral acceleration a_y or the ultimate displacement du), then calculating a single average value between the areas relative to the 8 bilinear curves (4 in X and 4 in Y) obtained for each model. The bilinear area was considered to be the best parameter to summarize the structural response in terms of both strength, stiffness and ductility, and hence of global energy dissipation.

The weight w_i of each parameter p_i in the modified vulnerability index method has been determinate as follow.

1. For each structural model m_{ij} relative to the parameter p_i and derived from both the PRE 1974 and POST 1974 prototype buildings, the areas underlying the 8 equivalent bilinear curves (4 horizontal load patterns in X direction and 4 in Y direction) has been computed.
2. Then the average of the 8 areas, A_{ij} , was computed for both classes. In this way, only a value representative of the global capacity was considered for every structural model m_{ij} , even if a different seismic capacity exists between to two main directions of the buildings.

$$A_{ij} = \frac{1}{8} \sum_i A_{xy,i} \quad (5.1)$$

3. The average value $A_{ij,m}$ of the two A_{ij} values relative to PRE and POST 1974 classes was calculated (eq. 5.2). This choice is to take into account the uncertainty in structural response, because a general building can have a structural scheme different from those used to represent the two classes. Anyway, it worse noting that for most parameters the response in terms of relative values is similar between the two classes.

$$A_{ij,m} = \frac{1}{2} [A_{ij} (\text{PRE 1974}) + A_{ij} (\text{POST 1974})] \quad (5.2)$$

Thus, an average bilinear curve is obtained for each configuration of the parameter p_i (fig. 5.21) and relative areas $A_{ij,m}$ can be compared.

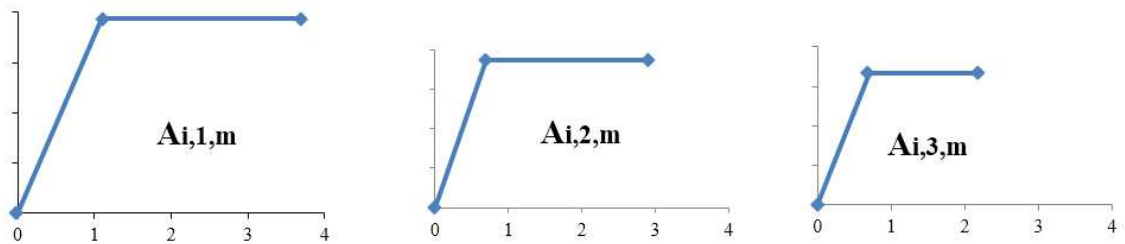


Figure 5.21. Comparison of the average bilinear curves relative to several configurations of the same parameter.

4. For each parameter, the ratios between the $A_{ij,m}$ values relative to the prototype building and to other models m_{ij} , used to represent the several configurations of the same parameter p_i , have been computed in order to find the maximum ratio $R_{i,max}$ (the maximum variation in terms of capacity and so a measure of the maximum incidence of the parameter on the global vulnerability) with eq. 5.3:

$$R_{i,max} = \frac{\max [A_{ij,m}]}{\min [A_{ij,m}]} \quad (5.3)$$

5. The sum S of the $R_{i,max}$ values of the all parameters was computed and then each $R_{i,max}$ value was divided for S (normalization), obtaining 15 scores w_i representing the maximum influence of each parameter p_i on the global vulnerability (eq. 5.4):

6.

$$w_i = \frac{R_{i,max}}{S} \quad (5.4)$$

7. Thus, the weight w_i was assumed as the score for the class C, while the half of w_i was assigned to the class B. For class C a score equal to zero was adopted, representing the best condition in terms of capacity for the parameter.

The 15 parameters and the scores assigned are shown in tab. 5.14.

Table 5.14. Vulnerability indicators and relative scores proposed by the author

Vulnerability indicators	Classes and scores		
	A	B	C
1 - Age of building	0	0.35	0.70
2 – Reference Code	0	0.50	1.00
3 – Built in seismic zone	0	0.75	1.50
4 – Typology of the resistant system	0	0.30	0.60
5 – Quality of the resistant system	0	0.35	0.70
6 – Critical elements	0	0.40	0.80
7 – Irregularity in plan shape	0	0.30	0.60
8 – Irregularity in elevation shape	0	0.15	0.30
9 – Irregularity in plan stiffness	0	0.25	0.50
10 - Irregularity in elevation stiffness	0	0.50	1.00
11 – Position and type of stairs	0	0.30	0.60
12 – Stiffness of floor slabs	0	0.20	0.40
13 – Position of foundations	0	0.10	0.20
14 – Irregularity of storey mass	0	0.20	0.40
15 – Degradation of materials	0	0.35	0.70

In general, it can be said that the scores obtained appear to be balanced and consistent with the influence that individual indicators may have on the global vulnerability.

However, these are related to a specific type of buildings (schools), with well-defined typological characteristics, so their reliability is limited to this context. In fact, any parameter may have a different weight on the vulnerability if inserted into another structural scheme.

For example, in the present case, it was decided to evaluate the parameters on a scheme that was as close as possible to the analyzed typology rather than to an abstract scheme, so the models have ribbon windows that delimit short columns along the longitudinal direction, whose premature collapse could nullify any improvements to the structural response.

It is also to be noted that in some cases non-adaptive and unimodal pushover analysis may fail to accurately investigate the nonlinear structural response, as there are situations in which a structural model that has an additional vulnerability compared to another and, therefore, it should be more vulnerable, but the pushover analysis has provided a greater average capacity. This may be due to the fact that with this type of analysis, one cannot grasp the actual evolution of the dynamic behaviour and thus the negative contribution to the response due to irregularities of a certain type.

Parameters that have the highest scores and thus affect most the vulnerability are:

- parameter n. 2 "*Reference Code*" with a score of 1.30 in class C, as it refers on the constructive details and the type of steel used (smooth or ribbed).
- parameter n. 3 "*Built in seismic zone*" with a score of 1.50 in class C, as it refers on the structural scheme adopted, i.e. accounting only for vertical loads or even for seismic actions.
- parameter n. 10 "*stiffness irregularity in elevation*" with a score of 1.10 in class A, as it evaluates the distribution of the infills along the height and, therefore, also the presence of a pilotis storey.
- parameter n. 15 "*Material deterioration*" with a score of 1.00 in class A, as it evaluates the presence of more or less extensive degradation, that is the reduction of cross-section due to the corrosion of the steel reinforcement which causes the expulsion of the concrete coverage.

While the parameters that least affecting, all with a score of 0.20 in class A, are:

- parameter n. 5 "*Quality of the Resistant System*", which assesses the presence and type of frames in to the two main directions of the building. It has been seen that considering a frame with high beams also in the transverse direction, designed without seismic criteria and, therefore, with weak columns-strong beam ratio, global capacity not increases very much.
- Parameter n. 13 "*Position of foundations*", which considers the position of foundations on different levels.
- Parameter n. 14 "*Irregularity of storey masses*", which considers a not uniform distribution of the storey masses.

Thus, comparing the method proposed by the author, specify for RC school buildings, with the 2nd level GNDT method, general for RC buildings, the following conclusions can be expressed:

- The number of parameters used by the author is greater than those of the GNDT method, in order to better capture even the smallest differences between buildings.
- Scores provided by the author have a greater variability among the several parameters, while those provided by the GNDT method are for the most part equal to each other. This allows a more accurate evaluation and differentiation of the final results, in terms of vulnerability index, for the buildings belonging to the stock under investigation.

In the following the criteria to assign the vulnerability classes to each parameter are shown.

1. Age of the building

A – Built before the 1970

B - Built between the 1970 - 2000

C – Built after the 2000

2. Reference Code

A – Buildings designed according to the Royal decree dated 1939.

B - Buildings designed according to the law n.1086 dated 1971 and relative decree.

C – Buildings designed according to OPCM 3274/ 2003 and NTC 2008.

3. Built in seismic prone area

A – Buildings located in non-seismic prone area at the construction period.

B - Buildings located in seismic prone area of 1st, 2nd or 3th category at the construction period. Building located in non-seismic prone area at the construction period but subjected to retrofitting interventions before the enforcement of the OPCM 3274 dated 2003.

C – Buildings located in seismic prone area defined according to the in force seismic map. Buildings subjected to retrofitting interventions after the enforcement of the OPCM 3274 dated 2003.

4. Typology of structural system

A – RC frames with weak infills (large openings such as ribbon windows, small thickness, non-resistant materials etc.).

B – RC frames with strong infills in some part of the building perimeter.

C – RC frames with strong infills widely spread on the building perimeter.

5. Quality of the resistant system

A – Unidirectional frames with strong beams-weak columns behaviour (es. $H_b > 2H_c$).

B – Bidirectional frames with strong beams-weak columns behaviour (es. $H_b > 2H_c$).

C – Bidirectional frames with strong columns -weak beams behaviour (es. $H_b > 2H_c$).

6. Critical elements

A - Contemporary presence of ribbon windows and stairs with knee beams that identify short columns.

B – Individual presence of ribbon windows or knife beams that identify short columns.

C – Absence of short elements.

7. Irregularity in the plan shape

A - Strongly irregular plan shapes (L, C or other shapes different from the compact one).

B – Compact plan shape with limited protrusions.

C - Regular plan (compact and without protrusions).

8. Irregularity in the elevation shape

A – Presence of large bow-windows (> 1 m) particularly wide (e.g. on the whole building side) or abrupt constrictions between a floor and the others ($L_c / L_s > 0.5$).

B - Presence of bow-windows with limited extension (e.g. only a part of the building side) or reduced constrictions between a floor and the others ($L_c / L_s < 0.5$).

C – No geometric irregularity in elevation.

9. Stiffness irregularity in plan

A – Infills with different materials (e.g. brick one side and glazed on the other) or infills with different shape (e.g. ribbon windows on one side and full height walls on the other) widespread on the sides of the building.

B – Infills with different materials (e.g. brick one side and glazed on the other) or infills with different shape (e.g. ribbon windows on one side and full height walls on the other) present in limited parts on the sides of the building.

C – Infills with the same characteristics on all sides for each building level.

10. Stiffness irregularity in elevation

A – Presence of pilotis storey at least on one side of the buildings.

B – Excessive reduction of the cross section of vertical resistant elements between the buildings levels. Irregular arrangement of infills in elevation.

C - None of the previous ones.

11. Position of the stairs

A – Stairs made of knee-beams and located in eccentric position in the plan.

B – Stairs made of rampant slabs and located in eccentric position. Stairs made of knee-beams and located in central position in the plan.

C – Stairs made of rampant slabs and located in central position in the plan.

12. Stiffness of floor slabs

A – Floor slabs with low in-plane stiffness (lack of reinforcement in the slabs, thickness lower than 4 cm, void in the slabs) placed on weak columns (absence of adequate seismic detailing).

B – Floor slabs with high in-plane stiffness placed on weak columns.

C – Floor slabs with high in-plane stiffness placed on strong columns (presence of adequate seismic detailing).

13. Position of foundations on the ground

A – Foundations placed on more ground levels for a large extension of the building.

B – Foundations placed on more ground levels for a large small extension of the building.

C – Foundations placed at the same ground level.

14. Irregularity of storey masses

A – Variation of floor masses due to different types of floor slabs, voids in the slabs (e.g. double heights).

B – High values of the live load at the upper levels of the building due to different use (library, archive etc.).

C – Storey masses are regularly distributed both in plan and elevation

15. Degradation of materials

A - Degradation of materials widespread on many structural elements (more than the 50% of elements are involved).

B - Limited degradation of materials (less than the 50% of elements are involved).

C – Materials are not deteriorated.

5.4.1. I_v – PGA relationship

The vulnerability Index I_v is a representative parameter of the global vulnerability/capacity of the structure, and thus it does not provide an absolute measure of the damage that the building could suffer for a certain intensity event, but only allows comparisons between buildings of the same type. For this reason, performing mechanical analysis, analytical relationships between the vulnerability index and capacity in terms of PGA was carried out with respect the condition of both slight damage

(D1 in the EMS-98 scale, operating limit state - SLO in EC8) and collapse (D4 to D5 in the EMS-98 scale, collapse limit state – SLC in EC8).

Thus, it is possible to compare the results provided from the rapid method with the ones provided by the mechanical method, validating the reliability of the vulnerability index method here developed.

Moreover, the capacity in terms of PGA then can be easily compared with the maximum expected PGA at the reference site obtained from the hazard analysis.

The Iv - PGA relationships were obtained in first publication (*Guagenti et al. 1989*) by statistical analysis of damage data detected from buildings affected by the earthquakes of Friuli 1976 and Abruzzo 1984.

In the Municipalities of Venzone, Tarcento, San Daniele and Barrea, etc. for buildings that suffered different damage levels, the damage was detected by using the datasheet for the survey of the damage in force at that time, thus establishing a certain damage level Dk. In parallel, for the same buildings the vulnerability index Iv was obtained by means the 2nd level GNDT method

Then, by correlating the values of Dk and Iv of each building and associating the macroseismic intensity with the detected damage levels, relationships between PGA and vulnerability index Iv was obtained. First though the macroseismic intensity I was converted into PGA by using the empirical relation of eq. 5.5 (*Guagenti et al. 1989*):

$$\ln y = a I + b \quad (5.5)$$

where y is the PGA and a and b are coefficients:

$$a = 0.602,$$

$$b = 7.073$$

Thus, the relationships Iv - PGA were then revised and calibrated within the GNDT (*Petrini 1995, Meroni et al. 2000*), reaching the form of eq. 5.6 and 5.7 respectively for the slight damage and the collapse.

$$PGA_s = 0.155 e^{[-0.0207 (Iv + 25)]} \quad (5.6)$$

$$PGA_c = \frac{1}{[0.625 + 0.00029 (Iv + 25)^{2.145}]} \quad (5.7)$$

where PGAs and PGAc represent respectively the acceleration for which the building suffers slight damage and collapse.

The presence of the term +25 in eq.5.6 and 5.7 is since for Iv values it was considered a range from -25 to 100, since that the negative values of Iv had to represent buildings designed with better

criteria than those of which damage was detected after the earthquake of Friuli (1976) and Abruzzo (1984), with which the same relationships were carried out but without the term +25.

Once know the PGA values relative to slight damage and the collapse, the trilinear damage curves can be developed. They constitute a useful tool to estimate the expected value of physical damage and losses in economic terms and casualties, once the hazard level of the site, the consistency of the building stock and its vulnerability are known.

Fig. 5.22 shows the trilinear damage curves for the I_v - PGA_c relationship provided by the GNDT method.

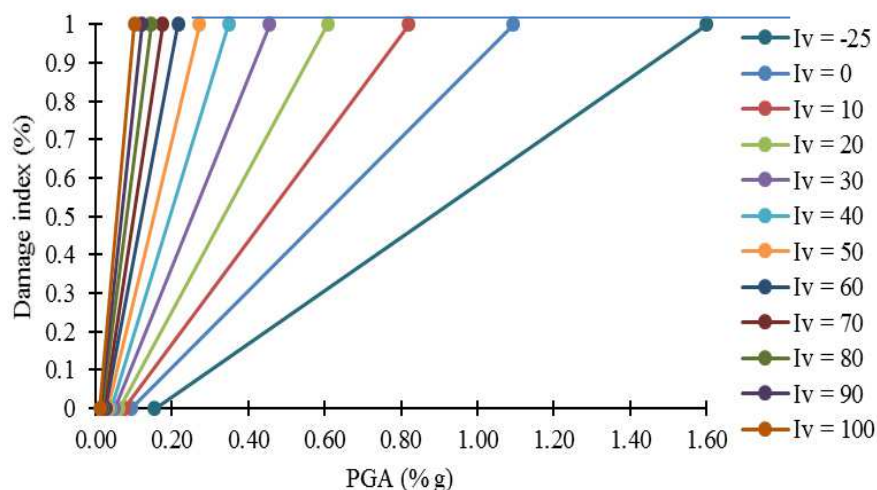


Figure 5.22. Trilinear damage curves provided from GNDT method

On the Y axis the economic damage index (DI, ranged between 0 and 1) is reported, calculated as the ratio between the expected repair cost and the total replacing cost. On the X axis the hazard level is represented in terms of PGA. Thus, each curve is immediately identified by assuming $DI = 0$ for the PGAs and $DI = 1$ for the PGA_c .

The two I_v - PGA relationships proposed by the author were determined by the best interpolation of the cloud of points representing the results from both the rapid and mechanical evaluations of each structural model used in the parametric analysis previously described. In the abscissa are shown the values of I_v obtained through the datasheet proposed by the author, while in the Y axis are reported the capacity in terms of PGA determined by means pushover analysis. In particular, the PGAs (slight damage) was determined in correspondence of the point with 0.7 ay on the average bilinear curve of the structural model considered, while the PGA_c (collapse) was determined in correspondence of the ultimate displacement point of the same average bilinear curve (please see the following part "procedure to calculate the PGA from pushover analysis" for a more depth description of the procedure adopted).

Fig. 5.23 shows the cloud of points respectively for the I_v - PGAs and I_v - PGA_c pairs.

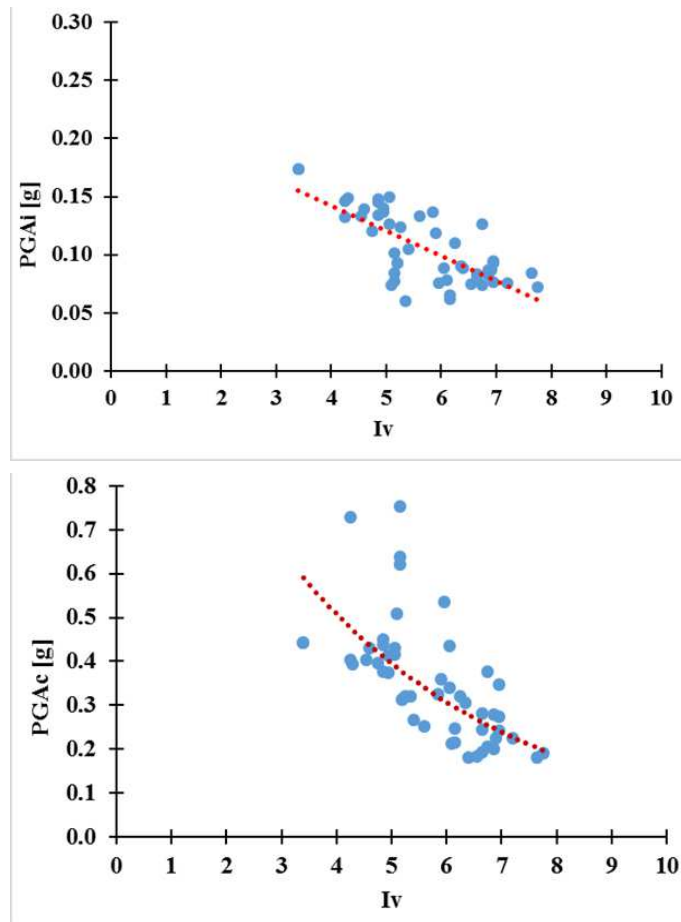


Figure 5.23. *Iv - PGA relationship for the slight damage (upper) and the collapse condition (lower)*

Thus, the analytical relationships, valid for both PRE and POST 1974 classes, are eq. 5.8 and 5.9.

$$PGAs = 0.2288 - 0.0215 Iv \quad (5.8)$$

$$PGAc = 1.39 * e^{-0.25 Iv} \quad (5.9)$$

It should be noted that the relationships are valid for RC structures which have the same characteristics of the two building classes here evaluated, and therefore without adequate seismic design, even though a range of Iv between 0 to 10 was assumed, that contemplates buildings designed according to any level of seismic design (absent, low, and high). In addition, the relationship is more reliable for Iv values within the range of 3 to 8, for which data are available, while for Iv values less than 3 and greater than 8 the PGAc is obtained by extrapolation.

The trilinear damage curves for the Iv - PGA relationships proposed by the author are shown in fig. 5.24.

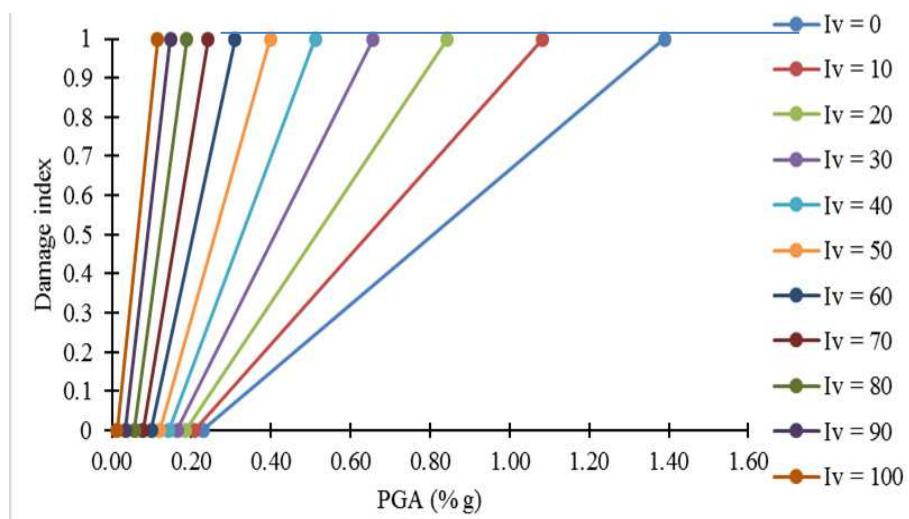


Figure 5.24. Trilinear damage curves provided from the author

In tab. 5.15 for some Iv values, the comparison of the PGAs and PGAc values calculated according to both the GNDT method and that proposed by the author, is reported for some Iv values. It is worth noting as the proposed method provides higher values of both PGAs and PGAc for every Iv value.

Table 5.15. Comparison between the PGA values provided from both methods

<i>Iv</i>	PGAs_ Author	PGAs_ GNDT	PGAc_ Author	PGAc_ GNDT
-25	-	0.155	-	1.600
0	0.229	0.092	1.390	1.094
1	0.207	0.075	1.083	0.820
2	0.186	0.061	0.843	0.608
3	0.164	0.050	0.657	0.456
4	0.143	0.040	0.511	0.349
5	0.121	0.033	0.398	0.272
6	0.099	0.027	0.310	0.217
7	0.078	0.022	0.242	0.176
8	0.056	0.018	0.188	0.145
9	0.035	0.014	0.147	0.121
10	0.013	0.012	0.114	0.103

Fig. 5.25 shows the trend of PGAc and PGAs by varying the Iv value, according to the formulations proposed by the GNDT and by author. To note how the curves are very close for the higher Iv values, while they are quite distant for Iv values between 0 and 50.

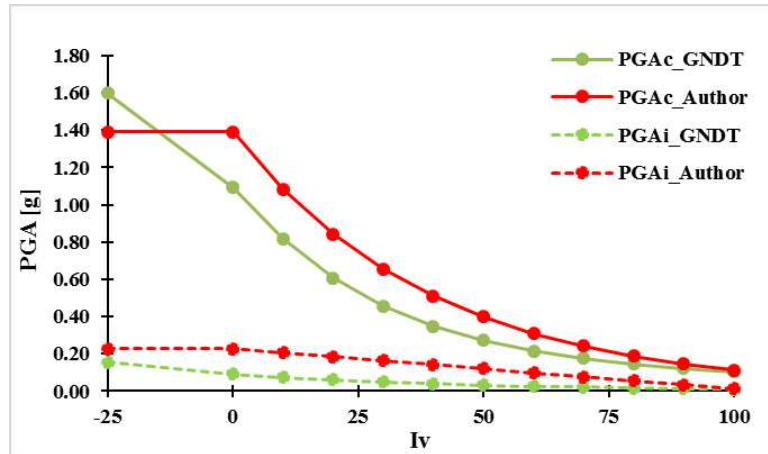


Figure 5.25. Comparison of the PGA values from the GNDT and the proposed methods

Procedure to calculate the capacity in terms of PGA from pushover analysis

PGA values relative to both collapse (PGAc) and slight damage (PGAs) condition were calculated for each model employed in the parametric analysis, as the mean of the values obtained from each of the 8 equivalent bilinear capacity curves, by means the procedure described below.

Assuming the ultimate capacity of the structure the point on the capacity curve of the MDOF system with a decay greater than the 20 % of the maximum base shear value, the equivalent bilinear curve according to the N2 method (Fajfar 2000) was determined for each analysis performed. Then the average bilinear curve was calculated as representative of each structural model.

Subsequently, in the Acceleration-Displacement Response Spectra - ADRS plane (Mahaney 1993), a spectral form was fixed and scaled up to individuate the:

- elastic spectrum in terms of acceleration, passing for the point $(d_i, 0.7 a_y)$ of the average bilinear curve, therefore characterized by the elastic vibration period T_{el} and spectral acceleration $S_{ae}(T_{el})$.
- the inelastic spectrum passing for the point $(d_u; a_y)$ of the average bilinear curve, characterized by the effective vibration period T_u , spectral acceleration $S_{ai}(T_u)$ and over strength factor R_{μ} .

Fig. 5.26 summarizes the incremental procedure.

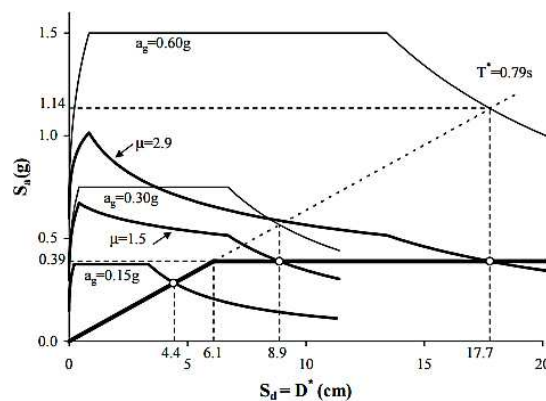


Figure 5.26. Incremental procedure to calculate the PGA

The acceleration of the two points considered on the bilinear is the same as the hardening is not considered in N2 method, while the vibration period changes. In fact, in the first case, the period is the elastic one, instead in the second case it is the inelastic one (effective period T_{eff}), which relates to the very damaged structure imminent to collapse. To calculate the effective periods the secant stiffness (Priestley *et al.* 2004) can be used as shown in fig. 5.27.

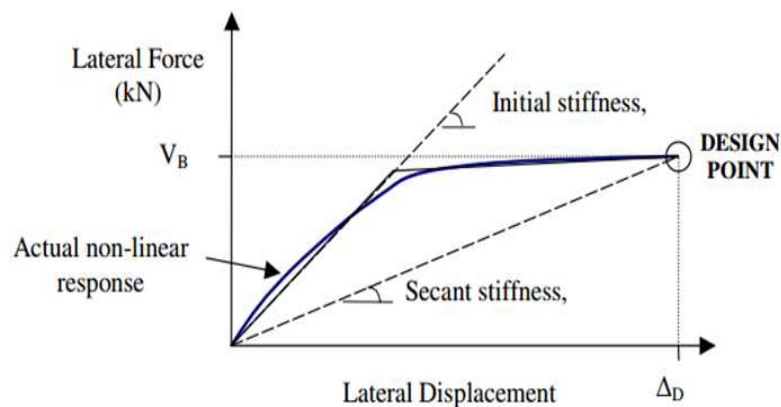


Figure 5.27. Initial and secant stiffness

Thus eq. 5.10 and 5.11 were employed:

$$T_y = 2\pi \sqrt{\frac{dy}{ay}} \quad (5.10)$$

$$T_{eff} = 2\pi \sqrt{\frac{du}{ay}} \quad (5.11)$$

A spectral shape was fixed according to the provisions of the in force Italian seismic code, assuming the following values of the hazard parameters characteristic for the area of interest:

$F_0 = 2.46$ (maximum spectral amplification)

$T_c^* = 0.30$ s (corner period)

The values of T_{el} and T_{eff} were calculated for each structural model employed in parametric analysis, as the average of the values relative to the 8 bilinear curves available. They are always greater than $T_c = T_c * C_c$, thus the third equation was used to calculate the PGA.

In tab. 5.16 the average values of all structural models of the two classes are reported.

Table 5.16. Average elastic and effective periods for the classes

	T_{el} [s]	T_{eff} [s]
<i>PRE 1974</i>	0.662	0.820
<i>POST 1974</i>	0.459	0.648

It is possible to note that the periods relative to the PRE 1974 class are greater than the respective ones of the POST 1974 class, meaning a greater deformability of the former as expected.

Thus, the PGA values can be calculated by means eq. 5.12:

$$PGA = \frac{S_{ae}(T)}{(F_0 * n * S)} \frac{T}{T_c} \quad (5.12)$$

where:

- $n = 1/q$; q is the behaviour factor (or R_u , resistance reduction factor), the ratio between the maximum force F_{el} if the SDOF system remains elastic and yield force F_y .
- S is the coefficient that take into account the local amplification due to subsoil and topographic conditions.

Known the vibration periods, the spectral acceleration for the points of interest on the bilinear curve and the relative values of ductility, the PGAs and PGAc are obtained going backward on the response spectra.

In the case of the PGAs, $q = 1$ because it is in the elastic field, while for the ultimate condition the inelastic spectrum is assumed with $q = R_\mu$.

The resistance reduction factor R_μ due to ductility is calculated by means eq. 2.9 and 2.10:

Thus, it is possible to go from the acceleration on the inelastic spectrum $S_{ai}(T)$ to that of the elastic spectrum $S_{ae}(T)$ for the same period T by means eq. 5.13 (*Vidic et al. 1994*):

$$S_{ae}(T) = S_{ai}(T) * R_\mu \quad (5.13)$$

Figs. 5.28 and 5.29 show the PGAc and PGAs values for each structural model employed in parametric analysis, comparing the values relative to the PRE 1974 and POST 1974 models.

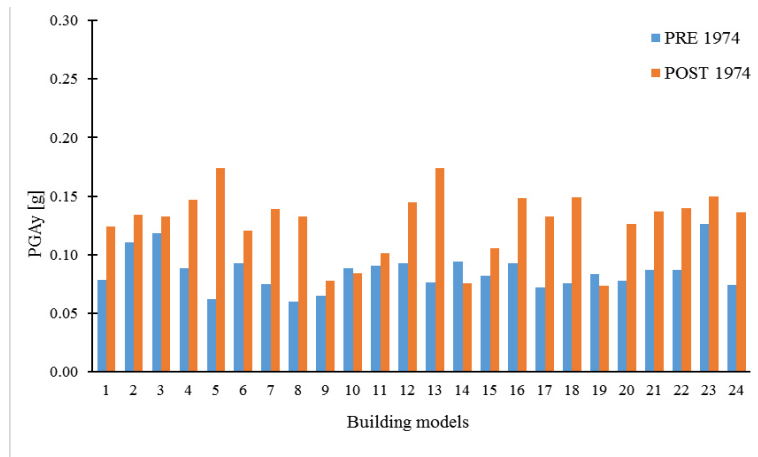


Figure 5.28. PGAi values for the PRE and POST 1974 buildings

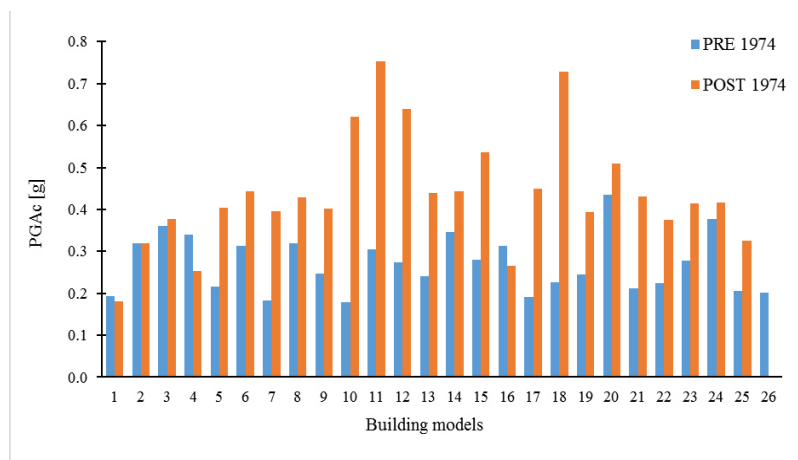


Figure 5.29. PGAc values for the PRE and POST 1974 models

Fig. 5.30 shows the Iv values for the same models.

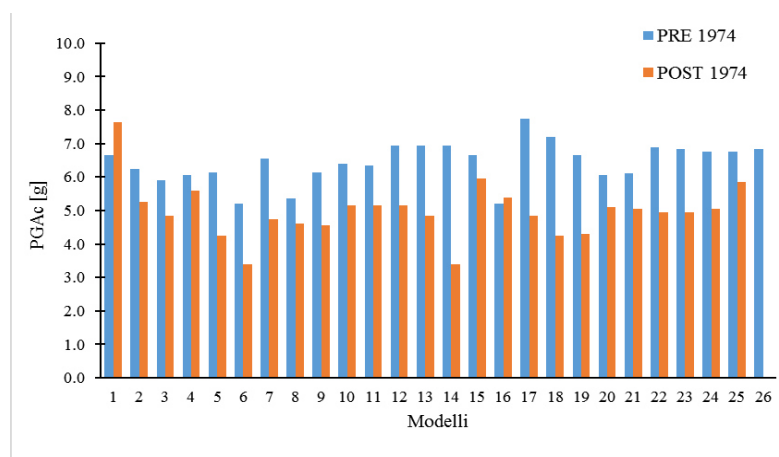


Figure 5.30. Iv values for the PRE and POST 1974 models

Average values of I_v and PGA from the all structural models representative of the two classes are shown in tab. 5.17.

Table 5.17. Average values of I_v and PGA for the PRE and POST 1974 classes

	<i>Average I_v</i>	<i>Average PAG_i [g]</i>	<i>Average $PGAc$ [g]</i>
<i>PRE 1974</i>	6.4	0.122	0.270
<i>POST 1974</i>	5.0	0.182	0.438

Obviously, the POST 1974 class has a lower average I_v value and higher average PGAs and $PGAc$ values than the PRE 1974 class.

It should be noted that the $PGAc$ values used to obtain the I_v - $PGAc$ relation refer to the global capacity of the structure, so the situation in which many elements are heavily damaged and so the structure has lost its bearing capacity. Thus, it is not the situation in which the collapse mechanism occurs in a single element (for flexure or shear) as it is usually assumed in the seismic safety assessments of the current seismic codes.

However, this hypothesis is supported by the fact that, considering the damage to buildings detected after past earthquake, they often do not exhibit severe damage or collapse due to levels of ground acceleration provided by the regulations for the most severe limit state (e.g. for the areas interested from this study, classified as of medium seismic hazard, the expected acceleration for these limit states and for the most frequent site conditions, oscillates between a minimum of 0.25 g and a maximum of 0.41 g).

However, the damage suffered by buildings is due more to the spectral acceleration $S_a(T)$ than the PGA, because the spectral acceleration takes into account the dynamic characteristics of the building. Indeed, it may happen that low PGA values cause more severe damage than higher PGA values, because the frequency content of the ground shaking could mainly affect a certain structural typology characterized by an own frequency similar to that of the earthquake.

References chapter 5

- Dolsek M. Estimation of Seismic Response Parameters Through Extended Incremental Dynamic Analysis. In: Papadrakakis M., Fragiadakis M., Lagaros N. (eds) Computational Methods in Earthquake Engineering. Computational Methods in Applied Sciences, vol 21. Springer, Dordrecht. 2011.
- Manfredi G. et al. Structural modeling uncertainties and their influence on seismic assessment of existing RC structures. *Structural Safety* 32 (2010) 220–228
- Masi and M. Vona, “Vulnerability assessment of gravity-load designed RC buildings: Evaluation of seismic capacity through non-linear dynamic analyses,” *Eng. Struct.*, vol. 45, pp. 257–269, Dec. 2012.
- Verderame G.M., Polese M., Mariniello C., Manfredi G., A simulated design procedure for the assessment of seismic capacity of existing reinforced concrete buildings, *Advanced in engineering software*, 41, 323-335, 2010.
- Verderame G.M., Stella A., Cosenza E., Mechanical properties of concretes adopted in R.C. structures in the age '60 (in Italian), *Proceedings of the 10th National ANIDIS Conference: Seismic Engineering in Italy*, Potenza-Matera, Italy, 2001.
- Verderame G.M., Stella A., Cosenza E., Mechanical properties of reinforcing steel adopted in R.C. structures in the age '60 (in Italian), *Proceedings of the 10th National ANIDIS Conference: Seismic Engineering in Italy*, Potenza-Matera, Italy, 2001.
- Krawinkler H. et al. Pros and cons of a pushover analysis of seismic performance evaluation. *Engineering Structures* Volume 20, Issues 4–6, April–June 1998, Pages 452-464
- Chopra A.K., Goel R.K. (2002). “A modal pushover analysis procedure for estimating seismic demands for buildings”. *Earthquake Engineering and Structural Dynamics*, 31, 561-582.
- Asteris P.G., Chrysostomou C.Z., Giannopoulos I., Ricci P. (2013) Modeling of Infilled Framed Structures. In: Papadrakakis M., Fragiadakis M., Plevris V. (eds) Computational Methods in Earthquake Engineering. Computational Methods in Applied Sciences, vol 30. Springer, Dordrecht

- Spacone E. et al. Localization Issues in Force-Based Frame Elements. *Journal of Structural Engineering* 127(11). 2001
- CEN (2005). Eurocode 8: Design of structures for earthquake resistance. Part 3: Assessment and retrofitting of buildings. EN 1998-3, Comité Européen de Normalisation, Brussels, Belgium.
- NTC 2008. Decreto Ministeriale 14/1/2008. Norme tecniche per le costruzioni (in Italian). Ministry of Infrastructures and Transportations, G.U. S.O. n. 29 on 2/4/2008 (2008).
- Panagiotakos T.B., Fardis M.N. (2001) Deformations of reinforced concrete members at yielding and ultimate *ACI Struct J* 98(2):135–148.
- Biskinis D. E., Roupakias G. K., & Fardis M. N. (2004). Degradation Of Shear Strength Of Reinforced Concrete Members With Inelastic Cyclic Displacements. *ACI Structural Journal*, (101), 773–783.
- Fabbrocino G, Verderame G.M., Manfredi G. (2005) Rotation capacity of old type RC columns. In: Proceedings of the fib symposium “keep concrete attractive”. Budapest, Hungary, May 23–25, pp 891–896.
- Verderame G.M., Ricci P., Manfredi G. et al. Ultimate chord rotation of RC columns with smooth bars: some considerations about EC8 prescriptions. *Bull Earthquake Eng* (2010) 8: 1351.
- Clementi F., Di Sciascio G., Di Sciascio S., and Lenci S., “Influence of the Shear-Bending Interaction on the Global Capacity of Reinforced Concrete Frames:,” in *Performance-Based Seismic Design of Concrete Structures and Infrastructures*, IGI Global, 2017, pp. 84–111.
- Uva G., Porco F., Raffaele D., Fiore A. On the role of equivalent strut models in the seismic assessment of infilled RC buildings. *Engineering Structures*, 42, 83–94, 2012.
- Crisafulli F.J, Carr A.J. and Park R. (2000), “Analytical modelling of infilled frame structures - a general review”, *Bull. New Zealand Soc. Earthquake Eng.*, 33(1), 30-47.
- Asteris P.G., Antoniou S.T., Sophianopoulos D.S. and Chrysostomou C.Z. (2011),

“Mathematical macromodeling of infilled frames: state-of-the-art”, ASCE J. Struct. Eng., 137(12), 1508–1517.

- Spacone E. et al. Masonry infilled frame structures: state-of-the-art review of numerical modelling. *Earthquakes and Structures*, Vol. 8, No. 1 (2015).
- Di Trapani F. et al. Masonry infills and RC frames interaction: literature overview and state of the art of macromodeling approach. *European Journal of Environmental and Civil Engineering*, 2015.
- Stafford Smith B. Lateral Stiffness of infilled frames. *Journal of Structural Division*, ASCE, 6, 183–99, 1963.
- Mainstone R.J. (1971) On the stiffnesses and strengths of infilled frames. *Proc Inst Civ Eng Suppl (iv)*:57–90.
- Mainstone R.J. Supplementary note on the stiffness and strength of infilled frames. Current paper CP13/74. *Build. Res. Establishment*. London, 1974.
- Bertoldi S. H., Decanini L. D., & Gavarini C. (1993). Infilled frames subjected to seismic actions, a simplified model: Experimental and numerical comparison. *Proceedings of the 6th national conference on seismic engineering ANIDIS* (pp. 815-824). Perugia.
- Panagiotakos T.B. and Fardis M.N., (1994), “Proposed nonlinear strut model for infill panels”, 1st Year Progress Report of HCM-PREC8 Project: University of Patras.
- Al-Chaar G.L. and Mehrabi A. (2008), “Constitutive Models for Nonlinear Finite Element Analysis of Masonry Prisms and Infill Walls”, No. ERDC/CERL-TR-08-19, Engineer Research and Development Center, Construction Engineering Research Lab, Champaign, IL, USA.
- Mouroux et al. The European RISK-UE project: an advanced approach to earthquake risk scenarios. 13th World Conference on Earthquake Engineering Vancouver, B.C., Canada August 1-6, 2004 Paper No. 3329.
- Guagenti E., Petrini V., 1989. *Il caso delle vecchie costruzioni: verso una nuova legge danni-*

intensità, Proceedings of the 4th Italian National Conference on Earthquake Engineering, - Milan - (Italy), 1, 145-153, Milano.

- Petrini V. (1995): Overview report on vulnerability assessment, Proceedings of the Fifth International Conference on Seismic Zonation - Nice - France, October 17th - 19th, 1995, volume III, pp. 1977-1988.
- Meroni F., Grimaz S., Petrini V. & Zonno G. (2000). Seismic vulnerability curves: the italian experience, submitted to Earthquake Spectra - EERI, Oakland, California.
- Fajfar P. A nonlinear analysis method for performance-based seismic design. Earthq Spectra, 16(3):573–591 (2000).
- Mahaney J. A., Paret T.F., Kehoe B. E., and Freeman S. A., (1993), “The Capacity Spectrum Method for Evaluating Structural Response During the Loma Prieta Earthquake”, National Earthquake Conference, Memphis
- Priestely M.J.N. et al. Initial stiffness versus secant stiffness in displacement based design. 13th World Conference on Earthquake Engineering Vancouver, B.C., Canada August 1-6, 2004 Paper No. 2888
- Vidic T., Fajfar P., and Fischinger M. (1994). Consistent inelastic design spectra: Strength and displacement, Earthquake Engineering and Structural Dynamics, 23(5): 507–521.
- Midas GEN. (2015). Analysis Manual.

Chapter 6

6. Rapid seismic vulnerability assessment for the school building stock

6.1. Assessment with macroseismic method

For the purposes of the macroseismic evaluation, the PRE 1974, POST 1974 and POST 2005 classes were associated respectively with RC 1 (frame with earthquake resistant design - ERD), RC 2 (frame with moderate level of ERD) and RC 3 (frame with high level of ERD) of the EMS-98 scale (Grunthal 1998).

Then, they were associated with the most likely vulnerability class, respectively C, D and E, and to the possible range of classes.

The number of buildings of the sample under investigation belonging to each class of the EMS-98 scale and the percentage on the total are shown in tab. 6.1.

Table 6.1. Association of the building stock to the typology classes of the EMS-98 scale

	Type of structure from EMS-98 scale	N° of buildings	% of buildings	Most likely class	Possible range
PRE 1974	RC1 - Without ERD (pre-Code not in seismic area)	32	30.5	C	B - C
POST 1974	RC2 - Moderate level of ERD (pre-Code in seismic area)	64	60.9	D	C - D - E
POST 2003	RC 3 - High level of ERD (post-Code)	9	8.6	E	E - F - G

Practically, a correspondence 1 to 1 was adopted between buildings belonging to the PRE 1974, POST 1974 and POST 2005 classes with those belonging respectively to the macroseismic classes RC 1, RC 2 and RC 3. However, it should be noted that a limited number of buildings of the POST 74 class was assigned to RC1(without seismic resistance criteria), since they were not built in an area classified as seismically at the construction time (most of the classification was made after 1984). Further, some buildings of the PRE 1974 class, although made in areas already classified as seismic at the construction time (Ancona was classified as seismic in 1935), were assigned to the RC1 class because the design rules (R.D. 1939) did not provide special requirements for buildings in seismic prone area.

For the EMS-98 typological classes, values of the parameter V_I - "Typological vulnerability index" (Giovinazzi et al. 2004) are available, representing the probable and plausible ranges of vulnerability classes (tab. 6.2) and thus allowing to obtain the vulnerability curves (macroseismic intensity - expected mean damage). In this study reference was made to the central value V_I^* (the most likely), while the other values in the table can be used to trace the upper and lower limits, probable or possible, of the expected damage according to the macroseismic intensity.

Table 6.2. Vulnerability index V_i values for the building typologies

Typologies		Building type	□ulnerabilità Classes				
			V_{Imin}	V_I^-	V_I^*	V_I^+	V_{Imax}
Masonry	M1	Rubble stone	0.62	0.81	0.873	0.98	1.02
	M2	Adobe (earth bricks)	0.62	0.687	0.84	0.98	1.02
	M3	Simple stone	0.46	0.65	0.74	0.83	1.02
	M4	Massive stone	0.3	0.49	0.616	0.793	0.86
	M5	Unreinforced M (old bricks)	0.46	0.65	0.74	0.83	1.02
	M6	Unreinforced M with r.c. floors	0.3	0.49	0.616	0.79	0.86
	M7	Reinforced or confined masonry	0.14	0.33	0.451	0.633	0.7
Reinforced Concrete	RC1	Frame in r.c. (without E.R.D)	0.3	0.49	0.644	0.8	1.02
	RC2	Frame in r.c. (moderate E.R.D.)	0.14	0.33	0.484	0.64	0.86
	RC3	Frame in r.c. (high E.R.D.)	-0.02	0.17	0.324	0.48	0.7
	RC4	Shear walls (without E.R.D)	0.3	0.367	0.544	0.67	0.86
	RC5	Shear walls (moderate E.R.D.)	0.14	0.21	0.384	0.51	0.7
	RC6	Shear walls (high E.R.D.)	-0.02	0.047	0.224	0.35	0.54
Stell	S	Steel structures	-0.02	0.17	0.324	0.48	0.7
Tiber	W	Timber structures	0.14	0.207	0.447	0.64	0.86

The typological vulnerability index V_I^* can be then corrected for each single building by applying the behaviour modifiers, that summed result in an increase or decrease in vulnerability ΔV_m , so the modified vulnerability index V_I of the single building is obtained through eq. 6.1.

$$V_I = V_I^* + \Delta V_m \quad (6.1)$$

Then calculating the average of the V_I values determined for all buildings within each typological class, the values in tab. 6.3 are obtained.

Table 6.3. Average modified vulnerability index for the typology classes

Typology class	V_I
RC 1 - PRE '74	0.718
RC 2 - POST '74	0.537
RC 3 - POST 2005	0.364

The vulnerability curves correlating the macroseismic intensity to the mean μ_D damage (from 0 to 5 according to the damage levels D_K of the EMS-98 scale) can be obtained by means the analytical relationship of eq. 2.4.

In fig. 6.1 the average vulnerability curves for the building belonging to the 3 typological classes are reported, calculated with the values of V_1^* in tab. 6.3.

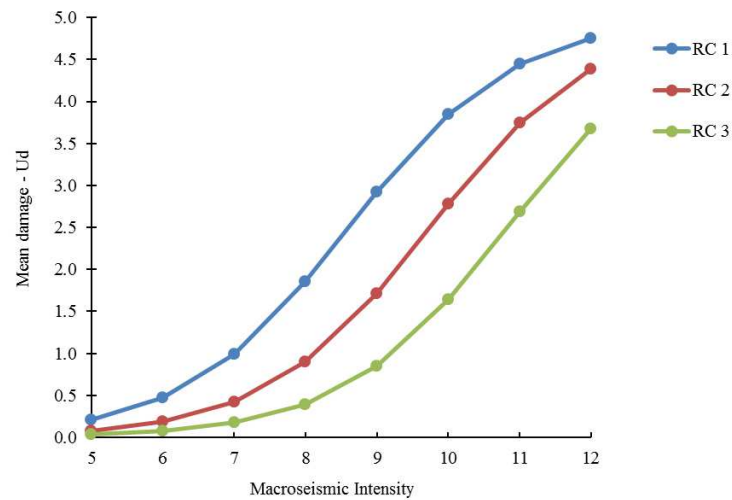
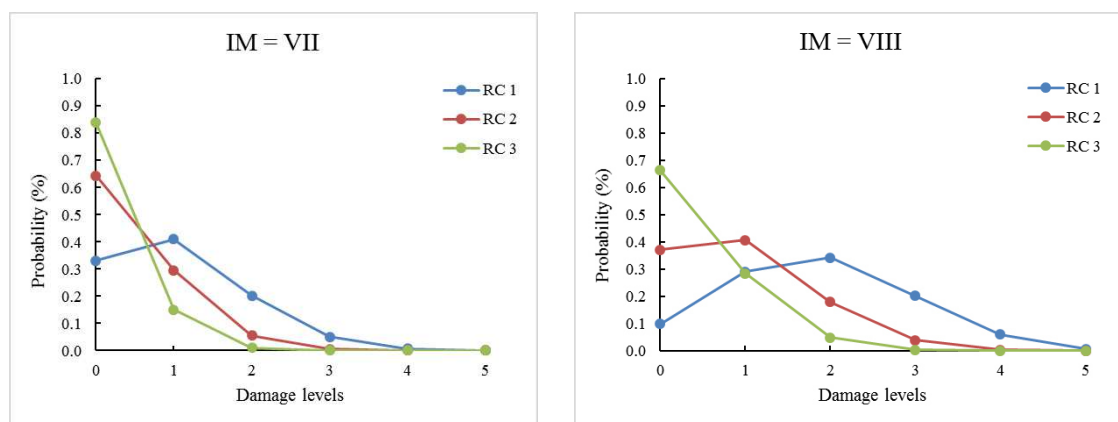


Figure 6.1. Average vulnerability curves for the 3 typological classes

Then, know the average damage for each macroseismic intensity level from the vulnerability curves, for each typological class it is also possible to graphically illustrate the DPMs, that are the probabilistic distribution of the damage. The probability distribution of damage p_k , with k ranged between 0 and 5, is assumed to be of binomial type with the only coefficient d^k as in eq. 2.1.

The graphs in fig. 6.2 show the binomial distributions of the mean damage μ_d , for the 3 typology classes RC1, RC2 and RC3.



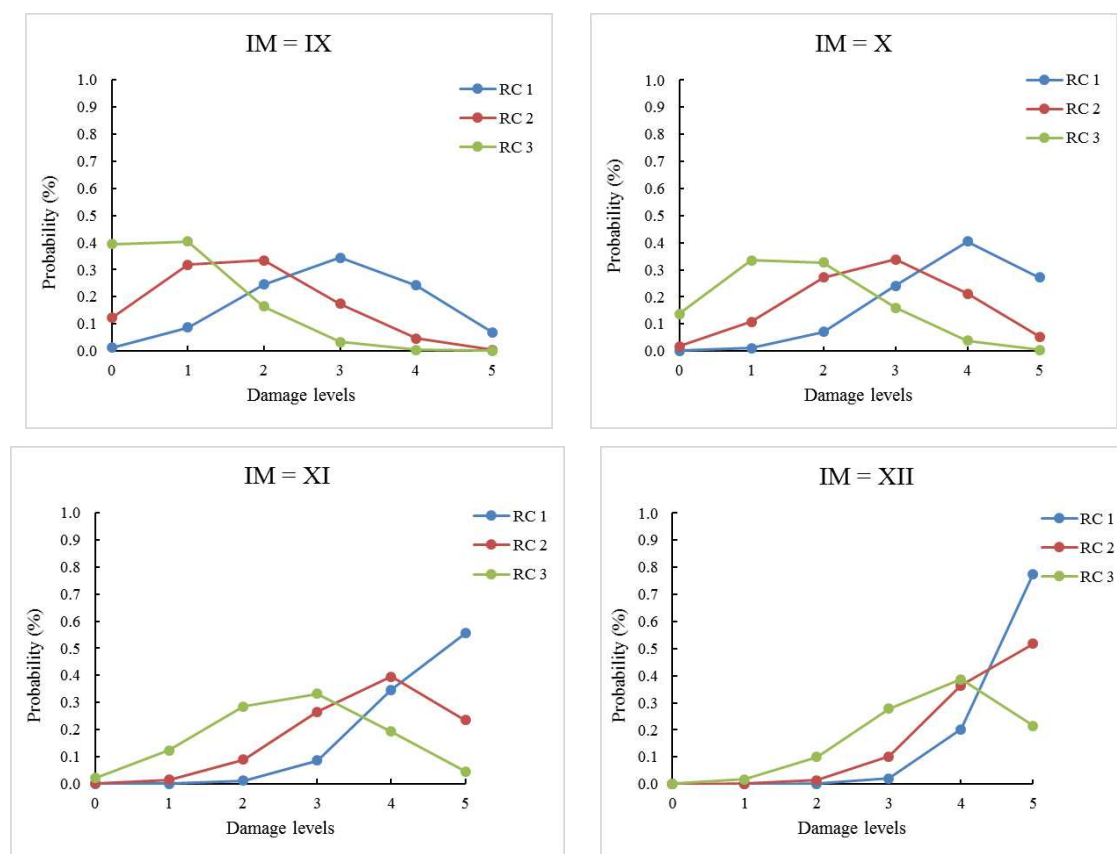


Figure 6.2. Binomial distribution of the expected mean damage

From the trend of the graphs it is possible to notice how increasing the intensity the probability distributions for the three classes shift to the right part of the graph, thus to higher damage levels.

Uncertainties assessment

In the macroseismic method, it is also possible to consider epistemic uncertainties, which takes into account the uncertainty in associating a specific vulnerability or typology class to the buildings analyzed.

In (Giovinazzi *et al.* 2004) the epistemic uncertainty is considered calculating the upper and lower bounds of V_I by means eq. 2.6 and 2.7, where ΔV_I can be assumed equal to 0.04 if data specifically detected to carry out a seismic vulnerability assessment are available, otherwise it would be assumed a value of 0.08, significant of greater uncertainty.

In fig. 6.3 the average damage curves related to the 3 typological classes here considered are shown with the upper and lower bounds of V_I .

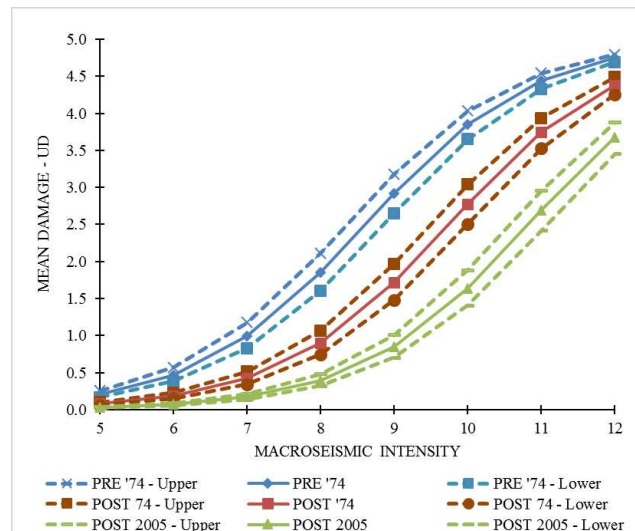


Figure 6.3. Average vulnerability curves for the classes accounting for epistemic uncertainty

6.1.2. Macroseismic intensity – PGA relationship

In large-scale evaluations, as in the case of building typology classes, it may be useful to estimate the expected damage as a function of the peak ground acceleration (PGA) instead of the macroseismic intensity. In fact, in some areas there may be available maximum acceleration values based on hazard analysis (PSHA), while reliable data on macroseismic intensity may be absent because no seismic events of certain intensities have occurred over time or the damage data has not been sufficiently detected to correlate them to macroseismic intensity in a reliable fashion.

Therefore, in order to obtain vulnerability curves in terms of PGA, it is necessary to convert the macroseismic

intensity into PGA. To this aim there are many relationships in the literature, some of them shown in fig. 6.4. (Murphy et al 1977, Margottini et al. 1985, Guagenti et al. 1989).

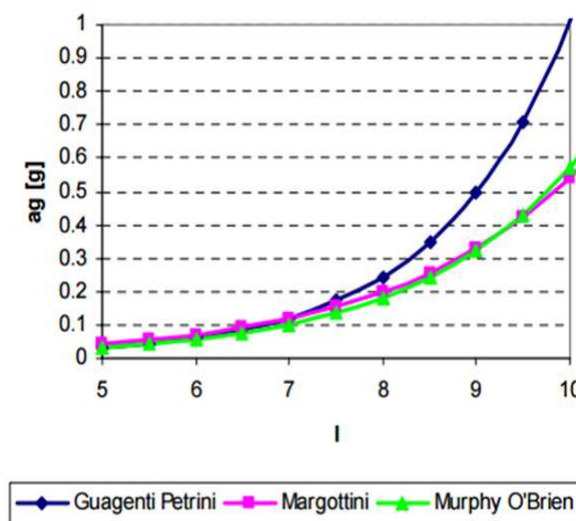


Figure 6.4. I – PGA relationships

Eq. 6.2 (Giovinazzi *et al.* 2004) allows to represent in a single form the relationship in fig. 6.4:

$$a_g = C_1 C_2 (I_{EMS} - 5) \tag{6.2}$$

where the values of C_1 and C_2 coefficients are suggested in (Giovinazzi *et al.* 2004) for some correlation laws and shown in tab. 6.4.

Table 6.4. values of C_1 and C_2 coefficients for some correlation laws

Correlation law	C_1	C_2
<i>Guagenti - Petrini</i>	0.03	2.05
<i>Margottini</i>	0.04	1.65
<i>Murphy O'Brien</i>	0.03	1.75

Eq. can also reverse to calculate the macroseismic intensity from the PGA as in eq. 6.3.

$$I = 5 + \frac{1}{\ln C_2} (\ln a_g - \ln C_1) \tag{6.3}$$

In the present case the relationship provided by Margottini was adopted in order to obtain the vulnerability curves in terms of PGA (fig. 6.5).

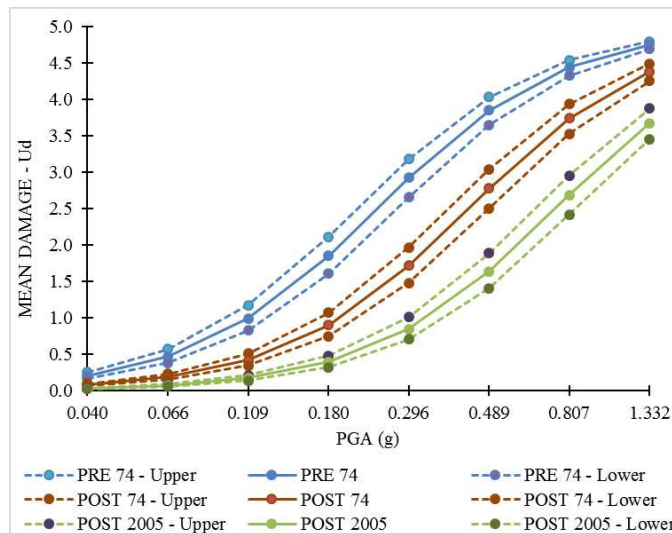


Figure 6.5. Macroseismic vulnerability curves in terms of PGA

Obviously, the transformation of the macroseismic intensity into PGA involves the introduction of a further source of uncertainty in the evaluation model, due to the way I is correlated to PGA.

Site amplification effects

The macroseismic scale refers to the horizontal rigid soil condition, so for a more accurate assessment it is necessary to introduce the local amplification effects in the estimation of vulnerability, such as stratigraphic and topographic amplification.

In this regard, it is possible to increase the value of the macroseismic intensity as suggested by (Giovinazzi *et al.* 2004) with eq. 6.4:

$$\Delta I = \frac{\ln(f_{PGA})}{\ln(C_2)} \quad (6.4)$$

where f_{PGA} is determined on the base of both subsoil category and the typology of the building (tab.6.5), as a function of the factor given by the ratio between spectral ordinates on soft soil (categories of subsoil B, C, D, E), and the spectral ordinates on stiff soil (category A), in the range of significant vibration periods.

Table 6.5. PGA multiplier factor f_{PGA} for several soil types and building categories

	B/A	C/A	D/A	E/A		B/A	C/A	D/A	E/A
M-Low	1.2	1.15	1.35	1.4	RC-Low	1.2	1.15	1.35	1.4
M-Medium	1.2	1.15	1.35	1.4	RC-Medium	1.5	1.725	2.5	1.75
M_Alti	1.32	1.265	1.485	1.54	RC-High	1.5	1.725	2.7	1.75

Whereas the value of C_2 depend on the adopted I-PGA relationship. In this case that of Margottini was used, then $\ln(C_2)$ is equal to 0.501.

Moreover, given the relation between V_I and I provided by eq. 2.4 for μ_d calculation, an increase ΔV_I can be associated with the increase ΔI (eq. 6.5):

$$\Delta V_i = \frac{\Delta I}{6.25} \quad (6.5)$$

In tab. 6.6 the ΔV_I values are directly provided on the base of the subsoil categories.

Table 6.6. ΔV_I values for EC8 soil types and for different building categories

	B/A	C/A	D/A	E/A		B/A	C/A	D/A	E/A
M_Low	0.04	0.03	0.08	0.09	RC_Low	0.04	0.03	0.08	0.09
M_Mediu m	0.04	0.03	0.08	0.09	RC_Mediu m	0.10	0.15	0.24	0.15
M_High	0.07	0.06	0.10	0.12	RC_High	0.10	0.15	0.26	0.15

In the present case, most of the school buildings have 2 or 3 floors and are located on soils of category B (high density), according to Italian seismic Code. The curves amplified for site effects are shown in fig. 6.6.

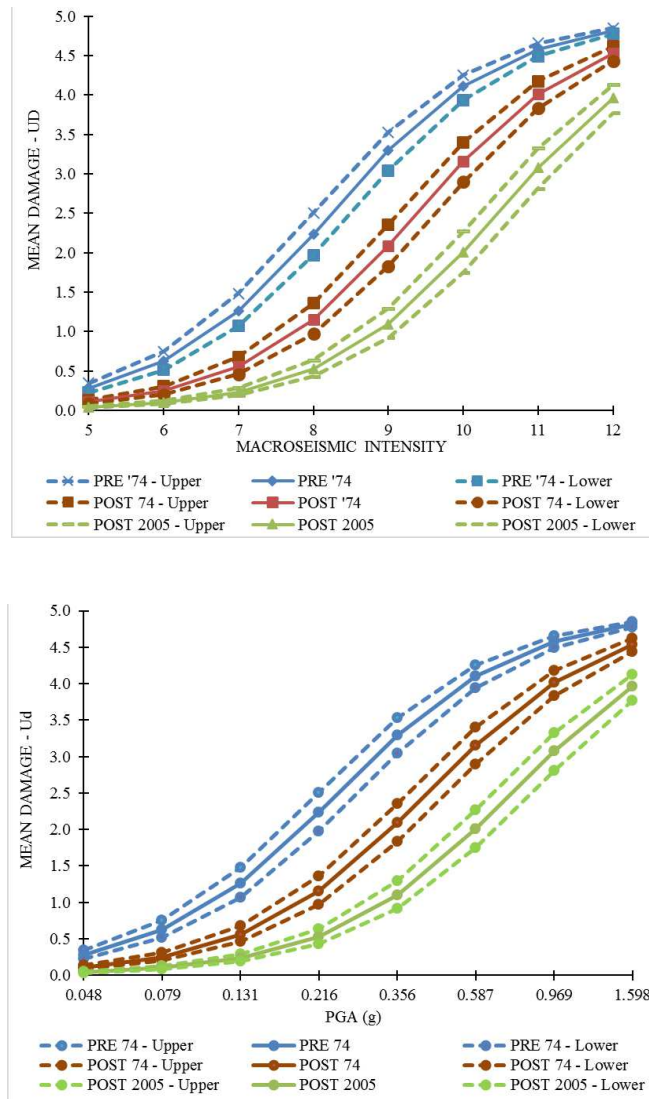


Figure 6.6. Vulnerability curves of the typological classes accounting for the site amplification effects in terms of both macroseismic intensity (upper) and PGA (lower).

Thus, for the same level of macroseismic intensity or PGA, there is a greater damage in the case in which the site effect amplification is accounted.

6.2. Assessment with vulnerability index method

The results in terms of both I_v and PGAc for the school buildings of the stock under investigation are illustrated, both for the 2nd level GNDT method and the one proposed by the author. Then they were compared distinguishing between the PRE and POST 1974 classes.

It is worth noting that I_v is to be considered a representative parameter of global vulnerability with respect the ultimate condition of the structure, i.e. when the collapse is reached.

The procedure consisted in evaluating the original design documents of each 2nd level school buildings of the province of Ancona and on-site inspections on the buildings to check the conformity with the design documents and the state of conservation of materials.

It should be pointed out that the assessment was carried out by expert judgment, trying to standardize the judgment between the two GNDT and proposed methods for indicators representing the same vulnerability factor in the two datasheets. This is to have as consistent results as possible between methods and thus to give more meaning the comparison. Obviously also trying to be as uniform as possible in the evaluation, the results obtained from the two methods are often different for the same building, being the two vulnerability datasheets quite different in the interpretation of the indicators and in the scores to assign.

The greatest difficulty in expressing a consistent judgment between the two methods is essentially due to the different interpretation of the vulnerability factors provided by the two methods and also to the different number of indicators (11 in the GNTD method and 15 in that proposed by the author).

In fact, as already explained in chap. 5, the method proposed by the author wants to break the vulnerability factors as much as possible into the correspondent indicators, in order to evaluate the vulnerability as precisely as possible.

Given the difference between the I_v range provided from the two methods (between 0 and 100 in the GNDT method, while between 0 and 10 in the proposed method) the I_v values of the proposed method were multiplied by 10 in order to directly compare the two methods.

6.2.1. 2nd level GNDT method

The scores to assign at the vulnerability indicators of the 2nd level GNDT method (*GNDT 1994, Regione Toscana 2003, Regione Marche 2004*) are shown in tab. 6.7.

Table 6.7. Vulnerability indicators and relative scores_2nd level GNDT method

Vulnerability indicators	Classes and scores			
	A	B	C	D
1 – Type and organization of the resistant system	0	-1	-2	0
2 – Quality of the resistant system	0	-0.25	-0.5	0
3 – Conventional resistance	0.25	0	-0.25	0
4 – Position of the building and foundations	0	-0.25	-0.5	0
5 – Floor slabs	0	-0.25	-0.5	0
6 – Planar configuration	0	-0.25	-0.5	0
7 - Elevation configuration	0	-0.50	-1.5	0
8 – Connection and critical elements	0	-0.25	-0.5	0
9 – Low ductility elements	0	-0.25	-0.5	0
10 – Non-structural elements	0	-0.25	-0.5	0
11 – Degradation of materials and damage	0	-0.50	-1	-2.45

Figs. 6.7, 6.8, 6.9 and 6.10 show the outcomes of the evaluation for each building belonging respectively to the PRE 1974 and POST 1974 classes, both in terms of I_v and ultimate capacity in terms of PGA (calculated according to the eq.). Obviously lower is the I_v values, greater is the correspondent PGA.

PRE-1974 buildings

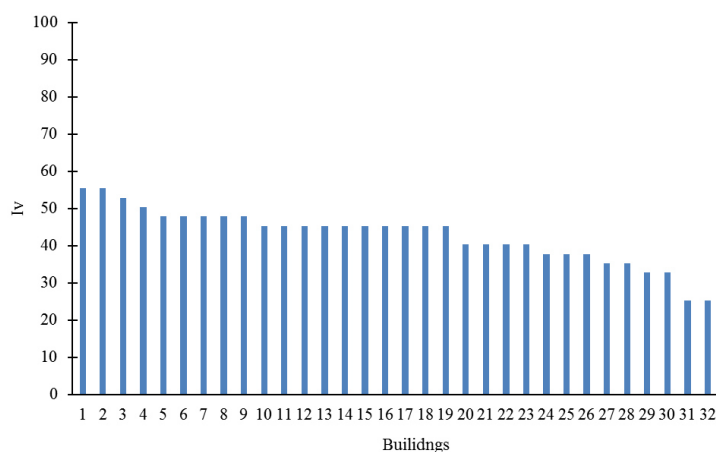


Figure 6.7. I_v values_PRE 1974 buildings

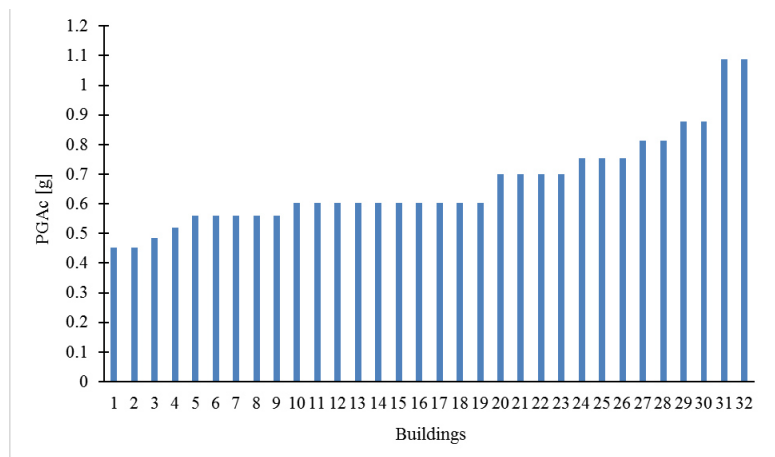


Figure 6.8. PGAc values_PRE 1974 buildings

Tab. 6.8 summarizes the results, showing some relevant statistics.

Table 6.8. Statistics of the results provided from the GNDT method _PRE 1974 buildings

PRE 74	mean	max	min	St.dev.	mode	confidence interval alfa = 0.5	variance
Iv GNDT	42.7	55.4	25.2	7.4	45.3	0.880	55.0
PGAc GNDT	0.333	0.523	0.240	0.069	0.305	0.008	0.005

POST 1974 buildings

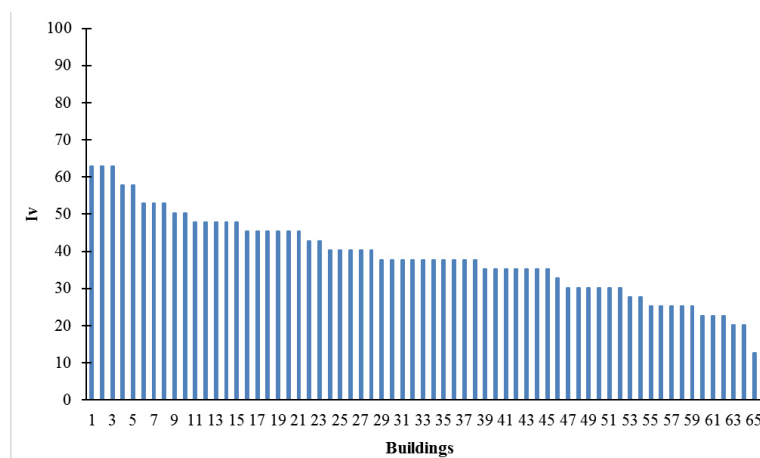


Figure 6.9. Iv values_POST 1974 buildings

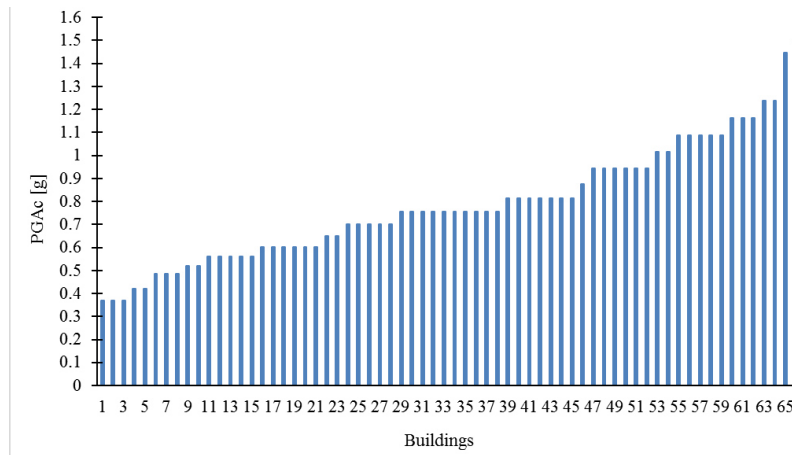


Figure 6.10. PGAc values_POST 1974 buildings

Tab. 6.9 summarizes the results, showing some relevant statistics.

Table 6.9. Statistics of the results provided from the GNDT method_POST 1974 buildings

POST 74	mean	max	min	St.dev.	mode	confidence interval alfa = 0.5	variance
Iv GNDT	38.1	62.9	10.1	11.6	37.8	0.96	134.7
PGAc GNDT	0.389	0.818	0.203	0.124	0.369	0.010	0.015

6.2.2. Proposed method

The vulnerability indicators and the relative scores proposed by the author are shown in tab. 6.10.

Table 6.10. Vulnerability indicators and relative scores_Author

Vulnerability indicators	Classes and scores		
	A	B	C
1 - Age of building	0	0.35	0.70
2 – Reference Code	0	0.50	1.00
3 – Built in seismic zone	0	0.75	1.50
4 – Typology of the resistant system	0	0.30	0.60
5 – Quality of the resistant system	0	0.35	0.70
6 – Critical elements	0	0.40	0.80
7 – Irregularity in plan shape	0	0.30	0.60
8 – Irregularity in elevation shape	0	0.15	0.30
9 – Irregularity in plan stiffness	0	0.25	0.50
10 - Irregularity in elevation stiffness	0	0.50	1.00
11 – Position and type of stairs	0	0.30	0.60
12 – Stiffness of floor slabs	0	0.20	0.40
13 – Position of foundation	0	0.10	0.20
14 – Irregularity of storey mass	0	0.20	0.40
15 – Degradation of materials	0	0.35	0.70

Figs. 6.11, 6.12, 6.13 and 6.14 show the results of the evaluation for each building belonging respectively to the PRE 1974 and POST 1974 classes, both in terms of I_v and $PGAc$.

PRE-1974 buildings

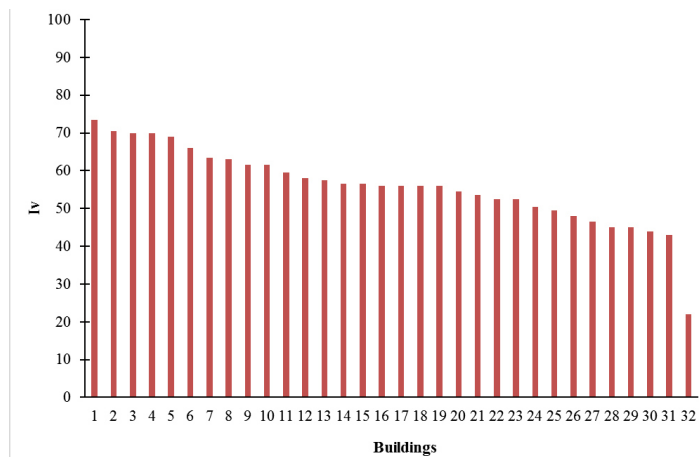


Figure 6.11. Iv values_PRE 1974 buildings

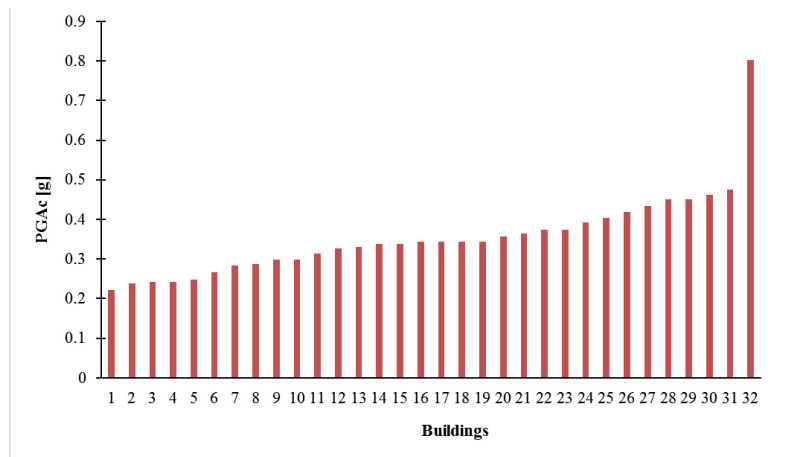


Figure 6.12. PGAc values_PRE 1974 buildings

Tab. summarizes the results, showing some relevant statistics.

Table 6.11. Statistics of the results provided from the proposed method _PRE 1974 buildings

PRE 74	mean	max	min	St.dev	moda	confidence interval alfa 0.5	variance
Iv Author	55.8	73.5	22.0	10.4	56.0	1.24	107.5
PGAc Author	0.356	0.802	0.221	0.107	0.343	0.013	0.011

POST 1974 buildings

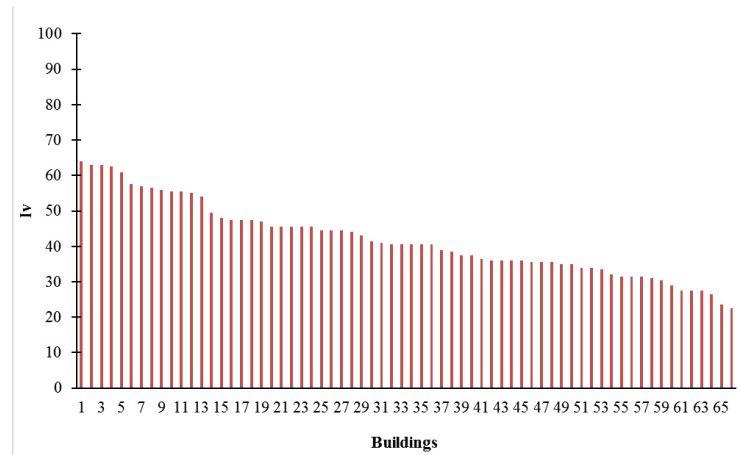


Figure 6.13. Iv values_POST 1974 buildings

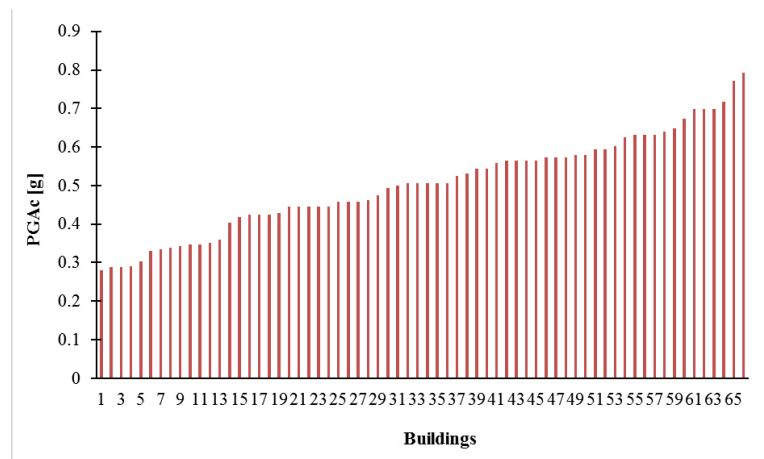


Figure 6.14. PGAc values_POST 1974 buildings

Tab. 6.12 summarizes the results, showing some relevant statistics.

Table 6.12. Statistics of the results provided from the proposed method_POST 1974 buildings

POST 74	mean	max	min	St.dev.	mode	confidence interval alfa = 0.5	variance
Iv Author	41.9	64.0	22.5	10.4	45.5	0.87	109.4
PGAc Author [g]	0.504	0.792	0.281	0.125	0.446	0.010	0.016

- **Comparison between PRE and POST 1974 classes**

The differences in outcomes in terms of I_v and PGAc relative to the two structural classes were evaluated, both in relation to the GNDT method and to the one proposed by the author.

I_v values

Fig. 6.15 shows the difference between average values of I_v , with a higher average value for the PRE-1974 class (the orange histogram) provided from both methods. The difference between the average I_v of the two classes is greater in the proposed method.

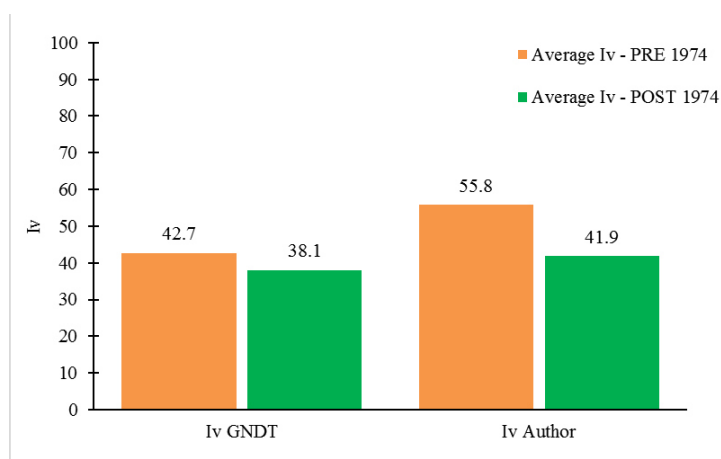


Figure 6.15. Comparison between PRE and POST 1974 classes in terms of average I_v obtained from both methods

Figs. 6.16 and 6.17 show the comparison of the buildings distributions in five I_v ranges (from low vulnerability (A) to high vulnerability (E)), of the PRE and POST 1974 classes, respectively for the GNDT and the proposed methods. The I_v ranges were determined subdividing the range 0 – 100 with step of 20.

This representation gives a global vision on the seismic vulnerability of the building stock under investigation, highlighting the possible critical situations (e.g. many buildings in the vulnerability range 0-20 (H) or 20-40 (MH)). Further, the representation in vulnerability ranges allows to compensate the statistical variability associated to the single I_v value.

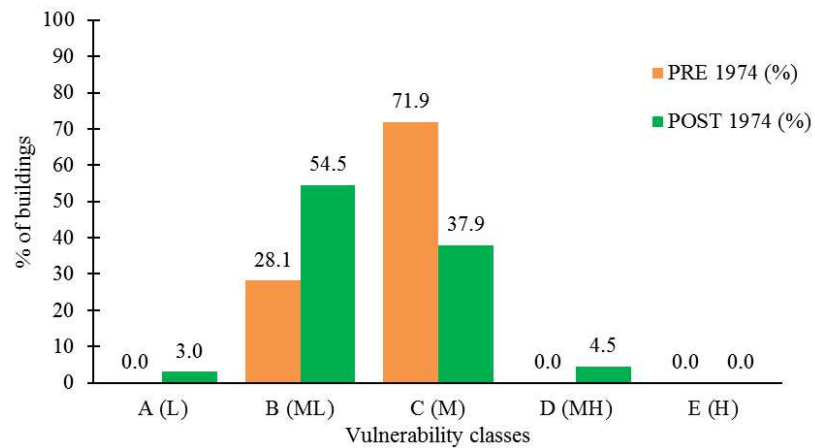


Figure 6.16. Comparison of the PRE and POST 1974 building distributions in the *Iv ranges_GNDT method*

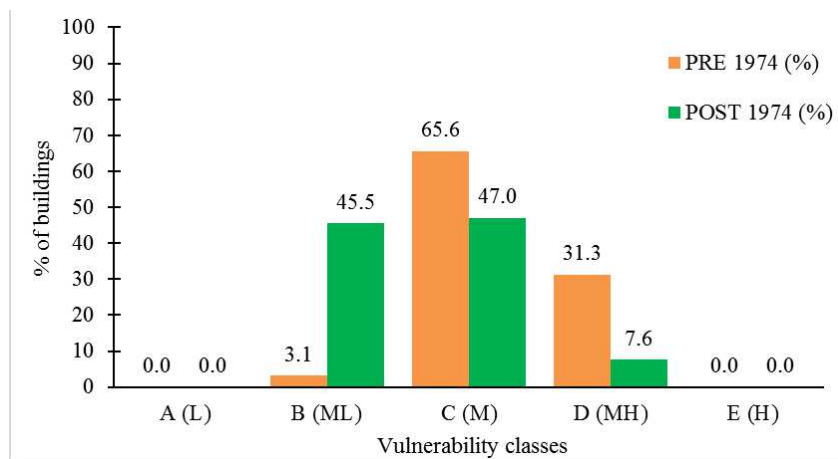


Figure 6.17. Comparison of the PRE and POST 1974 building distributions in the *Iv ranges_Proposed method*

For both methods, the PRE 1974 class (the orange histograms) has more buildings in worse vulnerability classes than the POST 1974 class.

According to the method proposed by the author, both structural classes have the distribution shifted to the right part, hence toward higher vulnerable ranges. In particular this occurs for the PRE 1974 class with many buildings moving to class D, while the redistribution for the POST 1974 class, with respect the GNDT method, is much more limited

PGAc values

Fig. 6.18 shows the comparison between average values of PGAc, with a higher average value for the POST 1974 class (the green histogram) provided from both methods. The difference between the average PGAc of the two classes is greater in the proposed method.

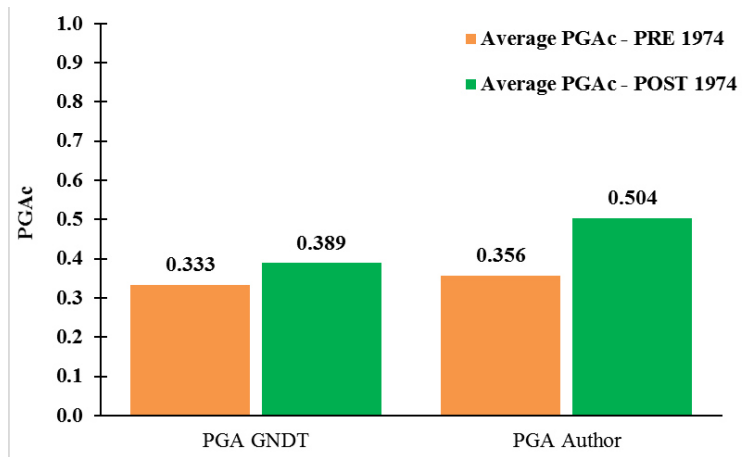


Figure 6.18. Comparison between PRE and POST 1974 classes in terms of average PGAc obtained from both methods

Figs. 6.19 and 6.20 show the comparison of the building distributions in five PGAc ranges with step of 0.2 g, of the PRE and POST 1974 classes, respectively for the GNDT and the proposed methods.

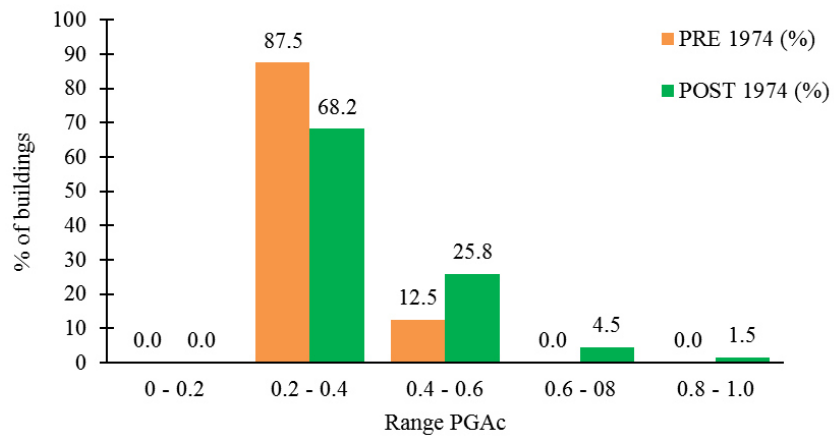


Figure 6.19. Comparison of the PRE and POST 1974 building distributions in PGAc ranges_GNDT method.

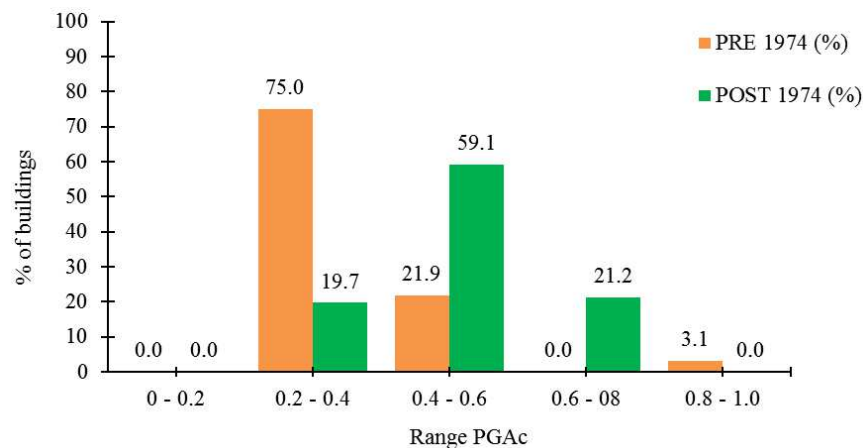


Figure 6.20. Comparison of the PRE and POST 1974 building distributions in PGAc ranges_Proposed method.

For both methods, the PRE 1974 class (the orange histograms) exhibits a higher percentage of buildings in PGAc range worse than POST 1974. However, no buildings belong in the range 0 - 0.2 g for both methods and this is a positive aspect for the vulnerability of the building stock under investigation.

The GNDT method (fig. 6.19), compared to that proposed from the author (fig. 6.20), has a building distribution of the PRE 1974 class (the orange histograms) more shifted on the left part, where 87.5% of the buildings are in the 0.2g - 0.4 g range, while in the proposed method the buildings in the same range are 68.2%.

The building distribution of the POST 1974 class (the green histograms) is shifted towards the higher values of capacity mostly for the proposed method with the buildings in the 21.2% of buildings in the range 0.6 g - 0.8 g, while in the GNDT method only the 4.5% of buildings is in the same range.

In general, the outcomes of both methods show that the analyzed school building stock do not has high vulnerability, as most of the buildings were built in areas seismically classified already at the time of the buildings construction (for some municipalities the first classification dates back to 1935). Indeed, the average PGAc for the two classes is not too low, although there are isolated cases of buildings that deviate sufficiently from the medium and present quite low values of PGAc.

6.2.3. Comparison between methods

The comparison between the results obtained from the GNDT and the proposed methods is illustrated below in terms of both Iv and PGAc.

Comparison in terms of Iv

Fig. 6.21 shows the comparison between the average Iv values provided from both methods, with a greater difference in the case of the PRE 1974 class (left side of fig. 6.21).

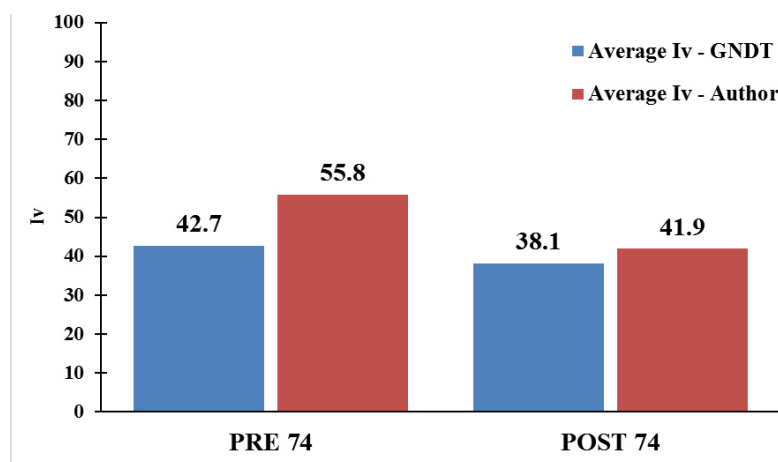


Figure 6.21. Comparison between methods in terms of average Iv of the PRE and POST 1974 classes

- **PRE 1974 class**

The histograms of fig. 6.22 show the comparison of the Iv values for each building obtained with both methods.

It is to be noted that for many buildings, the values provided from the method proposed by the author is greater than that provided by the GNDT method. However, in vulnerability index methods is not important the absolute Iv value, but the ranking of the buildings evaluated. Thus, even if the proposed method provides a greater Iv value with respect the GNDT method, it is possible that the ranking doesn't changes a lot.

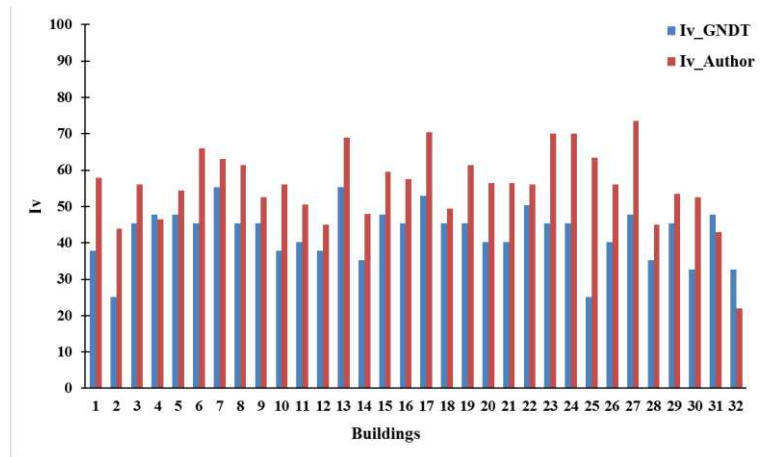


Figure 6.22. Comparison of Iv values provided from the proposed and GNDT methods_PRE 1974 buildings

Additionally, if it is analyzed the vulnerability ranking for both methods reported in Appendix to chapter 6, it is possible to note that the proposed method provides different Iv values between buildings, while the GNDT method often provides the same Iv values for several buildings, and hence the ranking is much more compact.

Therefore, it is possible to say that the proposed method allows to better grasp also small differences between the buildings, in order to differentiate the outcomes in terms of vulnerability. This was the main objective imposed in developing the proposed method.

Fig. 6.23 shows the percentage variation of Iv values for each building of the PRE 1974 class, when going from the GNDT to the proposed method.

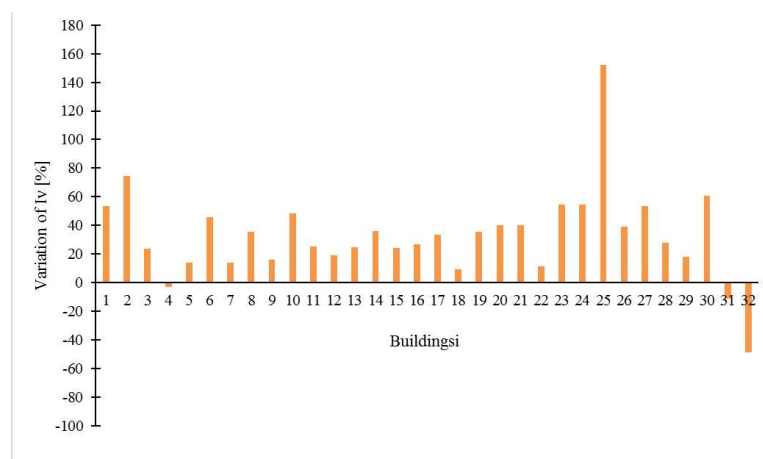


Figure 6.23. Percentage variation of the Iv values going from the GNDT to the proposed method_PRE 1974 buildings

The average variation is + 32.8%.

Tab. 6.13 and fig. 6.24 show the comparison, between the two methods, of some significant statistics relative to the Iv values of the PRE 1974 buildings.

Table 6.13. Comparison of the statistics for Iv values provided from both methods _PRE 1974 buildings

PRE 74	mean	max	min	St.dev.	mode	Confidence interval alfa 0.5	variance
Iv GNDT	42.7	55.4	25.2	7.4	45.3	0.88	55.0
Iv Author	55.8	73.5	22.0	10.4	56.0	1.24	104.1

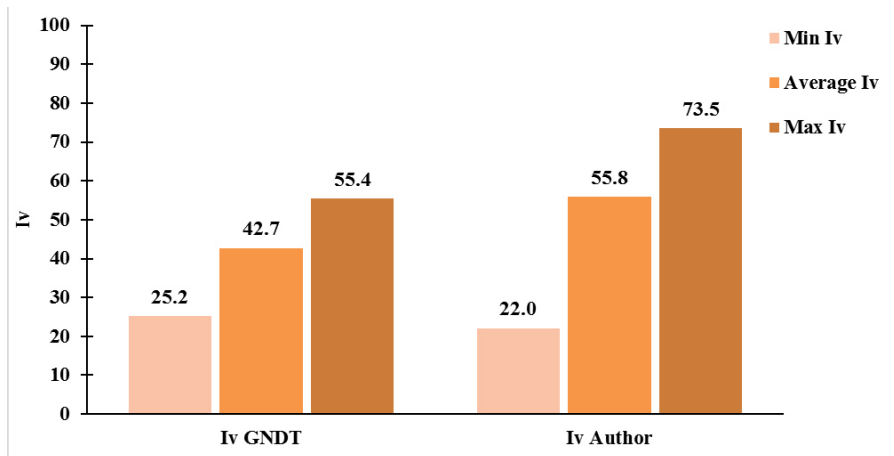


Figure 6.24. Minimum, mean and maximum Iv values provided from both methods _PRE 1974 class

The proposed method provides, for the PRE 1974 class, an average value of about 30% higher than the one provided from the GNDT method, and also a higher dispersion of the results because the variance is about the double.

Figs. 6.25 shows the comparison of the building distributions in the Iv range, provided from the GNDT and the proposed methods for the PRE 1974 buildings.

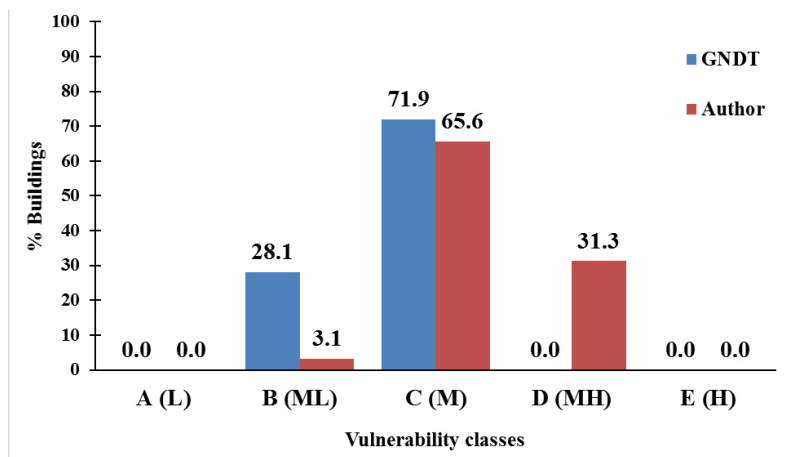


Figure 6.25. Comparison of the building distributions in the Iv ranges provided from the GNDT and proposed methods _PRE 1974 class

The proposed method provides a distribution more shifted to the right part, with 30% of buildings within the medium-high vulnerability class, and thus a general condition of greater vulnerability for buildings belonging to the PRE 1974 class.

For both methods, however, most buildings fall into the medium vulnerability class.

- **POST 1974 class**

The histograms of fig. 6.26 shows the comparison of the I_v values obtained with both methods for each building belonging to the POST 1974 class.

Also in this case, the proposed method provides higher I_v values for many buildings.

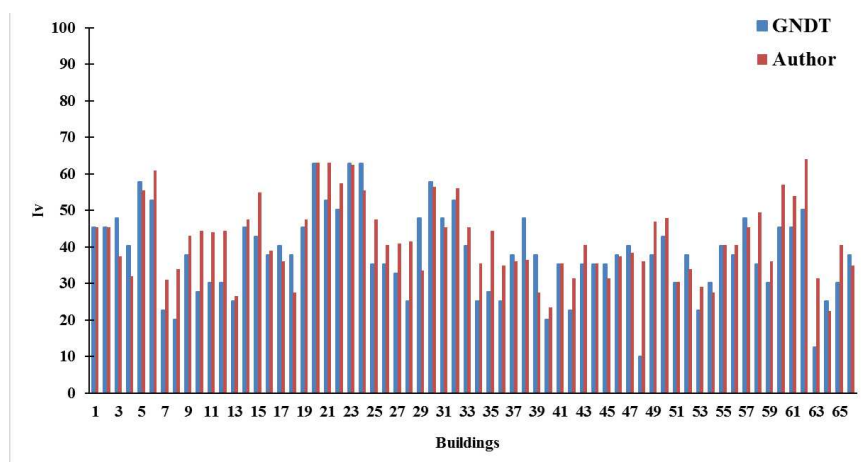


Figure 6.26. Comparison of I_v values provided from the proposed and GNDT methods_ POST 1974 buildings

By analysing the vulnerability ranking provided from both methods (Appendix to chapter 6), it is possible to say the same conclusion previously said with regard the ranking of the PRE 1974 buildings, that is a better differentiation of the buildings vulnerability provided from the proposed method.

Fig. 6.27 shows the percentage variation of I_v values for each building of the POST 1974 class, when going from the GNDT to the proposed method.

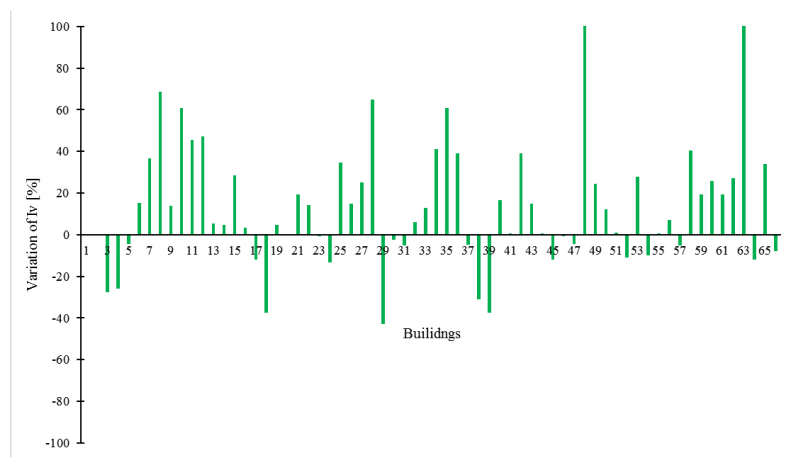


Figure 6.27. Percentage variation of the Iv values going from the GNDT to the proposed method_POST 1974 buildings

The average variation is 16.3%, but in some cases it is higher than 100%.

Tab. 6.14 and fig. 6.28 show the comparison, between the two methods, of some significant statistics relative to the Iv values of the POST 1974 buildings.

Table 6.14. Comparison of the statistics for Iv values provided from both methods _POST 1974 buildings

POST 74	mean	max	min	St.dev.	mode	Confidence interval alfa 0.5	variance
Iv GNDT	38.1	62.9	10.1	11.6	37.8	0.96	134.7
Iv Author	41.9	64.0	22.5	10.4	45.5	0.87	107.5

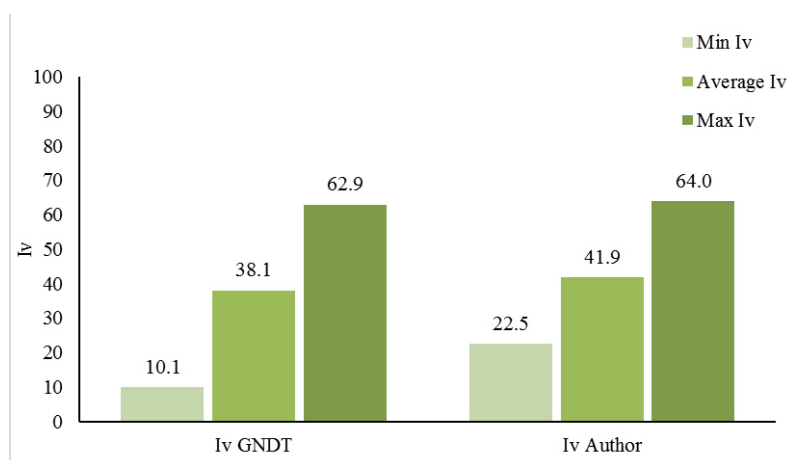


Figure 6.28. Minimum, mean and maximum Iv values provided from both methods_POST 1974 class

The proposed method, also for the POST 1974 building, provides an average value of I_v 10% higher than provided by the GNDT method. The latter method provides the larger variance, differently from the PRE 1974 case.

The building distributions in the vulnerability ranges shown in fig. 6.29 are very different from that relative to the PRE 1974 class. In fact, both for GNDT and proposed methods, the percentages of buildings are concentrated in the two vulnerability classes (medium-low and medium vulnerability classes). However, the distribution provided by the GNDT has most of buildings within the medium-low vulnerability class, confirming the greater conservativity of this method.

Anyway, both methods provide a situation of medium vulnerability for the POST 1974 school buildings under investigation.

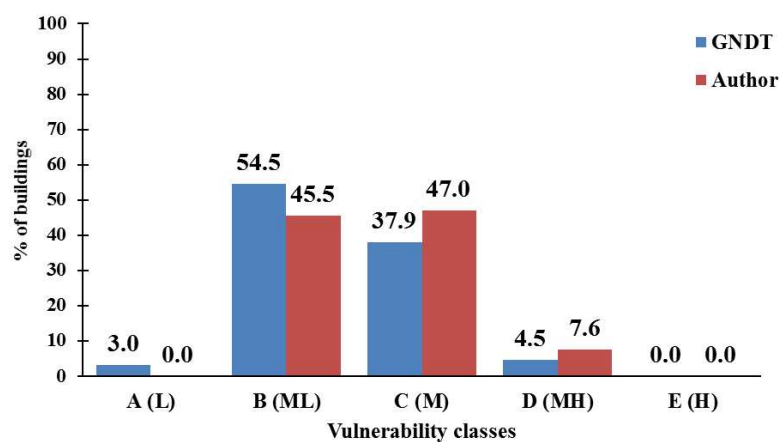


Figure 6.29. Comparison of the building distributions in the I_v ranges provided from the GNDT and proposed methods_POST 1974 class

Comparison in terms of PGAc

Fig. 6.30 shows the comparison between the average values of PGAc provided from both methods, with a greater difference for the POST 1974 buildings. Instead the PGAc are almost the same for the PRE 1974 buildings.

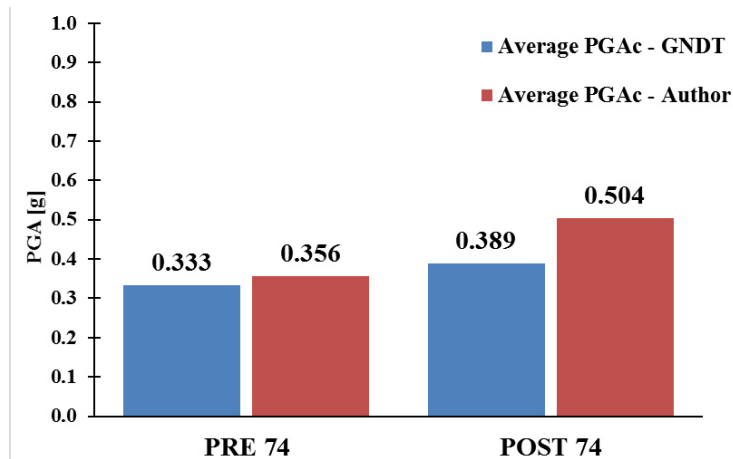


Figure 6.30. Comparison between methods in terms of average PGAc of the PRE and POST 1974 classes

- **PRE 1974 class**

The histograms of fig. 6.31 show the comparison of the PGAc obtained with both methods for each building belonging to the PRE 1974 class.

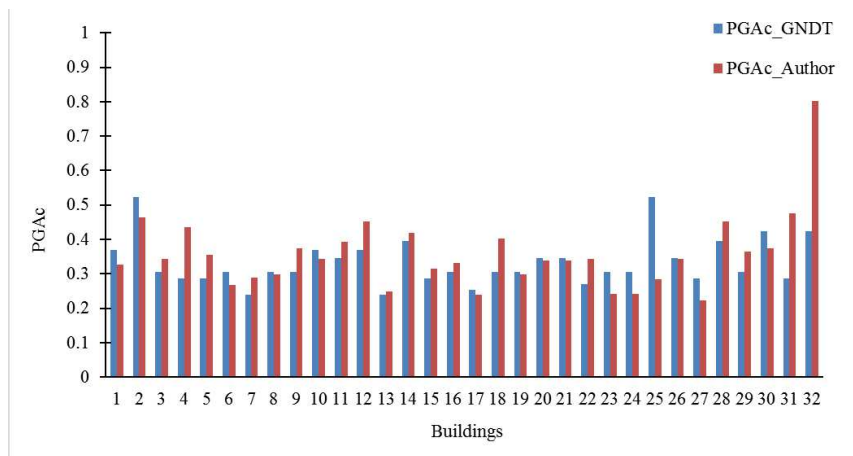


Figure 6.31. Comparison of PGAc values provided from the proposed and GNDT methods_PRE 1974 buildings

The PGAc values are very close for each building.

Fig. 6.32 shows the percentage variation of PGAc values for each building of the PRE 1974 class, when going from the GNDT to the proposed method. Most of buildings increase the own PGAc.



Figure 6.32. Percentage variation of the PGAc values going from the GNDT to the proposed method_PRE 1974 buildings

The average variation is of 6.23%, so the two methods provide on average about the same PGAc relative to the PRE 1974 class.

Tab. 6.15 and fig. 6.33 show the comparison, between the two methods, of some significant statistics for the PGAc values of the PRE 1974 buildings.

Table 6.15. Comparison of the statistics for PGAc values provided from both methods _PRE 1974 buildings

PRE 74	mean	max	min	St.dev.	mode	Confidence interval alfa 0.5	variance
PGA GNDT	0.333	0.523	0.240	0.069	0.305	0.008	0.005
PGAc Author	0.356	0.802	0.221	0.107	0.343	0.013	0.011

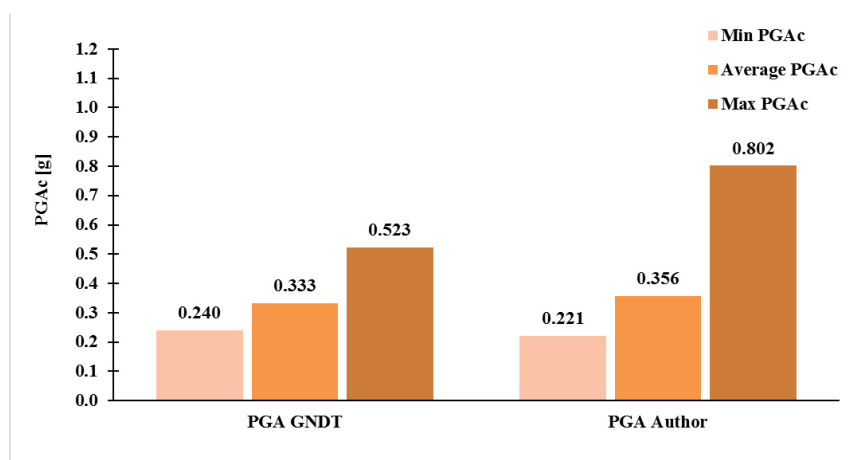


Figure 6.33. Minimum, mean and maximum PGAc values provided from both methods_PRE 1974 class

The proposed method provides a slightly higher average PGAc than the GNDT method and a double variance.

In addition, for a better interpretation of the results, fig. 6.34 shows the comparison of the building distributions in five PGAc ranges with step of 0.2 g (from 0 g to 1.0 g), provided from both methods for the PRE 1974 buildings.

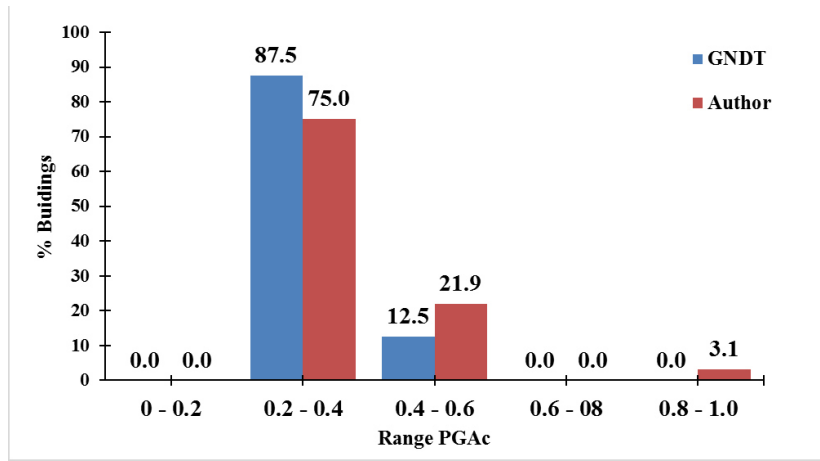


Figure 6.34. Comparison of the building distributions in the PGAc ranges provided from the GNDT and proposed methods_PRE 1974 class

In general, the two methods provide about the same structural capacity for the PRE 1974 class.

- **POST 1974 class**

The histograms in fig. 6.35 show the comparison of the PGAc obtained with both methods for each building of the POST 1974 class. In this case, the proposed method provides the higher value of the PGAc for most of buildings.

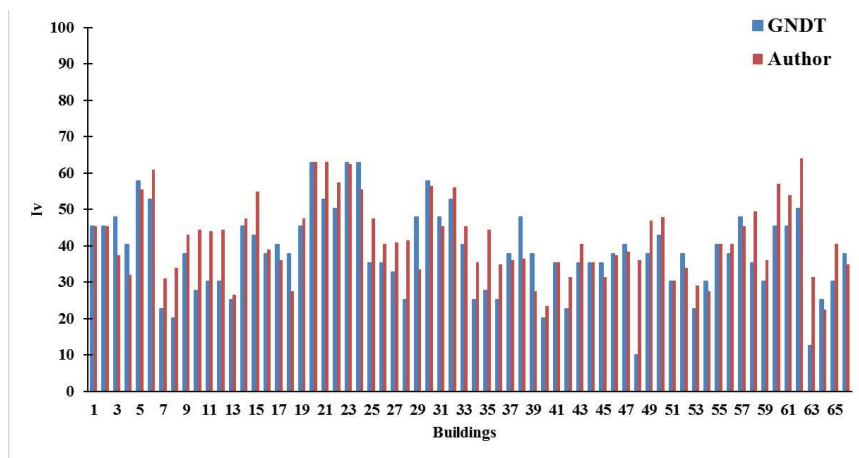


Figure 6.35. Comparison of PGAc values provided from the proposed and GNDT methods_POST 1974 buildings

Fig. 6.36 shows the percentage variation of PGAc values for each building of the POST 1974 class, when going from the GNDT to the proposed method. Almost all buildings increase the own PGAc.

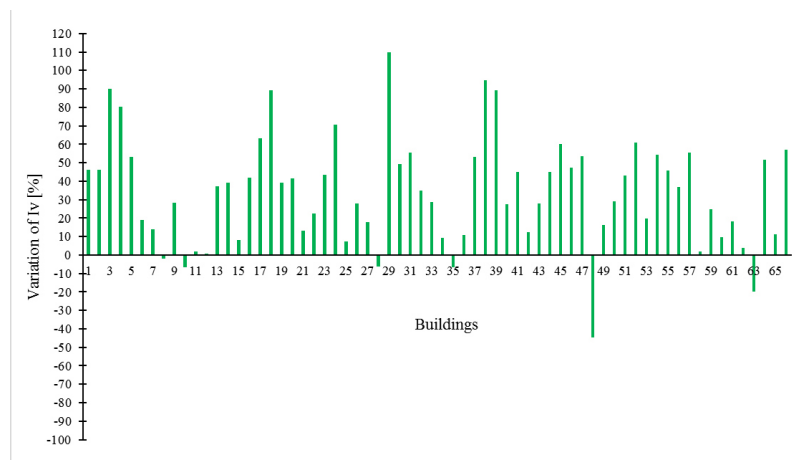


Figure 6.36. Percentage variation of the PGAc values going from the GNDT to the proposed method_POST 1974 buildings

The average variation is equal to 34.10%.

In this case, the number of buildings that increase their PGAc value with the proposed method, is higher than the number of buildings that decrease their Iv values with the same method. This is due to the different Iv-PGAc conversion relationships used by the two methods, whereby a building could to increase the level of vulnerability (higher Iv values) if evaluated according to the proposed method but at the same time the correspondent capacity in terms of PGAc could be higher than the value provided by the GNDT method.

Tab. 6.16 and fig. 6.37 show the comparison, between the two methods, of some significant statistics relative to PGAc values of the POST 1974 buildings.

Table 6.16. Comparison of the statistics for PGAc values provided from both methods _ POST 1974 buildings

POST 74	mean	max	min	St.dev.	mode	Confidence interval alfa 0.5	variance
PGA GNDT	0.389	0.818	0.203	0.124	0.369	0.010	0.015
PGAc Author	0.504	0.792	0.281	0.125	0.446	0.010	0.016

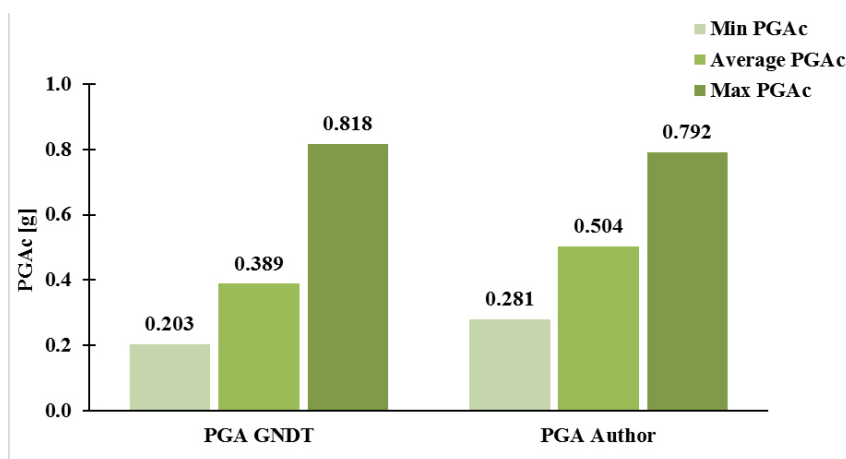


Figure 6.37. Minimum, mean and maximum PGAc values provided from both methods_ POST 1974 class

The proposed method provides an average value of PGAc that differs in excess of about 50% from the one provided from the GNDT method, while the variance is about equal.

The building distributions into the PGAc intervals of fig. 6.38 shows, for the GNDT method many buildings (68.2%) in the range 0.2 g - 0.4 g, whereas for the proposed method there is an enlarged distribution covering the range from 0.2 g to 0.8 g and with a concentration of buildings (59.1%) in the range 0.4 g – 0.6 g.

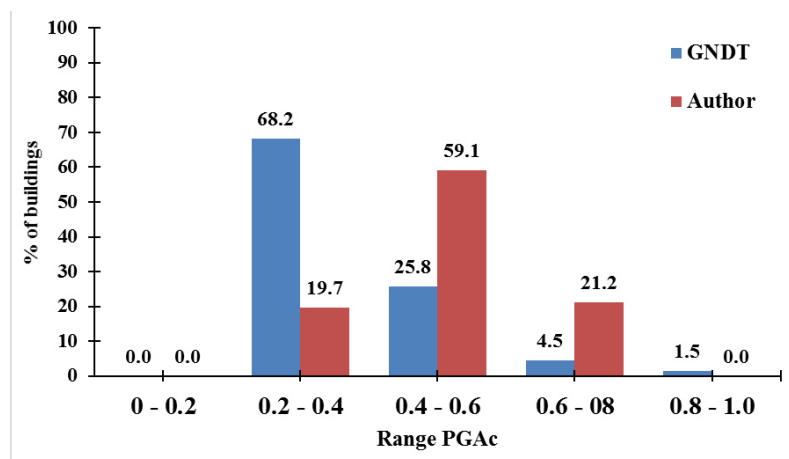


Figure 6.38. Comparison of the building distributions in the PGAc ranges provided from the GNDT and proposed methods_ POST 1974 class

In general, a situation of greater capacity is provided from the proposed method for the POST 1974 class.

The proposed method results less conservative than the GNDT method. In order to investigate more in depth this aspect, a numerical validation of the proposed method was performed, and it is illustrated in in chapter 7. Some case studies were analyzed through pushover analyses and the

results compared with those coming from the rapid methods. Further the two prototype buildings representing the PRE and POST 1974 classes were analyzed through both pushover and incremental dynamic analysis-IDA, thus comparing the vulnerability curves obtained from analytical method with the trilinear damage curves provided from the GNDT and the proposed methods.

In chapter 9 an experimental validation is illustrated, comparing the damage occurred on the school building stock of the province of Ancona and Macerata, during the Centre Italy 2016 sequence, with those estimated by means the trilinear damage curves provided from the GNDT and the proposed methods.

6.2.4. Trilinear damage curves for the classes

As already discussed in Chapter 2, the vulnerability index does not provide an absolute measure of the damage that the building can suffer when a certain seismic event occurs, but it only allows comparisons between the buildings. Then we also compared the results in terms of $PGAc$, so that we can match experimental, empirical (Iv-PGA relationships obtained empirically) and analytical evidence available in literature.

Known the vulnerability indices for each building and from both methods, $PGAc$ and $PGAi$ have been determined by means eq.

Hence, the trilinear damage curves ($PGA - DI$) can be developed to determine losses in a rapid fashion (please see chapter 9 for the loss scenarios relative to the building stock under investigation).

Then, considering the average value of the vulnerability index for the PRE and POST 1974 classes, calculated according to both the GNDT and the proposed methods, trilinear damage curves for the classes have been developed (fig. 6.39).

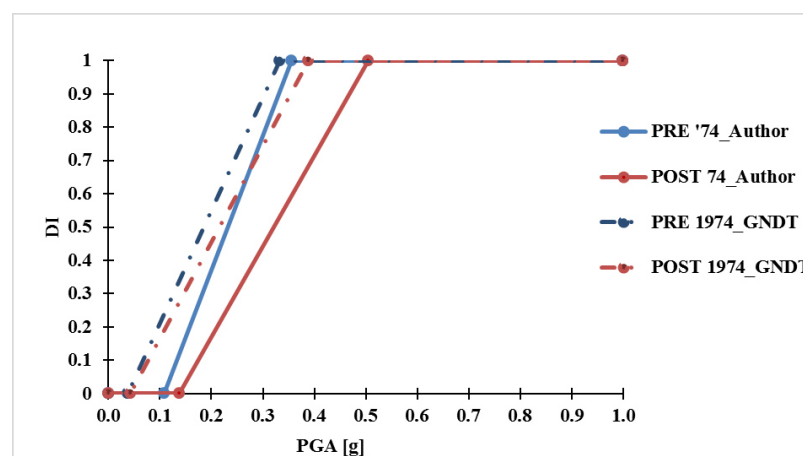


Figure 6.39. Comparison of trilinear damage curves provided from the author and GNDT methods obtained from the average Iv values for the two classes

The average values of I_v , PGAc and PGAs for both classes are shown in tab. 6.17.

Table 6.17. Average values of I_v , PGAc and PGAs for PRE and POST 1974 classes

	I_v	PGAs [g]	PGAc [g]
<i>PRE 1974_GNDT</i>	42.7	0.039	0.333
<i>PRE 1974_Autore</i>	55.8	0.108	0.356
<i>POST 1974_GNDT</i>	38.1	0.043	0.389
<i>POST 1974_Autore</i>	41.9	0.138	0.504

From the comparison of the curves emerges, in both methods, that the curve relative to the POST 1974 class is shifted to the right with respect the one related to the PRE 1974 class, as expected. In addition, the curves are closer in correspondence of low PGA levels, while they tend to move away by increasing the seismic intensity because the quality of the structure affect more the seismic response. This aspect is marked by the trilinear damage curves obtained from the proposed method, while it is just evident in those provided from the GNDT method.

References chapter 6

- Grunthal G. “European Macroseismic Scale”. Centre Européen de Géodynamique et de Séismologie, Luxembourg 1998; Vol. 15.
- Giovinazzi S. and Lagomarsino S., “A Macroseismic Method for the Vulnerability Assessment of Buildings,” 13th World Conf. Earthq. Eng., no. 896, pp. 1–6, 2004.
- Margottini C., Molin D., Narcisi B. and Serva L. (1985) Intensity vs. acceleration: Italian data, Proc. of the Conference on Historical Seismicity of Central-eastern Mediterranean Region, pp. 213–226.
- Murphy J. R.; O'Brien L. J. The correlation of peak ground acceleration amplitude with seismic intensity and other physical parameters. Bulletin of the Seismological Society of America, 67-3, 877-915. 1977.
- Guagenti E., Petrini V., 1989. Il caso delle vecchie costruzioni: verso una nuova legge danni-intensità, Proceedings of the 4th Italian National Conference on Earthquake Engineering, - Milan - (Italy), 1, 145-153, Milano.
- NTC 2008. Decreto Ministeriale 14/1/2008. Norme tecniche per le costruzioni (in Italian). Ministry of Infrastructures and Transportations, G.U. S.O. n. 29 on 2/4/2008 (2008).
- GNDT - Gruppo Nazionale per la Difesa dai Terremoti, 1994. Schede di 1° e 2° livello di vulnerabilità e di rilevamento del danno (edifici in c.a. e muratura).
- Regione Toscana, 2003. Manuale per la compilazione della scheda GNDT/CNR di II livello versione modificata della Regione Toscana, Direzione Generale delle Politiche Territoriali ad Ambientali, Settore: Servizio Sismico Regionale.
- Regione Marche, 2004. Manuale per la compilazione della scheda GNDT/CNR di II livello per edifici in calcestruzzo armato.

Chapter 7

7. Numerical validation through nonlinear analyses

The vulnerability index method here proposed needed of a validation through more reliable methods such as nonlinear numerical analysis.

Pushover analyses (*Dolsek et al. 2005*) and IDAs (*Vamvatsikos et al. 2002*) were performed on the two prototype buildings of the PRE and POST 1974 classes, with the aim to obtain first fragility curves and then vulnerability curves (PGA – DI) to compare with the trilinear damage curves provided from both the 2nd level GNDT and proposed methods.

Several authors have investigated the response of RC buildings for risk purpose by means non-linear analyses (*Bracci et al. 1995, Ellingwood et al. 2007, Liel et al. 2011, Faggella et al. 2013*). Other authors also compared results came from different non-linear procedures (*Elnashai 2001, Ferracuti et al. 2006, Vargas et al. 2013, Lantada et al. 2009, Magliuglio et al. 2007*). Further in (*D’Ayala et al. 2014*) a useful guideline for analytical vulnerability assessment of low/mid-rise buildings is provided.

Then some case studies were evaluated according to both GNDT and Author methods and the results in terms of capacity (PGA) compared with the one obtained through pushover analysis.

For prototype buildings analytical fragility curves have been developed from both pushover analyses and NLDAs (please see chapter 3 for a description of the procedure). Then fragility curves were used to calculate the probability of exceedance of each damage state, for increasing intensity levels, and consequently the expected damage level by means the vulnerability curves.

In this way, the validation of the rapid method proposed by the author has been done also for higher intensity level than the ones recorded during the Centre Italy sequence, as shown in chapter 8 for the experimental validation of the method.

Tab. 7.1 shows the relations assumed between the 5 damage levels of the EMS-98 scale (*Grunthal 1998*), the 4 damage states DS_k or performance levels usually provide by seismic Codes. Further the damage index thresholds according to (*Bramerini et al. 1995*) are reported.

Table 7.1. Correlation between damage levels, damage states, damage index values and after earthquake building condition

DL_k EMS-98	DS_k	DI Bramerini et al (1995)	Description	Condition
DL0	DS0	0.00	No damage	No damage
DL1	DS0	0.01		
DL2	DS1	0.10	Slight	Usable
DL3	DS2	0.35	Moderate	Usable with intervention
DL4	DS3	0.75	Extensive	Unusable
DL5	DS4	1.00	Complete	Collapsed

These relationships have been used to estimate damage level from rapid and pushover method. Whereas for IDAs the damage level was estimate thorough the IDR thresholds provided in tab. 7.2. (*Ghobarah 2004*):

Table 7.2. Values of the IDR toeholds for damage levels

	DL0	DL1	DL2	DL3	DL4	DL5
<i>Ghobarah 2004</i>	< 0.1 %	< 0.2 %	< 0.5 %	< 0.8 %	< 1.0 %	> 1.0%

7.1. Assessment of the prototype buildings

7.1.1. Incremental dynamic analysis (IDA)

Several NLDAs were carried out using 12 natural ground motion records, each one scaled with scale factors in order to have values of PGA from 0.1 to 1 with a step of 0.1.

In this way, the dynamic response and the displacement demand on the structure were investigated.

The structural model was developed by using unidimensional elements for columns and beams and diagonal struts for masonry infills. The stairs were considered in the model by mean plate elements. Deformable slabs were considered for the three storeys and fixed nodes were assumed at the foundation level.

Referring to the nonlinear behaviour the lumped plasticity method was used and the following assumption were done:

- plastic hinges for columns are PMM type, accounting the interaction between axial load and bending moments, while no interaction is considered for beams. Diagonal struts have only the axial plastic hinge.
- *Modified Takeda* model (*Takeda et al. 1970*) for flexure and shear hysteretic behavior, with stiffness reduction ratios α_1 and α_2 equal to 0.5 and 0.1 respectively. It was used for the ability to provide simple, numerically stable and sufficiently realistic hysteresis cycles.
- *Kinematic hardening* model for the axial hysteretic behavior.

Time history load cases were applied accounting for dead loads, live loads in a percentage suggested by the Code for the seismic combination and the records of the ground motions considered.

Direct integration of the ground motion according to Newmark method with $\gamma = 0.5$ and $\beta = 0.25$, and modal damping equal to 5 % for all modes were adopted.

Seismic input selection

The ground motions selection for non-linear dynamic analyses can follow several criteria (*Iervolino et al. 2005, Ghafory-Ashtiany et al. 2010, Masi et al. 2011, NIST 2011, Baker 2013*).

In this work a total number of 12 two-component natural accelerograms were employed, of which 9 accelerograms were selected to be compatible, according to as suggested from the Italian Code, with elastic response spectra for the hazard level of the area under investigation and relative to a return period of 712 years, corresponding to a 10% probability of occurrence in a reference period of 50 years. 712 years is reference return period to design a school building with respect the Limit State of Significant Damage (SLSD, or SLV in Italian) according to Italian Code. REXEL software (*Iervolino et al. 2009*) was used to select these records.

To consider the spatial distribution of the building stock, two reference response spectra were considered relative to the city of Ancona and Fabriano. Further, to account for the site amplification effect according to Italian seismic code, the soil categories B and C, and the T1 and T2 topographic conditions were assumed (these are the most common soil conditions for the building stock under investigation).

In this way, the aleatoric uncertainty in seismic demand was considered.

The other three records considered in the analysis, are not compatible with the reference response spectra for the return period of 712 years. These records refer to strong earthquakes occurred in Italy (Irpinia 1980, Amatrice 2016 and Norcia 2016) and they were chosen assuming the following conditions with respect the compatible records:

- the same fault mechanism (normal)
- the same soil type (B or C)
- a similar value of the maximum PGA

In tab. 7.3 the main features of the records used are described.

Table 7.3. Selected records for IDA

<i>Station ID</i>	<i>Earthquake Name</i>	<i>Date</i>	<i>Mw</i>	<i>Fault Mechanism</i>	<i>Epicentral Distance [km]</i>	<i>EC 8 Site classes</i>	<i>PGA_X [m/s²]</i>	<i>PGA_Y [m/s²]</i>
ST221	Umbria - Marche (IT)	26/09/1997	5.7	normal	3.0	C	3.38	2.56
MRN	Emilia (IT)_1st shock	20/05/2012	6.1	reverse	13.4	C	2.57	2.59
AQK	L'Aquila (IT)_mainshock	06/05/2009	6.3	normal	5.7	B	3.24	3.47
TLM1	Friuli (IT)_1st shock	06/05/1976	6.4	reverse	21.7	B	3.09	3.39
ST152	Lazio - Abruzzo (IT)	07/05/1984	5.9	normal	16.0	C	1.44	1.12
RHSC	Christchurch	13/06/2011	6.0	reverse	14.8	C*	1.88	1.89
ST271	Dinar	01/10/1995	6.4	normal	8.0	C	2.67	3.13
ST163	Kalamata	13/09/1986	5.9	normal	11.0	B	2.35	2.67
ST137 2	Kozani (aftershock)	19/05/1995	5.2	normal	16.0	B	2.60	1.84
CLT	Irpinia (IT)	23/11/1980	6.9	normal	18.9	B	1.72	1.55
NRC	Amatrice (IT)	24/08/2016	6.0	normal	15.3	B	3.53	3.67
NOR	Norcia (IT)	30/10/2016	6.5	normal	4.7	C*	3.06	2.88

Fig. 7.1 shows the spectral shape for the spectral-compatible records, while in fig. 7.2 are shown the not compatible records used in the analyses.

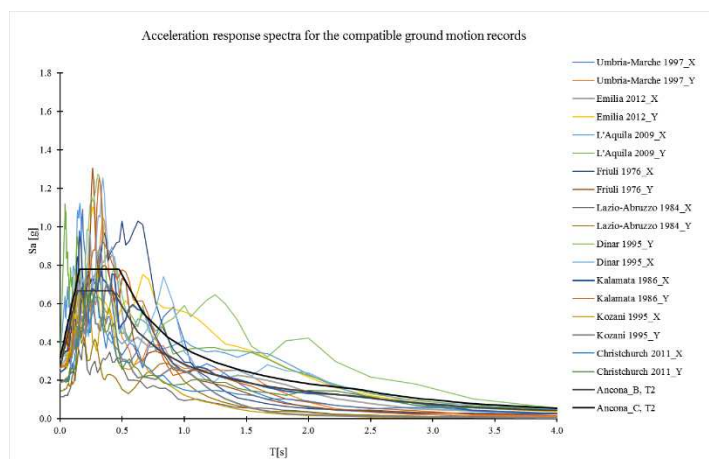


Figure 7.1. Response spectra of the compatible records

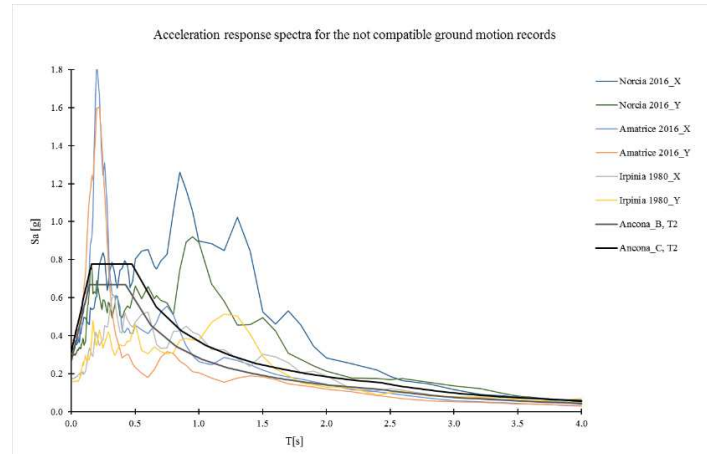


Figure 7.2. Response spectra of the not compatible records

Structural response

The structural response for both prototype building representative of the PRE and POST 1974 classes was analyzed by scaling the 12 natural records in order to have the maximum PGA from 0.1 g to 1 with intervals of 0.1 g. Thus, for each prototype building a total number of 120 time history analyses were performed.

The EDP considered is the maximum IDR between the two main directions (figs. 7.3 and 7.4).

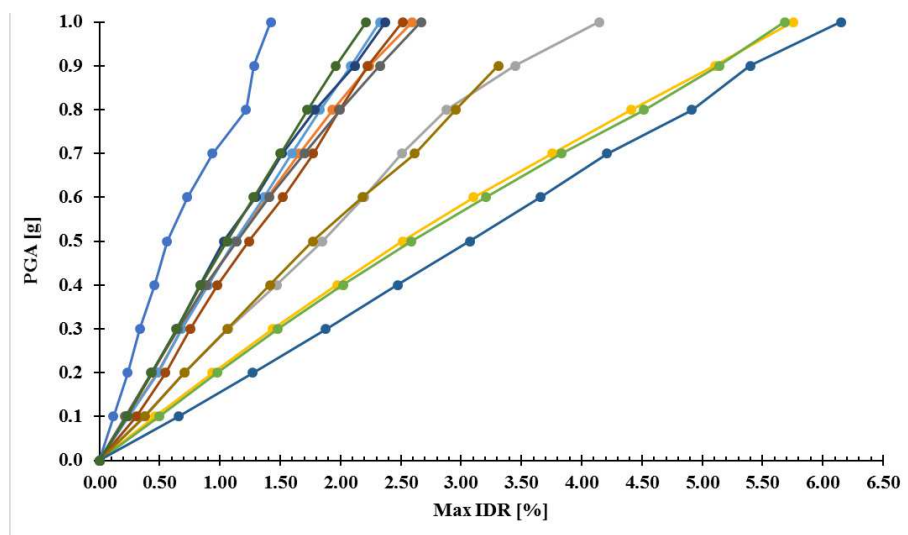


Figure 7.3. IDA curves for the PRE 1974 prototype building

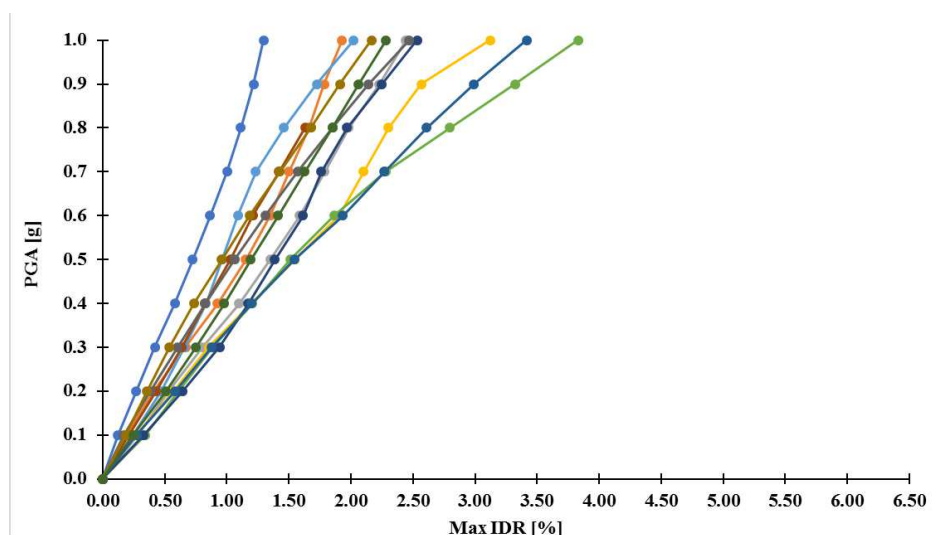


Figure 7.4. IDA curves for the POST 1974 prototype building

The differences in drift demands obtained under different ground motion ensembles reflect the epistemic uncertainty in ground motion modelling.

Several authors investigated the behaviour of the RCMF buildings through NLDAs. In (Masi *et al.* 2012) the response was evaluated for various configurations of RCMF such as bare, infilled and pilotis frames, providing results in terms of IDR and ductility demands in the members for increasing levels of both PGA and Housner Intensity (HI). The best correlation was provided between HI and IDR.

Therefore, different performances in terms of computed IDR values have been discussed by considering the building age, that is POST 1971 and PRE 1971, and identifying the role of building height and concrete strength.

With regard to Post71 types, results show that the lower drift values are always achieved in IF types. Drift values in BF types are always lower than in PF types, even though small differences are found irrespective of concrete strength and building height. Furthermore, drift values are always higher in structures with lower concrete strength with differences decreasing with building height. Similar results have been found in Ante71 types with respect to the role of concrete strength, infill distribution, and building height. Concerning the differences between Ante71 and Post71 types, results show that drift values are generally higher in Ante71 structures when considering BF and PF types having 2- and 4-storeys, while lower to negligible differences can be found in all IF and 8-storey types. Therefore, Post71 types generally show better performances than Ante71 types, even though differences decrease in the taller structures and, also in regularly infilled types. Among the considered structural parameters, infill distribution has the greatest influence on seismic response. This confirms results already found in previous studies on plane frames, related to the remarkable contribution provided by regularly arranged infills in reducing seismic vulnerability of gravity-load designed buildings.

Comparable trends can be seen in Old-Code (POST 1971) and Pre-Code types (PRE 1971) in relation to the qualitative role of infill and height. Generally, IDR values are higher for Pre-Code types, and the negative role of PF types is more marked.

The maximum Ductility Ratio (DR_{max}) values are generally obtained at the first story. Further the higher values are achieved for columns (DRC) rather than beams (DRB). It is interesting to note that for PF types (independent of the number of storeys in the buildings), the DRC_{max} at first story is always higher than other storeys.

Fragility curves

Fragility curves for both building classes relative to the damage states were developed from IDA curves and referring to eq. 3.10. Also, other procedures can be applied to derive fragility curves from NLDAs, as the cloud analyses (*Jalayer et al. 2014, Tesfamariam et al. 2014*) and the multiple stripe analyses (*Ni al. 2012*).

The median μ and the standard deviation β of the lognormal *CDF* ϕ were estimated by means the maximum likelihood method applied to the cumulative frequencies of exceedance of each limit state (*Baker 2015*).

The frequencies were computed as the ratio, for increasing PGA level with step of 0.05 g, between the number of IDA curves that exceed the specific DS threshold (the number of IDA curves that crossed the vertical lines intersecting the horizontal axis in correspondence of the IDR thresholds as shown in fig. 7.5) and the total number of IDA curves.

This approach is used when it is not possible to detect the exact IM and DM values corresponding to the occurrence of the damage states, as it happens when IM is increased in a discrete way (e.g. with scale factors as in this work). Instead, when continuous IDAs are performed, it's possible to know both IM and DM values for which the LSs occur in each IDA curve, thus the cloud of points representing the IM-DM pairs is employed to compute μ and β through a regression method.

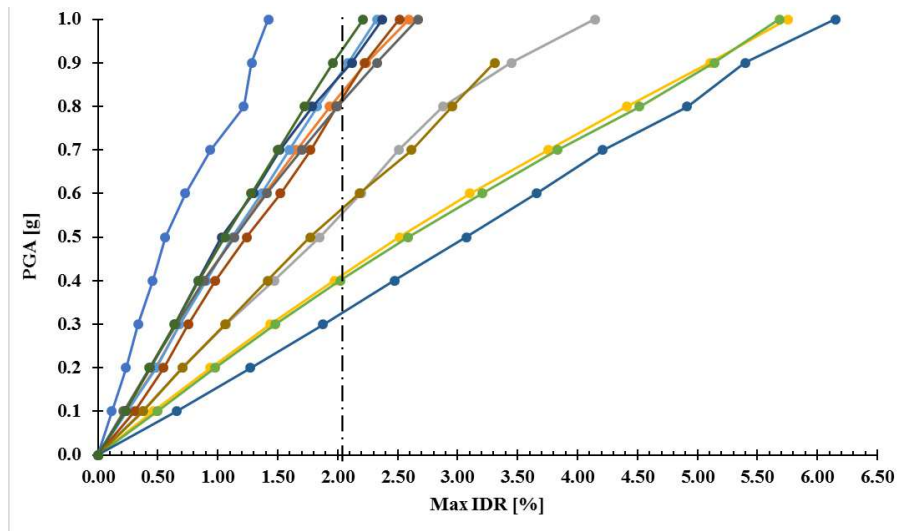


Figure 7.5. IDR threshold on IDA curves

The IDR threshold relative to the 4 damage state (DS1,...,DS4) was determined by means pushover analyses. This choice arises from the need to by-pass the higher costs linked to the evaluation of the occurrence of DSs by means IDAs, being the GMs scaled in a discrete way and not in a continuous manner as instead occurs for the horizontal load patterns in pushover analysis. Furthermore, pushover allows identifying general characteristics of system behaviour, i.e. elastic limit, redistribution of forces within the system subsequent to initial yielding, locations of plastic hinges.

Thus, the maximum IDR between the three stories of the buildings was selected, in correspondence of the points on the capacity curve for which the plastic hinges (fig. 7.6) of few close elements reached the damage states considered (damage limitation DL, significant damage SD, near collapse NC) in terms of chord rotation or shear strength according to the EC8 formulations.

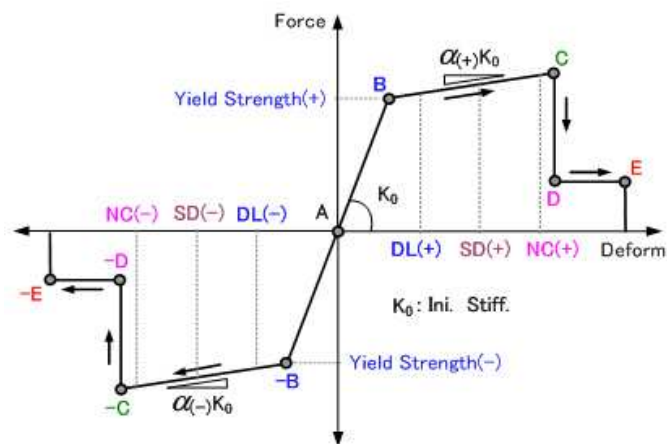


Figure 7.6. Plastic hinge for RC members

In particular, the DL damage state is reached when the yielding threshold is just exceeded; the SD occurs when the ultimate condition is almost achieved, and the NC limit state is reached when the members have reached their ultimate capacity.

Given that 8 capacity curves were performed for each building (4 in X direction and 4 in Y direction), the average value (tab. 7.4) between the eight maximum capacities in terms of IDR was assumed as thresholds for the damage state.

Table 7.4. IDR [%] for damage states

<i>Damage states</i>	IDR [%]	
	<i>PRE</i> <i>1974</i>	<i>POST</i> <i>1974</i>
DS1 - Light	< 0.20	< 0.20
DS2_Moderate	< 0.40	< 0.40
DS3_Extensive	< 0.70	< 0.90
DS4_Collapse	< 1.10	< 1.30

These values agree with some proposed in literature (*Ghobarah 2004, Vona 2014*). Thus, it can be noted that reliable structural models were used in the parametric analysis to quantify the vulnerability factors in the method proposed by the author (please see chapter 4).

In fig. 7.7 fragility curves from IDA are shown and the values of the statistical parameter are shown in tab. 7.5.

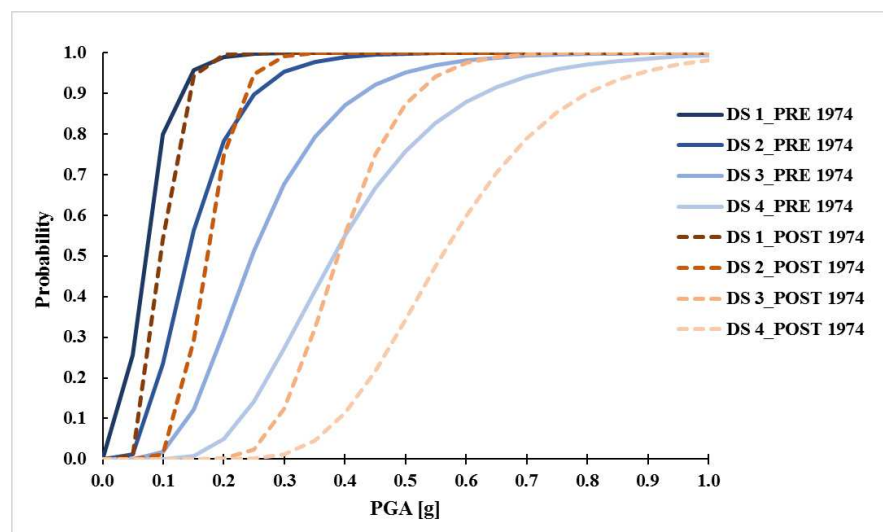


Figure 7.7. Fragility curves from IDA for the 4 damage states

It is worth noting that for the both prototype buildings the fragility curves are shifted on the left part of the graph and they are steeper for the LD damage state, while they are shifted on the right part

and are flatter by increasing the damage level. Furthermore, it is evident as the fragility associated with PRE 1974 model is larger than those of POST 1974 model for all the damage states, and this difference is increasing with the damage level.

Table 7.5. Statistical parameters of the CDF

	<i>Median PGA_{ds} [g]</i>				<i>β_{ds} [cm]</i>			
	<i>D_{S1}</i>	<i>D_{S2}</i>	<i>D_{S3}</i>	<i>D_{S4}</i>	<i>D_{S1}</i>	<i>D_{S2}</i>	<i>D_{S3}</i>	<i>D_{S4}</i>
PRE 1974	0.0678	0.1396	0.2467	0.3805	0.4636	0.4585	0.4272	0.3904
POST 1974	0.0972	0.1706	0.3879	0.5599	0.2729	0.2364	0.2218	0.2777

Then for the PGA levels corresponding to several return periods the DPMs (the probabilities to be in each damage state) relative to the prototype buildings representative of the PRE and POST 1974 building stocks were calculated (tabs. 7.6 and 7.7).

Table 7.6. DPM for PRE 1974 prototype building

<i>TR [years]</i>	<i>DS1</i>	<i>DS2</i>	<i>DS3</i>	<i>DS4</i>
30	0.57	0.08	0.00	0.00
50	0.78	0.21	0.01	0.00
75	0.90	0.40	0.05	0.00
100	0.95	0.55	0.12	0.01
201	0.99	0.78	0.31	0.05
475	1.00	0.94	0.63	0.23
712	1.00	0.96	0.72	0.32
975	1.00	0.98	0.80	0.42
1462	1.00	0.99	0.85	0.51
1950	1.00	0.99	0.89	0.58

Table 7.7. DPM for POST 1974 prototype building

<i>TR</i> <i>[years]</i>	<i>DS1</i>	<i>DS2</i>	<i>DS3</i>	<i>DS4</i>
30	0.15	0.00	0.00	0.00
50	0.49	0.01	0.00	0.00
75	0.81	0.09	0.00	0.00
100	0.94	0.28	0.00	0.00
201	1.00	0.74	0.00	0.00
475	1.00	0.98	0.08	0.01
712	1.00	1.00	0.19	0.02
975	1.00	1.00	0.33	0.05
1462	1.00	1.00	0.49	0.09
1950	1.00	1.00	0.61	0.14

In dark black are highlighted the rows corresponding to the four limit states of the Italian Code (SLO, SLD, SLV, SLC) provided for school building typology. Thus, damage indices were calculated through eq. 3.4.

Damage indices for each return period are shown in tab.7.8, while in fig. 7.8 the vulnerability curves in terms of PGA are shown for both classes.

Table 7.8. DI values for the prototype buildings

<i>TR</i> <i>[years]</i>	<i>PGA</i>	<i>PRE</i> <i>1974</i>	<i>POST</i> <i>1974</i>
30	0	0.15	0.03
50	0.073	0.25	0.10
75	0.097	0.37	0.20
100	0.124	0.49	0.30
201	0.148	0.73	0.50
475	0.199	1.00	0.65
712	0.285	1.00	0.73
975	0.318	1.00	0.83
1462	0.351	1.00	0.97
1950	0.386	1.00	1.00

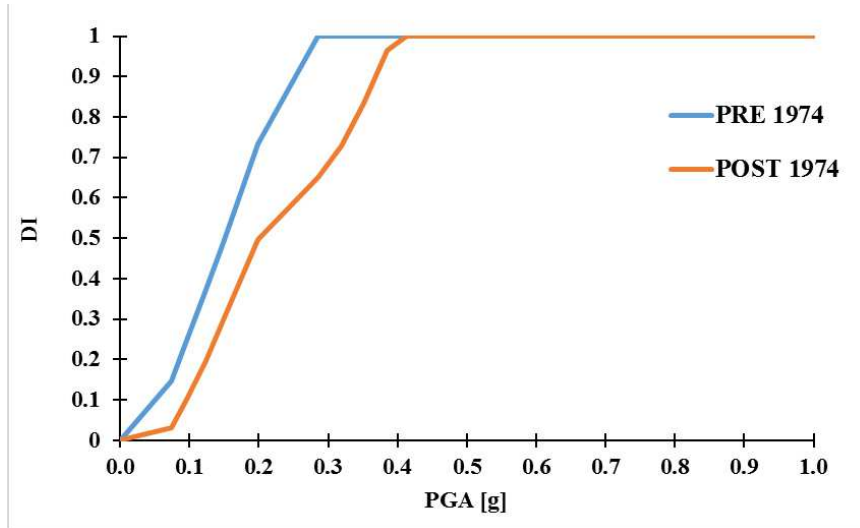


Figure 7.8. Vulnerability curves from IDAs

The vulnerability curves show as for an event with a PGA of about 0.25 g the PRE 1974 prototype reaches the collapse, while the POST 1974 collapse for PGA of about 0.40 g.

Thus, damage states for intensity levels of interest can be assigned according to the relationship between damage indices and damage states shown in tab.

7.1.2. Pushover analysis

Fragility curves were developed for the two prototype buildings from the average bilinear curves (fig. 7.9) obtained through pushover analyses (please see chapter 5).

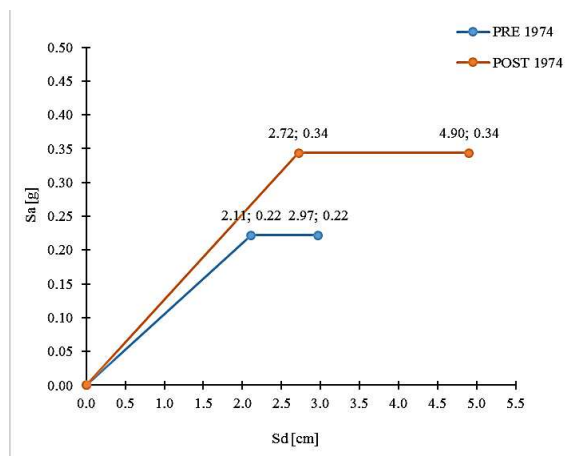


Figure 7.9. Average bilinear curves for the prototype buildings

The seismic demand was determined in terms of response spectra, for several return periods, by fixing a spectral shape and accounting for the site effects according to as suggested from the Italian seismic Code.

Because of the slight difference in the seismic hazard level of the cities under investigation in the Ancona province, only the hazard curve for a point in Ancona city and the relative response spectra were adopted for each return period.

Further, only the soil category C and topographic condition T2, with the ratio $h/H = 0.5$, were considered to obtain response spectra. These are the most common soil condition for the school building under investigation.

Fig. 7.10 shows the mean hazard curves (seismic intensity on the X axis and frequency of occurrence on the Y axis) and those for the 16th and 84th percentiles of the probabilistic distributions of the variables (intensity parameter).

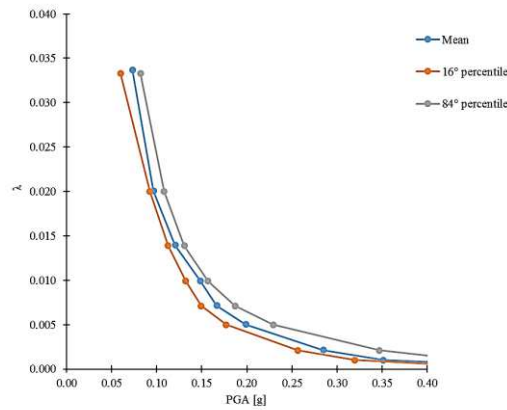


Figure 7.10. The mean, the 16th and 84th percentile hazard curves for the site.

The mean hazard curve accounts for epistemic uncertainty in seismic demand. It was determined amplifying the median curves (50th percentile) for a coefficient that consider the difference in terms of PGA values between the 84th and 16th percentile hazard curves for a given value of λ (eq. 7.1) (CNR-DT 212/2013):

$$\lambda_S(S)_{\text{mean}} = \lambda_S(S)_{\text{median}} * e^{\left(\frac{1}{2} \beta_H^2\right)} \quad (7.1)$$

where:

$$\beta_H = \frac{\ln(S_{84\%}) - \ln(S_{16\%})}{2} \quad (7.2)$$

Both hazard curves and response spectra were determined referring to a unique point for each city where the schools are located, because of the homogeneity of soil conditions was assumed within the city. Obviously, the local site conditions could differ between the school buildings, but in situ investigations should be done.

In tab. the values of PGA for some points of the hazard curves are shown.

Table. 7.9. Seismic demand in terms of PGA for several return periods

TR_D [years]	PGA [g]		
	50°	16°	84°
30	0.073	0.060	0.082
50	0.097	0.093	0.108
72	0.121	0.113	0.131
101	0.148	0.132	0.157
141	0.167	0.149	0.187
200	0.199	0.177	0.229
476	0.285	0.256	0.347
1000	0.351	0.319	0.443
2500	0.492	0.440	0.616

To estimate the performance of both buildings, the comparison in the ADRS (acceleration-displacement response spectra) plane between the response spectra, for the several return periods, and the structural capacity in terms of bilinear capacity curves (N2 method) was done (fig. 7.10).

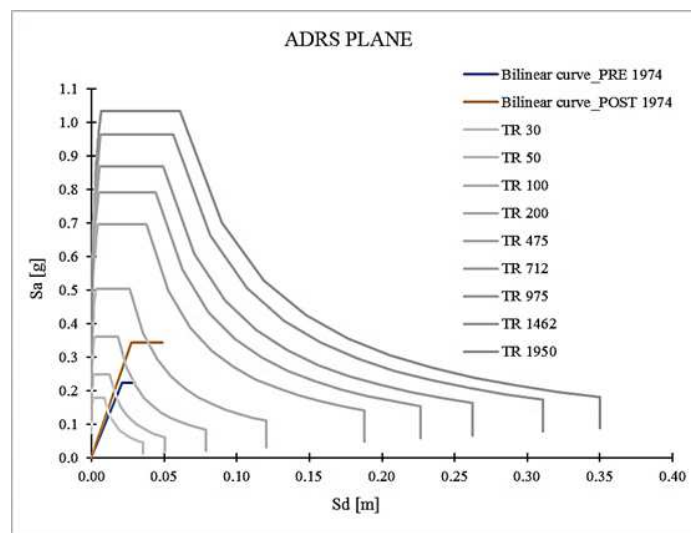


Figure 7.10. Bilinear capacity curves of buildings and response spectra for several return periods

The performance points for each return period were found and the value of seismic demands in terms of spectral displacement are reported in tab. 7.10.

Table 7.10. Seismic demand in terms of $S_d(T)$ obtained through the N2 method.

TR_D [years]	S_d for the performance point [m]	
	PRE 1974	POST 1974
30	0.013	0.011
50	0.018	0.015
75	0.021	0.018
100	0.024	0.022
201	0.035	0.032
475	0.050	0.046
712	0.059	0.052
975	0.065	0.058
1462	0.074	0.065
1950	0.081	0.072

Then the probability of occurrence of each damage state given a certain intensity level was determined from the relative fragility curves, developed according to eq. 7.3:

$$P [ds | S_d] = \phi \left[\frac{1}{\beta_{ds}} \ln \left(\frac{S_d}{S_{d,ds}} \right) \right] \quad (7.3)$$

The values of the median $S_{d,ds}$ and the standard deviation β_{ds} were determined from the average bilinear curves according to the RISK-UE formulations (Milutinovic et al. 2003) shown in tab. 7.11. In fact, building capacity curves provide a simple and reasonably accurate means of predicting inelastic building displacement response for damage estimation purposes.

Table 7.11. Formulations to calculate median and St. dev. for the damage states

Damage state - D_{Sk}	$S_{d,ds}$ Mediana	B_{ds} Dev. St.
D_{S1}	0.7 dy	$0.25 + 0.07 \ln(\mu)$
D_{S2}	1.0 dy	$0.20 + 0.18 \ln(\mu)$
D_{S3}	dy + 0.5 (du - dy)	$0.10 + 0.40 \ln(\mu)$
D_{S4}, D_{S5}	du	$0.15 + 0.50 \ln(\mu)$

For total standard deviation β_{ds} the formulations in tab. 7.11 are determined assuming that the probability of exceeding each damage state at its spectral displacement is the 50%, while the other damage states follows a beta distribution in a way that minimize the difference between the beta and lognormal cumulative distributions, obtained by varying the ductility values. Because of is the capability of the beta distribution (that is like the binomial one when its parameters assume certain values) to capture the real damage surveyed after past earthquake (*Braga et al. 1982*), thus β_{ds} can represent all the uncertainties involved in the process.

It is worth noting that, if under a specified level of ground motion the seismic response is linear or nearly linear, the building behaviour depends primarily on its stiffness and strength properties. In this case, the behaviour of the idealized SDOF system can adequately simulate the median response of the type of buildings it represents. Hence, it is relatively easy to establish the median spectral displacements (or interstorey drift ratios) for the yielding, the slight and the moderate damage states. However, difficulties will be encountered if the structure is shaken well into the inelastic range. In this case, the behaviour of the building depends not only on the stiffness and strength properties, but also on the inelastic deformation capacities (ductility) of structural members, that is their ability to develop plastic deformation while maintaining the lateral-load resisting capacity.

Hence, beyond the moderate damage state, the results of pushover analysis could not be used directly for determining the median spectral displacements for the extensive and the complete damage states. In fact, the latter segments of the capacity curve underestimate the inelastic deformation capacity of the structure. While this conservatism is desirable for the design of new buildings as well as for assessment and rehabilitation of existing buildings, it is nevertheless unsuitable for loss estimate. Damage functions should predict losses without bias. Hence, from the point of view of the loss estimation, conservatism in seismic design codes and guideline documents must be removed.

The values of median and standard deviation for the damage states are shown in tab. 7.12.

Table 7.12. Median and St. dev. Values for the damage states

	<i>Median $S_{d,ds}$</i> <i>[cm]</i>				<i>β_{ds}</i> <i>[cm]</i>			
	<i>D_{S1}</i>	<i>D_{S2}</i>	<i>D_{S3}</i>	<i>D_{S4}, D_{S5}</i>	<i>D_{S1}</i>	<i>D_{S2}</i>	<i>D_{S3}</i>	<i>D_{S4}, D_{S5}</i>
<i>PRE 1974</i>	1.48	2.11	2.54	2.97	0.27	0.26	0.24	0.32
<i>POST 1974</i>	1.90	2.72	3.81	4.90	0.29	0.31	0.34	0.44

Fig. 7.11 shows the fragility curves for each damage state in terms of spectral displacement.

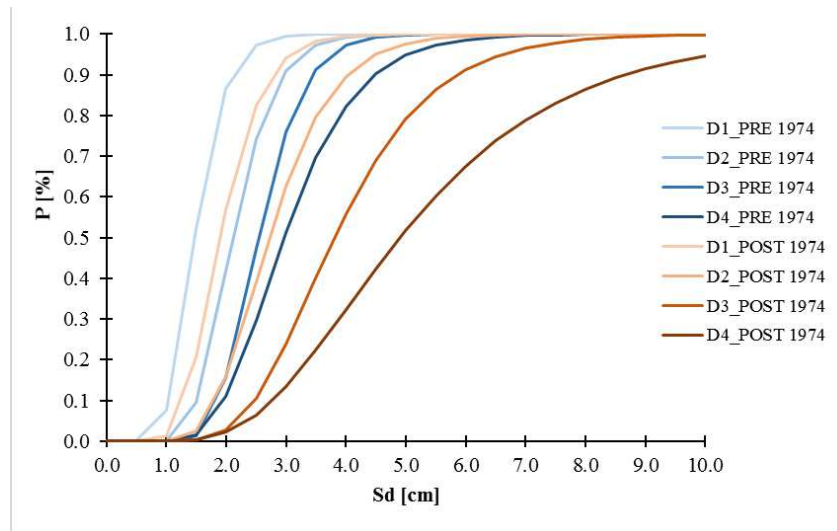


Figure 7.11. Comparison of fragility curves in terms of spectral displacement (S_d) for the PRE and POST 1974 prototype buildings

Furthermore, the fragility curves in terms of PGA were developed and showed in fig. 7.12, by replacing in the equations in tab. the terms dy and du with PGA_y and PGA_u respectively. The values of median and standard deviation for the damage states are shown in tab. 7.13.

Table 7.13. Median and St. dev. Values for the damage states

	Median PGA_{ds} [g]				β_{ds} [cm]			
	D_{S1}	D_{S2}	D_{S3}	D_{S4}	D_{S1}	D_{S2}	D_{S3}	D_{S4}
<i>PRE 1974</i>	0.078	0.112	0.160	0.208	0.27	0.26	0.24	0.32
<i>POST 1974</i>	0.124	0.177	0.246	0.315	0.29	0.31	0.34	0.44

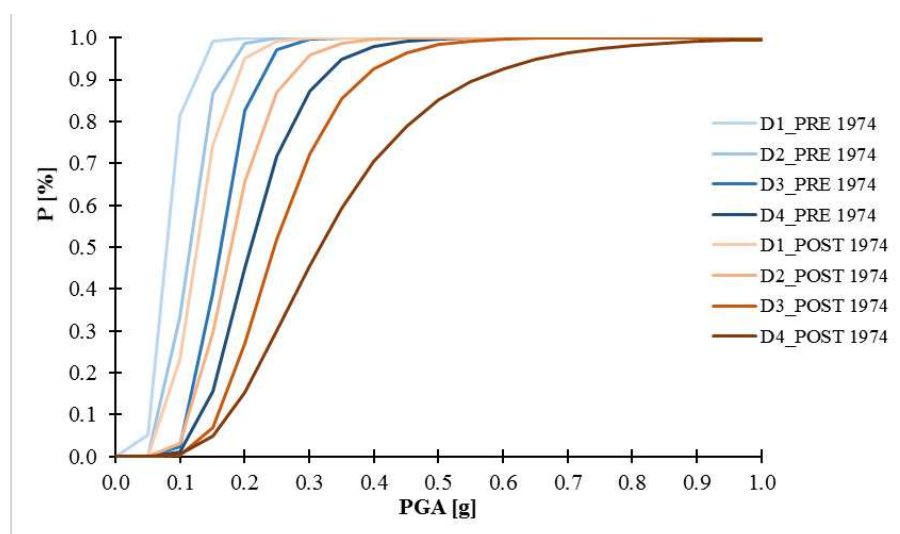


Figure 7.12. Comparison of fragility curves in terms of PGA for the PRE and POST 1974 prototype buildings

As expected, the fragility curves relative to the PRE 1974 class are steeper than the ones relative to the POST 1974, in particular for the higher damage levels. Thus PRE 1974 class reach the damage thresholds with a lower seismic intensity level.

For the performance points previously determined (tab. 7.10) the DPMs (the probabilities to be in each damage state) relative to the prototype buildings representative of the PRE and POST 1974 building stocks were calculated (tabs. 7.14 and 7.15).

Table 7.14. DPM for PRE 1974 prototype building

<i>TR</i> [years]	<i>DS1</i>	<i>DS2</i>	<i>DS3</i>	<i>DS4</i>
30	0.04	0.00	0.00	0.00
50	0.20	0.02	0.00	0.00
75	0.50	0.12	0.02	0.02
100	0.73	0.28	0.07	0.05
201	0.95	0.65	0.26	0.15
475	1.00	0.94	0.67	0.41
712	1.00	0.97	0.78	0.51
975	1.00	0.99	0.86	0.60
1462	1.00	0.99	0.91	0.68
1950	1.00	1.00	0.94	0.73

Table 7.15. DPM for POST 1974 prototype building

<i>TR_D</i> [years]	<i>DS1</i>	<i>DS2</i>	<i>DS3</i>	<i>DS4</i>
30	0.40	0.05	0.00	0.00
50	0.78	0.28	0.02	0.01
75	0.95	0.65	0.14	0.05
100	0.99	0.86	0.37	0.15
201	1.00	0.99	0.82	0.44
475	1.00	1.00	0.99	0.84
712	1.00	1.00	1.00	0.91
975	1.00	1.00	1.00	0.95
1462	1.00	1.00	1.00	0.97
1950	1.00	1.00	1.00	0.98

The damage index is calculated according eq. 3.4, thus a damage state can be assigned according to the relationship between damage index and damage state shown in tab. 7.1.

The damage index for each return period are shown in tab. 7.16, while in fig. the vulnerability curves are shown in terms of PGA (fig. 7.13).

Table 7.16. DI values for the prototype buildings

<i>TR</i>	<i>PGA</i> [g]	<i>PRE</i> 1974	<i>POST</i> 1974
30	0	0.10	0.01
50	0.073	0.29	0.05
75	0.097	0.58	0.18
100	0.124	0.88	0.33
201	0.148	1.00	0.73
475	0.199	1.00	1.00
712	0.285	1.00	1.00
975	0.318	1.00	1.00
1462	0.351	1.00	1.00
1950	0.386	1.00	1.00

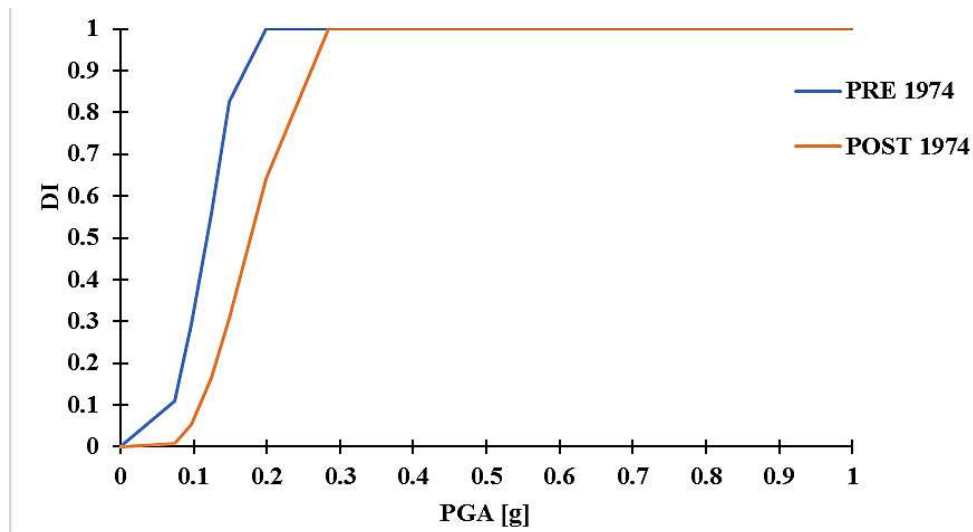


Figure 7.13. Comparison of vulnerability curves in terms of PGA for the PRE and POST 1974 prototype buildings

The vulnerability curves show as for an event with a PGA of about 0.2 g the PRE 1974 prototype reaches the collapse, while the POST 1974 collapse for PGA of about 0.35 g.

7.1.3. Comparison of the results

Finally, the vulnerability curves estimated for the prototype buildings through nonlinear analyses are compared with the ones obtained by means the rapid methods. In this way, the reliability of the trilinear damage curves here proposed can be validated also for higher intensity levels with respect those recorded during the Centre Italy sequence, as shown in chapter 8 for the experimental validation of the method.

Thus, the damage index was calculated for both PGA levels corresponding to the limit states (return periods of 50, 75, 712 and 1462 years), and the relative damage states were assigned through the relation of Bramerini showed in tab.

In fig. 7.14 are shown the trilinear damage curves for the two prototype buildings, obtained by means both 2nd level GNDT and proposed methods.

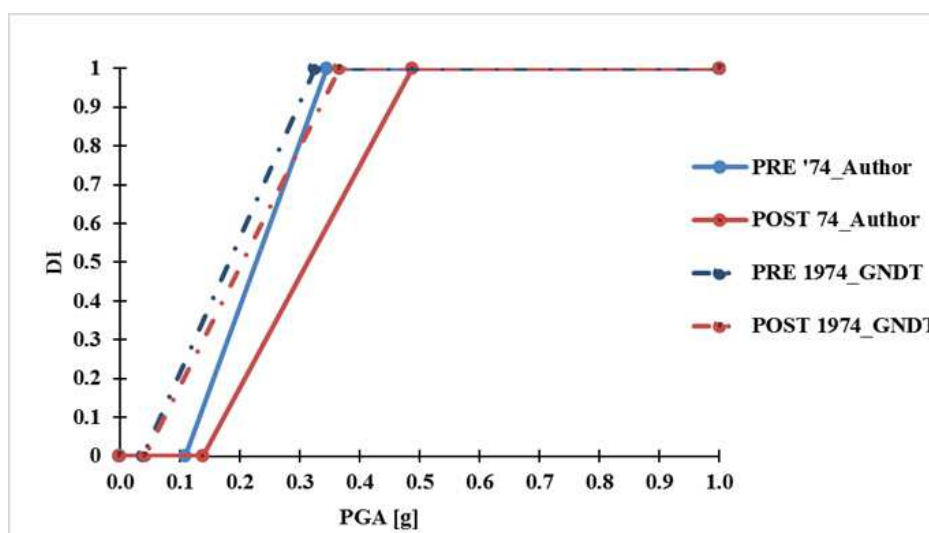


Figure 7.14. Comparison of trilinear damage curves for the two prototype buildings obtained by means both methods.

In tab. 7.17, for the proposed method, and in tab. 7.18, for the 2nd level GNDT method, the damage indices and the relative damage states are shown for the return periods corresponding to the limit states provided by the Code.

Table 7.17. Damage states provided from the proposed method

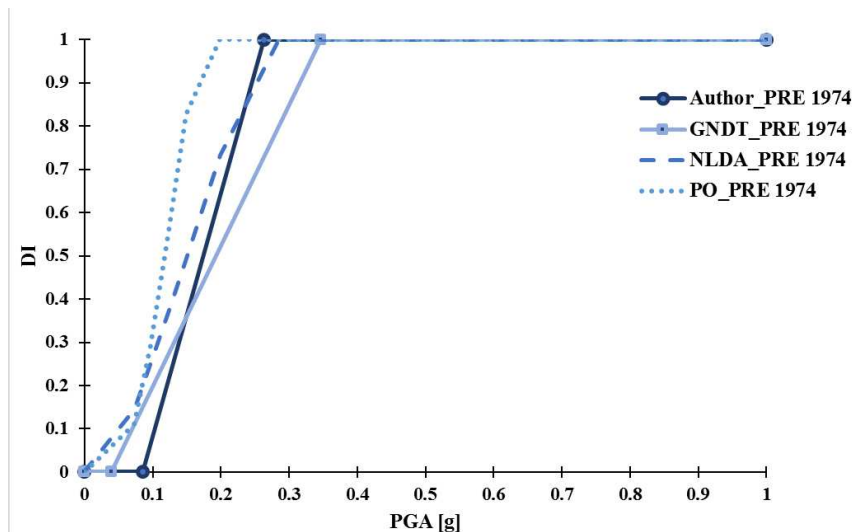
			PRE 1974		POST 1974	
LS	TR	PGAD	DI	DSk	DI	DSk
SLO	50	0.097	0.07	DS0	0.00	DS0
SLD	75	0.124	0.22	DS1	0.00	DS0
SLV	712	0.318	1.31	DS5	0.67	DS2
SLC	1462	0.386	1.69	DS5	0.91	DS3

Table 7.18. Damage states provided from the 2nd level GNDT method

			PRE 1974		PRE 1974	
LS	TR	PGAd	DI	DSk	DI	DSk
SLO	50	0.097	0.19	DS2	0.13	DS2
SLD	75	0.124	0.27	DS3	0.21	DS2
SLV	712	0.318	0.91	DS4	0.72	DS3
SLC	1462	0.386	1.13	DS5	0.90	DS4

Then the comparison between the vulnerability curves obtained from rapid and numerical methods was done. It can be seen as for PRE 1974 prototype building (fig. 7.15) the proposed curve is so far from the numerical ones for lowest intensity levels (it is not conservative), while the GNDT curve is very close to them. For the highest intensity levels the proposed curve approximates very well the curve from IDA, while the curve from pushover is too conservative.

The same is for the POST 1974 prototype building (fig. 7.16).

**Figure 7.15.** Comparison of vulnerability curves for the PRE 1974 building

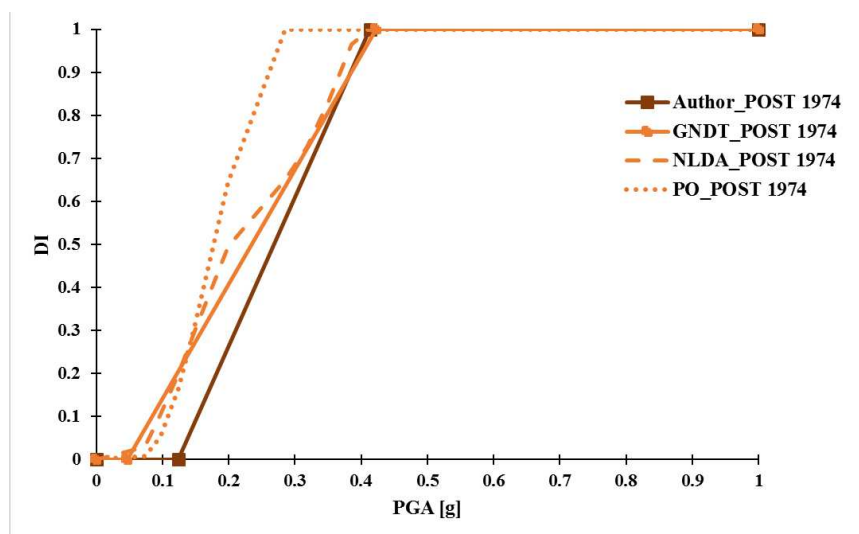


Figure 7.16. Comparison of vulnerability curves for the POST 1974 building

In tabs. 7.19 (for PRE 1974 prototype building) and 7.20 (for POST 1974 prototype building) the comparison of the estimated damage states from the several methods is illustrated for the return periods corresponding to the occurrence of the 4 damage states for school buildings designed according to the prescription of the Italian seismic Code. The damage states were estimated by means the Bramerini relationship of tab. 7.1 once the value of the damage index is known from the vulnerability curve.

Table 7.19. Comparison of the estimated damage levels for the PRE 1974 prototype building

Limit state	TR	PGAD [g]	Author	GNDT	Pushover	NLDA
SLO	50	0.097	DS0	DS2	DS2	DS2
SLD	75	0.124	DS1	DS2	DS3	DS2
SLV	712	0.318	DS5	DS4	DS5	DS5
SLC	1462	0.386	DS5	DS5	DS5	DS5

Table 7.20. Comparison of the estimated damage levels for the POST 1974 prototype building

Limit state	TR	PGAD [g]	Author	GNDT	Pushover	NLDA
SLO	50	0.097	DS0	DS2	DS0	DS1
SLD	75	0.124	DS0	DS2	DS1	DS2
SLV	712	0.318	DS3	DS3	DS5	DS3
SLC	1462	0.386	DS4	DS4	DS5	DS4

It is worth noting that for both PRE and POST 1974 prototype buildings the proposed method provides better results in correspondence of the highest intensity levels, thus for the SLV and SLC. While it is less conservative than the other methods for low intensity level.

7.2. Assessment of case studies

Pushover analyses were carried out on ten case studies in order to obtain the average bilinear curve from which to calculate the average capacity in terms of PGA, with regard the initial damage (PGA_i) and collapse (PGA_c) (please see chapter 5 for the description of the procedure applied). These values of structural capacity were then compared with those obtained from both the 2nd level GNDT and the proposed methods as a function of the global vulnerability index.

Below it is exemplified the rapid and pushover assessment for one of the case study.

Case study: ITC Gentili Macerata

The school building is in the city of Macerata. It was built in the 1979 and it has the classical characteristics of the schools of that period, such as large windows on the longitudinal façades, identifying short columns, and masonry infills on the transverse (fig. 7.17 -left). The plan shape is an elongated rectangular (fig. 7.17 – right) and the number of storeys is 3.

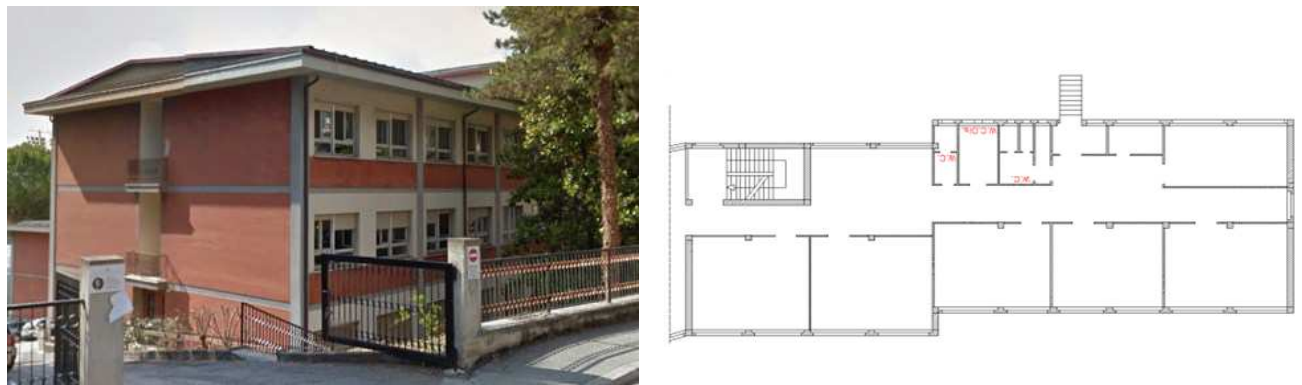


Figure 7.17. Lateral view (left) and plan shape (right) of the school

The RC frames are arranged only along the longitudinal direction and on the perimeter of the transverse direction.

First the rapid evaluation was performed. In tab. 7.21 the scores assigned to the vulnerability indicators according to the proposed method are shown.

Table 7.21. Evaluation by means the proposed vulnerability datasheet

Vulnerability indicators	w_i
1 - Age of building	0.40
2 – Reference Code	0.65
3 – Built in seismic zone	1.50
4 – Typology of the resistant system	0.35
5 – Quality of the resistant system	0.20
6 – Critical elements	0.25
7 – Irregularity in plan shape	0.30
8 – Irregularity in elevation shape	0
9 – Irregularity in plan stiffness	0.50
10 - Irregularity in elevation stiffness	0
11 – Position and type of stairs	0.30
12 – Stiffness of floor slabs	0.25
13 – Position of foundation	0
14 – Irregularity of storey mass	0
15 – Degradation of materials	0

$$I_v = 4.70$$

$$PGA_i = 0.127 \text{ g}$$

$$PGA_u = 0.429 \text{ g}$$

While for the 2nd level GNDT method the results are:

$$I_v = 27.7$$

$$PGA_i = 0.052 \text{ g}$$

$$PGA_u = 0.486 \text{ g}$$

Then pushover analyses were performed by applying 2 groups of lateral loads, the push mode and push mass for each main direction X and Y (total of 8 analyses).

Structural models of the two case studies were developed by using unidimensional elements for beams and columns. Further masonry infills were considered as equivalent diagonal struts with a certain equivalent area/stiffness and resistance.

The lumped plasticity method was used to take into account nonlinearities, so plastic hinges according to EC8 were assigned to columns, beams and diagonal struts. The plastic hinge for

columns is PMM type, accounting for interaction between axial load and bending moments, while no interaction is considered for beams.

In diagonal struts axial plastic hinges are considered and the local effect of the infill panel on the frame is not considered, because only the global behaviour is of interest.

Thus the 8 capacity curves of the MDOF system (fig. 7.18 left) and the average equivalent bilinear curve of the SDOF system (7.18 right) were obtained.

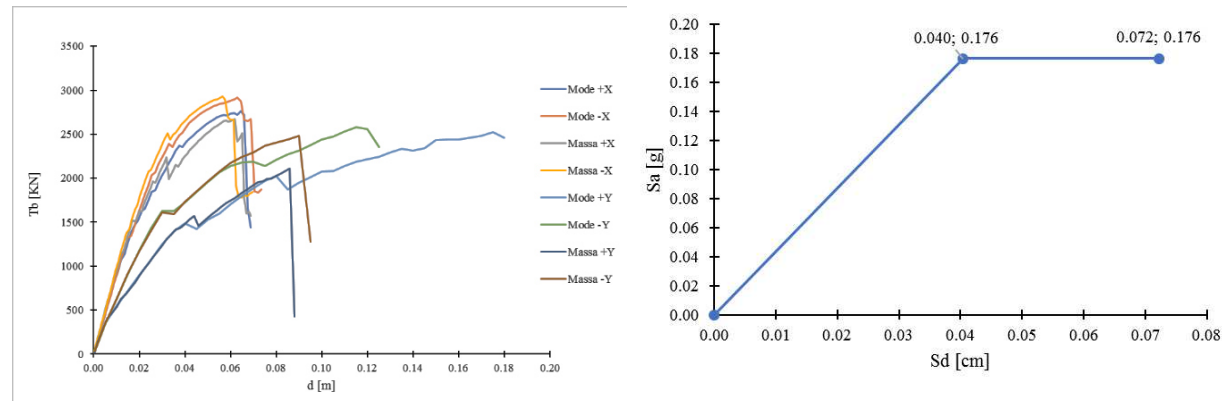


Figure 7.18. Capacity curves of the MDOF system (left) and the average equivalent bilinear curve of the SDOF system (right).

The capacity values in terms of PGA in correspondence of the initial damage and collapse are calculated as shown in chapter 5 by fixing a spectral shape and applying the N2 method backward.

$$PGA_i = 0.096 \text{ g}$$

$$PGA_u = 0.350 \text{ g}$$

By comparing the results, the proposed method provides a greater value of PGA_i , with respect both GNDT method and pushover, while the PGA_c value is comprised between the lower value provide by the pushover and the higher value provided by the GNDT method.

The same procedure was applied for all case studies and the comparison of the results in terms of both PGA_i and PGA_c are shown respectively in fig. 7.19 and fig. 7.20.

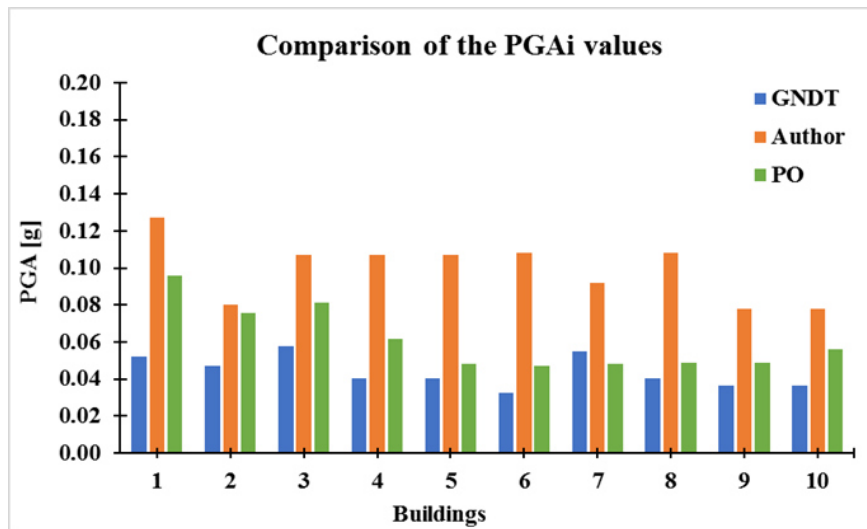


Figure 7.19. Comparison of $PGAI$ calculated for the case studies by means pushover and rapid methods

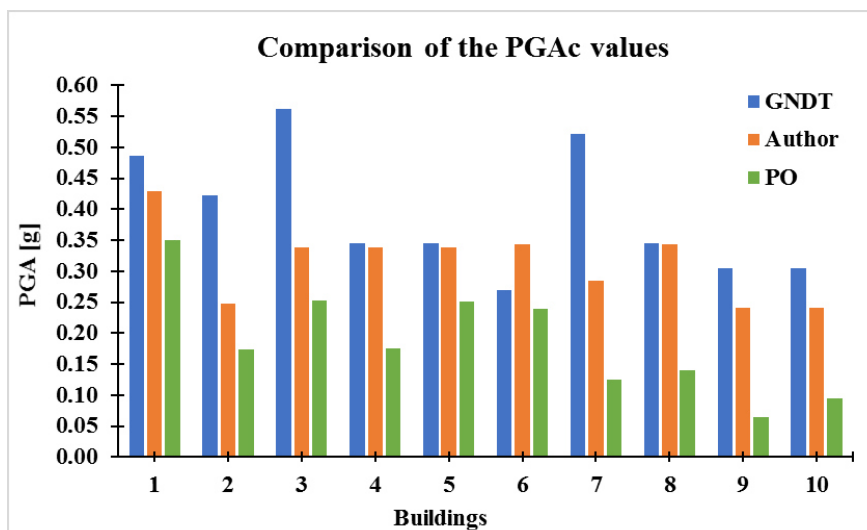


Figure 7.20. Comparison of $PGAc$ calculated for the case studies by means pushover and rapid methods

Results confirm the non-conservativity, previously founded also for the two prototype buildings, of the proposed method for the initial damage condition. While for the collapse condition the proposed method provides in most cases $PGAc$ values closer than those provided from both pushover analyses and 2nd level GNDT method.

References chapter 7

- Dolšek M, Fajfar P. 2005. Simplified non-linear seismic analysis of infilled reinforced concrete frames. *Earthquake Engineering and Structural Dynamics* 34(1): 49–66. DOI: 10.1002/eqe.411.
- Vamvatsikos D. and Cornell C. A., “Incremental dynamic analysis,” *Earthq. Eng. Struct. Dyn.*, vol. 31, no. 3, pp. 491–514, Mar. 2002.
- Bracci J. M. G., Reinhorn A. M., and Mander J. B. (1995). “Seismic resistance of reinforced concrete frame structures designed for gravity loads: Performance of structural system.” *ACI Struct. J.*, 2(5), 597–609.
- Ellingwood B. R., Celik O. C., and Kinali K., “Fragility assessment of building structural systems in Mid-America,” *Earthq. Eng. Struct. Dyn.*, vol. 36, no. 13, pp. 1935–1952, Oct. 2007.
- Liel, A. B., Haselton, C. B., and Deierlein, G. G. (2011). “Seismic Collapse Safety of Reinforced Concrete Buildings. II: Comparative Assessment of Nonductile and Ductile Moment Frames.” *Journal of Structural Engineering*, 137(4), 492.
- Faggella M. et al. Probabilistic seismic response analysis of a 3-D reinforced concrete building. *Structural Safety* Volume 44, September 2013, Pages 11-27.
- Elnashai A.S. Static pushover versus dynamic collapse analysis of RC buildings. *Engineering Structures* 23 (2001) 407–424.
- Ferracuti B., Savoia M., Pinho R., Francia R., Conventional and Adaptive Pushover Procedures Against Dynamic Analysis, in: *GIMC 2006 :XVI Convegno Italiano di Meccanica Computazionale*, GIMC, Bologna, Italy, 26-28 June 2006.
- Vargas Y. F., Pujades L. G., Barbat A. H., and Hurtado J. E., “Incremental Dynamic Analysis and Pushover Analysis of Buildings. A Probabilistic Comparison,” in *Computational Methods in Stochastic Dynamics*, M. Papadrakakis, G. Stefanou, and V. Papadopoulos, Eds. Springer Netherlands, 2013, pp. 293–308.

- Lantada N., Pujades L.G., Barbat A.H.: Vulnerability index and capacity spectrum based methods for urban seismic risk evaluation. A comparison. *Nat. Hazards* 51, 501–524 (2009).
- Magliulo G., Maddaloni G., & Cosenza, E. (2007). Comparison between non-linear dynamic analysis performed according to EC8 and elastic and non-linear static analyses. *Engineering Structures*, 29(11), 2893–2900.
- D’Ayala D., Meslem A., Vamvastikos D., Porter, K., Rossetto T., Crowley H., Silva V., 2014. Guidelines for analytical vulnerability assessment of low/mid-rise Buildings – Methodology. Vulnerability Global Component project. Available from: www.nexus.globalquakemodel.org/gem-vulnerability/posts/
- Grunthal G. “European Macroseismic Scale”. Centre Européen de Géodynamique et de Séismologie, Luxembourg 1998; Vol. 15.
- Bramerini F., Di Pasquale G., Orsini G., Pugliese A., Romeo R., Sabetta F., “Rischio sismico del territorio italiano. Proposta per una metodologia e risultati preliminari”. SSN/RT/95/01, Rome, 1995 (In Italian).
- Ghobarah A. “On Drift Limits Associated with Different Damage Levels,” Proceedings of International Workshop on Performance-Based Seismic Design, Department of Civil Engineering, McMaster University, Bled, 28 June-1 July 2004.
- Takeda T., Sozen M. A., and Nielsen N. N., “Reinforced Concrete Response to Simulated Earthquakes,” *J. Struct. Div.*, vol. 96, no. 12, pp. 2557–2573, 1970.
- Iervolino, J., and Cornell, C. A. (2005). “Record selection for nonlinear seismic analysis of structures.” *Earthquake Spectra*, 21(3), 685–713.
- Ghafory-Ashtiany M., Mousavi M., Azarbakht A.R.. 2010. Strong ground motion record selection for the reliable prediction of the mean seismic collapse capacity of a structure group. *Earthquake Engineering and Structural Dynamics*.
- Masi A. et al. Selection of Natural and Synthetic Accelerograms for Seismic Vulnerability Studies on Reinforced Concrete Frames. *J. Struct. Eng.* 2011.137:367-378.

- NIST. (2011). Selecting and Scaling Earthquake Ground Motions for Performing Response-History Analyses. NIST GCR 11-917-15, Prepared by the NEHRP Consultants Joint Venture for the National Institute of Standards and Technology, Gaithersburg, Maryland.
- Baker J. Trade-offs in ground motion selection techniques for collapse assessment of structures. Vienna Congress on Recent Advances in Earthquake Engineering and Structural Dynamics 2013. Vienna, Paper No. 123
- Iervolino I., Galasso C., and Cosenza E., “REXEL: computer aided record selection for code-based seismic structural analysis,” Bull. Earthq. Eng., vol. 8, no. 2, pp. 339–362, Apr. 2010.
- Masi A. and Vona M., “Vulnerability assessment of gravity-load designed RC buildings: Evaluation of seismic capacity through non-linear dynamic analyses,” Eng. Struct., vol. 45, pp. 257–269, Dec. 2012.
- Jalayer F., et al. Bayesian Cloud Analysis: efficient structural fragility assessment using linear regression. Bulletin of Earthquake Engineering April 2015, Volume 13, Issue 4, pp 1183–1203.
- Tesfamariam et al. Probabilistic seismic demand model for RC frame buildings using cloud analysis and incremental dynamic analysis, Tenth U.S. National Conference on Earthquake Engineering Frontiers of Earthquake Engineering, At Anchorage, Alaska 2014.
- Ni P. P., et al., "Seismic Risk Assessment of Structures Using Multiple Stripe Analysis", Applied Mechanics and Materials, Vols. 226-228, pp. 897-900, 2012.
- Baker J. W., “Efficient Analytical Fragility Function Fitting Using Dynamic Structural Analysis,” Earthq. Spectra, vol. 31, no. 1, pp. 579–599, Feb. 2015.
- Vona M., “Fragility Curves of Existing RC Buildings Based on Specific Structural Performance Levels,” Open J. Civ. Eng., vol. 4, no. 2, pp. 120–134, 2014.
- CNR, Consiglio Nazionale delle Ricerche. (2013). CNR-DT 212/2013 - Istruzioni per la Valutazione Affidabilistica della Sicurezza Sismica di Edifici Esistenti (in italian). Rome.

- Milutinovic Z.V.and Trendafiloski G.S., WP4: Vulnerability of current buildings, in RISK-UE project. 2003.
- Braga F., M. Dolce e D. Liberatore, 1982. A statistical study on damaged buildings and an ensuing review of the M.S.K - 76 scale. 7th European Conference on Earthquake Engineering, Athens.

Chapter 8

8. Experimental validation: the 2016 Centre Italy earthquake

8.1. The seismic sequence and the damage suffered to the building stock

Experimental validation of the proposed rapid method has been possible, unfortunately, thanks to the seismic sequence that from August 2016 to January 2017 involved the Centre Italy causing a lot of damage in a large area. To this aim the damage occurred was detected also on RC high school building stock of the province of Macerata, being closer to the epicentres of the sequence than those of the province of Ancona. In fact, the school buildings belonging to the province of Macerata suffered larger intensity levels and consequently higher damage levels.

After strong earthquakes occurred in the recent past, many authors detected the performance (Augenti et al. 2004, Decanini et al. 2004, Ricci et al. 2011, Braga et al. 2011, Manfredi et al. 2013) and the damage on RC buildings with the aim to develop empirical fragility curves (De Luca et al. 2014, Del Gaudio et al. 2015, Del Gaudio et al. 2016) and damage scenarios (Liel et al. 2012, Verderame et al. 2014, Del Gaudio 2016).

Some authors also compared the damage detected after earthquakes with that estimated by means numerical investigations (Spence et al. 2003, Sabetta et al. 2013, Del Gaudio et al. 2017-a, Del Gaudio et al. 2017-b).

Fig. 8.1 shows the epicentre of the main events with a magnitude M_w higher than 5.5.

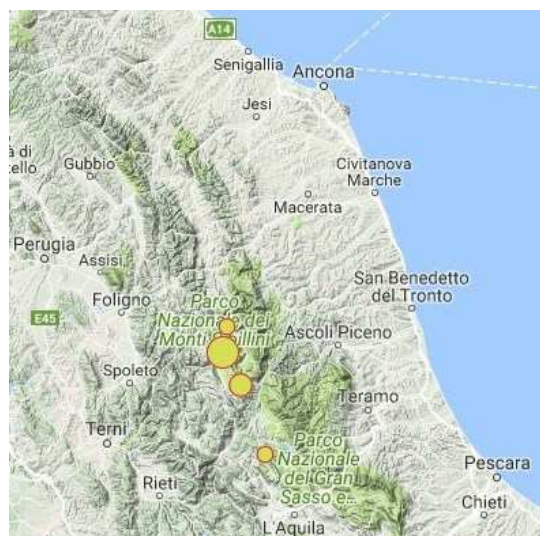


Figure 8.1. Epicentres of the main earthquakes occurred in Centre Italy
(font: <http://esm.mi.ingv.it>)

The epicentres are closer to the Macerata province, but also some cities of the Ancona province are not so far.

The first strong event of $M_w = 6.0$ occurred in the night of the 2016/08/24 with epicentre in Accumoli. It destroyed the cities of Amatrice, Accumoli and Pescara del Tronto and 299 people died.

The second events of maximum $M_w = 5.9$ occurred on the 2016/10/26 with epicentre in Ussita. It fortunately didn't cause death but increases damage level of buildings.

The strongest event of magnitude $M_w = 6.5$ occurred on the 2106/10/30 with epicentre close to Norcia, spreading damage in a large part of the Centre Italy.

The last events occurred on the 2017/01/18, when some earthquakes very close in time occurred in the area a North of L'Aquila. The maximum M_w was of 5.5 and the

Tab. 8.1 summarizes data relative to the main events of the Centre Italy 2016 sequence.

Table 8.1. Main events of the Centre Italy 2016 sequence

<i>Event date</i>	<i>Epicentre</i>	<i>Magnitude</i>	<i>Depth</i>	<i>Style of faulting</i>
2016/08/24	Accumoli	6.0	8.1	Normal
2016/10/26	Ussita	5.9	7.5	Normal
2106/10/30	Norcia	6.5	9.2	Normal
2017/01/18	Amatrice	5.5	9.1	Normal

During the largest magnitude events ($M_w = 6.0$ and $M_w = 6.5$) very high accelerations were recorded in areas closer the epicentre (fig. 8.2), maybe the highest never recorded in Italy.

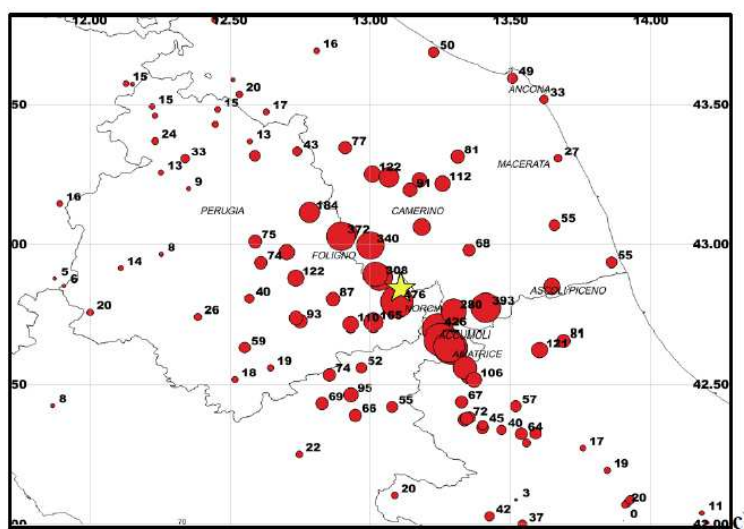


Figure 8.2. Recorded acceleration for the 2016/10/30 earthquake (font: INGV)

With regard the spectral accelerations, in fig. 8.3 are shown the spectra recorded to the stations of Amatrice (AMT) and Norcia (NRC) for 4 main events. It can be seen as in both stations the maximum values of $Sa(T)$ reached almost 2.0 g for the events occurred on the 2016/08/24 and 2016/10/30.

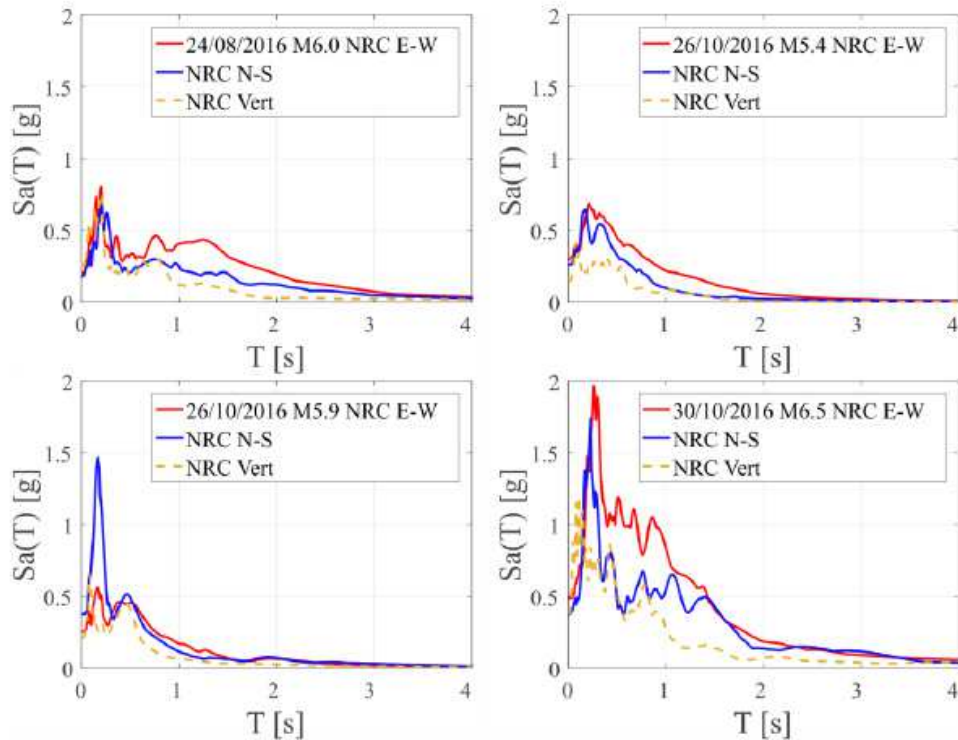


Figure 8.3. Pseudo-acceleration elastic response spectra recorded by the NRC station

Fig. 8.4 shows the comparison between the elastic spectra recorded to 4 closest stations with respect the epicentre for the 2016/08/24 event ($M_w = 6.0$) and the elastic spectra provided by the Italian seismic Code.

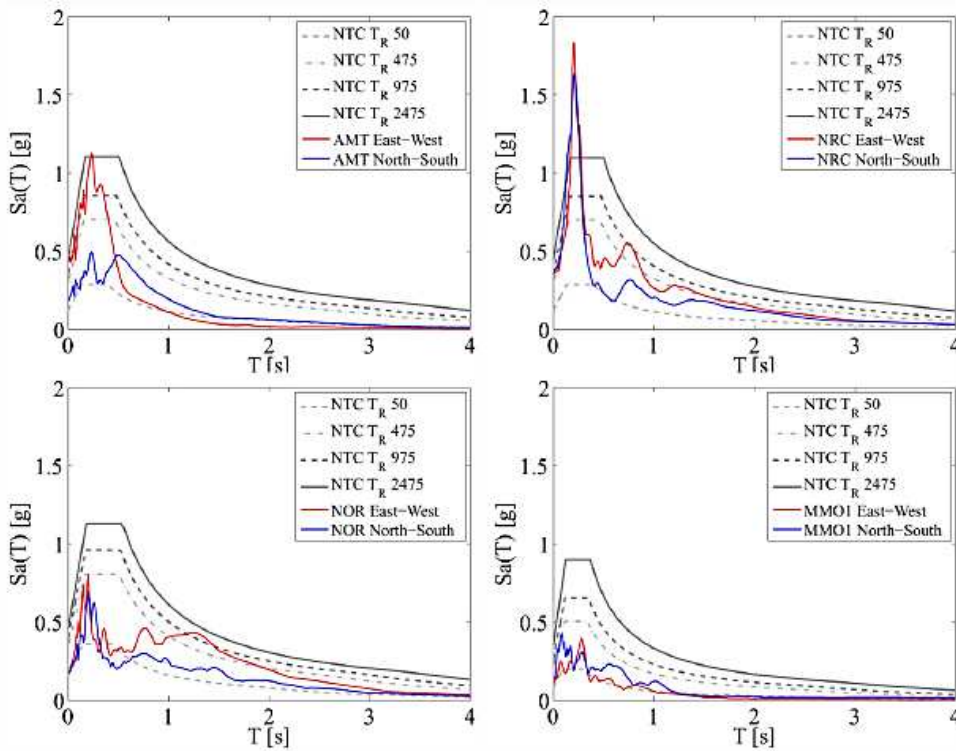
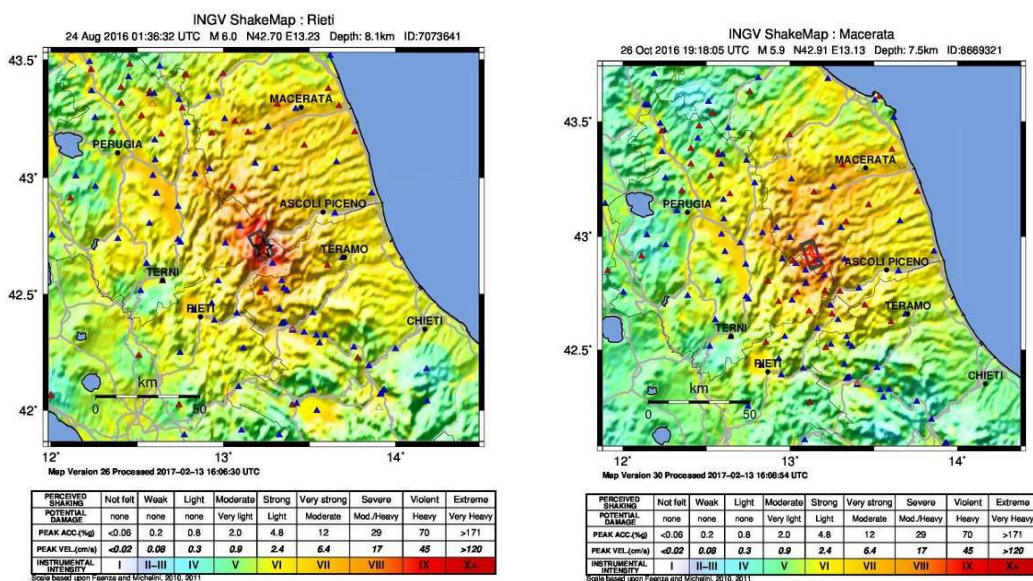


Figure 8.4. Comparison of four response spectra (horizontal components) recorded in the epicentral station with respect to the Italian code elastic response spectra at various return period

The MCS instrumental intensity shake maps provided by the INGV (*Michelini et al. 2008*) for these events are shown in fig. 8.5. They illustrate the spatial distribution of the macroseismic intensity and so also of the damage distribution.



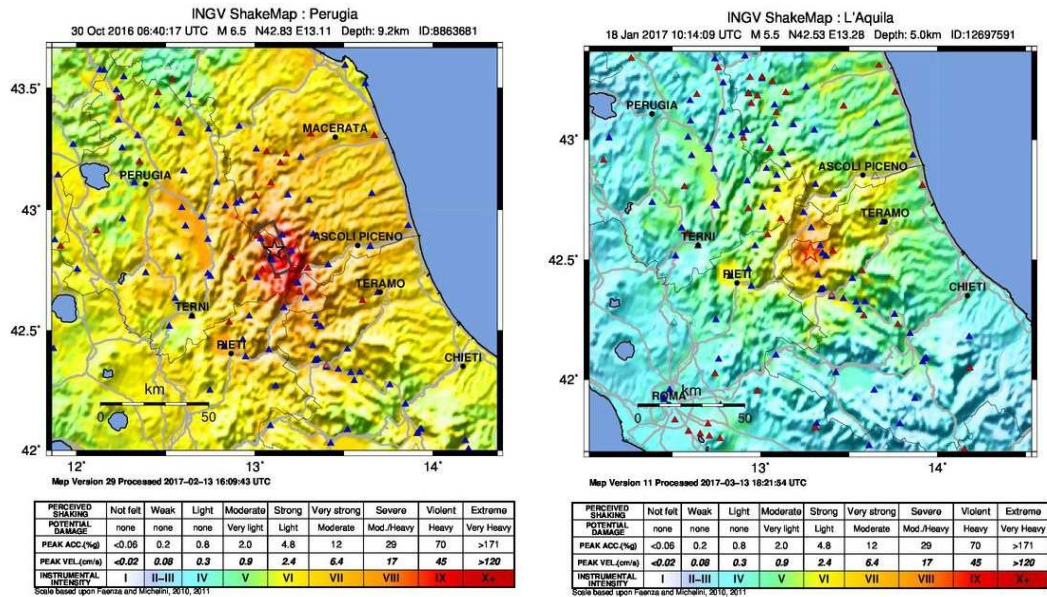


Figure 8.5. MCS instrumental intensity shake maps for the main Centre Italy earthquake (font: INGV)

It is worth noting the differences in colours indicate the zones with a higher or lower damage. The area closer to the epicentres reached a macroseismic intensity equal to IX and X.

For the area under investigation (Ancona and Macerata provinces) the strongest events produced a macroseismic intensity between VII and VIII for the Macerata province and V and VI for the Ancona Province.

Figs. 8.6, 8.7, 8.8 and 8.9 show the damage suffered from RC buildings due to the Centre Italy sequence.



Figure 8.6. Total collapse of buildings due to soft-storey mechanism in the municipalities of Amatrice (left) and Norcia (right)



Figure 8.7. Damage to the beam-column joint in the municipality of Amatrice



Figure 8.8. Short column effect in the municipality of Visso



Figure 8.9. Damage to masonry infills in the municipalities of Urbino (left) and Norcia (right)

In the following part, the damage assessment was done for the school building stock through the expeditious method proposed by the author and the results were compared with the damage surveyed.

Further some nonlinear dynamic analyses (NLDAs) were performed on a school building of the Macerata province, one of those shown in chapter 5 for the numerical validation of the proposed

vulnerability index method. The choice of this building is because it suffered both non-structural and structural damage.

8.2. Rapid damage estimation for the building stock

The Centre Italy seismic sequence was considered as a scenario to do an empirical validation of the vulnerability index method developed in this work.

To this aim the damage levels were estimated through the trilinear damage curves and compared with those actually occurred. For the main events in tab. the ground motion records close the school buildings were selected and the maximum PGA was assumed as seismic demand parameters.

The localization of the accelerometric stations in the area under investigation is shown in fig. 8.10.



Figure 8.10. Accelerometric stations in the area under investigation

It is worth noting that the spatial distribution of the stations is not good because it doesn't cover homogeneously the whole territory under consideration, thus the seismic demands for each school building are affected by high uncertainty. For the main events, the recorded accelerations in the stations of interest are shown in fig. 8.11.

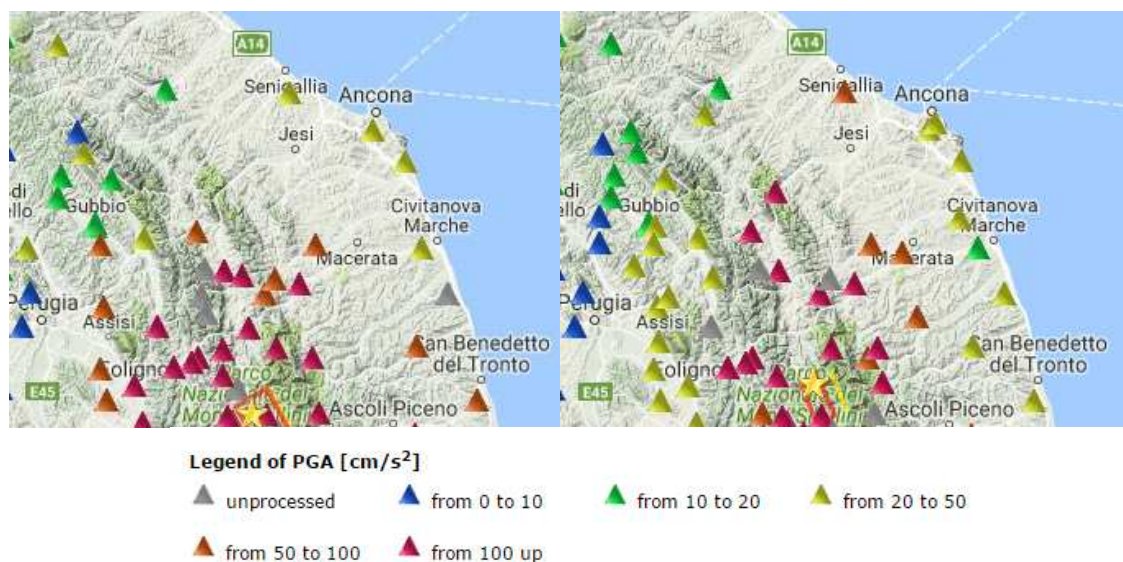


Figure 8.11. Recorded accelerations for the main events of the Centre Italy sequence 2016 (font: <http://esm.mi.ingv.it>)

The acceleration values considered for each city are the maximum recorded between the 4 events. When a station is very close to a city, its maximum PGA value was used, while when more stations are close to a city the weighted average values accounting for distance was assumed.

Tabs. 8.2 and 8.3 show the acceleration levels recorded closer as possible to the city under investigation, respectively for the province of Ancona and Macerata.

Table 8.2. Maximum recorded acceleration for cities of interest in the province of Ancona

<i>City</i>	<i>Event date</i>	<i>Station code</i>	<i>PGA [g]</i>	<i>Soil type (EC 8)</i>	<i>Topography</i>
<i>Ancona</i>	2016/10/30	ANB	0.049	B*	T1
<i>Arcevia</i>	2016/10/26	MMUR	0.102	A*	T1
<i>Fabriano</i>	2016/10/26	FBR	0.150	C*	T1
<i>Falconara M.</i>	2016/10/30	average	0.049	-	-
<i>Castelfidardo</i>	2016/10/30	average	0.041	-	-
<i>Chiaravalle</i>	2016/10/30	average	0.049	-	-
<i>Jesi</i>	2016/10/26	average	0.055	-	-
<i>Loreto</i>	2016/08/24	PP3	0.049	C*	T1
<i>Osimo</i>	2016/10/30	average	0.041	-	-
<i>Sassoferrato</i>	2016/08/24	average	0.126	-	-
<i>Senigallia</i>	2016/10/26	SNG	0.052		

Table 8.3. Maximum recorded acceleration for cities of interest in the province of Macerata

<i>City</i>	<i>Event date</i>	<i>Station code</i>	<i>PGA [g]</i>	<i>Soil type (EC 8)</i>	<i>Topography</i>
<i>Macerata</i>	2016/08/24	MCT	0.080	B*	T1
<i>Matelica</i>	2016/10/26	MTL	0.240	B	T1
<i>Recanati</i>	2016/08/24	PP3	0.049	C*	T1
<i>San Severino</i>	2016/10/30	SSM1	0.098	B*	T1
<i>Sarnano</i>	2016/10/30	SNO	0.114	B*	T1

The damage detected after the seismic sequence for each school of the Ancona and Macerata province, provided a general situation of no damage except for few buildings in which non-structural damage was found. It is mostly a damage on partition walls that detached from the RC frames.

However, in some school buildings of the Macerata province, closer to the epicentres of the seismic sequence, the non-structural damage reached the moderate and heavy level, while the structural damage reached the slight and moderate levels (D3 and D4). In one case, the structural damage can be classified as moderate because cracks on column tops and in the end parts of beams were found. This agrees with the recorded acceleration level that are higher for the area of the Macerata province.

Fig. 8.12 shows the detected building losses for the school building stock of the Province of Ancona and Macerata.

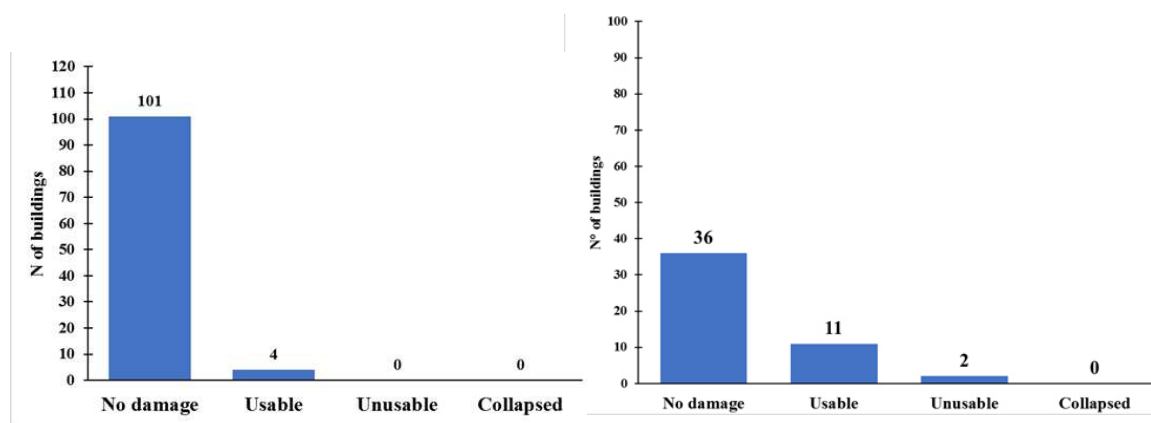


Figure 8.12. Detected physical losses (number of buildings): Province of Ancona (left) and Macerata (right)

Thus, in the province of Ancona none school suffered a damage level that implied the unusable or collapse, while in the province of Macerata some schools suffered moderate and heavy structural and non-structural damage.

The damage suffered from some RC school buildings within the area affected by the Centre Italy 2016 seismic sequence is illustrated in figs. 8.13, 8.14 and 8.15 with respect the structural damage and in figs. 8.16 and 8.17 with respect non-structural damage.

Damage to structural elements



Figure 8.13. Damage to beam-column joints



Figure 8.14. Short column effect



Figure 8.15. Strong beam-weak column effect

Damage to non-structural elements



Figure 8.16. Damage to partition walls



Figure 8.17. Damage to masonry infills (left) and to roof eaves (right)

With regard human losses, fortunately nobody died or injured, also because the strongest earthquakes happened when the schools were closed. While the occurred economical losses are not known from the author.

The estimation of the damage levels for both building stocks was done by using the trilinear damage curves developed by the author and the seismic demands in terms of maximum PGA recorded closer to each school building. Fig. 8.18 show the building losses, in terms of number of schools, for the building stock of the Ancona and Macerata province.

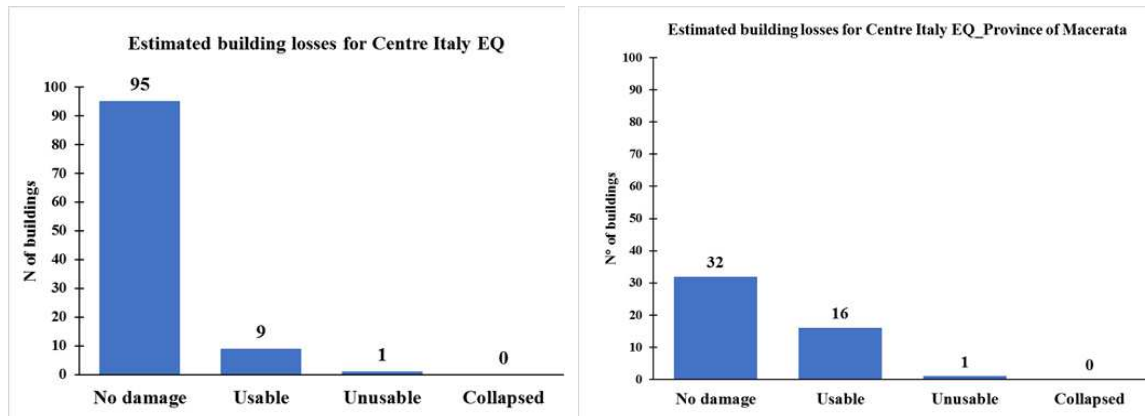


Figure 8.18. Estimated physical losses (number of buildings): Province of Ancona (left) and Macerata (right)

The estimation of casualties and injuries by using the Hazus, Bramerini and Coburn and Spence methods provided in all cases no death and injured.

The estimated economical loss amount to 4.800.000 € for the province of Ancona, equal to the 2.2 % of the entire rebuilt cost of the building stock, and 4.200.000 € for the province of Macerata, equal to the 0.05 % of the entire rebuilt cost.

In general, the rapid damage estimation provides a good agreement between the damage detected. In the following is shown the comparison with damage estimated through non-linear analysis on a case study.

8.3. Analytical damage estimation for a case study

The seismic response and the damage caused from the Centre Italy seismic sequence for a school building is analyzed more in depth through pushover and NLDAs.

The case study (fig. 8.19) is one already analyzed in chapter 7 for the numerical validation of the vulnerability index method proposed by the author. It is located in Macerata and from the survey of the damage suffered after the seismic sequence, it can say that it suffers slight non-structural damage on partition walls (fig. 8.19).

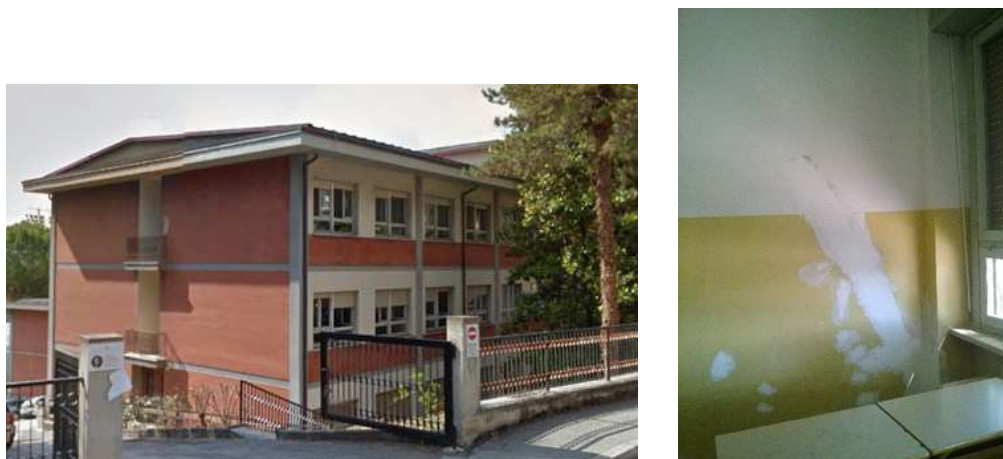


Figure 8.19. ITC Macerata: Lateral view (left) and slight damage on partition walls (right)

Thus, a damage level corresponding about to DL1 of the EMS-98 scale (*Grunthal 1998*) was assigned and the building was declared usable.

Tab. 8.4 shows the relations assumed between the damage levels of the EMS-98 scale, the damage states or performance levels usually provide by seismic Code and the damage index values provided by (*Bramerini et al. 1995*).

Table 8.4. Correlation between EMS-98 damage levels, damage index and replacing cost

Dk	Description	DI Bramerini	Condition	% cost of replacing (L'Aquila)
DL0	No damage	0.00 – 0.01	Usable	0.00
DL1	Slight	0.01 – 0.10		0.07
DL2	Moderate	0.10 – 0.35	Usable with intervention	0.15
DL3	Heavy	0.35 – 0.75		0.50
DL4	Very heavy	0.75 -1.00	Unusable	0.80
DL5	Collapse	> 1.00	Collapsed	1.00

Assuming the maximum acceleration recorded from the stations closer the school building under investigation, that is equal to 0.118 g, the estimated damage index by means the trilinear damage curve (fig. 8.20) from the proposed method ($PGAs = 0.127$ g and $PGAc = 0.429$ g) is equal to 0.

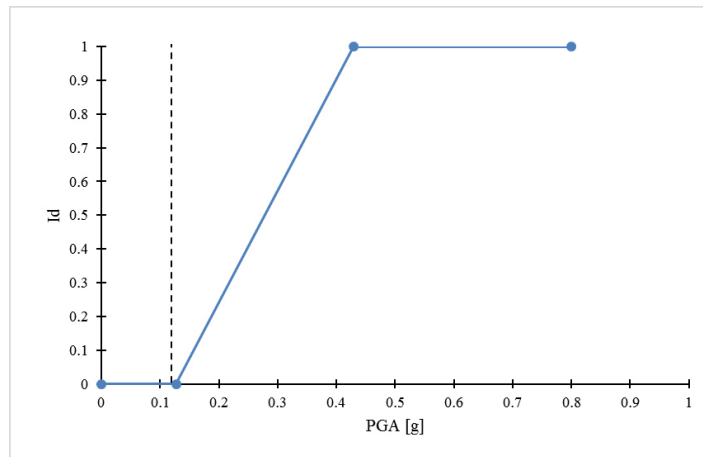


Figure 8.20. Estimation of damage from trilinear curve: demand in terms of PGA

Thus, according to tab. the damage level is DL0.

It doesn't correspond to the occurred one, because a slight damage occurred on non-structural elements. However, the recorded PGA from the stations could be lower than to one occurred where the school building is located. Further this way to estimate damage doesn't take into account the dynamic response of the structure, while the damage estimation through pushover analyses, by comparing capacity and demand in the ADRS plane, and through NLDAs allow to consider the dynamic effects due to earthquake.

Thus, also the trilinear damage curve in terms of spectral acceleration is developed (fig) and the damage estimated taking into account the maximum spectral value for the fundamental vibration period T_1 of the building, calculated through the eq. 8.1:

$$T_1 = 0.075 H^{3/4} \quad (8.1)$$

And it is equal to 0.45 s.

The response spectra relative to the ground motion records are shown in fig. 8.21 with the vertical line for the fundamental period.

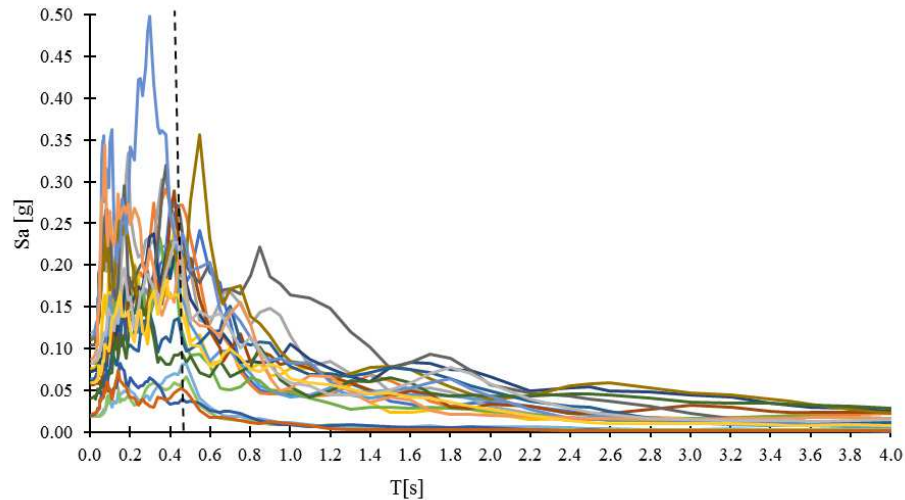


Figure 8.21. Estimation of spectral acceleration from the main ground motion of Centre Italy 2016 sequence

The maximum spectral acceleration is equal to 0.22 g.

The capacity in terms of $S_a(T)$ was calculated from PGA through the simplified relationship provided by (Dolce et al. 2005), that assume the spectral acceleration value coming from a linear static analysis (eq. 8.2)

$$S_{a,C}(T1) = \frac{PGA_C * \alpha_{PM} * \alpha_{AD} * \alpha_{DT}}{q} \quad (8.2)$$

- α_{PM} is the modal participation coefficient (T/T_c), which is assumed, in a simple way, to be 1.0 for buildings with only one storey and 0.8 in other cases.
- α_{AD} is the spectral amplification coefficient and is assumed to be 2.46.
- α_{DT} is a coefficient that takes into account dissipative phenomena. If the resistant contribution of infills is significant with respect to that of main resistant system and is considered in the analysis, α_{DT} assumes unitary value, otherwise if such contribution is ignored α_{DT} is equal to 0.80.
- q is the behaviour factor assumed equal to 2.

Thus, we have:

$$S_a(T1)_i = 0.178 \text{ g}$$

$$S_a(T1)_u = 0.600 \text{ g}$$

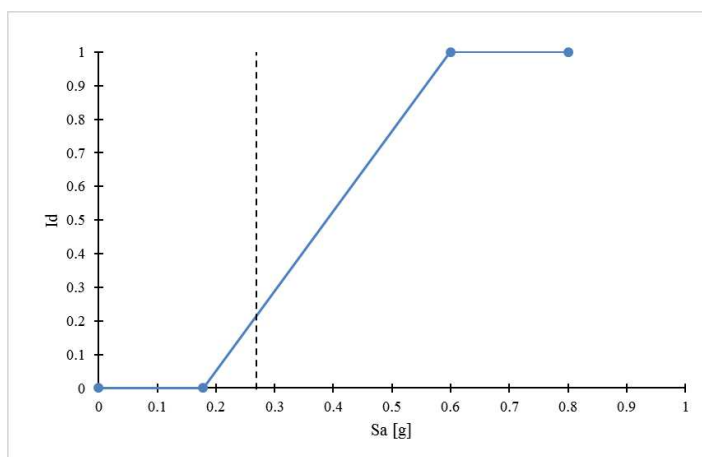


Figure 8.22. Estimation of damage from trilinear curve: demand in terms of spectral acceleration

The DI value is equal to 0.10 and so the estimated damage level according to tab. is DL1 (slight), that agrees with the damage occurred.

8.3.1. Non-linear dynamic analysis (NLDA)

Several NLDA were performed by using as seismic input the ground motion recorded in stations closer to the school building (fig. 8.23) for the main events of the seismic sequence in Centre Italy.



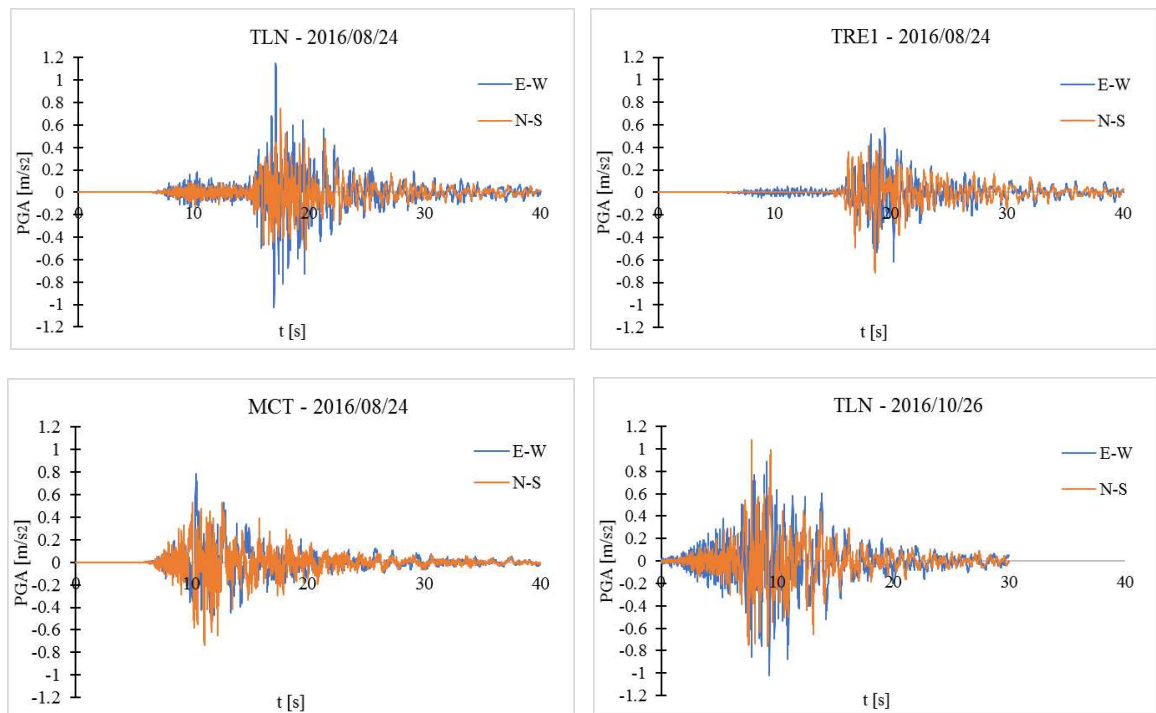
Figure 8.23. Reference stations for records selection

Tab. 8.5 shows data for these records.

Table 8.5. Maximum accelerations recorded from the stations closer to the school under investigation

<i>Event date</i>	<i>Station code</i>	<i>max PGA [m/s²]</i>
2016/08/24	MCT	0.082
2016/08/24	TLN	0.118
2016/08/24	TRE1	0.073
2016/10/26	MCT	0.073
2016/10/26	TLN	0.110
2016/10/26	TRE1	0.060
2016/10/30	TLN	0.114
2016/10/30	TRE1	0.083
2017/01/18	MCT	0.019
2017/01/18	TLN	0.021

Fig. 8.24 shows the records for the stations considered.



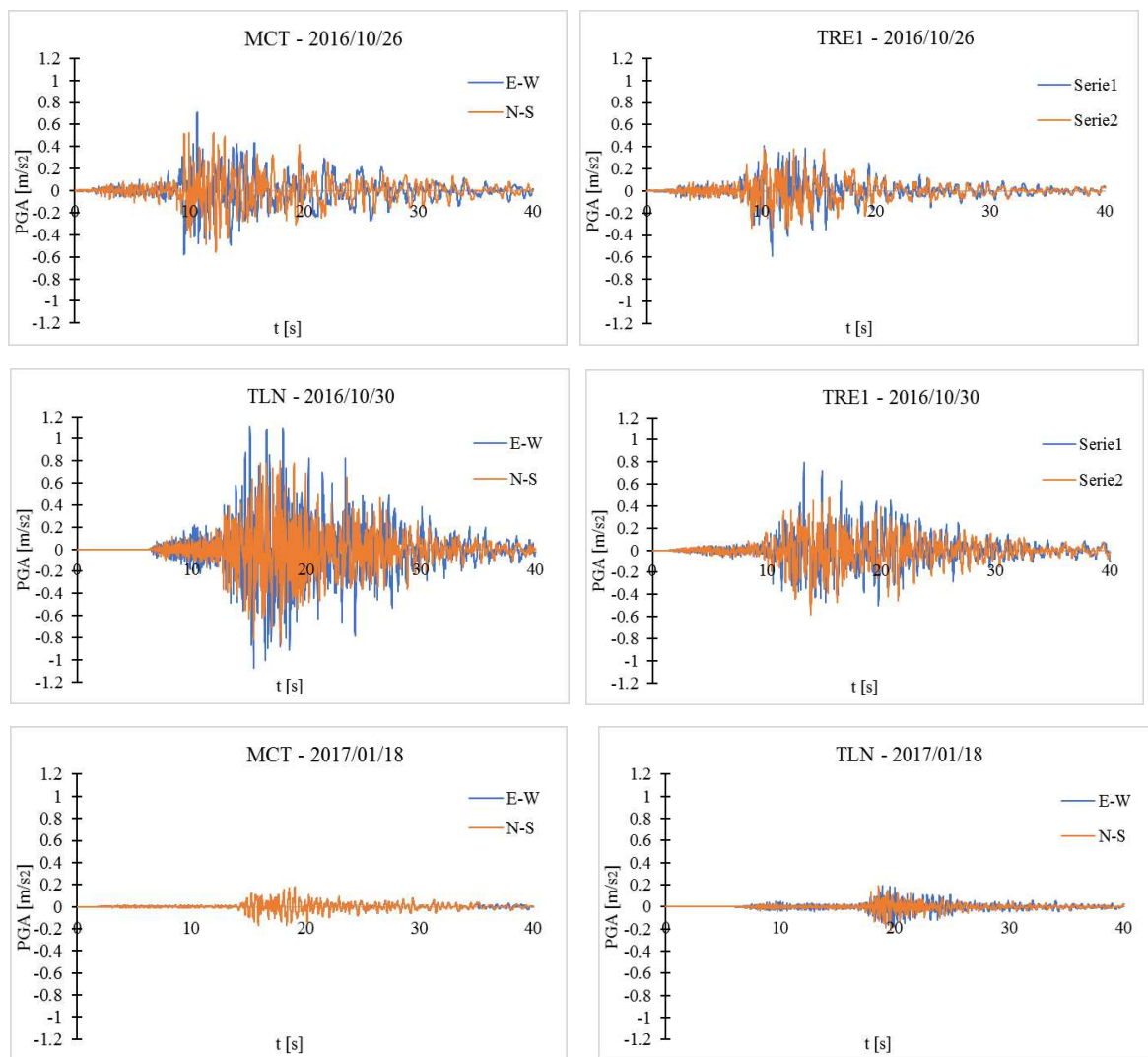


Figure 8.24. Accelerograms recorded close to the school building under investigation during the Centre Italy 2016 seismic sequence

The structural model was developed by using unidimensional elements for columns and beams and diagonal struts for masonry infills. The stairs were considered in the model by mean plate elements. Deformable slabs were considered for the three storeys and fixed nodes were assumed at the foundation level.

Referring to the nonlinear behaviour the lumped plasticity method was used and the following assumption were done:

- plastic hinges for columns are PMM type, accounting for interaction between axial load and bending moments, while no interaction is considered for beams. Diagonal struts have only the axial plastic hinge.
- Modified Takeda model for flexure and shear hysteretic behaviour, with stiffness reduction ratios α_1 and α_2 equal to 0.5 and 0.1 respectively.

- Kinematic hardening model for the axial hysteretic behaviour.

Time history load cases were applied accounting for dead loads, live loads in a percentage suggested by the Code for the seismic combination and the records of the ground motions considered.

Direct integration of the ground motion according to *Newmark method* with $\gamma = 0.5$ and $\beta = 0.25$, and modal damping equal to 5 % for all modes were adopted.

The results in terms of absolute maximum interstorey drift ratio (figs.8.25 and 8.26) allow to estimate the damage suffered through the relations between the drift ratio and the damage state for RC frames building shown in tab. 8.6.

It can be noted as in the X direction the maximum drift occurs at the third level for all simulations, with a higher value of about 0.25 %.

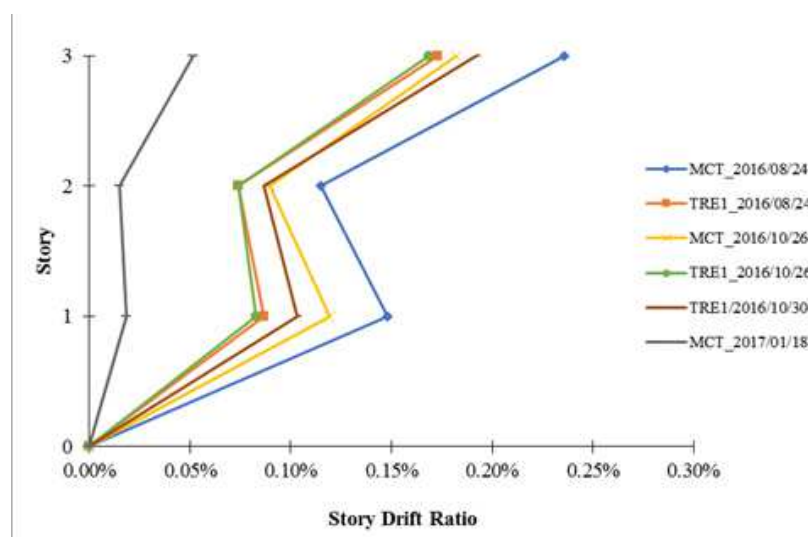


Figure 8.25. Maximum IDR in the X direction

Also in the Y direction, the maximum drift is at the last floor for all the simulation, with a higher value of about 0.25 %.

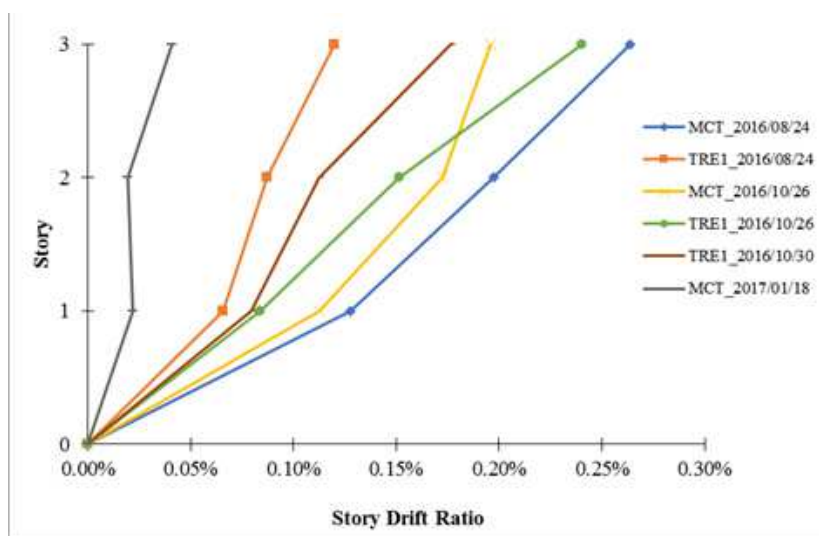


Figure 8.26. Maximum IDR in the Y direction

The adopted interstorey drift thresholds for the damage states are shown in tab. 8.6. according to (Ghobarah 2004).

Table 8.6. IDR thresholds for damage states of Non-ductile RCMF structures

	DL0	DL1	DL2	DL3	DL4	DL5
<i>Ghobarah 2004</i>	< 0.1 %	< 0.2 %	< 0.5 %	< 0.8 %	< 1.0 %	> 1.0%

Thus, the maximum IDR obtained from NLDSs (0.3%) was compared with the threshold values for the damage states and so the DL1 was assigned.

This result agrees with those obtained from the rapid method and the damage occurred.

8.3.2. Pushover analysis

The pushover analyses performed are described in chapter 5 for the building under investigation. To estimate damage, the comparison in the ADRS plane between the seismic demands from the several ground motions and the structural capacity in terms of SDOF equivalent bilinear capacity curve was done.

In fig. 8.27 the ADRS format for the same records of the Centre Italy earthquakes used for NLDAs is illustrated.

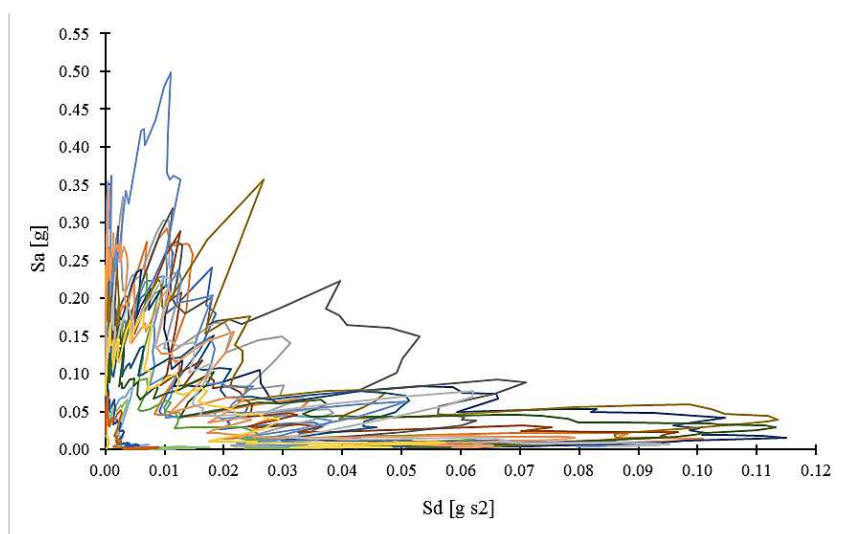


Figure 8.27. Selected records in ADRS format

The average bilinear curve obtained from the pushover analyses (see chapter 5) was overlapped to the demand spectra in ADRS format (fig. 8.28), so that the performance point can be calculated.

The yield and the ultimate points of the average bilinear curve have displacement of 4.0 cm and 7.2 cm respectively and the same spectral acceleration of 0.176 g.

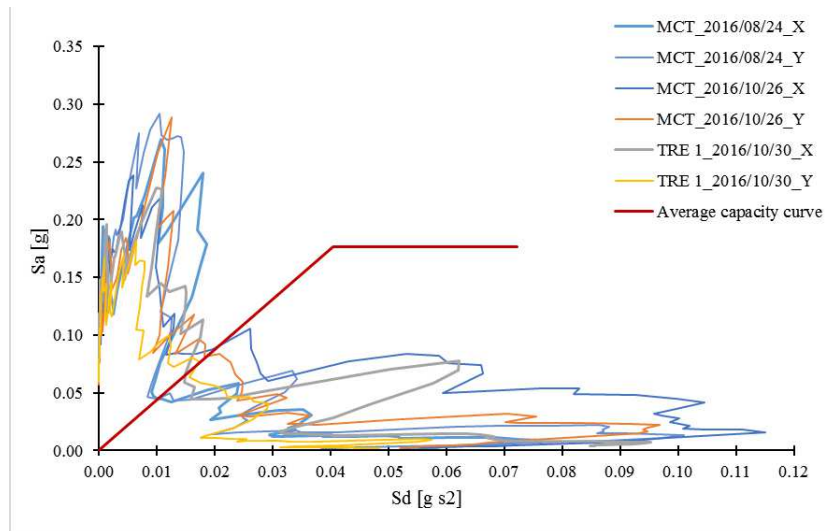


Figure 8.28. Determination of the maximum displacement demand

The performance point provided from the strongest demand spectrum (TLN_2016/10/30/_X) gives a displacement about equal to the yield point (4.0 cm).

Consequently, the probability to suffer each damage level for the calculated performance point can be obtained from the fragility curves in terms of displacement.

Analytical fragility curves were developed (please see chapter 3) from the average bilinear curve of the eight pushover analyses performed (fig. 8.29) and assuming the following relationship between the thresholds of the displacement capacity for the SDOF and the four damage states (Vacareanu et al. 2004):

$$DS1 = 0.7 dy$$

$$DS2 = dy$$

$$DS3 = dy + 0.5 (du - dy)$$

$$DS4 = du$$

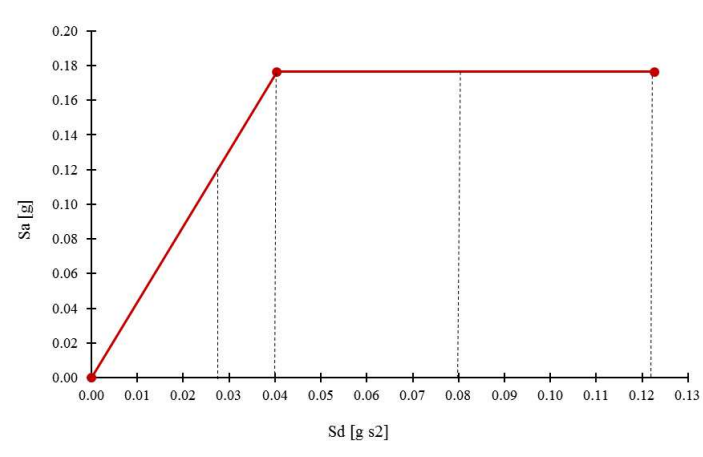


Figure 8.29. Damage states thresholds on the average bilinear curve

The fragility curves for the damage states DS_k are shown in fig. 8.30 with the vertical line for the target displacement.

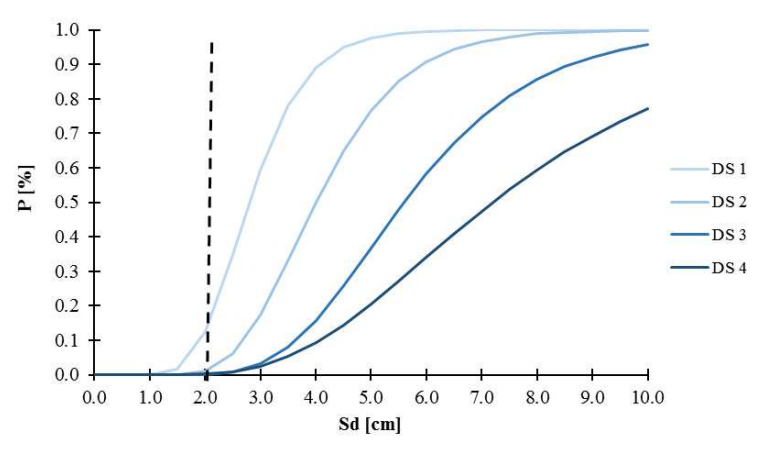


Figure 8.30. Fragility curves for the DS_k

Thus, the damage index DI can be estimate through the relationship n. 3.4. In this case the DI value is equal to 0.03, thus a damage state equal to DL1 (slight) is assumed according to tab. 8.4.

Summarizing, the estimated damage level is DL0 from the rapid method, while it is DL1 from both pushover analysis and NLDA. This difference in results could be due to the relations, proposed in the Risk-UE project, used to calculate the values for both threshold displacements $S_{d,ds}$ and standard deviations β_{ds} relatively to the fragility curves of the damage states.

Generally, the validation done by comparing the damage occurred on the case study with those estimated from both nonlinear analyses and the rapid method proposed by the author, gives good results.

The method proposed by the author provides the best result when it considers the spectral acceleration in terms of both capacity and demand, instead the PGA, because in this way the dynamic effects due to seismic excitation are accounted.

Of course, many uncertainties should affect damage estimation such as those in structural modelling, in structural response (i.e. interstorey drift ratio), in the definition of the damage states thresholds in terms of spectral displacement on the mean bilinear curve, in the damage scales employed etc.

References chapter 8

- Augenti N. et al. Performance of School Buildings during the 2002 Molise, Italy, Earthquake. *Earthquake Spectra*, Volume 20, No. S1, pages S257–S270, July 2004.
- Decanini L. D., De Sortis A., Goretti A., Liberatore L., Mollaioli F., Bazzurro L. (2004) Performance of reinforced concrete buildings during the 2002 Molise, Italy, earthquake. *Earthquake Spectra* 20(S1):S221–S255.
- Ricci P, De Luca F., and Verderame, G.M., (2011), “6th April 2009 L'Aquila earthquake, Italy: reinforced concrete building performance”, *Bull. Earthquake Eng.*, 9, 285-305.
- Braga F., Manfredi V., Masi A. et al. Performance of non-structural elements in RC buildings during the L'Aquila, 2009 earthquake. *Bull Earthquake Eng* (2011) 9: 307.
- Manfredi G., Prota A., Verderame G.M., De Luca F., Ricci P., (2013). 2012 Emilia earthquake, Italy: Reinforced Concrete buildings response, *Bulletin of Earthquake Engineering* (under review).
- De Luca F. et al. Analytical versus observational fragilities: the case of Pettino (L'Aquila) damage data database. *Bulletin of Earthquake Engineering* 13(4). April 2014.
- Del Gaudio C., Ricci P., Verderame G.M., Manfredi G., 2015. Development and urban-scale application of a simplified method for seismic fragility assessment of RC buildings. *Engineering Structures*, 91, 40-57.
- Del Gaudio C., De Martino G., Di Ludovico M., Manfredi G., Prota A., Ricci P. and Verderame G. M. (2016). "Empirical fragility curves from damage data on RC buildings after the 2009 L'Aquila earthquake." *Bull. Earthq. Eng.*, 15(4), 1425-1450.
- Liel A.B., Lynch K.P., Vulnerability of Reinforced-Concrete-Frame Buildings and Their Occupants in the 2009 L'Aquila, Italy, Earthquake, *Natural Hazards Review*, Feb, 11-23, 2012.

- Verderame G.M., et al. Damage scenarios for RC buildings during the 2012 Emilia (Italy) earthquake. *Soil Dynamics and Earthquake Engineering* Volume 66, November 2014, Pages 385-400.
- Del Gaudio C. et al. First remarks about the expected damage scenario following the 24th August 2016 earthquake in central Italy. 16th World Conference on Earthquake, 16WCEE 2017 Santiago Chile, January 9th to 13th 2017 Paper N° 5005.
- Spence R., Bommer J.J., Del Re D., Bird J., Aydinoglu N., Tabuchi S. “Comparison Loss Estimation with Observed Damage: A study of the 1999 Kocaceli Earthquake in Turkey”. *Bulletin of Earthquake Engineering*, 2003; Vol. 1, pp: 83-113.
- Sabetta F., Speranza E., Borzi B., Faravelli M. (2013) -Scenari di danno empirici e analitici a confronto con recenti terremoti italiani. 32° National Conference GNGTS, Trieste, Vol. 2, 136-141.
- Del Gaudio C. et al. A class-oriented large-scale comparison with post-earthquake damage for Abruzzi region. *COMPDYN 2017 - 6th ECCOMAS Thematic Conference on Computational Methods in Structural Dynamics and Earthquake Engineering*, At Rhodes Island, Greece.
- Del Gaudio C. et al. A single-building comparison with observed post-earthquake damage: the case study of L’Aquila municipality. 16th World Conference on Earthquake, 16WCEE 2017 Santiago Chile, January 9th to 13th 2017 Paper N° 4155
- Michelini A., Faenza L., Lauciani V. and Malagnini L. (2008). ShakeMap implementation in Italy. *Seismological Research Letters* 79.5: 688-697.
- Grunthal G. “European Macroseismic Scale”. Centre Européen de Géodynamique et de Séismologie, Luxembourg 1998; Vol. 15.
- Bramerini F., Di Pasquale G., Orsini G., Pugliese A., Romeo R., Sabetta F., “Rischio sismico del territorio italiano. Proposta per una metodologia e risultati preliminari”. SSN/RT/95/01, Rome, 1995 (In Italian).

- Dolce M., Moroni C., 2005. La valutazione della vulnerabilità e del rischio sismico degli edifici pubblici mediante le procedure VC e VM. Progetto SAVE, Atti di Dipartimento N. 4/2005.
- Ghojarah A. “On Drift Limits Associated with Different Damage Levels,” Proceedings of International Workshop on Performance-Based Seismic Design, Department of Civil Engineering, McMaster University, Bled, 28 June-1 July 2004.
- Vacareanu R., Lungu D., Aldea A., and Arion C.: WP07 Report. Seismic Risk Scenarios Handbook, Risk-UE Project, Bucharest, 50 pp., 2004.

Chapter 9

9. Rapid damage scenario for the building stock

Damage scenarios due several seismic events have been developed for the school building stock belonging to the province of Ancona (105 buildings) and the province of Macerata (41 buildings). The starting points are the results in terms of vulnerability come from the rapid methods, such as the macroseismic one and the vulnerability index method. Then taking into account the seismic hazard for each school buildings, the losses in terms of physical damage (number of buildings in each damage state), economic (total rebuilding costs) and casualties and injuries.

Many authors have developed risk scenarios for population of buildings at different scales, as cities (*Facciolli et al. 1999, Dolce et al. 2000, Spence et al. 2006, Marulanda et al. 2013*), regions (*Meroni et al. 2008, Asteris et al. 2016, D'Amico et al. 2015*) and entire countries (*Di Pasquale et al. 2005, Zuccaro et al 2009*), by using the several frameworks available in literature (please see chapter 3). The seismic hazard can be defined in terms of different parameters (PGA, spectral acceleration) and determined by deterministic or probabilistic methods. Both approaches require the identification of seismogenic areas that affect the seismicity of the site and the definition of appropriate attenuation laws.

- *Deterministic Seismic Hazard Assessment (DSHA)*: it does not provide any indication on the probability of occurrence of a reference earthquake and on the effect of uncertainties. The hazard parameter is obtained on the basis of the several scenarios depending on the various seismic sources.
- *Probabilistic Seismic Hazard Assessment (PSHA)*: it does not provide indications on the reference earthquake and on the magnitude-distance pairs that allow to define the expected scenario. The hazard parameter is expressed in terms of probability of exceedance at the site in a predetermined time interval.

It is obtained by means a standard probabilistic approach (*Cornell 1968*), that cumulates the effects of all potential sources in the area under investigation and produces maps representative of the seismic input level expected in each point for several return periods.

Generally, the best choice is to use both approaches in an integrated fashion (PSHA disaggregation, *Bazzurro et al. 1999*).

When specific seismic events are selected (*deterministic approach*), we have a *scenario analysis* instead of a *risk analysis*, because in the latter case all the possible seismic sources and so a very large number of events are considered (*probabilistic approach*). The former is better for preventions purpose, thus to project interventions for risk mitigation, while the latter is better to project the emergency management after an earthquake occurs.

According to the definitions above, here both scenario and risk analyses are proposed, accounting for each building of the vulnerability curves $I-\mu_d$, from the macroseismic method, and the trilinear damage curves $PGA - Id$, from the vulnerability index method proposed (please see chapter 6).

In particular “*uniform hazard scenarios*” and “*epicentre-distance scenarios*” were developed.

1. In the *uniform hazard scenarios*, the macroseismic intensity and the PGA values were selected for each city in which the school buildings are located.

In the first case was selected the maximum historical event, obtained from the earthquake catalogue (CPTI). Also, macroseismic intensity computed from PGA by using the correlation law proposed from Margottini, in which the PGA values are provided by the hazard curve for the site, accounting for the site amplification effect due to the soil type and topography.

Then, to estimate losses from the trilinear damage curves $PGA - DI$ developed in chapter 6, both PGA and $S_a(T)$ were employed as seismic demand parameters (to highlight the differences in the results when the vibration period is considered), assuming values from the hazard map of Italy relative to increasing return periods of the seismic events.

To consider also the parameter $S_a(T)$, the conversion of the trilinear damage curves according to this parameter needed. Thus, the capacity in terms of $S_a(T)$ was calculated through the simplified relationship of eq. 8.2.

2. In the *epicentre-distance scenarios*, some events are selected on the base of the active fault system of the region, thus fixing a magnitude level, a hypocentre depth and an epicentral distance. The PGA values and were calculated for each zone of interest through an attenuation law (*Sabetta e Pugliese 1987*).

9.1. Seismic hazard of the region

The area under investigation is historically a seismic region. In the centuries several strong earthquakes occurred, the last seismic sequence is very recent dating from August 2016 to January 2017 (please see chapter 8 for a more depth discussion of this topic).

Fig. 9.1 shows the maximum observed macroseismic intensities for Italy and for the area under investigation.

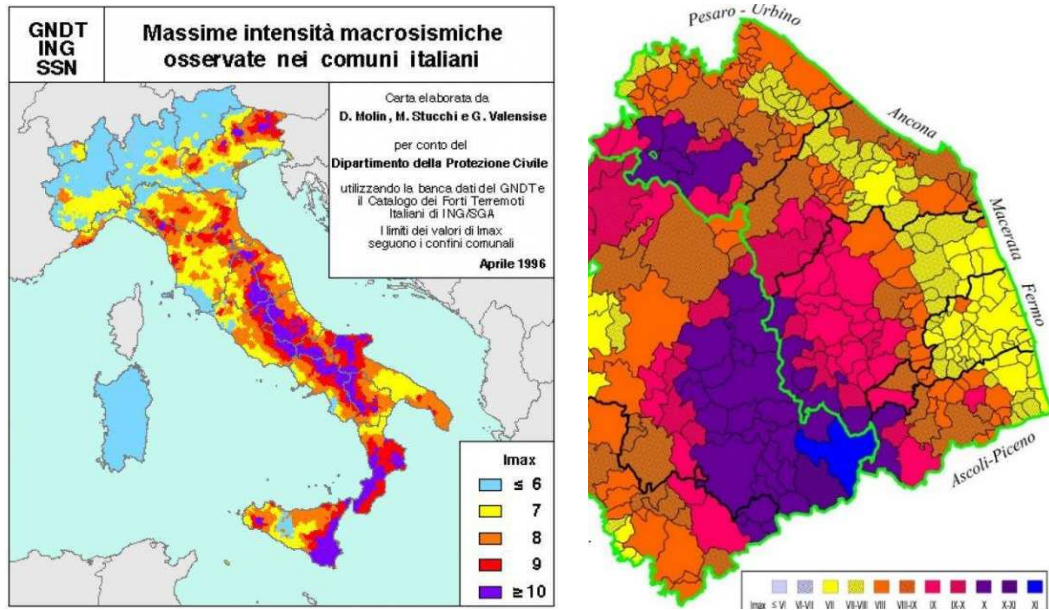


Figure 9.1. Maximum observed macroseismic intensities

In the past there have been events of intensity even of IX and X in some of the cities of interest. The main cause of the earthquakes in Italian territory is the relative movement between the Eurasian and African plaques (fig. 9.2), which is creating a stretch of the Apennine dorsal.

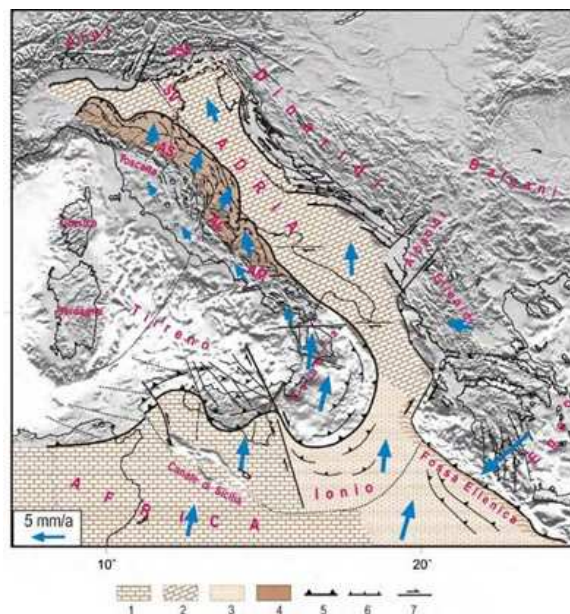


Figure 9.2. Tectonic movement that affects Italy

Active fault systems are shown in fig. 9.3 for the entire Italian territory and specifically for the area of interest. The latter has two main fault systems, one affecting the Adriatic coastline and the other the Apennines.

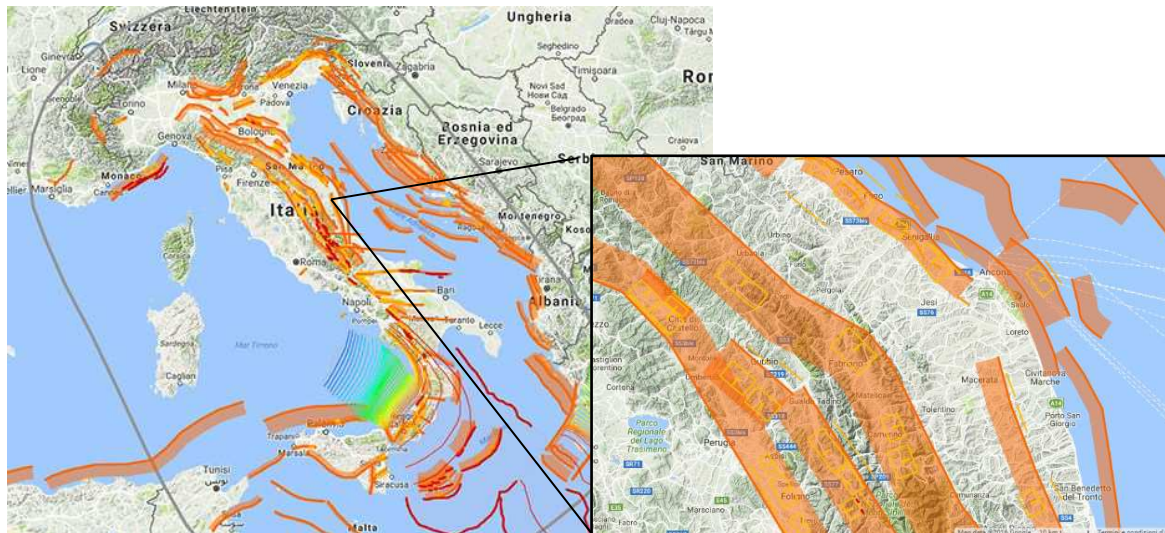


Figure 9.3. Fault system in Italy and in the Region of interest

The fault system of the Apennines area could generate earthquakes with a maximum magnitude of 7.0, while those relatives to the Adriatic coast could generate magnitude max 6.0 events.

Fig 9.4 shows a map with the major earthquakes for Italy (*font: CPTI15 - Parametric Catalogue of Italian Earthquakes v.15 (Rovida et al. 2016)*).

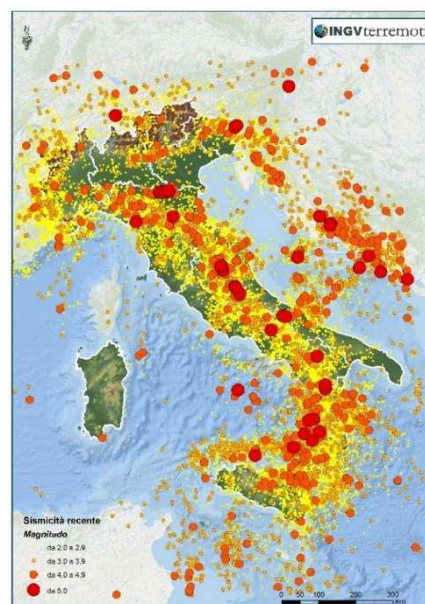


Figure 9.4. Major earthquakes occurred in Italy

For the purposes of determining the seismic hazard of the site for each school building, reference has been made to the seismic classification of the territory adopted by the in force Italian seismic Code (*NTC 2008*), carried out by a probabilistic analysis (PSHA) based on the observation of active faults and on the statistical study of past earthquakes (please see chapter 3 for a more depth description).

The Hazard map provides a basic hazard expressed by the following parameters for each node of the 5x5 Km grid and for nine values of the probabilities of exceedance in 50 years:

ag: maximum acceleration on rigid horizontal soil

F0: maximum value of the amplification factor

T_c^* : corner period at which begin the constant velocity part of the spectra

The relative values are provided for the 50^o, 16^o and 84^o percentile to take into account epistemic uncertainty in seismic input. From these, it is possible to obtain the response spectra by appropriate relationships provided by the regulations for the calculation of the corner periods (T_B , T_C , T_D) and of the spectral ordinates.

The map below (fig. 9.5) shows the hazard in terms of acceleration on rigid soil, at 50^o percentile and for a return period of 475 years, in the area of interest. A medium-high base hazard is provided, as the municipalities belonging to the provincial territory have an acceleration oscillating between 0.15 g and 0.25 g (most of them have about 0.18 g).

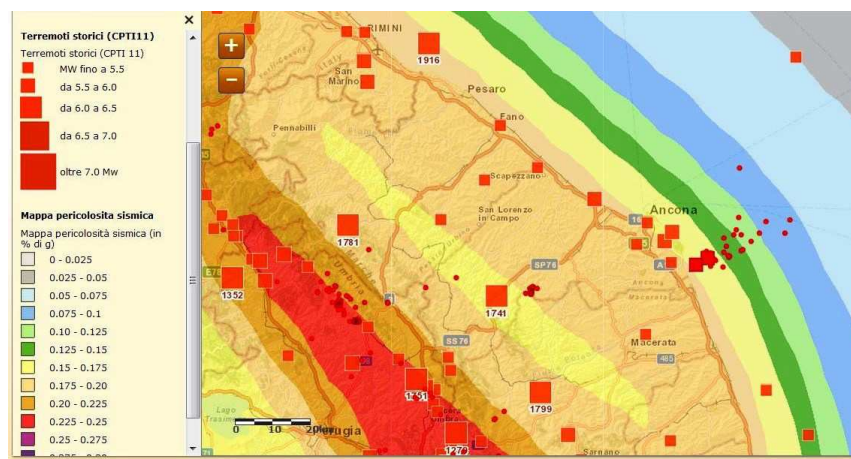


Figure 9.5. Hazard map for the region of interest and main historical events

Tabs. 9.1 and 9.2 provide the maximum expected acceleration on rigid soil relative to the 50^o percentile for the municipalities of interest, with regard several probabilities of occurrence in 50 years.

Table 9.1. Maximum PGA on rigid soil for several probabilities of occurrence in 50 years_Province of Ancona

City	ag [g]				
	P_{vr}	5%	10%	63%	81%
<i>Ancona</i>		0.234	0.179	0.059	0.044
<i>Arcevia</i>		0.225	0.174	0.071	0.056
<i>Castelfidardo</i>		0.237	0.183	0.061	0.048
<i>Chiaravalle</i>		0.237	0.183	0.062	0.048
<i>Fabriano</i>		0.233	0.183	0.078	0.062
<i>Falconara M.</i>		0.236	0.182	0.060	0.047
<i>Jesi</i>		0.246	0.185	0.066	0.052
<i>Loreto</i>		0.236	0.181	0.060	0.046
<i>Osimo</i>		0.237	0.183	0.062	0.048
<i>Sassoferrato</i>		0.226	0.175	0.073	0.058
<i>Senigallia</i>		0.238	0.183	0.062	0.048

Table 9.2. Maximum PGA on rigid soil for several probabilities of occurrence in 50 years_Province of Macerata

City	ag [g]				
	P_{vr}	5%	10%	63%	81%
<i>Macerata</i>		0.227	0.175	0.068	0.054
<i>Matelica</i>		0.234	0.183	0.078	0.063
<i>Recanati</i>		0.237	0.183	0.063	0.049
<i>San Severino</i>		0.226	0.175	0.073	0.058
<i>Sarnano</i>		0.236	0.183	0.077	0.061

However, to the basic seismic hazard must be added the possible amplification effects of the seismic motion due to the stratigraphic, geomorphological and topographic characteristics of the reference site. If seismic microzonation studies (MZS) have been carried out, it is possible to refer to them to obtain the peak ground acceleration values, otherwise reference is made to the in force Italian seismic Code (*NTC 2008*), which provides, in a simplified manner, the adoption of a coefficient S (eq. 9.2) multiplicative of the peak acceleration on rigid soil:

$$S = S_s * S_T \quad (9.2)$$

where S_s is the subsoil coefficient that takes into account the subsoil stratigraphy and S_T is the topographic coefficient.

In this case, the most common subsoil categories are B and C as described in the in force Italian seismic Code (respectively high density and medium density soil).

While in terms of topographic effects, given the strictly hilly configuration of the territory, for most buildings it can reasonably be assumed the topographic condition T2 as described in the Italian Code.

In some cases, the conditions of flat ground and top hills were considered.

A single elastic spectrum was assumed within each city, assuming for simplicity that hazard is uniform within the municipal territory.

9.1.1. Determination of the seismic intensity level

The choice of the intensity level can follow several approaches:

- **Strongest historical event**

It can be characterized by a low probability of occurrence and it lead to an unsustainable quantification of resources. Moreover, this probability of occurrence is not uniform across the different areas and to determine resources on the base of the historical event can lead to a different level of civil protection.

- **The most significant event from the point of view of the seismic hazard of the site.**

It has the advantage to consider events with the same probability, uniform on the territory.

The determination of the resources can be graded in function of the probability of occurrence from which you want to protect, but the hazard analyzes are performed with reference to a site that, in the should be representative of the entire territory under examination. Moreover, a high hazard level does not always correspond to a high level of damage.

- **Most significant event from the point of view of the damage.**

It takes into account the impact of the earthquake on the territory, assessing the change in the state of the territory produced by the event, both in direct terms (physical damage) and in terms of consequences of this, that are casualties, injuries, homeless, etc.

To this end, it is necessary to review all the events of different gravity that may originate in one of the seismogenic zones (characterized by a constant seismicity spread throughout the entire area) that affect the territory under consideration and to select those susceptible to have a greater impact.

Hence, n damage scenarios are elaborated for the area under examination with different levels of severity (in terms of losses) with epicenter migrating within the above-mentioned seismogenic zones.

The events characterized by higher magnitude values and whose epicenter is barycentric to the area of interest, they involve the entire territory and so they are a critical situation for the area. Less critical events or those localized near the boundary of the investigated area, however, affect only a part of the whole territory analyzed, it is therefore necessary to identify events that affect different portions of the territory and compare them.

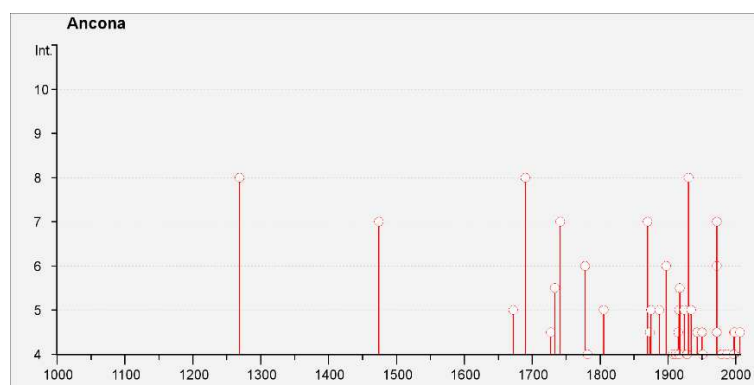
The results of the elaborations allow the selection of significant interventions, defining, where necessary, different impact thresholds for increasing gravity and/or for different return periods, to which could correspond different levels of activation of the emergency plan.

Macroseismic intensity

The macroseismic intensities (IM) usually were estimated on the base of damage data and the number of casualties found in the chronicles of the time.

The events can be selected from the macroseismic catalogue or through correlation law between PGA and MI (e.g. using eq. 6.3), assuming PGA values from the hazard map for a certain return period.

Thus, the maximum value between the previous two is considered in each city for the “uniform hazard scenario”. The highest historical macroseismic intensities recorded were VIII and VII respectively for the cities of Ancona and Macerata (fig. 9.6).



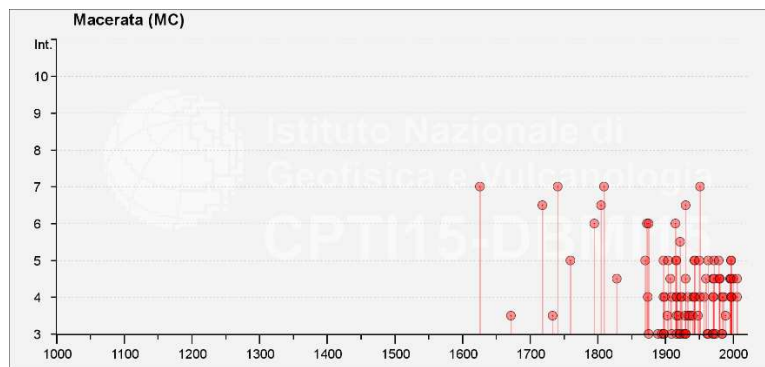


Figure 9.6. Maximum historical macroseismic intensities for the cities of Ancona and Macerata (font: DBMI – Italian Macroseismic Database (Locati et al. 2016)).

Fig. 9.7 shows the overlap of the main events from the year 1000 and the map of the maximum macroseismic intensities MCS with a probability of exceedance of 10% over 50 years, calculated using the same probabilistic procedure used for official hazard estimations.

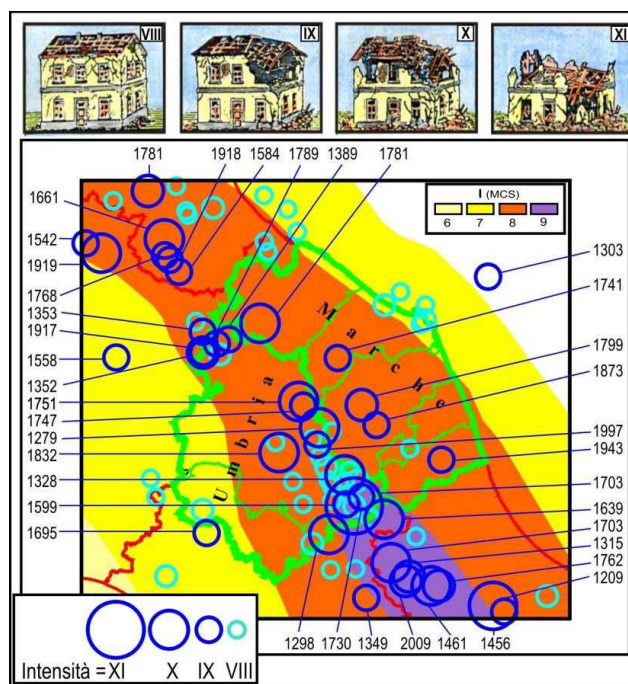


Figure 9.7. Map of the maximum macroseismic intensities MCS with a probability of exceedance of 10% over 50 years and the main events from the year 1000.

For the whole area under investigation the expected I with a p_{VR} of 10% in 50 years is equal to 8, but in this study a p_{VR} of 5% (collapse limit state) and a reference period of 75 years (school buildings) are considered.

Thus, the MI values relative to this hazard level are calculated and shown in tab. 9.3 which summarize the macroseismic intensity values for the cities under investigation.

Table 9.3. Maximum historical I_Province of Ancona

<i>City</i>	<i>Max I_{MCS} from catalogue</i>	<i>Epicentre</i>	<i>M_w (estimated)</i>	<i>Date</i>
Ancona	8	Costa Anconetana	5.58	1690/12/23
Arcevia	8	Appennino Umbro- Marchigiano	6.2	1279/04/30
Castelfidardo	7	Senigallia	5.8	1930/10/30
Chiaravalle	8	Senigallia	5.8	1930/10/30
Fabriano	9	Fabrianese	6.17	1741/04/24
Falconara M.	8	Senigallia	5.8	1930/10/30
Jesi	8	Senigallia	5.8	1930/10/30
Loreto	7	Senigallia	5.8	1930/10/30
Osimo	8	Senigallia	5.8	1930/10/30
Sassoferrato	8	Appennino Umbro- Marchigiano	6.05	1747/04/17
Senigallia	9	Senigallia	5.8	1930/10/30

Fig. 9.8 shows the macroseismic intensities for the 30/10/1930 and 24/04/1741 events.

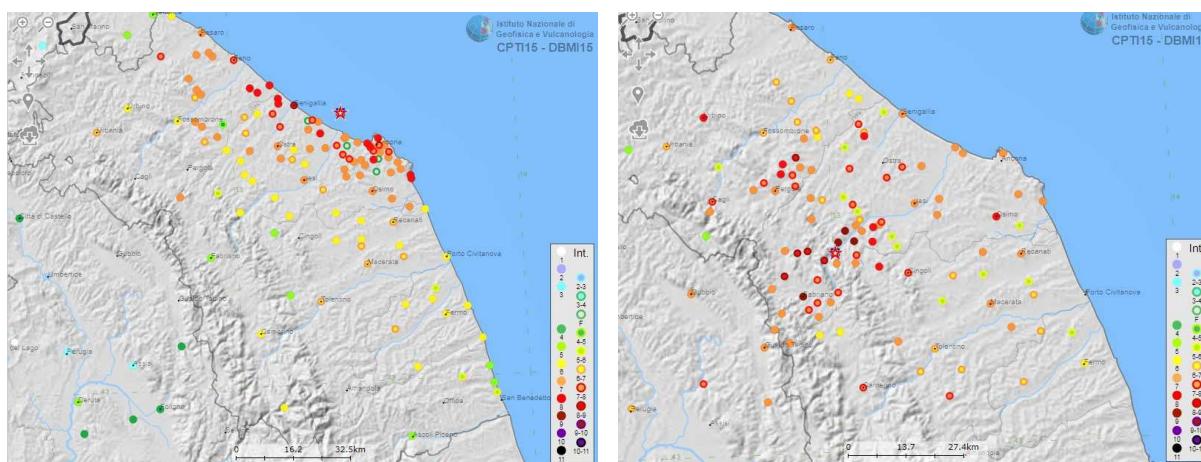


Figure 9.8. Events of the 30/10/1930 and 24/04/1741 (font: CPTI15 - DBMI15)

The intensities for the province of Macerata are summarized in tab. 9.4.

Table 9.4. Maximum historical I_Province of Macerata

<i>City</i>	<i>Max I MCS from catalogue</i>	<i>Epicenter</i>	<i>Mw (estimated)</i>	<i>Date</i>
<i>Macerata</i>	7	Macerata	5.1	1626/05/12
<i>Matelica</i>	8	Appennino Umbro- Marchigiano	6.2	1279/04/30
<i>Recanati</i>	7	Fabrianese	6.17	1741/04/24
<i>San Severino</i>	8	Aquilano	6.67	1703/02/02
<i>Sarnano</i>	8	Appennino Marchigiano	6.18	1799/07/28

Hazard curves and response spectra

PGA and Sa(T) values from the hazard map accounting for the site effects are used to evaluate the losses for an earthquake with a certain return period (or probability of exceedance) in the reference period of the building. In the case of school buildings, the Italian Code suggests assuming a reference period equal to 75 years ($50 \times C_u$, with $C_u = 1.5$). Thus, the return period assumed is equal to 712 years for the safety life limit state (SLV) and 1462 years for collapse limit state (SLC). The elastic response spectrum is able to represent the level and frequency content of seismic excitation that controls the peak building response, so it is an extremely useful tool characterizing ground motions demand. It also provides convenient means to summarize the peak responses of all possible linear SDOF systems to a particular component of ground motion. It is usually computed for 5 percent damping being representative for a vast majority of structures.

Both hazard curves (fig.9.9) and response spectra for several return periods (figs. 9.10 and 9.11), were determined referring to a unique point for each city where the schools are located, because of the homogeneity of soil conditions within the city. Obviously, the local site conditions could differ between the school buildings, but in situ investigations should be done.

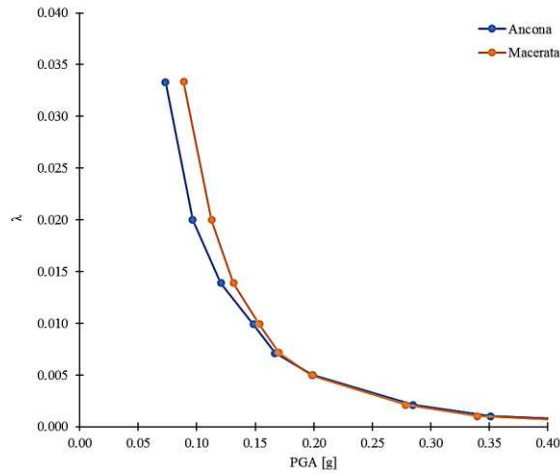


Figure 9.9. Hazard curves for the cities of Ancona and Macerata

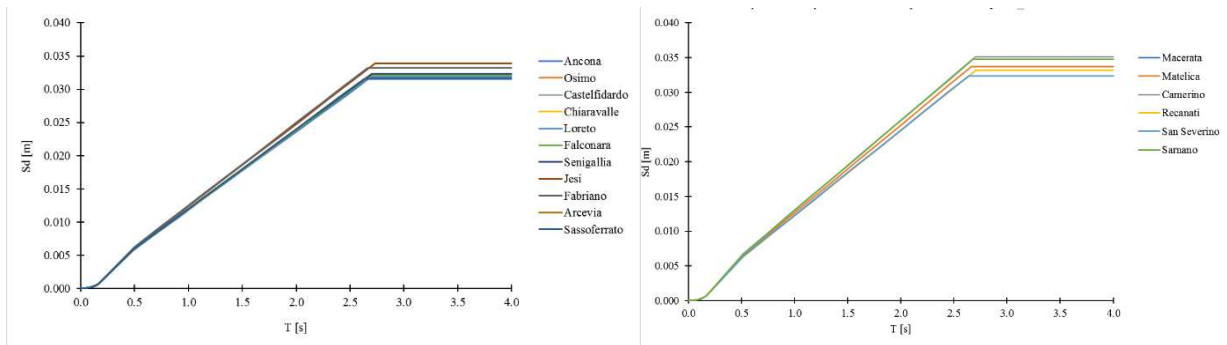


Figure 9.10. Displacement response spectra for a return period of 1462 year. Cities of the province of Ancona (left) and Macerata (right)

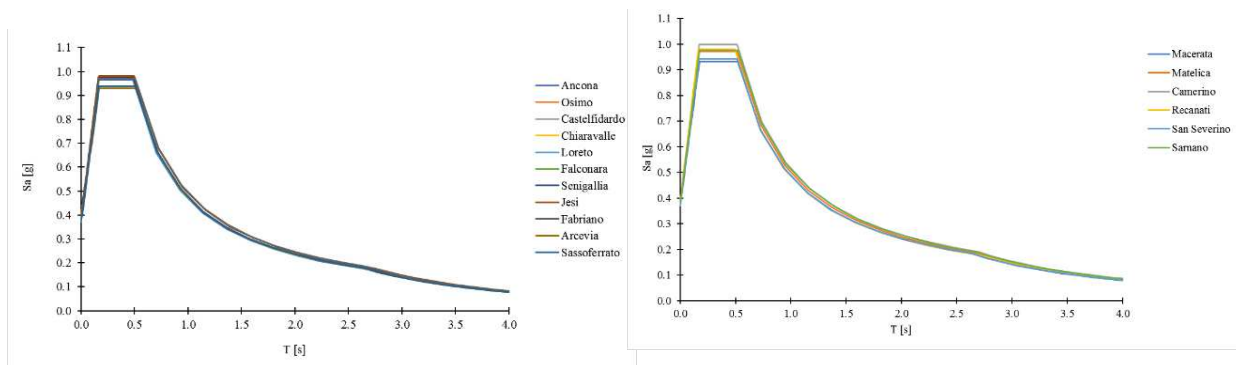


Figure 9.11. Acceleration response spectra for a return period of 1462 year. Cities of the province of Ancona (left) and Macerata (right)

As showed by the spectra there is a very low difference between the hazard of the cities and so also the hazard within each city is negligible as assumed.

Tabs. 9.5 and 9.6 summarize the PGA values relative to a return period of 1462 year ($p_{vr} = 5\%$ in 75 years) for a subsoil of category C and topographic condition T2.

Table 9.5. PGA values for several return periods I_Province of Ancona

City	<i>PGA_soft soil</i>				
	<i>[g]</i>				
	<i>TR = 200</i>	<i>TR = 475</i>	<i>TR = 912</i>	<i>TR = 1462</i>	<i>TR = 2475</i>
<i>Ancona</i>	0.199	0.285	0.331	0.386	0.492
<i>Arcevia</i>	0.199	0.276	0.338	0.373	0.461
<i>Castelfidardo</i>	0.202	0.290	0.355	0.389	0.500
<i>Chiaravalle</i>	0.204	0.291	0.356	0.389	0.500
<i>Fabriano</i>	0.214	0.290	0.350	0.377	0.471
<i>Falconara M.</i>	0.203	0.289	0.354	0.388	0.497
<i>Jesi</i>	0.205	0.294	0.369	0.399	0.510
<i>Loreto</i>	0.200	0.288	0.353	0.387	0.495
<i>Osimo</i>	0.203	0.291	0.356	0.389	0.501
<i>Sassoferrato</i>	0.201	0.277	0.339	0.372	0.463
<i>Senigallia</i>	0.205	0.291	0.378	0.390	0.501

Table 9.6. PGA values for several return periods I_Province of Macerata

City	<i>PGA_soft soil</i>				
	<i>[g]</i>				
	<i>TR = 200</i>	<i>TR = 475</i>	<i>TR = 912</i>	<i>TR = 1462</i>	<i>TR = 2475</i>
<i>Macerata</i>	0.198	0.278	0.340	0.374	0.463
<i>Matelica</i>	0.215	0.291	0.351	0.377	0.472
<i>Recanati</i>	0.203	0.291	0.356	0.391	0.506
<i>San Severino</i>	0.202	0.279	0.340	0.372	0.463
<i>Sarnano</i>	0.212	0.291	0.354	0.382	0.481

9.2. Exposure data

In order to estimate the expected losses, the exposure data in terms of number of school buildings, students and replacing cost for each building of both samples were calculated. In tab. 9.7 aggregate data for provinces are shown, while in tab. 9.8 exposure data are disaggregate for cities.

Table 9.7. Exposure data for school buildings of both provinces

<i>City</i>	<i>N° of school</i>	<i>N° of independent buildings</i>	<i>N° of students</i>	<i>Replacing cost [mln €]</i>
<i>Province of Ancona</i>	42	105	19.201	216.5
<i>Province of Macerata</i>	11	41	5.956	88.4

Tab. 9.8. Number of schools and f independent buildings for each city

<i>City</i>	<i>N° of school</i>	<i>N° of independent buildings</i>	<i>N° of students</i>	<i>Replacing cost [mln €]</i>
<i>Ancona</i>	10	29	5244	58.4
<i>Arcevia</i>	1	3	247	3.9
<i>Fabriano</i>	7	9	1791	31.1
<i>Falconara M.</i>	2	5	870	10.7
<i>Castelfidardo</i>	1	3	423	5.5
<i>Chiaravalle</i>	1	2	249	6.0
<i>Jesi</i>	8	13	3364	33.7
<i>Loreto</i>	2	6	1281	11.5
<i>Osimo</i>	3	11	1256	17.5
<i>Sassoferrato</i>	1	1	60	2.1
<i>Senigallia</i>	6	23	4416	35.9
<i>Macerata</i>	4	21	2464	30.9
<i>Matelica</i>	2	6	341	9.3
<i>Recanati</i>	2	6	2152	12.0
<i>San Severino</i>	1	2	687	9.9
<i>Sarnano</i>	2	6	312	9.7

Disaggregate data shown as the cities of Ancona, Senigallia, Fabriano, Jesi and Macerata have the most part of students and economic value.

To estimate the human losses, the total amount of students of each institute has been subdivided between the structural independent buildings, proportionally to their floor surfaces.

The casualties and injuries because due to the physical damage were estimated according to the several models shown in chapter 3 (*Bramerini 1995, Coburn et al. 2002, HAZUS 99*) and the results were compared.

The economic model has to take into account the repair costs for each level of damage considered and the cost of replacing for a typical RC school building. Generally, a local market investigation should be performed to get these costs or a damage index

In the case of school buildings, the most part of economic losses is direct loss due to the damage of structural and non-structural components. The contents are not so important as vice versa in the case of industrial buildings or other type of buildings which contain goods with a relevant economical value (i.e. hospitals that have expansive machineries). Further neither the economic losses due to the business interruption are accounted for school buildings.

Thus, it is needed to correlate the damage level suffered by the buildings with the repair cost. To this aim the threshold values for damage levels shown in tab. 9.9 are used respectively for macroseismic and vulnerability index methods. Further the assumed percentages of the replacing cost for each damage level are shown.

Table 9.9. Correlation between EMS-98 damage levels, damage indices and % of replacing cost

<i>Dk</i>	<i>Description</i>	<i>ud</i>	<i>DI Bramerini</i>	<i>Condition</i>	<i>% Replacing cost</i>
DL0	No damage	0 - 1	0.00 – 0.01	Usable	0.00
DL1	Slight	1 - 2	0.01 – 0.10		0.07
DL2	Moderate	2 - 3	0.10 – 0.35	Usable with intervention	0.15
DL3	Heavy	3 - 4	0.35 – 0.75		0.50
DL4	Very heavy	4 - 5	0.75 -1.00	Unusable	0.80
DL5	Collapse	> 5	> 1.00	Collapsed	1.00

The percentages of the replace costs were determined according to (*Di Ludovico et al. 2016 a-b*), which considers a replacing cost equal to 1200 €/m², based on the post L'Aquila earthquake (2009) cost reconstruction data.

Thus, the economic loss for each building is calculated by multiplying the percentage of the replacing cost, depending on to damage level suffered, for the total replacing cost calculated by multiplying the total floor areas and the replacing cost equal to 1200 €/m².

9.3. Uniform hazard scenarios

It is a scenario that provides unrealistic loss estimation if the entire sample is considered, so a territorial scale, since it is unlikely that events with the same intensity will occur simultaneously in all cities and in the two provinces. However, it makes it possible to measure the risk level of the population of buildings and to estimate realistically the expected losses at the city scale if there when an event with a certain return period occurs.

The highest historical macrocosmic intensities and the PGA provided by the hazard map for several return periods and amplified for site effects were adopted for the evaluation.

Both macroseismic vulnerability curves and trilinear damage curves (please see chapter 6) for each building under investigation are used to estimate losses.

Macroseismic scenario

In this scenario, the maximum historical intensities for each city shown in tab. were assumed to estimate losses through the mean damage curve of each building belonging to the stocks of the province of Ancona and Macerata.

Fig. 9.12 shows, for the two provinces, the distribution of the after-earthquake condition in terms of percentage of buildings.

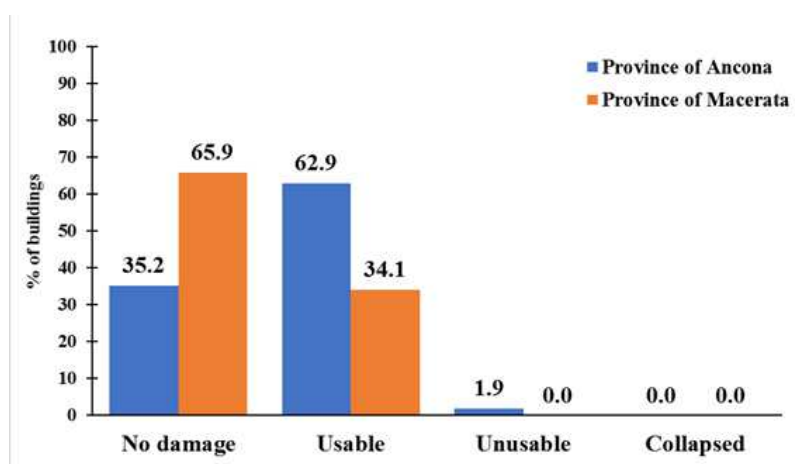


Figure 9.12. Distribution of the physical losses for the provinces

The total number of buildings in each after earthquake condition for both the province of Ancona and Macerata are shown in tab. 9.10.

Table 9.10. Building losses disaggregated for the provinces.

	<i>No damage</i>	<i>Usable</i>	<i>Unusable</i>	<i>Collapsed</i>
<i>Province of Ancona</i>	37	66	2	0
<i>Province of Macerata</i>	27	14	0	0

In tab. 9.11 the building losses are disaggregated for each city under investigation.

Table 9.11. Building losses disaggregated for each city under investigation.

	No damage		Usable		Unusable		Collapsed	
	N°	%	N°	%	N°	%	N°	%
<i>Ancona</i>	11	37.9	18	62.1	0	0	0	0
<i>Arcevia</i>	1	33.3	2	66.7	0	0	0	0
<i>Fabriano</i>	0	0	8	88.9	1	11.1	0	0
<i>Falconara M.</i>	3	60.0	2	40.0	0	0	0	0
<i>Castelfidardo</i>	3	100	0	0	0	0	0	0
<i>Chiaravalle</i>	0	0	2	100	0	0	0	0
<i>Jesi</i>	3	23.1	10	76.9	0	0	0	0
<i>Loreto</i>	6	100	0	0	0	0	0	0
<i>Osimo</i>	7	63.6	4	36.4	0	0	0	0
<i>Sassoferrato</i>	0	0	1	100	0	0	0	0
<i>Senigallia</i>	3	13.0	19	82.6	1	4.3	0	0
<i>Macerata</i>	16	76.2	5	23.8	0	0	0	0
<i>Matelica</i>	5	83.3	1	16.7	0	0	0	0
<i>Recanati</i>	3	50.0	3	50.0	0	0	0	0
<i>San Severino</i>	0	0	2	100	0	0	0	0
<i>Sarnano</i>	3	50.0	3	50.0	0	0	0	0

Economic losses (fig. 9.13) amount to the 8.2 % of the total replacing cost for the stock of the province of Ancona, and the 3.3% for those of the province of Macerata.

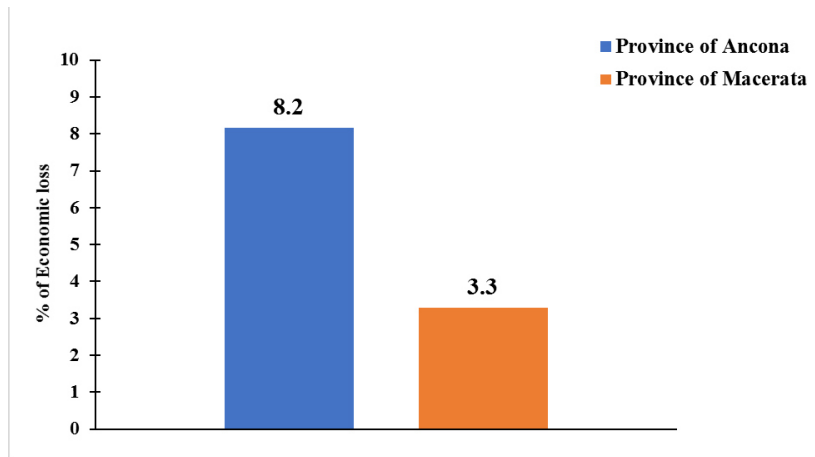
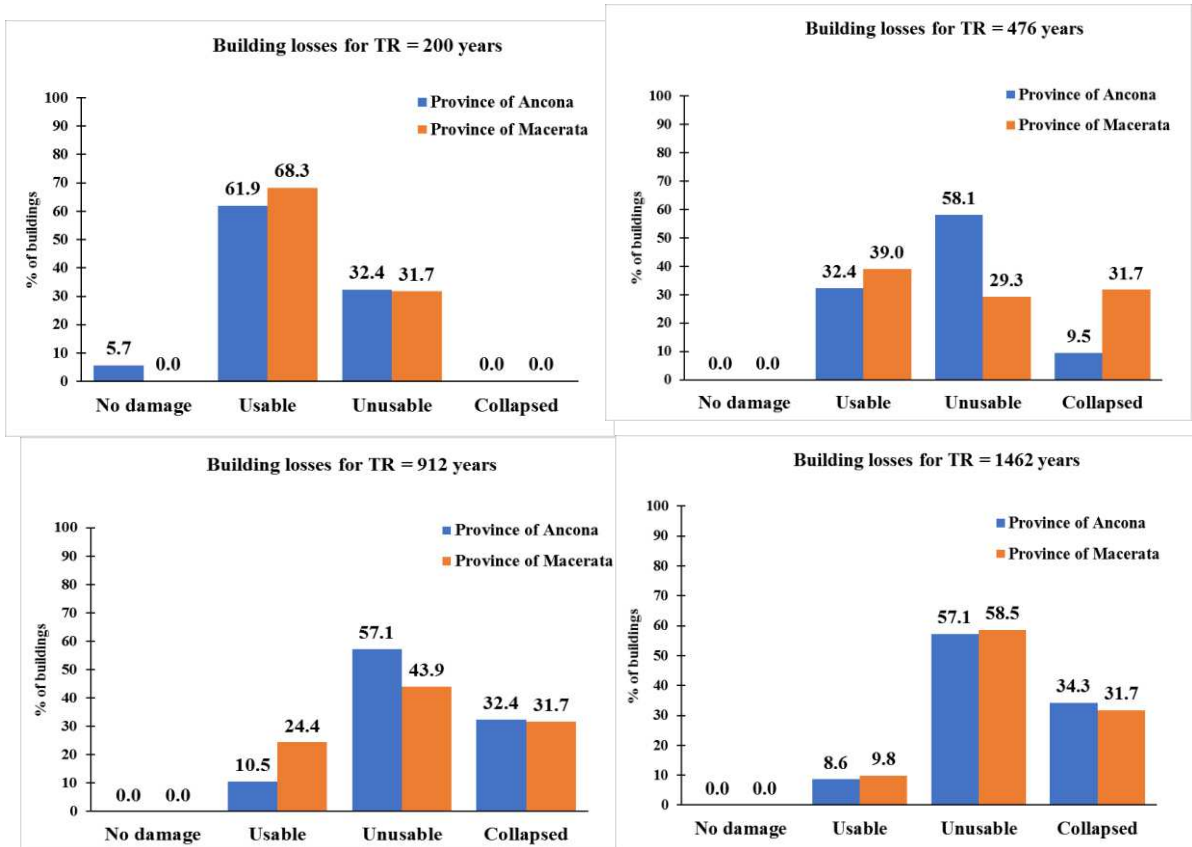


Figure 9.13. % of economic loss on the total amount for the provinces

No casualties and injuries are provided from all methods here adopted (Hazus, Bramerini and Coburn and Spence).

Scenarios for increasing hazard levels

Several scenarios were developed accounting for a seismic demand calculated for return periods of 200, 476, 912, 1462 and 2475 years. Fig. show the building losses for the two stocks in terms of percentage of buildings.



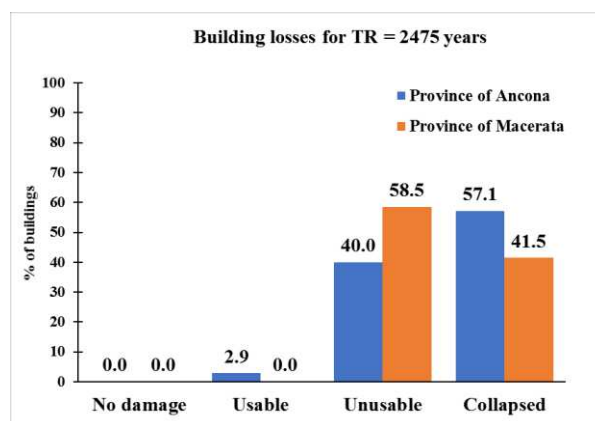


Figure 9.14. Distributions of building losses disaggregate for the provinces and for several return periods of the seismic event.

It can be seen as for both building stocks the distributions are shifted on the left for the lower return periods, thus more buildings with no damage or with slight non-structural damage (usable) are estimated, while for the higher return periods the distributions are shifted on the right toward the unusable and collapse condition.

For mostly return periods the higher percentage of buildings exhibits the unusable condition, except for the TR = 200 years for which the higher percentage of buildings exhibits the usable condition. The total number of buildings losses are shown in tab. 9.12, disaggregated for provinces, and in tab. 9.13, disaggregated for cities.

Table 9.12. N° of buildings in each after-earthquake condition_Data disaggregated for provinces

TR	No damage		Usable		Unusable		Collapsed	
	Ancona	Macerata	Ancona	Macerata	Ancona	Macerata	Ancona	Macerata
200	6	0	65	28	34	13	0	0
476	0	0	34	16	61	12	10	13
912	0	0	11	10	60	18	34	13
1462	0	0	9	4	60	24	36	13
2475	0	0	3	0	42	24	60	17

Table 9.13. Comparison of n° and percentages on the total amount of **unusable and collapsed buildings**_Data disaggregated for cities

	TR = 200		TR = 476		TR = 912		TR = 1462		TR = 2475		Historical I max	
	N°	%	N°	%	N°	%	N°	%	N°	%	N°	%
<i>Ancona</i>	10	34.5	20	69.0	21	72.4	24	82.8	27	93.1	0	0
<i>Arcevia</i>	0	0	2	66.7	3	100	3	100	3	100	0	0
<i>Fabriano</i>	7	77.8	9	100	9	100	9	100	9	100	1	11.1
<i>Falconara M.</i>	1	20.0	4	80.0	5	100	5	100	5	100	0	0
<i>Castelfidardo</i>	0	0	1	33.3	2	66.7	3	100	3	100	0	0
<i>Chiaravalle</i>	1	50.0	2	100	2	100	2	100	2	100	0	0
<i>Jesi</i>	3	23.1	8	61.5	11	84.6	12	92.3	13	100	0	0
<i>Loreto</i>	3	50.0	3	50.0	4	66.7	6	100	6	100	0	0
<i>Osimo</i>	4	36.4	8	72.7	10	90.9	11	100	11	100	0	0
<i>Sassoferrato</i>	1	100	1	100	1	100	1	100	1	100	0	0
<i>Senigallia</i>	4	17.4	13	56.5	16	69.6	20	87.0	22	95.7	1	4.3
<i>Macerata</i>	5	23.8	11	52.4	11	52.4	17	81.0	21	100	0	0
<i>Matelica</i>	0	0.0	1	16.7	6	100	6	100	6	100	0	0
<i>Recanati</i>	3	50.0	6	100	6	100	6	100	6	100	0	0
<i>San Severino M.</i>	2	100	2	100	2	100	2	100	2	100	0	0.
<i>Sarnano</i>	3	50.0	5	83.3	6	100	6	100	6	100	0	0

Casualties and injuries were estimated accounting for the Hazus, Bramerini and Coburn and Spence methods.

In figs. 9.15 and 9.16 are shown the values obtained with the Bramerini method (please see chapter 3), respectively for school buildings of the province of Ancona and Macerata.

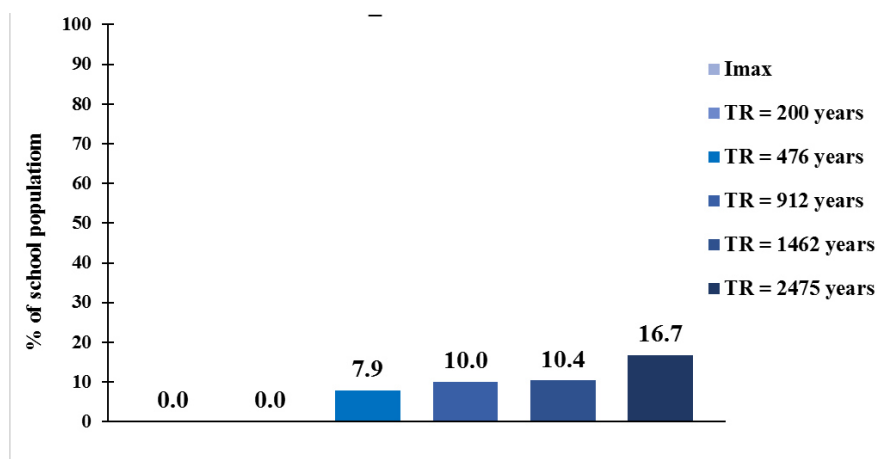


Figure 9.15. % of human loss on the total amount - Province of Ancona

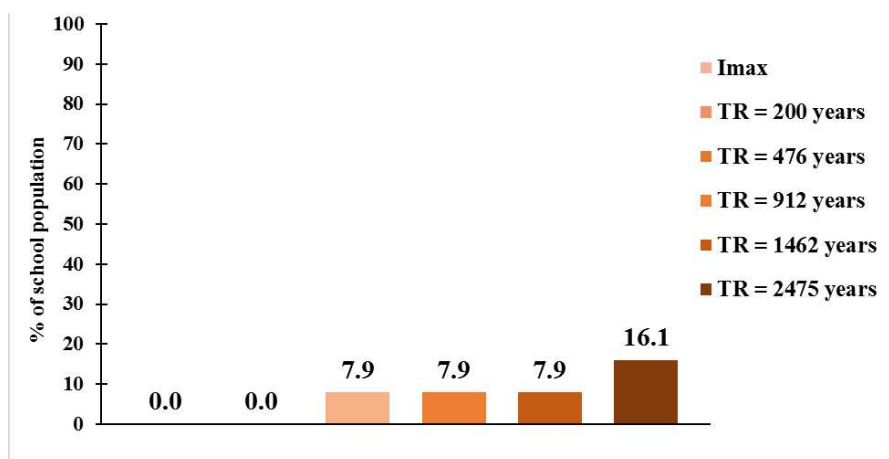


Figure 9.16. % of human loss on the total amount - Province of Macerata

Human losses disaggregate for cities are shown in tab. 9.14.

Table 9.14. Comparison of number and percentage of casualties/injuries (from Bramerini) - Data disaggregated for cities

	TR = 200		TR = 476		TR = 912		TR = 1462		TR = 2475		Historical I max	
	N°	%	N°	%	N°	%	N°	%	N°	%	N°	%
Ancona	0	0	229	4.4	421	8.0	663	12.7	1030	19.6	0	0
Arcevia	0	0	0	0	0	0	0	0	42	17.0	0	0
Fabriano	0	0	159	8.9	253	14.1	357	19.9	404	22.5	0	0
Falconara M.	0	0	66	7.6	66	7.6	66	7.6	157	18.1	0	0
Castelfidardo	0	0	0	0	0	0	0	0	0	0	0	0
Chiaravalle	0	0	0	0	0	0	37	14.9	75	30.0	0	0
Jesi	0	0	0	0	138	4.1	204	6.1	492	14.6	0	0

<i>Loreto</i>	0	0	0	0	0	0	22	1.7	22	1.7	0	0
<i>Osimo</i>	0	0	188	15.0	188	15.0	212	16.8	212	16.8	0	0
<i>Sassoferrato</i>	0	0	18	30.0	18	30.0	18	30.0	18	30.0	0	0
<i>Senigallia</i>	0	0	49	1.1	49	1.1	409	9.3	752	17.0	0	0
<i>Macerata</i>	0	0	0	0	0	0	0	0	21	0.1	0	0
<i>Matelica</i>	0	0	229	4.4	603	11.5	663	12.7	34	2.7	0	0
<i>Recanati</i>	0	0	159	8.9	357	19.9	357	19.9	646	11.1	0	0
<i>San Severino M.</i>	0	0	66	7.6	66	7.6	66	7.6	206	15.0	0	0
<i>Sarnano</i>	0	0	0	0	0	0	0	0	53	5.6	0	0

Finally, economic losses for the several return periods are compared in figs. 9.17 and 9.18, respectively for school buildings of the province of Ancona and Macerata.

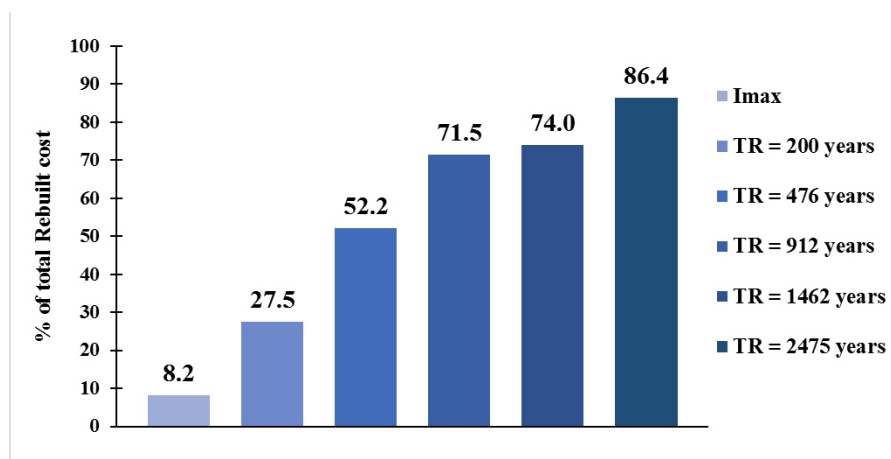


Figure 9.17. % of economic loss on the total amount_Province of Macerata

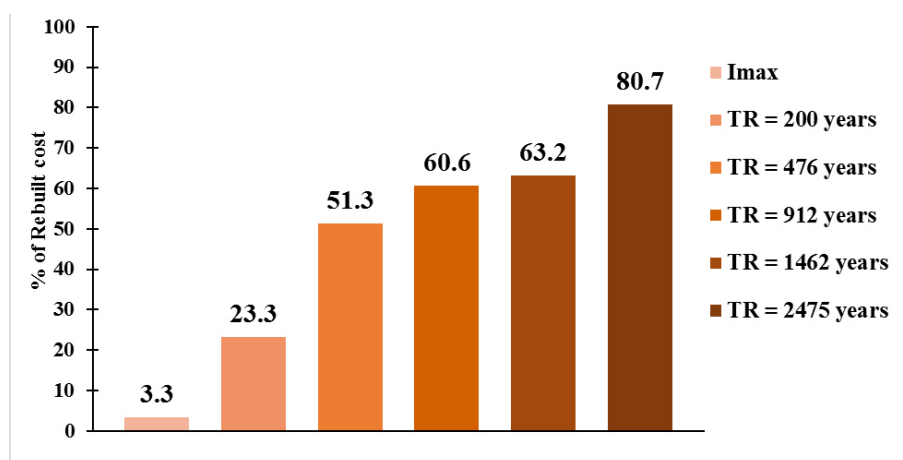


Figure 9.18. % of economic loss on the total amount_Province of Macerata

Results disaggregate for cities are shown in tab. 9.15.

Table 9.15. Repair cost and percentage on the total amount of the replacing cost_Data
disaggregated for cities

	TR = 200		TR = 476		TR = 912		TR = 1462		TR = 2475		Historic I _{max}	
	Mln €	%	Mln €	%	Mln €	%	Mln €	%	Mln €	%	Mln €	%
<i>Ancona</i>	16.4	28.1	32.0	54.8	36.5	62.5	45.5	77.9	51.2	87.6	13.6	23.4
<i>Arcevia</i>	0.6	15.0	1.3	34.9	1.9	50.0	2.6	67.0	3.5	91.4	1.1	28.8
<i>Fabriano</i>	12.8	41.1	22.9	73.6	24.1	77.4	28.0	89.9	30.3	97.3	11.3	36.3
<i>Falconara M.</i>	2.3	21.7	5.4	50.8	6.3	59.5	7.2	67.4	9.5	89.0	1.2	11.1
<i>Castelfidardo</i>	0.6	11.3	1.7	31.0	1.9	34.0	2.8	50.0	3.7	66.3	0.4	7.0
<i>Chiaravalle</i>	1.9	32.4	3.0	50.0	3.9	64.9	5.4	89.9	6.0	100	0.9	15.0
<i>Jesi</i>	7.1	21.1	14.6	43.3	16.8	50.0	21.7	64.3	27.6	81.8	5.9	17.7
<i>Loreto</i>	2.6	22.7	4.2	36.2	5.0	43.4	7.6	66.3	8.3	72.4	0.8	7.0
<i>Osimo</i>	6.5	37.0	11.0	62.8	12.1	68.8	13.0	74.3	15.2	87.0	3.9	22.2
<i>Sassoferrato</i>	1.7	80.0	2.1	100	2.1	100	2.1	100	2.1	100	0.3	15.0
<i>Senigallia</i>	6.9	19.3	14.8	41.2	18.4	51.3	24.3	67.6	29.4	82.1	10.4	29.0
<i>Macerata</i>	5.0	16.3	12.4	40.3	12.4	40.3	14.8	47.9	21.1	68.4	0.32	1.0
<i>Matelica</i>	1.1	12.2	2.9	30.8	5.9	63.5	5.9	63.5	6.8	72.5	0.29	3.2
<i>Recanati</i>	4.5	37.8	8.8	73.4	10.7	89.4	10.7	89.4	11.9	100	0.39	3.3
<i>San Severino M.</i>	4.9	50.0	9.9	100	9.9	100	9.9	100	9.9	100	1.5	15.0
<i>Sarnano</i>	4.9	18.8	11.2	42.9	14.5	55.4	14.5	55.4	21.5	82.2	0.4	1.6

Tabs. 9.16 and 9.17 summarize the losses in terms of total number of collapsed buildings, casualties and repair cost for both the building stocks by increasing the return period of the seismic events.

Table 9.16. Losses for the province of Ancona

TR	N° of collapsed buildings	N° of casualties			Economical losses Mln [€]
		Hazus	Bramerini	Coburn	
200	0	30	0	0	59.5
476	10	214	708	1258	113.1
912	34	380	1928	3425	154.7

1462	36	431	1988	3532	160.2
2475	60	652	3202	5689	186.9

Table 9.17. Losses for the province of Macerata

TR	N° of collapsed buildings	N° of casualties			Economical losses Mln [€]
		Hazus	Bramerini	Coburn	
200	0	25	0	0	20.6
476	13	120	470	1296	45.3
912	13	139	470	1296	53.6
1462	13	163	470	1296	55.9
2475	17	227	959	2164	71.3

The total losses for both building stock can be obtained by summing the losses for each province.

9.4. For single event scenarios

Some scenarios were developed assuming epicentres on the base of the fault system of the region, so magnitude values were chosen on the base of the maximum expected value for the specific fault within the seismogenic zones according to the ZS9 map.

These zones are those affecting the cities under investigations, that are the n. ZS917, ZS918 and ZS919 as shown in fig. 9.18.

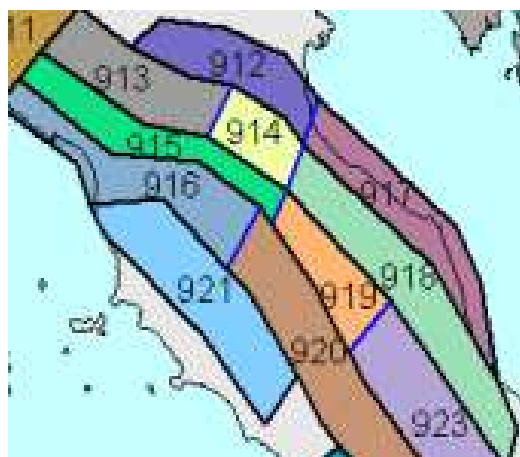


Figure 9.18. Seismogenic zones for the area of interest

The epicentres could be located in any point on the fault system of each seismogenic zones. Adopting a deterministic approach, the epicentres were assumed to be located in the city with the highest exposure (the most part of the school buildings and students).

Three epicentres are (fig. 9.19):

1. Ancona
2. Fabriano
3. Macerata

This would be a way to keep into account some of the most severe scenarios, even if the worst scenario could be one provided from an epicentre different from those selected (to develop all the possible scenarios considering all possible epicentral positions it is a very hard work).



Figure 9.19. Active faults and epicentres for the scenario analyses

However, the most part of other cities with school building is close to Ancona, so that the epicentre in Ancona become very meaningful.

Tab. 9.18 shows data relative to the three seismic sources considered for the scenarios.

Table 9.18. Data of the seismic sources considered for the scenarios

<i>Epicentre city</i>	<i>Seismogenic Zone</i>	<i>Source</i>	<i>Type of fault mechanism</i>	<i>Fault depth</i>	<i>max Mw</i>
<i>Ancona</i>	Rimini-Ancona (ZS917)	ITCS008_Coneronshore	Reverse	3.0 – 6.5	5.9

<i>Fabriano</i>	Umbrian Apennine (ZS919)	ITCS027_Bore-Montefeltro-Fabriano-Laga	Normal	12.0 – 22.0	6.2
<i>Macerata</i>	Medium Marche-Abruzzo (ZS918)	ITCS020_Southern Marche	Normal	3.0 – 9.0	5.9

Further for each city in which the schools are located, the linear distances from the epicentres were calculated (tab. 9.19). The epicentres were assumed located about in the centre of the cities and the same epicentral distance was assumed for school buildings located within a city.

Table 9.19. Epicentral distances for the cities under investigation

	<i>Epicentral distances [Km]</i>		
	<i>Ancona</i>	<i>Fabriano</i>	<i>Macerata</i>
<i>Ancona</i>	5	58	35
<i>Arcevia</i>	49	18	47
<i>Fabriano</i>	58	5	20
<i>Falconara M.</i>	9	51	35
<i>Castelfidardo</i>	17	53	45
<i>Chiaravalle</i>	16	44	37
<i>Jesi</i>	24	34	30
<i>Loreto</i>	20	58	20
<i>Osimo</i>	15	49	21
<i>Sassoferrato</i>	57	11	50
<i>Senigallia</i>	27	48	50
<i>Macerata</i>	35	43	5
<i>Matelica</i>	57	12	36
<i>Recanati</i>	22	53	14
<i>San Severino</i>	50	25	23
<i>Sarnano</i>	66	45	32

Then attenuation law according to Sabetta e Pugliese (1987), was used to calculate the intensity level in terms of PGA on the ground surface for each city under investigation, assuming the soft soil condition according to the ground characteristic of the zone under investigation. The PGA values are shown in tab. 9.20.

Table 9.20. PGA values for the cities under investigation

	<i>PGA_soft soil</i>		
	<i>[g]</i>		
	<i>Ancona</i>	<i>Fabriano</i>	<i>Macerata</i>
<i>Ancona</i>	0.396	0.055	0.073
<i>Arcevia</i>	0.052	0.169	0.055
<i>Castelfidardo</i>	0.144	0.060	0.124
<i>Chiaravalle</i>	0.152	0.072	0.073
<i>Fabriano</i>	0.044	0.489	0.057
<i>Falconara M.</i>	0.241	0.062	0.069
<i>Jesi</i>	0.105	0.093	0.085
<i>Loreto</i>	0.124	0.055	0.124
<i>Osimo</i>	0.161	0.065	0.119
<i>Sassoferrato</i>	0.045	0.257	0.051
<i>Senigallia</i>	0.094	0.066	0.051
<i>Macerata</i>	0.073	0.074	0.338
<i>Matelica</i>	0.045	0.240	0.071
<i>Recanati</i>	0.114	0.060	0.171
<i>San Severino</i>	0.051	0.124	0.109
<i>Sarnano</i>	0.039	0.070	0.079

The losses estimated for each single event scenario are shown below. In this case the results are shown both in the disaggregate form, for the two provinces and cities, and in the total form merging together the two building stocks. This latter assumption is done because in the single event scenario all the buildings under investigation are interested to the event at the same time and so is meaningful to represent the global situation. While the disaggregation of results is done only to compare the losses suffered to the two building stocks when they are interested from a specific event.

Below the building losses for the **Ancona earthquake** in the total form (fig. 9.20), disaggregate for the two provinces (fig. 9.21) and for the cities (tab. 9.21).

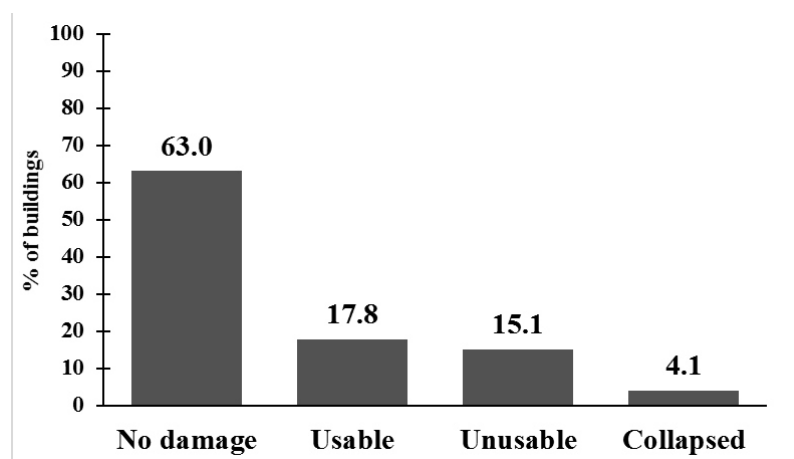


Figure 9.20. Total building losses_Ancona EQ

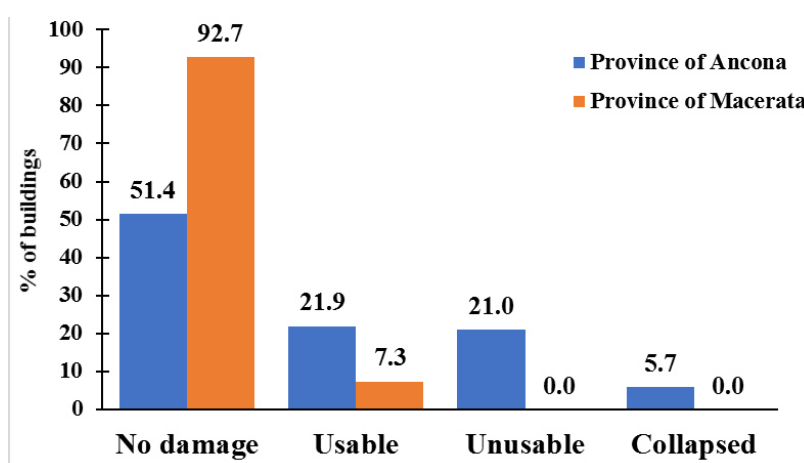


Figure 9.21. Building losses disaggreate for provinces_Ancona EQ

Table 9.21. Building losses disaggreate for cities_Ancona EQ

	No damage		Usable		Unusable		Collapsed	
	N°	%	N°	%	N°	%	N°	%
<i>Ancona (epicenter)</i>	0	0	5	17	12	41	12	41
<i>Arcevia</i>	3	100	0	0	0	0	0	0
<i>Fabriano</i>	9	100	0	0	0	0	0	0
<i>Falconara M.</i>	0	0	3	60	2	40	0	0
<i>Castelfidardo</i>	3	100	0	0	0	0	0	0
<i>Chiaravalle</i>	1	50	1	50	0	0	0	0
<i>Jesi</i>	13	100	0	0	0	0	0	0
<i>Loreto</i>	6	100	0	0	0	0	0	0
<i>Osimo</i>	6	55	2	18	3	27	0	0

<i>Sassoferrato</i>	1	100	0	0	0	0	0	0
<i>Senigallia</i>	23	100	0	0	0	0	0	0
<i>Macerata</i>	21	100	0	0	0	0	0	0
<i>Matelica</i>	6	100	0	0	0	0	0	0
<i>Recanati</i>	3	50	3	50	0	0	0	0
<i>San Severino</i>	2	100	0	0	0	0	0	0
<i>Sarnano</i>	6	100	0	0	0	0	0	0

Collapsed buildings are only ones located in the epicentre cities.

Below the building losses for the **Fabriano earthquake** in the total form (fig. 9.22), disaggregate for the two provinces (fig. 9.23) and for the cities (tab. 9.22).

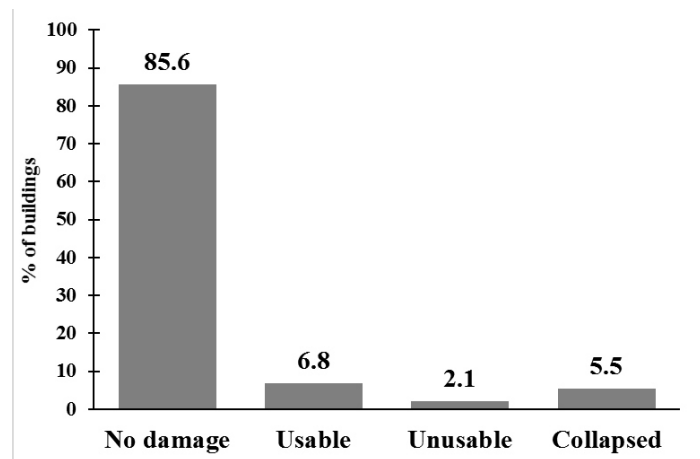


Figure 9.22. Total building losses_Fabriano EQ

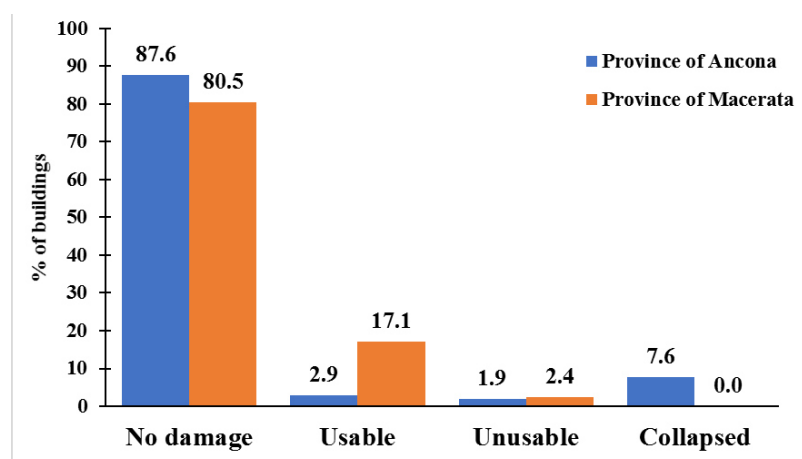


Figure 9.23. Building losses disaggregate for provinces_Fabriano EQ

Table 9.22. Building losses disaggregate for cities_Fabriano EQ

	No damage		Usable		Unusable		Collapsed	
	N°	%	N°	%	N°	%	N°	%
<i>Ancona</i>	29	100	0	0	0	0	0	0
<i>Arcevia</i>	1	33	2	67	0	0	0	0
<i>Fabriano (epicentre)</i>	0	0	0	0	1	11	8	89
<i>Falconara M.</i>	5	100	0	0	0	0	0	0
<i>Castelfidardo</i>	3	100	0	0	0	0	0	0
<i>Chiaravalle</i>	2	100	0	0	0	0	0	0
<i>Jesi</i>	13	100	0	0	0	0	0	0
<i>Loreto</i>	6	100	0	0	0	0	0	0
<i>Osimo</i>	11	100	0	0	0	0	0	0
<i>Sassoferrato</i>	0	0	0	0	0	0	1	100
<i>Senigallia</i>	23	100	0	0	0	0	0	0
<i>Macerata</i>	21	100	0	0	0	0	0	0
<i>Matelica</i>	0	0	5	83	1	17	0	0
<i>Recanati</i>	6	100	0	0	0	0	0	0
<i>San Severino M.</i>	0	0	2	100	0	0	0	0
<i>Sarnano</i>	6	100	0	0	0	0	0	0

Below the building losses for the **Macerata earthquake** in the total form (fig. 9.24), disaggregate for the two provinces (fig. 9.25) and for the cities (tab. 9.23).

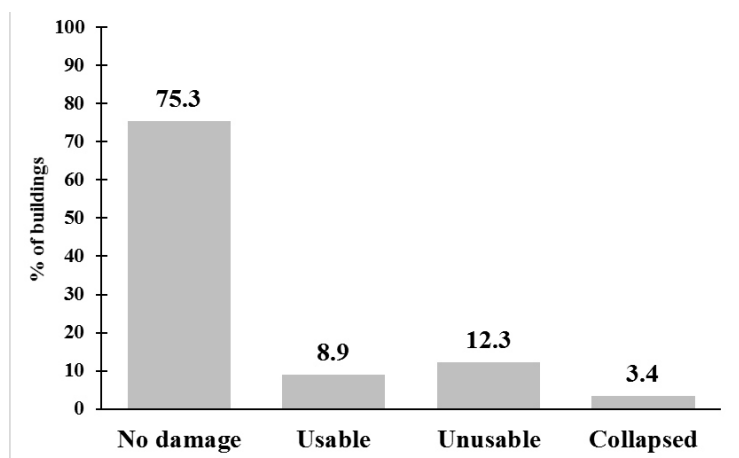


Figure 9.24. Total building losses_Macerata EQ

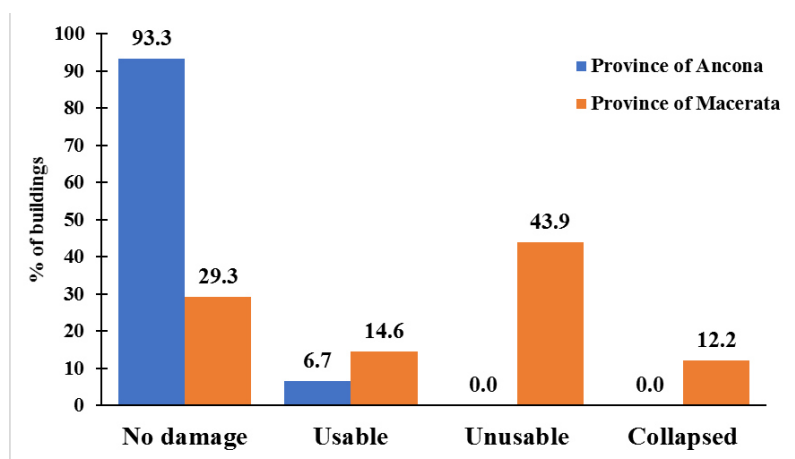


Figure 9.25. Building losses disaggregate for provinces_Macerata EQ

Table 9.23. Building losses disaggregate for cities_Macerata EQ

	No damage		Usable		Unusable		Collapsed	
	N°	%	N°	%	N°	%	N°	%
<i>Ancona</i>	29	100	0	0	0	0	0	0
<i>Arcevia</i>	3	100	0	0	0	0	0	0
<i>Fabriano</i>	9	100	0	0	0	0	0	0
<i>Falconara M.</i>	5	100	0	0	0	0	0	0
<i>Castelfidardo</i>	3	100	0	0	0	0	0	0
<i>Chiaravalle</i>	2	100	0	0	0	0	0	0
<i>Jesi</i>	13	100	0	0	0	0	0	0
<i>Loreto</i>	3	50	3	50	0	0	0	0
<i>Osimo</i>	7	64	4	36	0	0	0	0
<i>assoferrato</i>	1	100	0	0	0	0	0	0
<i>Senigallia</i>	23	100	0	0	0	0	0	0
<i>Macerata (epicentre)</i>	0	0	1	5	15	71	5	24
<i>Matelica</i>	6	100	0	0	0	0	0	0
<i>Recanati</i>	0	0	3	50	3	50	0	0
<i>San Severino M.</i>	0	0	2	100	0	0	0	0
<i>Sarnano</i>	6	100	0	0	0	0	0	0

The buildings losses for the three events are shown in tab. 9.24, in the aggregate form, in tab. 9.25, disaggregate for the provinces, and in tab. 9.26, disaggregated for cities.

Table 9.24. Comparison of the n° of buildings in each post-earthquake condition_Aggregate data

	<i>No damage</i>	<i>Usable</i>	<i>Unusable</i>	<i>Collapsed</i>
<i>Ancona EQ_Mw = 5.9</i>	92	26	22	6
<i>Fabriano EQ_Mw = 6.2</i>	125	10	3	8
<i>Macerata EQ_Mw = 5.9</i>	110	13	18	5

Table 9.25. Comparison of the n° of buildings in each post-earthquake condition_Disaggregation for provinces

<i>Event</i>	<i>No damage</i>		<i>Usable</i>		<i>Unusable</i>		<i>Collapsed</i>	
	<i>Ancon</i>	<i>Macerat</i>	<i>Ancon</i>	<i>Macerat</i>	<i>Ancon</i>	<i>Macerat</i>	<i>Ancon</i>	<i>Macerat</i>
	<i>a</i>	<i>a</i>	<i>a</i>	<i>a</i>	<i>a</i>	<i>a</i>	<i>a</i>	<i>a</i>
<i>Ancona EQ</i>	54	38	23	3	22	0	6	0
<i>Fabriano EQ</i>	92	33	3	7	2	1	8	0
<i>Macerata EQ</i>	98	12	7	6	0	18	0	5

Table 9.26. Comparison of the numbers and percentages on the total amount of **unusable and collapsed buildings**_ Data disaggregated for cities

	Ancona EQ		Fabriano EQ		Macerata EQ	
	<i>N°</i>	<i>%</i>	<i>N°</i>	<i>%</i>	<i>N°</i>	<i>%</i>
<i>Ancona</i>	24	82.8	0	0.0	0	0
<i>Arcevia</i>	0	0	0	0.0	0	0
<i>Fabriano</i>	0	0	9	100	0	0
<i>Falconara M.</i>	2	40.0	0	0.0	0	0
<i>Castelfidardo</i>	0	0.0	0	0.0	0	0
<i>Chiaravalle</i>	0	0.0	0	0.0	0	0
<i>Jesi</i>	0	0.0	0	0.0	0	0
<i>Loreto</i>	0	0.0	0	0.0	0	0
<i>Osimo</i>	3	27.3	0	0.0	0	0
<i>Sassoferrato</i>	0	0.0	1	100.0	0	0
<i>Senigallia</i>	0	0.0	0	0.0	0	0

<i>Macerata</i>	0	0.0	0	0	0	0.0
<i>Matelica</i>	0	0.0	1	16.7	20	95.2
<i>Recanati</i>	0	0.0	0	0.0	3	50.0
<i>San Severino M.</i>	0	0.0	0	0.0	0	0.0
<i>Sarnano</i>	0	0.0	0	0.0	0	0.0

The human losses due to the three events, computed according the Bramerini method, are shown in aggregate form both in terms of total number of casualties (fig. 9.26) and of percentages (fig. 9.27) on the total population.

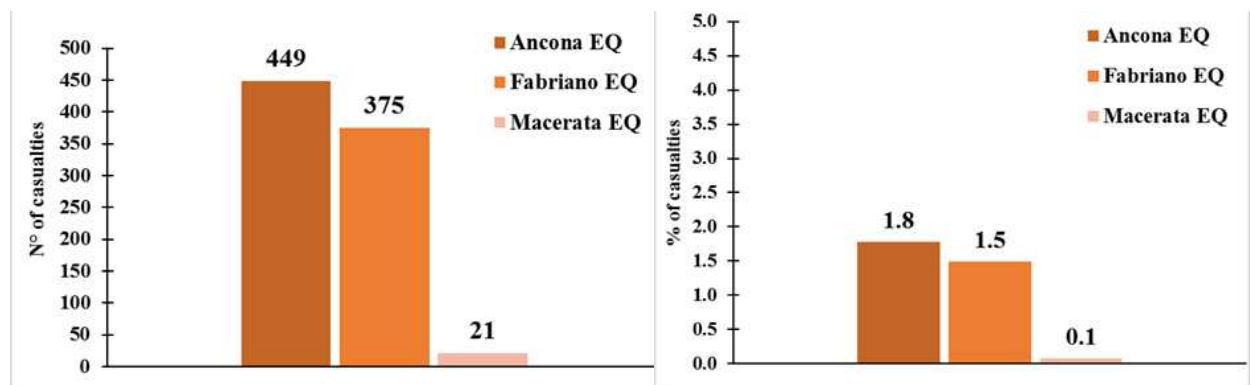


Figure 9.26. Comparison of the n° of casualties (left) and of the percentage on the total population (right)_Aggregate data

Casualties provided from the three methods are a small percentage of the total amount of students. In tab. 9.27 the number and the percentages of casualties are disaggregated for cities.

Table. 9.27. Comparison of number and percentage of casualties/injuries (from Bramerini) _Data disaggregated for cities

	Ancona EQ		Fabriano EQ		Macerata EQ	
	N°	%	N°	%	N°	%
<i>Ancona</i>	735	14.0	0	0	0	0
<i>Arcevia</i>	0	0	0	0	0	0
<i>Fabriano</i>	0	0	404	22.5	0	0
<i>Falconara M.</i>	0	0	0	0	0	0
<i>Castelfidardo</i>	0	0	0	0	0	0
<i>Chiaravalle</i>	0	0	0	0	0	0

<i>Jesi</i>	0	0	0	0	0	0
<i>Loreto</i>	0	0	0	0	0	0
<i>Osimo</i>	0	0	0	0	0	0
<i>Sassoferrato</i>	0	0	18	30.0	0	0
<i>Senigallia</i>	0	0	0	0	0	0
<i>Macerata</i>	0	0	0	0	21	0.1
<i>Matelica</i>	0	0	0	0	0	0
<i>Recanati</i>	0	0	0	0	0	0
<i>San Severino M.</i>	0	0	0	0	0	0
<i>Sarnano</i>	0	0	0	0	0	0

Finally, aggregate economic losses due to the three events are compared in fig. 9.27.

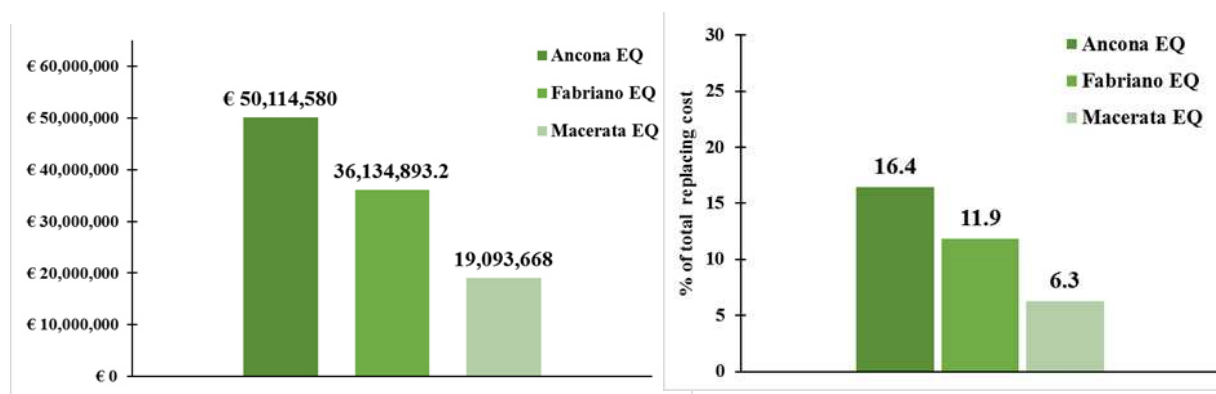


Figure 9.27. Comparison of the total repair cost (left) and of the percentage on the total replacing cost (right)_Aggregate data

In tab. 9.28 the total repair cost and the percentages on the total replacing cost are disaggregated for cities.

Table 9.28. Repair cost and percentage on the total amount of the replacing cost_Data disaggregated for cities

	Ancona EQ		Fabriano EQ		Macerata EQ	
	Mln €	%	Mln €	%	Mln €	%
<i>Ancona</i>	39.9	68.2	0	0	0	0
<i>Arcevia</i>	0	0	0.4	11.5	0	0
<i>Fabriano</i>	0	0	30.3	97.3	0	0
<i>Falconara M.</i>	3.9	36.5	0	0	0	0

<i>Castelfidardo</i>	0	0	0	0	0	0
<i>Chiaravalle</i>	0.7	11.0	0	0	0	0
<i>Jesi</i>	0.3	0.9	0	0	0	0
<i>Loreto</i>	0.3	2.3	0	0	0.3	2.3
<i>Osimo</i>	4.2	23.8	0	0	1.1	6.4
<i>Sassoferrato</i>	0	0	2.1	100	0	0
<i>Senigallia</i>	0.1	0.3	0	0	0	0
<i>Macerata</i>	0	0	0	0	0	0
<i>Matelica</i>	0	0	2.9	30.8	12.4	40.3
<i>Recanati</i>	0.8	7.0	0	0	3.8	31.4
<i>San Severino M.</i>	0	0	1.5	15.0	1.5	15.0
<i>Sarnano</i>	0	0	0	0	0	0

Tab. 9.29 summarizes the aggregate losses in terms of total number of collapsed buildings, casualties and economic losses due to the three events.

Table 9.29. Comparison of the n° of collapsed buildings, casualties and economic losses

_Aggregate data

	<i>N° of collapsed buildings</i>	<i>N° of casualties (Bramerini)</i>	<i>Economic losses Mln [€]</i>
<i>Ancona EQ_Mw =5.9</i>	6	449	50.11
<i>Fabriano EQ_Mw=6.2</i>	8	375	36.1
<i>Macerata EQ_Mw = 5.9</i>	5	21	19.1

Tab. 9.29 compares the losses in terms of total number of collapsed buildings, casualties and economic losses due to the three events, disaggregate for provinces.

Table 9.30. Comparison of the n° of collapsed buildings, casualties and economic losses

_Disaggregation for provinces

<i>Event</i>	<i>N° of collapsed buildings</i>		<i>N° casualties (Bramerini)</i>		<i>Economic losses Mln [€]</i>	
	<i>Ancona</i>	<i>Macerata</i>	<i>Ancona</i>	<i>Macerata</i>	<i>Ancona</i>	<i>Macerata</i>
<i>Ancona EQ</i>	6	0	449	0	49.3	0.8
<i>Fabriano EQ</i>	8	0	375	0	31.8	4.4
<i>Macerata EQ</i>	0	5	0	21	1.4	17.7

The per event damage scenarios have been developed considering earthquakes with a maximum magnitude estimated on the base of the fault system present in the area of interest.

Epicenters in Ancona, Fabriano and Macerata have been chosen because of the most presence of schools in these cities.

Thus, epicentre position and maximum magnitude are fixed such as in a deterministic approach.

The uniform hazard scenarios assume PGA values relative to return periods of 200, 476, 912, 1462 and 2475 years, referring to Italy hazard map carried out by means a PSHA.

Obviously, it provides higher losses than the per event scenarios (figs. 9.28, 9.29 and 9.30), because about the same intensity is considered acting coterporally in all cities under investigation.

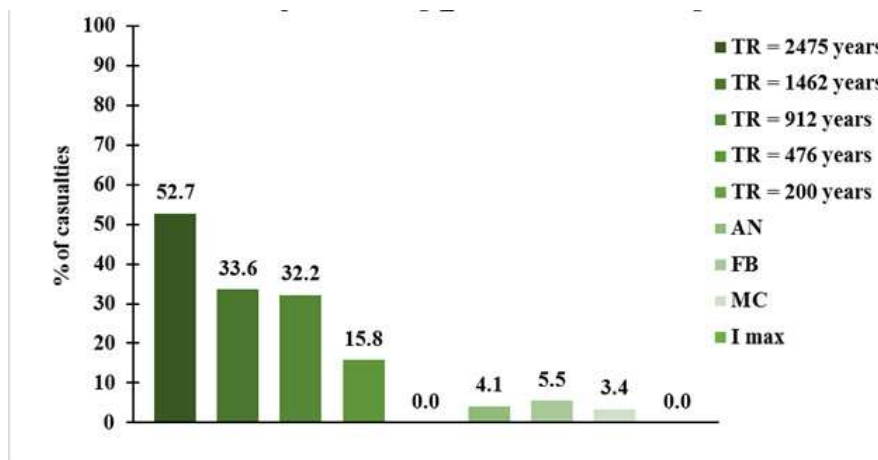


Figure 9.28. Percentage of the collapsed buildings for the all scenarios

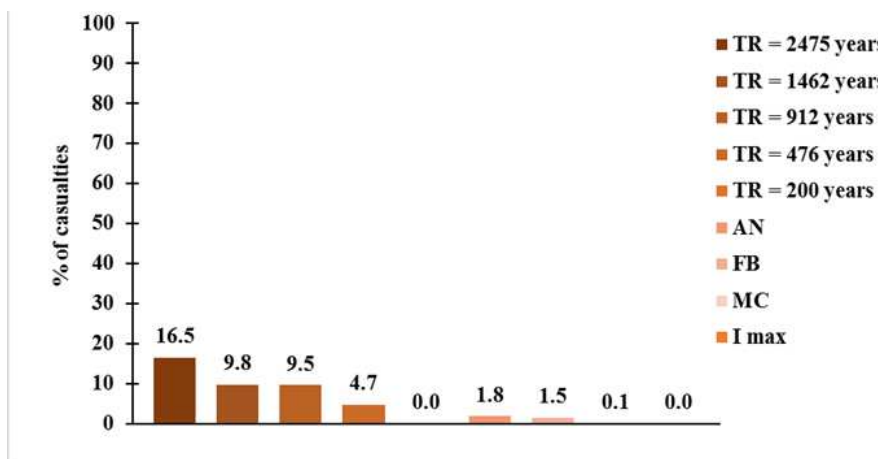


Figure 9.29. Percentage of the casualties for the all scenarios

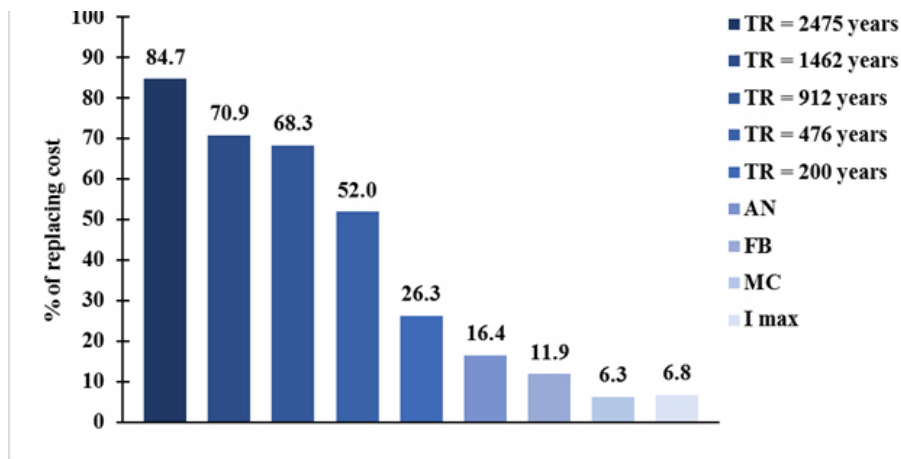


Figure 9.30. Percentage of the replacing cost for the all scenarios

In *uniform hazard scenarios* can be noted as the physical and economic losses increase almost linearly with the hazard level, while the number of casualties increase much less depending only from the number of building collapsed, that is fairly high only for the return period of 2475 years. In *per event scenarios*, even if the scenario with epicentre in Ancona (Mw = 5.9) has a lower magnitude than the one with epicentre in Fabriano (Mw = 6.2), the losses are higher because of most part of exposure (buildings and students) are closer to Ancona and so they suffer in a greater way the Ancona earthquake. While the city of Fabriano is far enough other cities in which school buildings are located.

The same is for the Macerata earthquake (Mw = 5.9), that causes high losses mainly in the city of Macerata.

Therefore, in all three scenarios most of loss is concentrated close to the epicenter.

Other scenarios could be developed by varying the position of the epicentre along the fault lines in order to estimate losses and compare them to understand the worst epicentre position for the whole province of Ancona.

Instead, to understand the maximum expected losses for each city, the epicentre of an earthquake with the maximum expected magnitude for the closest fault systems, could be located as close as possible the city under investigation (the epicentre location depends on the relative position between the fault system and city).

References chapter 9

- Faccioli E. et al. A study on damage scenarios for residential buildings in Catania city. *Journal of Seismology* 3: 327–343, 1999.
- Dolce M., Marino M., Masi A., Vona M. (2000), “Seismic Vulnerability Analysis and Damage Scenarios of Potenza Town”, *International Workshop on Seismic Risk and Earthquake Damage Scenarios of Potenza*, Potenza.
- Spence R. and Le Brun B., eds. (2006). “Earthquake scenarios for European cities—The RISK-UE project.” *Bull. Earthquake Eng.*, 4(4), 319–463.
- Marulanda M.C., Carreño M.L., Cardona O.D. et al. Probabilistic earthquake risk assessment using CAPRA: application to the city of Barcelona, Spain. *Nat Hazards* (2013) 69: 59.
- Meroni F. et al. Damage risk and scenarios in the Veneto - Friuli area (NE Italy). *Bollettino di Geofisica Teorica ed Applicata* Vol. 49, n. 3-4, pp. 485-503; December 2008.
- Asteris P.G. Definition of Seismic Vulnerability Maps for Civil Protection Systems: The Case of Lampedusa Island. *The Open Construction and Building Technology Journal*, 2016, 10, (Suppl 1: M5) 87-105.
- D’Amico et al. Building vulnerability and seismic risk analysis in the urban area of Mt. Etna volcano (Italy). *Bulletin of Earthquake Engineering* July 2016, Volume 14, Issue 7, pp 2031–204.
- Di Pasquale et al. New Developments in Seismic Risk Assessment in Italy. *Bulletin of Earthquake Engineering* January 2005, Volume 3, Issue 1, pp 101–128.
- Zuccaro G., Cacace F. (2009) Revisione dell’inventario a scala nazionale delle classi tipologiche di vulnerabilità ed aggiornamento delle mappe nazionali di rischio sismico. *Atti del XIII Convegno ANIDIS “L’ingegneria sismica in Italia”*, June 28–July 2, Bologna, Italy. Paper S14.39 (in Italian).
- Cornell C.A. 1968: *Engineering seismic risk analysis*. *Bull. Seism. Soc. Am.*, 58, 1583-1606.

- Bazzurro P., Cornell C. A. (1999). Disaggregation of Seismic Hazard. *Bulletin of the Seismological Society of America*, 89 (2), 501-520.
- Sabetta F., Pugliese A. Attenuation of Peak Horizontal Acceleration and Velocity from Italian Strong-motion Records. *Bull. Seism. Soc. Am.* Vol. 77, 1987.
- Ministro dei Lavori Pubblici e dei Trasporti, “DM 14/01/2008 – NTC - Norme tecniche per le costruzioni (in Italian),” *Suppl. Ordin. Gazz. Uff. n. 29*, 2008.
- Rovida A., Locati M., Camassi R., Lolli B., Gasperini P. (eds), 2016. CPTI15, the 2015 version of the Parametric Catalogue of Italian Earthquakes. Istituto Nazionale di Geofisica e Vulcanologia.
- Locati M., Camassi R., Rovida A., Ercolani E., Bernardini F., Castelli V., Caracciolo C.H., Tertulliani A., Rossi A., Azzaro R., D’Amico S., Conte S., Rocchetti E. (2016). DBMI15, the 2015 version of the Italian Macroseismic Database. Istituto Nazionale di Geofisica e Vulcanologia.
- Brammerini F., Di Pasquale G., Orsini G., Pugliese A., Romeo R., Sabetta F., “Rischio sismico del territorio italiano. Proposta per una metodologia e risultati preliminari”. SSN/RT/95/01, Rome, 1995 (In Italian).
- HAZUS 99 “Earthquake Loss Estimation Methodology - Technical and User Manuals” Federal Emergency Management Agency, Washington, D.C. 1999.
- Coburn A. and Spence R. J. S.: *Earthquake Protection*, John Wiley and Sons, 2002.
- Di Ludovico M, Prota A, Moroni C, Manfredi G, Dolce M (2016-a) a, “Reconstruction process of damaged residential buildings outside the historical centres after L’Aquila earthquake—part I: “light damage” reconstruction. *Bull Earthq Eng.*
- Di Ludovico M, Prota A, Moroni C, Manfredi G, Dolce M (2016-b) b. Reconstruction process of damaged residential buildings outside historical centres after the L’Aquila earthquake—part II: “heavy damage” reconstruction. *Bull Earthq Eng.*

Conclusions

A new vulnerability index method for seismic vulnerability and risk assessment of RCMF school buildings was illustrated. It allows to rapidly calculate the global vulnerability index (Iv), that is a comparative measure of the vulnerability, by evaluating 15 vulnerability indicators through expert judgment and assigning scores to them, such as in the 2nd level GNDT method.

The proposed method was derived from mechanicals simulations on several structural models (chapter 5) representative of some relevant structural characteristics detected from the school building stock under investigation (chapter 4).

To this aim the building stock was divided into two structural classes, the PRE and POST 1974, to take into account the different reference design Codes and so the variability in seismic response.

The scores to assign to the vulnerability indicators were derived from the comparison of the capacities of the structural models generated for the parametric analysis. The area comprised under the average equivalent bilinear curve (of the 8 curves for each models) was assumed as the capacity parameter.

The several structural models were generated in a deterministic way by assuming the frequentist configurations detected for each indicator investigated. This could be an aspect to improve in future development, considering also other possible configurations especially with regard the mechanical parameters of the materials.

Further the proposed method didn't investigate the vulnerability aspects due to non-structural elements, such as partition walls and ceilings, that in some situations could be very dangerous for students. Thus this could be an aspect to investigate in future studies.

Most of structural models exhibited a better response, in terms of resistance, stiffness and ductility, along the longitudinal direction, because of the presence of shear type frames, especially for the structural models conforming to the POST 1974 design procedure. However, the presence of the ribbon windows delimiting short columns on the façade causes the brittle collapse of them.

In the transverse direction, the lack of shear type frames except on the perimeter induces lower resistance and stiffness, especially for the structural models conforming to the PRE 1974 design procedure. However, a positive contribution in terms of both stiffness and resistance, for the elastic range, is due to the presence of full height walls on the sides and of the stairs with knee-beams.

The evaluation of the building stock was performed according to the macroseismic method, associating the building classes to the typologies of the EMS-98 scales (RC1, building without earthquake resistance details, and RC2, building with medium earthquake resistance details). Thus, the mean damage curves were developed and then used for the damage scenario with macroseismic intensities.

Further the assessment according to the proposed and the 2nd level GNDT methods were carried out.

As expected, the proposed method provides a higher average vulnerability for the POST 1974 class with respect to the PRE 1974 class, such as the 2nd level GNDT method (chapter 6). However, the proposed method provides a more precise assessment of each building and so a better differentiation of the results. In fact, the 2nd level GNDT method usually provides the same I_v value for different buildings, because of many scores to assign to the vulnerability indicators are equal to each other. Instead, in the proposed procedure the scores are different for most vulnerability indicators and so the obtained I_v values differ from one another.

This aspect is of fundamental importance when a vulnerability ranking has to be carried out in order to establish the destination of the limited resources available for risk mitigation interventions.

Then, by transforming the I_v values into the capacity in terms of PGA using the relationships provided from the author (chapter 5), both with respect to the slight damage (PGAs) and the collapse (PGAc), the trilinear damage curves (PGA – DI) were obtained. They make it possible the evaluation of the reliability of the proposed method, by means the comparison with numerical and experimental investigations, and the risk assessment.

It is worth noting that the I_v - PGA relationships were obtained by interpolating the cloud of points representing the pairs I_v – PGA for the structural models employed in the parametric analysis, where the PGAs and PGAc values were calculated in the ADRS plane by intersecting the demand spectra and the average equivalent bilinear curves of each structural models, respectively in correspondence of the points $(d(0,7 a_y), 0.7 a_y)$ and (d_u, a_u) of the curves. This means that the capacity determined in terms of PGA is a mean capacity and the uncertainties in the structural response were not considered because the upper and lower bound were not calculated.

The average PGAc values with respect to the collapse for the PRE and POST 1974 building classes (0.356 g and 0.504 g respectively), showed a fairly safe condition if compared with the PGA levels provided by the Italian seismic Code for the design of new school building. However, the intensity levels could be much higher as shown from the recent earthquakes, even if they act for a short time. Analytical fragility curves for the four damage states DS_k were developed from both pushover analysis and IDAs on the PRE and POST 1974 prototype buildings (chapter 7). As expected, the fragility curves relative to the PRE 1974 building are shifted on the left with respect to the ones of the POST 1974 building, meaning a greater fragility of the former especially for the higher damage states (DS3 and DS4).

The fragility curves here developed are based on global mechanisms, thus they measure the capacity reserves that the structure is able to exhibit, beyond the local damage mechanisms (conventionally set by structural Codes), up to their propagation into a global failure mechanism.

Then, introducing the seismic hazard for the area of interest, analytical vulnerability curves (PGA – DI) were obtained from fragility curves (PGA – P). The comparison between analytical

vulnerability curves and the trilinear damage curves, obtained from the rapid methods (chapter 6), shows that for low seismic intensity the rapid method is less conservative than both the GNDT method and the non-linear analyses. Instead, for the higher intensity levels the proposed method is very close to the vulnerability curves from both IDA and GNDT, while the curve form pushover analysis is too conservative.

The evaluation of 10 case studies of RC school buildings by means pushover analyses confirmed as seen for the prototype buildings.

The experimental validation, performed by comparing the damage occurred during the Centre Italy 2016 seismic sequence, with the damage estimated from the proposed trilinear damage curves for the same intensity levels, provides a good correspondence for the physical damage (no damaged, usable, unusable and collapsed buildings) and human losses. With regard economic losses no data are available at moment and so a validation wasn't possible.

A case study was evaluated in depth by means non-linear analyses and considering several accelerograms selected closer as possible the school building investigated. Also in this case a good correspondence was found between the estimated damage level and the occurred one.

Obviously, many uncertainties affect these results, such as the damage scale assumed to estimate damage through the damage index (Bramerini et al. 1995), thus in the thresholds values corresponding to the damage levels DLk. Further, the intensity levels recorded during the sequence are not those exactly suffered from school buildings, because the stations are not located in the buildings and in some cases are fairly far. Local amplification effects could have had an important role in the damaging of some schools.

Also, the damage detection could have a little bit of uncertainty in the choice of the exact damage level suffered, being made by means expert judgment.

Even if more case studies should be analytically evaluated and an experimental for higher intensity level to have more robust validation, the proposed method can be considered fairly reliable for the purpose of rapid and comparative assessment.

Finally, several damage scenarios were developed for the school buildings under investigation, by considering the seismic hazard in two different ways.

In the first way, uniform hazard was considered on the region of interest. The hazard levels were assumed from the Italian seismic map, thus PGA values corresponding to five return periods of the seismic events.

In the second way, three hypocentres-magnitude pairs on the basis of the seismogenic sources present in the region were assumed.

In *uniform hazard scenarios* can be noted as the physical and economic losses increase almost linearly with the hazard level, while the number of casualties increase much less depending only from the number of building collapsed, that is fairly high only for the return period of 2475 years.

For mostly return periods the higher percentage of buildings exhibits the unusable condition, except for the TR = 200 years for which the higher percentage of buildings exhibits the usable condition. In *per event scenarios*, most of losses are due to the Ancona EQ because the most part of school buildings is located close to the city of Ancona. Therefore, in all three scenarios most of loss is concentrated close to the epicenter.


The estimated losses have to be considered as mean values because the average capacity of the buildings and the median hazard (50^opercentile) were considered.


Thus, the present work could be a significant support for the owners of the school buildings (provinces of Ancona and Macerata) in order to understand which are the buildings with higher risk and so to prioritize the interventions for seismic risk mitigation.


Further they can have an estimation of the average expected economic losses due to several seismic events, so an idea of the required resources.


Appendix A_Data sheets of high school buildings (province of Ancona)


School building: I.T.N “Elia”		City: ANCONA
Age	1969	
Seismic design level	Low	
N° of independent structures	2	
Average n° of storeys	5	


School building: Liceo artistico “Mannucci”		City: ANCONA
Age	1966	
Seismic design level	Low	
N° of independent structures	3	
Average n° of storeys	3	


School building: Liceo scientifico “Savoia”		City: ANCONA
Age	1972	
Seismic design level	Low	
N° of independent structures	2	
Average n° of storeys	4	


School building: I.T.I.S. “Volterra”		City: ANCONA
Age	1963, 1970	
Seismic design level	Low	
N° of independent structures	7	
Average n° of storeys	3	


School building: I.T.A.S. “Angelini”		City: ANCONA
Age	1995	
Seismic design level	Low	
N° of independent structures	1	
Average n° of storeys	3	

School building: I.T.C. “Benincasa”		City: ANCONA
Age	1976	
Seismic design level	Low	
N° of independent structures	2	
Average n° of storeys	3	


School building: Liceo scientifico “Galilei”		City: ANCONA
Age	1976, 2006	
Seismic design level	Low, High	
N° of independent structures	3	
Average n° of storeys	4	


School building: I.T.C.G. “Vanvitelli - Stracca”		City: ANCONA
Age	1988	
Seismic design level	Low	
N° of independent structures	4	
Average n° of storeys	3	

School building: I.I.S. “Podesti-Onesi”		City: ANCONA
Age	2010	
Seismic design level	High	
N° of independent structures	5	
Average n° of storeys	2	

School building: I.P.S.I.A. “Padovano”		City: ARCEVIA
Age	1980, 1985	
Seismic design level	No, Low	
N° of independent structures	3	
Average n° of storeys	5	


School building: I.T.I.S. “Meucci”		City: CASTELFIDARDO
Age	2003	
Seismic design level	Medium	
N° of independent structures	3	
Average n° of storeys	3	

School building: I.P.C. “Medi”		City: CHIARAVALLE
Age	1990	
Seismic design level	Low	
N° of independent structures	2	
Average n° of storeys	4	


School building: I.T.I.S. “Merloni”		City: FABRIANO
Age	1966, 1967	
Seismic design level	No	
N° of independent structures	2	
Average n° of storeys	3	

School building: Liceo Scientifico “Volterra”		City: FABRIANO
Age	1950	
Seismic design level	No	
N° of independent structures	1	
Average n° of storeys	3	


School building: I.T.C.G. “Morea”		City: FABRIANO
Age	1988	
Seismic design level	Low	
N° of independent structures	4	
Average n° of storeys	3	


School building: Liceo artistico “Mannucci”		City: FABRIANO
Age	1989	
Seismic design level	Low	
N° of independent structures	1	
Average n° of storeys	3	


School building: Liceo classico “Stelluti”		City: FABRIANO
Age	1985	
Seismic design level	Low	
N° of independent structures	1	
Average n° of storeys	3	


School building: Liceo scientifico “Cambi”		City: FALCONARA
Age	1976	
Seismic design level	Low	
N° of independent structures	2	
Average n° of storeys	3	


School building: I.T.C. Serrani		City: FALCONARA
Age	1982	
Seismic design level	Low	
N° of independent structures	3	
Average n° of storeys	3	


School building: I.I.S. “Galiliei”		City: JESI
Age	1976	
Seismic design level	Medium (retrofit 1996)	
N° of independent structures	3	
Average n° of storeys	2	

School building: Liceo artistico “Mannucci”		City: JESI
Age	< 1960	
Seismic design level	No	
N° of independent structures	1	
Average n° of storeys	3	

School building: Liceo scientifico “Da Vinci”		City: JESI
Age	1973, 2000, 2004	
Seismic design level	No, Medium	
N° of independent structures	3	
Average n° of storeys	4	


School building: .T.C.G. “Cuppari”		City: JESI
Age	1984, 1987	
Seismic design level	Low	
N° of independent structures	3	
Average n° of storeys	3	

School building: I.T.I.S. “Marconi”		City: JESI
Age	1992, 2005, 2009	
Seismic design level	Low, High	
N° of independent structures	3	
Average n° of storeys	2	

School building: I.T.C. “Einstein”		City: LORETO
Age	1966	
Seismic design level	No	
N° of independent structures	3	
Average n° of storeys	4	


School building: I.P.A.S. “Nebbia”		City: LORETO
Age	2004	
Seismic design level	High	
N° of independent structures	3	
Average n° of storeys	3	


School building: Liceo clas.sc. “Campana”		City: OSIMO
Age	1967, 2005	
Seismic design level	No, High	
N° of independent structures	3	
Average n° of storeys	3	


School building: I.T.G.C. “Corridoni”		City: OSIMO
Age	1987, 1994, 2006	
Seismic design level	Low, High	
N° of independent structures	6	
Average n° of storeys	3	

School building: I.P.S.I.A. “Laeng”		City: OSIMO
Age	1962	
Seismic design level	No	
N° of independent structures	2	
Average n° of storeys	6	


School building: Liceo scientifico “Volterra”		City: SASSOFERRATO
Age	1962	
Seismic design level	No	
N° of independent structures	1	
Average n° of storeys	3	

School building: I.T.C.G. “Corinaldesi”		City: SENIGALLIA
Age	1981, 2003	
Seismic design level	Low, Medium	
N° of independent structures	2	
Average n° of storeys	3	

School building: Liceo scientifico“Medi”		City: SENIGALLIA
Age	1965	
Seismic design level	Low	
N° of independent structures	2	
Average n° of storeys	4	

School building: Liceo scienze umane “Marinelli”		City: SENIGALLIA
Age	1972, 2007	
Seismic design level	Low, High	
N° of independent structures	2	
Average n° of storeys	3	

School building: Liceo classic “Peticari”		City: SENIGALLIA
Age	1967	
Seismic design level	High (retrofit 2007)	
N° of independent structures	2	
Average n° of storeys	2	

School building: I.P.A.S. “Panzini”		City: SENIGALLIA
Age	1974, 1986, 1995, 2004	
Seismic design level	Low, Medium	
N° of independent structures	10	
Average n° of storeys	2, 5	

School building: I.P.S.I.A. "Padovano"		City: SENIGALLIA
Age	2001	
Seismic design level	Medium	
N° of independent structures	4	
Average n° of storeys	2	